Towards Development of a 3-State Self-Paced Brain Computer Interface System

by

ALI BASHASHATI

B.Sc., Sharif University of Technology, 2000

M.Sc., Amirkabir University of Technology (Tehran Polytechnic), 2002

A THESIS SUBMITTED IN PARTIAL FULFILLMENT OF
THE REQUIREMENTS FOR THE DEGREE OF

DOCTOR OF PHILOSOPHY

In

THE FACULTY OF GRADUATE STUDIES
(Electrical and Computer Engineering)

THE UNIVERSITY OF BRITISH COLUMBIA

September 2007

© Ali Bashashati, 2007

Abstract

Brain computer interface (BCI) systems aim at helping individuals with motor disabilities by providing them the ability to control devices such as wheelchairs and computers, using their brain activity only.

The majority of BCI research to-date has focused on developing technology for "synchronous" BCIs. These systems allow the user to affect control during specified time periods only. Self-paced (asynchronous) BCIs on the other hand, are designed to respond whenever the user intends to control the system, otherwise they remain in the so called "inactive output state".

This dissertation pursues two main objectives: 1) improving the performance of the existing 2-state self-paced BCI system developed at the Neil Squire Society, Vancouver, Canada (initial evaluations of this system on eight subjects showed mean true positive (TP) rates of 51.3% and 27.5% at false positive (FP) rates of 2% and 1%, respectively.) and 2) designing the first 3-state self-paced BCI.

At first, a comprehensive survey of signal processing algorithms in BCI systems is conducted. This survey is the first comprehensive review that covers more than 300 BCI published papers and introduces a taxonomy for signal processing in BCI systems.

To achieve the first objective, four separate studies related to the feature extraction and feature classification blocks of the 2-state self-paced BCI are conducted. These studies increase the mean TP rate of the existing system to 73.5% and 47.3% at the FP rates of 2% and 1%, respectively. In these studies, the users were not allowed to control the BCI in 15-34% of the time due to the presence of eye blinks. Thus, another study is also conducted to evaluate the system when the users were allowed to control the output even during eye blinks. Results show slight decrease in TP rates (mean TP rates of 68.0% and 40.6% at the FP rates of 2% and 1%, respectively) with the advantage of providing full control of the system.

To achieve the second objective, two new set of movements (right and left hand extension movements) which have not been previously used in the context of BCI systems are used to control the new 3-state self-paced BCI. Results on four able-bodied subjects show significant improvements in detecting the presence of a movement when the system is used in the context of a 2-state self-paced BCI. The mean TP rate is 73.4% at the FP rate of 1%. Initial evaluations of the proposed 3-state self-paced BCI show promise with mean right and left true positive rates of 42.2% and 51.9% at a false positive rate of 1%.

Table of Contents

Chapter 1 Introduction 1
1.1. Functional Model of a BCI system 2
1.2. Background 5
1.2.1. Self-Paced and Synchronized BCI Systems 9
1.2.2. BCI Research at the Neil Squire Society (NSS) and the University of British Columbia (UBC) 13
1.3. Objectives and Contributions 15
1.4. Thesis Scope and Organization 18
1.5. References 21
Chapter 2 A Survey of Signal Processing Algorithms in Brain-Computer Interfaces Based on Electrical Brain Signals 29
2.1. Introduction 29
2.2. General Structure of a BCI System 30
2.2.1. Electrophysiological Sources of Control in Current BCIs 32
2.3. Methods 34
2.4. Results 37
2.5. Discussion 49
2.5.1. Signal Enhancement 53
2.5.2. Feature Extraction 55
2.5.3. Feature Selection 57
2.5.4. Feature Classification 58
2.5.5. Post-Processing 60
2.6. Conclusions 62
2.7. References 63
2.8. Appendix A. Index of Terms 94
Chapter 3 Brain Computer Interface (BCI) Design for Asynchronous Control Applications: Improvements to the LF-ASD Asynchronous Brain Switch 96
3.1. Introduction 96
3.2. New Asynchronous Brain Switch Designs 99
3.3. Description of New Components and Methods 100
3.4. Evaluation Methods 102
3.5. Results and Discussion 103
3.5.1. Debounce Analysis 103
3.5.2. New vs. Old Transducer Designs 105
3.5.3. Spinal Cord-Injured Subjects vs. Able-Bodied Subjects 108
3.6. Conclusion 109
3.7. References 110
Chapter 4 A Comparative Study on Generating Training-Data for Self-Paced Brain Interfaces 113
4.1. Introduction 113
4.2. Data Generation Methods 115
4.2.1. Parzen-Based Training-Data Generation (TR_Gen1) 116
4.2.2. kMeans-Based Training-Data Generation (TR_Gen2) 118
4.2.3. Averaged kMeans-Based Training-Data Generation (TR_Gen3) 118
4.3. Evaluation 119

4.3.1. Experimental Data 120
4.3.2 Method of Evaluation 121
4.4. Results 123
4.5. Discussion 125
4.6. References 128
Chapter 5 User Customization of the Feature Generator of an Asynchronous Brain Interface 131
5.1. Introduction 131
5.2. Background 133
5.2.1. LF-ASD Feature Generator 134
5.3. Data Recording 135
5.4. Methods 136
5.4.1. Delay Parameter Customization 136
5.4.2. Cross-validation and Stratified Cross-validation 138
5.5. Results 140
5.6. Conclusions 147
5.7. References 150
Chapter 6 An Improved Asynchronous Brain Interface: Making Use of the Temporal History of the LF-ASD Feature Vectors 152
6.1. Introduction 152
6.2. Proposed design of the LF-ASD-V5 156
6.2.1. Path Template Generation 157
6.3. Evaluation Method 158
6.4. Results 161
6.5. Conclusions 166
6.6. References 168
Chapter 7 Effects of Eye Blinks on a Self-paced Brain Interface Design 170
7.1. Introduction 170
7.2. Methods 173
7.2.1. Brain Interface Designs 173
7.2.2. Experiments 175
7.2.3. Evaluation 177
7.3. Results 179
7.4. Discussion 187
7.5. References 189
Chapter 8 Towards Development of a 3-State Self-Paced Brain Interface Based on Hand Extension Movements 191
8.1. Introduction 191
8.2. Experimental paradigm 195
8.3. Proposed 3-state self-paced Brain computer interface 196
8.3.1. Detector 1 197
8.3.2. Detector 2 200
8.4. Evaluation 201
5. Results 202
8.5. Discussion 204
8.6. References 207
Chapter 9 Improving the Performance of a 3-State Self-Paced Brain Computer Interface ..210

9.1. Introduction 210
9.2. 3-State Self-Paced BCI 213
9.2.1. Detector 1 (DET1) 214
9.2.2. Detector 2 (DET2) 217
9.3. Experimental Paradigm 218
9.4. Evaluation 219
9.5. Results 221
9.6. Conclusions 223
9.7. References 226
Chapter 10 Summary and Conclusions 229
10.1. Summary and Concluding Remarks 229
10.2. Summary of Contributions 232
10.3. Discussions and Future Directions 234
10.4. Applications of 2-State and 3-State Self-Paced BCIs 237
10.5. References 239
Appendix A. UBC Research Ethics Board Certificate 241
Appendix B. Expanded Tables of Chapter 2 242
Appendix C. Details of Methods 257
C.1. Linear Discriminnat Analysis (Lachenbruch 1975) 257
C.2. Principal Components Analysis (Jolliffe 2002) 258
C.3. K-Means Clustering (Hartigan 1979) 259
C.4. Parzen Probability Density Estimation Method (Parzen 1962) 260
C.5. Description of the LF-ASD Feature Generator (Mason and Birch 2000) 261
C.6. Fuzzy Adaptive Resonance Theory (Carpenter et al 1991) 262
C.7. Learning Vector Quantization (Kohonen 1990) 263
C.8. k-Nearest Neighbor Classification: 264
C.9. References 264

List of Tables

Table 1.1 Description of the BCI transducer components....4
Table 2.1 Taxonomy for BCI Transducer designs....32
Table 2.2 Electrophysiological activities used in BCI designs and their definitions....33
Table 2.3 Pre-processing (signal enhancement) methods in BCI designs....39
Table 2.4 Feature selection/dimensionality reduction methods in BCI designs....40
Table 2.5 Feature extraction methods in BCI designs. refer to appendix 2 for A more detailed version of this table....41
Table 2.6 Feature classification methods in BCI designs that use EEG and ECoG recording technology....45
Table 2.7 Feature classification methods in BCI designs that are based on neural cortical recordings....48
Table 2.8 Post processing methods in BCI designs....49
Table 2.9 Index of Terms....94
Table 3.1 Configurations of the New Asynchronous Brain Switch Designs, where nLF-ASD = normalized-Low-Frequency Asynchronous Switch Design, ENT = Energy Normalization Transform, KLT = Karhunen-Loève Transform, fuzzy ART = fuzzy Adaptive Resonance Theory, LVQ3 = Learning Vector Quantization....100
Table 3.2 Mean True Positive Rates For All Subjects With Different Debounce Values, where nLF-ASD = normalized-Low-Frequency Asynchronous Switch Design, STD = standard deviation of True Positive Rates, s = seconds, Tdb.= debounce period. Note: all False Positive rates = 2%....105
Table 3.3 True Positive Rates for Individual Subjects. Note: all False Positive rates = 2%. Debounce values of 16 are shown....107
Table 4.1 Area under ROC curve (for FP<2%) averaged over 10 runs of the algorithms for each subject for different training-data generation methods....123
Table 4.2 Overall significance level (p-value) of *improvements* and percentage of improvements (in parentheses) of the area under ROC curve (for FP<2%) when using the proposed training-data generation method. Items that has '-' indicate performance decrease and thus no values is reported....124
Table 4.3 Average true positive rates (across eight subjects) at fixed false positive rates of 1% and 2% for the training-data generation methods....124
Table 5.1 Delay parameters (measured in seconds) estimated from the ensemble averages of the bipolar EEG signals (F2-FC2) generated from the training data set. Note that the same delay parameters are used for all six bipolar channels....138
Table 5.2 True positive (TP) rates (%) at false positives (FP) of 2% for different training and test sets. TS_i represents the case in which the data of the i^{th} session were used for training and the other sessions for testing....139
Table 5.3 Performance of the LF-ASD together with standard deviations across 10 runs of stratified cross-validation with original and new delay parameters....143
Table 5.4. Average standard deviation (STD) of TP rates (at fixed FP=2%) across each cross-validation set....144
Table 6.1. Details of the eeg data of the evaluation set that were blocked by the test system due to eye-blink....161
Table 6.2 True positive (tp) rates at fixed False Positive (fp) rates of 1% and 2% for able-bodied subjects....164

Table 6.3 True Positive (tp) rates at fixed False Positive (fp) rates of 1% and 2% for SCI subjects. 164
Table 7.1 Details of the EEG data of the evaluation set that were blocked by the test system due to eye-blinks. 172
Table 7.2 True positive (TP) rates at fixed False Positive (FP) rates of 1% and 2% for both able-bodied and spinal cord injured subjects for LF-ASD-V4 and LF-ASD-V5 designs using Case 1 and Case 3 evaluation methods. 180
Table 7.3 True positive (TP) rates at fixed False Positive (FP) rates of 1% and 2% for both able-bodied and spinal cord injured subjects for LF-ASD-V4 and LF-ASD-V5 designs using Case 2 and Case 3 evaluation methods. 181
Table 7.4 True positive (TP) rate (%) change of the LF-ASD-V4 when eye-blinks are present (LF-ASD-V4-Case3) versus the original LF-ASD-V4 when the output is blocked due to eye-blinks (LF-ASD-V4-Case2) 181
Table 7.5 True positive (TP) rate (%) change of the LF-ASD-V5 when eye-blinks are present (LF-ASD-V5-Case3) versus the original LF-ASD-V5 when the output is blocked due to eye-blinks (LF-ASD-V5-Case2) 181
Table 7.6 True positive rate (%) change of the LF-ASD-V5 when eye-blinks are present (LF-ASD-V5-Case3) versus the original LF-ASD when the output is blocked due to eye-blinks (LF-ASD-V4-Case2) 182
Table 8.1 Estimated α_i and α_j parameters for each subject. Note all values are in milliseconds. 198
Table 8.2 Percentage of true positives (TP_{IC}) at fixed false positive rate of 1% for the two designs of DET1 202
Table 8.3 Percentage of right and left true positives (TP_R and TP_L) of the two proposed 3-state brain computer interfaces (when false positive rate is set at 1%) . The TP_R and TP_L values of the best design combination for each subject is highlighted. 203
Table 8.4 Best design combination for each subject together with the performances of the 2-state and 3-state systems (at false positive of 1%), where A = <DET1-LF-1NN + DET2-PSD-LDA> and B = <DET1-PSD-LDA + DET2-PSD-LDA> 203
Table 9.1 Percentage of true positives (TP_{IC}) at fixed false positive rate of 1% for the two designs of DET1 222
Table 9.2 Percentage of right and left true positives (TP_R and TP_L) of the two proposed 3-state brain computer interfaces (when false positive rate is set at 1%) . The TP_R and TP_L values of the best design combination for each subject is highlighted. 222
Table 10.1 comparison between 2-state self-paced BCI systems 231
Table 10.2 Comparison between multi-state bci systems 232
Table B.0.1 Feature extraction methods in BCI designs 242
Table B.0.2 Feature classification methods in BCI designs that use EEG and ECoG recording technology 248
Table B.0.3 Feature classification methods in BCI designs that are based on neural cortical recordings 255

List of Figures

Figure 1.1. Simple block diagram of a BCI system....2
Figure 1.2 Functional model of a BCI system depicting the principle functional components, where amp = amplifier. Note the 'Control Display' is optional....4
Figure 1.3 (a) Self-paced brain computer interface operating paradigm, (b) synchronized brain computer interface paradigm....11
Figure 1.4 High-level design of LF-ASD brain computer interface. The 'Feature Classifier' continually monitors the 6-dimensional feature vectors and when a feature vector enters a pre-defined sub-space "IC", the output of the classifier is activated (IC state). Otherwise, the output state remains inactive (NC state)....14
Figure 1.5 Sample outputs of the 2-state BCI (the LF-ASD) and proposed 3-state BCI....17
Figure 1.6 Organization of chapters....21
Figure 2.1 Functional model of a BCI system (Mason and Birch 2003). Note the control display is optional. This review focuses on the shaded components of BCI systems....31
Figure 2.2 Signal-enhancement, feature selection and post-processing methods in BCI designs....50
Figure 2.3 Feature extraction methods in BCI designs based on Sensorimotor Activity, VEP, P300, SCP, Response to Mental Tasks, Activity of Neural Cells, and Multiple Neuromechanisms....51
Figure 2.4 Feature classification methods in BCI designs. 'In/Out Modeling' refers to those ANC-based BCIs that directly map the input neural recordings to the output without using a feature extraction technique....52
Figure 3.1 Functional model of a BCI System depicting the principle functional components (Mason and Birch 2003, Mason *et al* 2003). Note the Control Display is optional....97
Figure 3.2 General asynchronous system control sequence....98
Figure 3.3 Components of nLF-ASD transducers with new components shown in gray, where ENT = Energy Normalization Transform, KLT = Karhunen-Loève Transform, and 1-NN = 1-Nearest Neighbor....99
Figure 3.4 Distribution of false switch activations. A. Schematic diagram showing the metrics used to characterize false switch activations: L_i = length of the *i*th switch activation block (i.e. the number of activations that occur in consecutive sample times); and P_i = the *i*th inter-activation period (i.e. the distance from start of the *i*th activation block to the end of the *ith*+1 block). B. Histogram of switch activation block length (L_i values). C. Histogram of inter-activation period (P_i values). The arrows indicate the primary debounce values used in evaluation of the new ABS designs....101
Figure 3.5 ROC curves for Subject SC2 using system design nLF-ASD-A. A. Analysis of the 8 different values of debounce (T_{db}) used in this study with corresponding Areas under the ROC curve to indicate overall system performance. B. An expanded view of A. Only those values of false positives below 8% are shown for clarity....104
Figure 3.6 ROC curves for Subject SC2 with debounce set to 16 samples. Analysis of the five different processing methods used in this study. Only those values of false positives below 8% are shown for clarity....106
Figure 3.7 ROC curve of the true positive rate means for all 8 subjects (depicted with standard error of the mean error bars) with debounce set to 16 samples. Solid line = LF-ASD. Dashed line = nLF-ASD-A. The difference is significant ($p < 0.05$, 2-way ANOVA). Only those values of false positives below 8% are shown for clarity....107

Figure 3.8 ROC curve of the mean true positive rates for AB subjects vs. SCI subjects (depicted with standard error of the mean error bars) with debounce set to 16 samples. Solid line = able-bodied subjects. Dashed line = spinal cord-injured subjects. A. System design nLF-ASD-A. B. System design LF-ASD. 109
Figure 4.1 Structure of an IC trial, where TEIC: time of the expected IC, ERW: expected response window, IC: intended control, NC: no control, T_{Cue}: time of the cue appearance. 116
Figure 4.2 IC state training-data generation using TR_Gen1 method, IC: intended control, NC: no control, FV: feature vector, $f_{NC}(x)$: probability density function of NC features. 117
Figure 4.3 IC state training-data generation using TR_Gen2 method, IC: intended control, NC: no control, $f_{NC}(x)$: probability density function of NC features. 118
Figure 4.4 Components of the Low Frequency Asynchronous Switch Design (the LF-ASD) (from (Borisoff *et al* 2004)). ENT: energy normalization transform, KLT: Karhounen-Loéve transform, 1-NN: one nearest neighbour 120
Figure 4.5 Average ROC curves (for false positives less than 2%, as we are interested in false positives less than 2%) across eight subjects for the seven training-data generation methods (TR_Gen1 (dashed line with rectangles), TR_Gen2 (dashed line with plus signs), TR_Gen3 (solid line with circles), TR_TEIC (solid line with stars), TR_3TEIC (solid line with lozenges), TR_All (solid line with crosses), TR_Ran (dashed line with triangles)) 125
Figure 5.1 Components of the Low Frequency Asynchronous Switch Design (the LF-ASD) (from (Borisoff *et al* 2004)).ENT: energy normalization transform, KLT: Karhounen-Loéve transform, 1-NN: one nearest neighbor 134
Figure 5.2 Desired pattern of the bipolar EEG during movement. $E_i(n)$: amplitude difference between local maximum before the movement and local minimum after the movement, $E_j(n)$: amplitude difference between local maximum before the movement and local minimum before the movement 134
Figure 5.3 The ensemble averages of the normalized EEG in bipolar channel F2-FC2 for subject AB2. Time of the expected movement (TEM) is at t=1.8 s. 137
Figure 5.4 2-dimensional output of the feature generator for normalized bipolar EEG channel F2-FC2 for subject AB2 for the customized delay parameters (solid line: feature values of the first dimension, dashed line: feature values of the second dimension, and solid line with cross: bipolar EEG). Note that the vertical line at t=1.8 s corresponds to the time of the attempted movement (TEM). 141
Figure 5.5 2-dimensional output of the feature generator for normalized bipolar EEG channel F2-FC2 for subject AB2 for the original delay parameters (solid line: feature values of the first dimension, dashed line: feature values of the second dimension, and solid line with cross: bipolar EEG). Note that the vertical line at t=1.8 s corresponds to the time of the attempted movement (TEM) 142
Figure 5.6 ROC curve for subject AB1 (solid line with circles: ROC curve for the customized BI system, solid line: ROC curve for the original BI system). Note that, for clarity, only false positives below 4% are shown. 144
Figure 5.7 ROC curve for subject AB2 (solid line with circles: ROC curve for the customized BI system, solid line: ROC curve for the original BI system). Note that, for clarity, only false positives below 4% are shown. 145

Figure 5.8 ROC curve for subject AB3 (solid line with circles: ROC curve for the customized BI system, solid line: ROC curve for the original BI system). Note that, for clarity, only false positives below 4% are shown. 146
Figure 5.9 ROC curve for subject SCI1 (solid line with circles: ROC curve for the customized BI system, solid line: ROC curve for the original BI system). Note that, for clarity, only false positives below 4% are shown. 147
Figure 6.1 Functional model of a BI system depicting the principle functional components. More details can be found in (Mason and Birch 2003). 153
Figure 6.2 (a) Ensemble averages of the EEG of subject ID and (b) the corresponding feature vectors over time. The attempted movement is at t=1.875s. 155
Figure 6.3 Components of the LF-ASD-V5 transducer, where ENT = Energy Normalization Transform, KLT = Karhunen-Loève Transform, and 1-NN = 1-Nearest Neighbour.... 158
Figure 6.4 Path template generation procedure (also known as classifier training) 158
Figure 6.5 Structure of each 2-minute sub-session of EEG recording, where TEM=time of the expected (attempted) movement 160
Figure 6.6 *Path templates* for subject LB for the two cases 1) movement (IC) state (lines with circles) and 2) no movement (NC) state (lines with crosses). Time=0 corresponds to the time of the expected (attempted) movement (TEM). Note that the algorithm estimates three path templates per class. However, as can be seen in this figure, the three path templates of the NC state 162
Figure 6.7 *Path templates* for subject ID for the two cases 1) movement (IC) state (lines with circles) and 2) no movement (NC) state (lines with crosses). Time=0 corresponds to the time of the expected (attempted) movement (TEM). Note that the algorithm estimates three path templates per class. However, as can be seen in this figure, two of the three path templates of the IC state were very similar and are seen as one template. This is also can be seen for NC state path templates. 163
Figure 6.8 Truncated ROC curves for SCI subject BK for LF-ASD-V4 system (Dashed line) and our proposed LF-ASD-V5 design (Solid line with circles). 165
Figure 6.9 Truncated ROC curves for SCI subject RT for LF-ASD-V4 system (Dashed line) and our proposed LF-ASD-V5 design (Solid line with circles). 166
Figure 7.1 Components of the LF-ASD-V4 transducer (Borisoff et al., 2004), where ENT = Energy Normalization Transform, KLT = Karhunen-Loève Transform, 1-NN = 1-Nearest Neighbour, amp = amplifier, and FV_{V4} = extracted feature vector. 174
Figure 7.2 Desired pattern of the bipolar EEG during movement, where $e(n)$ = amplitude of the signal, $E_i(n)$ = amplitude difference between local maximum before the movement and local minimum after the movement, $E_j(n)$ = amplitude difference between local maximum before the movement and local minimum before the movement, $t=n$ is the time of the expected movement attempt, and α_i and α_j are the delay parameters. 174
Figure 7.3 Components of the LF-ASD-V5 transducer (Bashashati et al., 2006 a), where ENT = Energy Normalization Transform, KLT = Karhunen-Loève Transform, 1-NN = 1-Nearest Neighbour, amp = amplifier, FV_{V4} = extracted feature vector of LF-ASD-V4, and FV_{V5} = extracted feature vector of LF-ASD-V4 175
Figure 7.4 Structure of each 2-minute sub-session of EEG recording, where TEM = time of the expected (attempted) movement, NC = no-control, and IC = intentional control... 176
Figure 7.5 (a) Periods of intended control. Total length of experiment, in seconds, is **T**. (b) Timing of LF-ASD activations. (c) Timing of ocular artifacts detected using EOG electrodes, where IC = intentional control, $OA_{1,2,3}$ = ocular artifact periods. 178

Figure 7.6 True positive rate change (at false positive rate of 2%) of the LF-ASD-V4 and LF-ASD-V5 designs between Case 2 and Case 3 evaluation methods. 182
Figure 7.7 Truncated receiver operation characteristic (ROC) curves for subject ID (line with lozenges: LF-ASD-V5-Case2, line with circles: LF-ASD-V4-Case2, line with stars: LF-ASD-V5-Case3, line with triangles: LF-ASD-V4-Case3). As we are interested in lower FP rate levels, only those values of FPs below 3% are shown in the ROC curves. The numbers in the parentheses show the false positive and true positive percentages, respectively, for identical classification parameters for LF-ASD-V5-Case2 and LF-ASD-V5-Case3. 183
Figure 7.8 Truncated receiver operation characteristic (ROC) curves for subject CB (line with lozenges: LF-ASD-V5-Case2, line with circles: LF-ASD-V4-Case2, line with stars: LF-ASD-V5-Case3, line with triangles: LF-ASD-V4-Case3). As we are interested in lower FP rate levels, only those values of FPs below 3% are shown in the ROC curves. The numbers in the parentheses show the false positive and true positive percentages, respectively, for identical classification parameters for LF-ASD-V5-Case2 and LF-ASD-V5-Case3. 183
Figure 7.9 Truncated receiver operation characteristic (ROC) curves for subject CS (line with lozenges: LF-ASD-V5-Case2, line with circles: LF-ASD-V4-Case2, line with stars: LF-ASD-V5-Case3, line with triangles: LF-ASD-V4-Case3). As we are interested in lower FP rate levels, only those values of FPs below 3% are shown in the ROC curves. The numbers in the parentheses show the false positive and true positive percentages, respectively, for identical classification parameters for LF-ASD-V5-Case2 and LF-ASD-V5-Case3. 184
Figure 7.10 Truncated receiver operation characteristic (ROC) curves for subject KT (line with lozenges: LF-ASD-V5-Case2, line with circles: LF-ASD-V4-Case2, line with stars: LF-ASD-V5-Case3, line with triangles: LF-ASD-V4-Case3). As we are interested in lower FP rate levels, only those values of FPs below 3% are shown in the ROC curves. The numbers in the parentheses show the false positive and true positive percentages, respectively, for identical classification parameters for LF-ASD-V5-Case2 and LF-ASD-V5-Case3. 184
Figure 7.11 Truncated receiver operation characteristic (ROC) curves for subject AJ (line with lozenges: LF-ASD-V5-Case2, line with circles: LF-ASD-V4-Case2, line with stars: LF-ASD-V5-Case3, line with triangles: LF-ASD-V4-Case3). As we are interested in lower FP rate levels, only those values of FPs below 3% are shown in the ROC curves. The numbers in the parentheses show the false positive and true positive percentages, respectively, for identical classification parameters for LF-ASD-V5-Case2 and LF-ASD-V5-Case3. 185
Figure 7.12 Truncated receiver operation characteristic (ROC) curves for subject LB (line with lozenges: LF-ASD-V5-Case2, line with circles: LF-ASD-V4-Case2, line with stars: LF-ASD-V5-Case3, line with triangles: LF-ASD-V4-Case3). As we are interested in lower FP rate levels, only those values of FPs below 3% are shown in the ROC curves. The numbers in the parentheses show the false positive and true positive percentages, respectively, for identical classification parameters for LF-ASD-V5-Case2 and LF-ASD-V5-Case3. 185
Figure 7.13 Truncated receiver operation characteristic (ROC) curves for subject BK (line with lozenges: LF-ASD-V5-Case2, line with circles: LF-ASD-V4-Case2, line with stars: LF-ASD-V5-Case3, line with triangles: LF-ASD-V4-Case3). As we are interested in

lower FP rate levels, only those values of FPs below 3% are shown in the ROC curves. The numbers in the parentheses show the false positive and true positive percentages, respectively, for identical classification parameters for LF-ASD-V5-Case2 and LF-ASD-V5-Case3. 186
Figure 7.14 Truncated receiver operation characteristic (ROC) curves for subject RT ((line with lozenges: LF-ASD-V5-Case2, line with circles: LF-ASD-V4-Case2, line with stars: LF-ASD-V5-Case3, line with triangles: LF-ASD-V4-Case3). As we are interested in lower FP rate levels, only those values of FPs below 3% are shown in the ROC curves. The numbers in the parentheses show the false positive and true positive percentages, respectively, for identical classification parameters for LF-ASD-V5-Case2 and LF-ASD-V5-Case3. 186
Figure 8.1 Samples of outputs of 2-state and 3-state self-paced BCIs, where NC = No Control state, IC = Intended Control state 193
Figure 8.2 Screen contents for each of the right hand (a) and left hand (b) extension movement trials, t=0 is the time of movement execution 196
Figure 8.3 Structure of the 3-state self-paced brain computer interface design 197
Figure 8.4 Structure of the two designs of DET1, where KLT = Karhunen-Loève Transform, and 1-NN = 1-Nearest Neighbour, PSD = power spectral density, and LDA: linear discriminant analysis. 197
Figure 8.5 Description of delay terms (α_i, α_j), where e(n) is the amplitude of the bipolar signal 198
Figure 8.6 Structure of DET2-PSD-LDA, where PSD = power spectral density, and LDA = linear discriminant analysis. 200
Figure 9.1 Sample of output of a 3-state self-paced BCIs, where NC = No Control state, IC = Intended Control state 212
Figure 9.2 Overall structure of the 3-state self-paced BCI design 214
Figure 9.3 Structure of the two designs of DET1, where KLT = Karhunen-Loève Transform, and 1-NN = 1-Nearest Neighbour, PSD = power spectral density, and LDA: linear discriminant analysis. Note, shaded designs are new designs of DET1 implemented in this study. 217
Figure 9.4 Structure of DET2, where LDA = Linear Discriminant Analysis, PSD = Power Spectral Density 218
Figure 10.1 Example of a BCI user interface 239
Fig. C.1. Desired pattern of the bipolar EEG during movement 261

Acknowledgements

I would like to express my deepest gratitude to my supervisors, Drs. Rabab Ward and Gary Birch, for providing the opportunity to work under their supervision. Their constant guidance, patience and encouragements have been of great value to me.

My sincere thanks to my committee member, Dr. Peter Lawrence, for his constructive criticism and advice during this thesis.

I wish to thank Drs. Steve Mason and Jaimie Borisoff for their help, useful comments and criticisms during this work. I also wish to thank my friend and colleague Borna Noureddin and other lab-mates in the Brain Interface Lab at the GF Strong Hospital for their useful discussions throughout this work.

Finally, my loving thanks to my wife, my Mehrnoush, for her support during this work and for being with me in the good and bad days. Without her, it would be impossible to get to this point.

I dedicate this thesis to my parents who believed in me and the countless sacrifices they made to make my dreams come true.

Co-Authorship Statement

1- Ali Bashashati, Mehrdad Fatourechi, Rabab K. Ward, and Gary E. Birch, "A Survey of Signal Processing Algorithms in Brain-Computer Interfaces Based on Electrical Brain Signals," *Journal of Neural engineering*, vol. 4, no. 2, pp. R35-55, Jun 2007.

AB reviewed all papers, interpreted the results, wrote manuscript and acted as the corresponding author.

MF helped in manuscript writing, results interpretation and manuscript evaluation.

RW and GB supervised development of work, helped in manuscript writing and manuscript evaluation.

2- J. Borisoff, S. Mason, A. Bashashati, and G. Birch, "Brain Computer Interface (BCI) Design for Asynchronous Control Applications: Improvements to the LF-ASD Asynchronous Brain Switch," *IEEE Trans. Biomed. Eng.*, vol. 51, no. 6, pp. 985-92, June 2004.

AB developed codebook generation mechanisms and dimensionality reduction algorithms, helped in writing and evaluation of the manuscript.

JB developed other signal processing components, analyzed the data, interpreted the results, wrote manuscript and acted as corresponding author.

SM contributed to data interpretation and manuscript evaluation.

GB supervised development of work, helped in results interpretation and manuscript evaluation.

3- Ali Bashashati, S.G. Mason, Jaimie Borisoff, Rabab K. Ward, and G. Birch, "A Comparative Study on Generating Training-Data for Self-Paced Brain Interfaces," *IEEE Trans. Neural Systems and Rehabilitation*, vol. 15, no. 1, Mar 2007.

AB developed the methods, analyzed the data, interpreted the results, wrote manuscript and acted as the corresponding author.

SM and JB contributed to results interpretation and manuscript evaluation.

RW and GB supervised development of work, helped in data interpretation and manuscript evaluation.

4- A. Bashashati, M. Fatourechi, R. Ward, and G. Birch, "User Customization of the Feature Generator of an asynchronous Brain Interface," *Annals of Biomedical Engineering*, vol. 34, no. 6, pp. 1051-60, June 2006.

AB developed the methods, analyzed the data, interpreted the results, wrote manuscript and acted as the corresponding author.

MF contributed to study design, helped in shaping the manuscript, results interpretation and manuscript evaluation.

RW and GB supervised development of work, helped in manuscript writing and evaluation.

5- A. Bashashati, S.G. Mason, Rabab K. Ward, and G. Birch, "An Improved Asynchronous Brain Interface: Making Use of the Temporal History of the LF-ASD Feature Vectors," *Journal of Neural Engineering*, vol. 3, no. 2, pp. 87-94, June 2006 *(Invited paper)*.

AB developed the methods, analyzed the data, interpreted the results, wrote manuscript and acted as the corresponding author.

SM contributed to the development of the initial concept, results interpretation and manuscript evaluation.

RW and GB supervised development of work, helped in results interpretation and manuscript evaluation.

6- Ali Bashashati, Borna Noureddin, Rabab Ward, Peter Lawrence, and Gary Birch, "Effects of Eye Blinks on the Performance of a Self-paced Brain Interface," *Clinical Neurophysiology,* vol. 118, no. 7, pp. 1639-47, July 2007.

AB developed the methods, analyzed the results, interpreted the results, wrote manuscript and acted as the corresponding author.

BN contributed to development of evaluation methods, results interpretation and manuscript evaluation.

PL, RW and GB supervised development of work, helped in manuscript writing, results interpretation and manuscript evaluation.

7- Ali Bashashati, Rabab Ward, and Gary Birch, "Towards Development of a 3-State Self-Paced Brain Interface Based on Hand Extension Movements," *J Computational Intelligence & Neuroscience,* In press (Accepted in Aug 2007).

AB developed the 3-state BCI system, collected and analyzed the EEG data, interpreted the results, wrote manuscript and acts as the corresponding author.

RW and GB supervised development of work, helped in manuscript writing, results interpretation and manuscript evaluation.

8- Ali Bashashati, Rabab Ward, and Gary Birch, "Improving the Performance of a 3-State Self-Paced Brain Computer Interface," to be submitted.

AB developed the system, collected and analyzed the EEG data, interpreted the results, wrote manuscript and will act as the corresponding author.

RW and GB supervised development of work, helped in results interpretation and manuscript evaluation.

List of Abbreviations

Abbreviation	Description
1-NN	One nearest neibour
AAR	Adaptive auto-regressive
AB	Able bodied
AEP	Auditory evoked potential
AGR	Adaptive Gaussian representation
ALN	Adaptive logic network
ANC	Activity of neural cells
ANN	Artificial neural networks
AR	Auto-regressive
ARTMAP	Adaptive resonance theory MAP
ARX	Autoregressive with exogenous input
BCI	Brain computer interface
BPF	Band-pass filter
CAR	Common average referencing
CBR	Changes in brain rhythms
CCTM	Cross-Correlation based template matching
CER	Coarse-grained entropy rate
CHMM	Coupled hidden markov model
CSP	Common Spatial Patterns
CSSD	Common spatial subspace decomposition
CSSP	Common spatio-spectral patterns
CTFR	Correlative time-frequency representation
CTFSR	Correlative time-frequency-space representation
DFT	Discrete Fourier transform
DSLVQ	Distinctive sensitive learning vector quantization
EEG	Electro-encephalogram
EOG	Electro-oculogram
ENT	Energy normalization transform
ERD	Event related desynchronization
ERN	Event related negativity
ERS	Event related synchronization
ERW	Expected response window
FLD	Fisher's linear discriminat
FFT	Fast Fourier transform
FP	False positive
Freq-Norm	Frequency normalization
GA	Genetic algorithm
GAM	Generalized additive models
GLA	Generalized linear models
GPER	Gaussian process entropy rates
HMM	Hidden markov model
IC	Intentional control
ICA	Independent component analysis
IFFT	Inverse fast Fourier transform
KLT	Karhounen-Loeve transform
k-NN	k-nearest neighbour
LDA	Linear discriminant analysis
LDS	Linear dynamical system
LGM	Linear Gaussian models implemented by Kalman filter
LMS	Least mean square

Abbreviation	Description
LPC	Linear predictive coding
LPF	Low pass filter
LRP	Lateralized readiness potential
LVQ	Learning vector quantization
MD	Mahalanobis distance
MLP	Multi-Layer perceptron neural networks
MN	Multiple neuro-mechanisms
MNF	Maximum noise fraction
MRA	Movement related activity
MRP	Movement related potential
NC	No control
NMF	Non-negative matrix factorization
NN	Neural networks
OLS1	Orthogonal least square
OPM	Outlier processing method
PCA	Principal Component Analysis (a.k.a. Karhounen Loeve Transform)
PLV	Phase locking values
PPM	Piecewise Prony method
PSD	Power spectral density
RBF	Radial basis function
RFE	Recursive feature/channel elimination
RNN	Recurrent neural network
ROC	Receiver operating characteristic
ROCC	Receiver operating characteristic curve
SA-UK	Successive averaging and/or considering choice of unknown
SCI	Spinal cord injury
SCP	Slow cortical potentials
SE	spectral entropy
SFFS	Sequential forward feature selection
SL	Surface Laplacian
SOFNN	Self organizing feature neural network
SOM	Self organizing map
SSEP	Somatosensory evoked potential
SSP	Signal space projection
SSVEP	Steady state visual evoked potential
STD	Standard Deviation
SVD	Singular value decomposition
SVM	Support vector machine
SVR	Support vector machine regression
SWDA	Stepwise discriminant analysis
TBNN	Tree-based neural network
TEIC	Time of expected intentional control
TEM	Time of expected attempted movement
TFR	Time-frequency representation
TP	True positive
VEFD	Variable epoch frequency decomposition
VEP	Visual evoked potential
WE	Wavelet entropy
WK	Wiener-Khinchine
ZDA	Z-scale based discriminant analysis

Chapter 1 Introduction

Many different disorders and injuries can disrupt the neuromuscular channels through which the brain communicates and controls the body. These disorders can impair the neural pathways that control muscles or impair the muscles themselves. Those who are severely affected may lose all voluntary muscle control, including eye movement and respiration, and may be completely 'locked in' to their brain.

In the absence of methods for repairing the damage done by these disorders, various assistive devices have been developed to liberate these individuals, but the effectiveness of devices in assisting severe disabilities is often limited. An option for restoring the function to those with motor impairment is to provide the brain with a new, non-muscular communication and control channel; a direct brain computer interface (BCI[1]) for conveying messages and commands to the external world. The ultimate purpose of direct brain computer interface (BCI) research is to allow an individual with severe motor disabilities to have effective control over devices such as computers, speech synthesizers, assistive appliances, and neural prostheses. Such an interface would thus increase an individual's independence, leading to an improved quality of life and reduced social costs.

Over the past two decades, a variety of studies have evaluated the possibility that brain signals recorded from the scalp or from within the brain could provide new augmentative technology that does not require muscle control. Using various signal processing algorithms, brain computer interface (BCI) systems detect the presence of specific patterns in a person's ongoing brain activity that relates to the person's intention to initiate control. The BCI system translates these patterns into meaningful control commands. These control signals are then used as input to intelligent devices to assist these individuals. Fig. 1.1 shows a simple block diagram of a BCI system, in which the BCI transducer translates the person's brain activity into useful control signals that will drive the assistive device.

Studies show that non-muscular communication and control are possible (for example see (Mason *et al* 2007, Vaughan *et al* 2003, Wolpaw *et al* 2002)) and might serve useful purposes for those who cannot use conventional technologies. To people who are 'locked-in'

[1] Brain computer interfaces may be referred to as brain machine interfaces (BMI), brain interfaces (BI), or direct brain interfaces (DBI) in some studies.

(e.g. by end-stage amyotrophic lateral sclerosis (ALS), brainstem stroke, or severe polyneuropathy) or lack any useful muscle control (e.g. due to severe cerebral palsy), a BCI system could give the ability to answer simple questions quickly, control the environment, perform slow word-processing, or even operate a neuro-prosthesis. At the same time, the performance of this new technology, measured in communication speed and accuracy is modest. Communication speed refers to the speed at which a person can send commands to the system or answer yes/no questions. Thus, they have limited practical value and are only for those with most severe disabilities. As a result, the ultimate value of this new technology will depend largely on the degree to which its accuracy and communication rate can be increased and the extent to which BCI systems can be applied to the communication and control needs of many people with motor disabilities of different origins and varying severity.

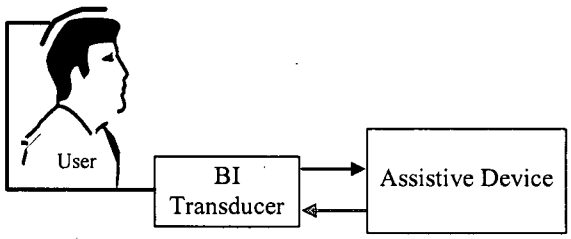

Figure 1.1. Simple block diagram of a BCI system.

1.1. Functional Model of a BCI system

Fig. 1.2 shows detailed functional model of a BCI system (Mason and Birch 2003, Mason et al 2003, Mason et al 2007). The figure depicts a generic BCI system in which a person controls a device in an operating environment (e.g., a powered wheelchair in a house) through a series of functional components. In this context, the user's brain activity is used to generate the control signals that operate the BCI system. The user monitors the state of the device to determine the result of his/her control efforts. In some systems, the user may also be presented with a control display, which displays the control signals generated by the BCI system from his/her brain activity.

The electrodes placed on the head of the user record the brain signal from the scalp (or the surface of the brain, or the neural activity within the brain) and convert this brain activity to electrical signals. The 'artifact processor' block shown in Fig. 1.2, removes the artefacts from

the electrical signal after it has been amplified. Note that many transducer designs do not include artifact processing. The 'feature generator' block transforms the resultant signals into feature values that correspond to the underlying neurological mechanism (neuromechanism2) employed by the user for control. For example, if the user is to control the power of his/her Mu (8-12Hz) and Beta (18-25Hz) rhythms, the feature generator would continually generate features relating to the power-spectral estimates of the user's Mu and Beta rhythms. The feature generator generally can be a concatenation of three components, the 'signal-enhancement', the 'feature extraction', and the 'feature selection' components, as shown in Fig. 1.2.

In some BCI designs, pre-processing (signal enhancement) is performed on the brain signal prior to the extraction of features so as to increase the signal-to-noise ratio of the signal. A feature selection component is sometimes added to the BCI system after the feature extraction stage. The aim of feature selection is to reduce the number of features and/or channels used so that very high dimensional and noisy data are excluded. Ideally, the features that are meaningful or useful in the classification stage are identified and chosen, while others (including outliers and artefacts) are omitted.

The 'feature translator' translates the features into logical (device-independent) control signals, such as a two-state discrete output. The translation algorithm uses linear classification methods (e.g., classical statistical analyses) or nonlinear ones (e.g., neural networks). According to the definition in (Mason and Birch 2003), the resultant logical output states are independent of any semantic knowledge about the device or how it is controlled. As shown in Fig. 1.2, a feature translator may consist of two components: 'feature classification' and 'post-processing'. The main aim of the feature classification component is to classify the features into logical control signals. Post-processing methods such as a moving average block may be used after feature classification to reduce the number of error activations of the system.

The control interface translates the logical control signals from the feature translator into semantic control signals that are appropriate for the particular type of device used. Finally, the device controller translates the semantic control signals into physical control signals that

[2] According to the Merriam-Webster Medical dictionary, a bodily regulatory mechanism based in the structure and functioning of the nervous system is called a *neuromechanism*.

are used by the device. The device controller also controls the overall behavior of the device. For more detail refer to (Mason and Birch 2003). Table 1.1 provides a simplified description of the BCI transducer components.

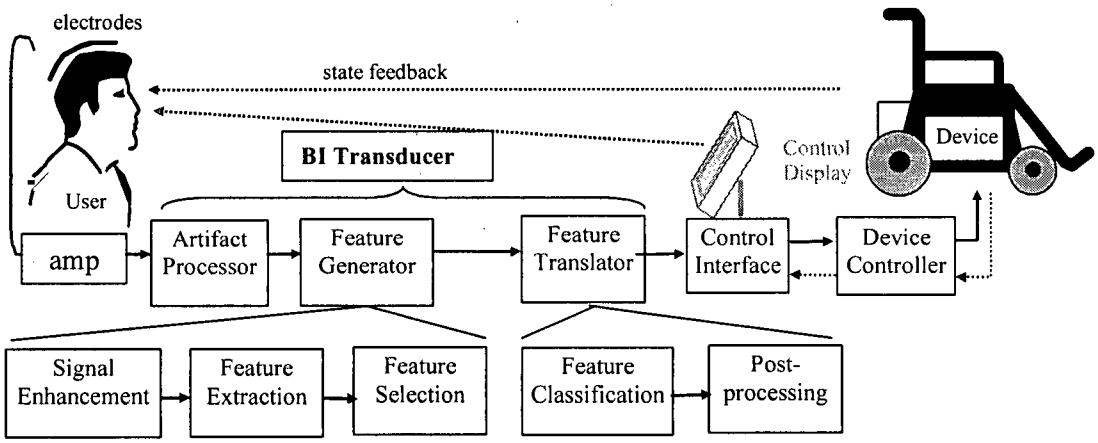

Figure 1.2 Functional model of a BCI system depicting the principle functional components, where amp = amplifier. Note the 'Control Display' is optional.

TABLE 1.1 DESCRIPTION OF THE BCI TRANSDUCER COMPONENTS

Item	Terms		Definition
BCI	Artifact Processor		Removes artifact from the input signal
Transducer	Feature Generator	Signal Enhancement	(1) Enhance signal-to-noise ratio of brain signals (2) The output of this block is a signal with the same nature as the input (i.e. the output like the input is in the temporal domain).
		Feature Extraction	Generates the feature vectors
		Feature Selection	Selects a subset of features
	Feature Translator	Feature Classification	Classifies the features into logical control signals
		Post-Processing	Increases the performance after feature classification e.g., by blocking the activations with low certainty

1.2. Background [3]

Present-day BCIs use a variety of electrophysiological mechanisms such as visual evoked potentials (VEP), slow cortical potentials (SCP), P300 evoked potentials, Mu and Beta rhythms associated with movement execution or imagination, movement related potentials (MRP), cortical neuronal action potentials, and BCIs that are based on the response to mental tasks. In BCI systems, electrophysiological sources refer to the neurological mechanisms or processes employed by a BCI user to generate control signals.

In the 1970s, Vidal developed a BCI system based on VEP recorded from the scalp over the visual cortex to determine the direction of gaze, and thus to determine the direction in which the user wished to move a cursor (Vidal 1977). Sutter (Sutter 1992) described a similar BCI system called the brain response interface (BRI). This system uses the VEPs produced by brief visual stimuli and recorded from the scalp over the visual cortex. The user faces a video screen displaying 64 symbols (e.g. letters) in an 8*8 grid and looks at the symbol he or she wants to select. Subgroups of these 64 symbols undergo an equiluminant red/green alterations 40-70 times/s. each symbol is included in several subgroups, and the entire set of subgroups is presented several times. Each subgroup's VEP amplitude about 100 ms after the stimulus is computed and compared to a VEP template already established for the user. From these comparisons the system determines with high accuracy the symbol that the user is looking at (Sutter 1984, Sutter 1992). Middendorf et al. reported another method for using VEPs to determine gaze direction. Several virtual buttons appear on a screen and flash at different rates. The user looks at a button and the system determines the frequency of the response over the visual cortex. When this frequency matches that of a button, the system concludes that the user wants to select it (Middendorf *et al* 2000).

Among the lowest frequency features of the scalp-recorded EEG are the slow voltage changes generated in the cortex. These potential shifts occur over 0.5–10.0 seconds and are called slow cortical potentials (SCP). Negative SCPs are typically associated with movement and other functions involving cortical activation, while positive SCPs are usually associated with reduced cortical activation (Rockstroh *et al* 1984). Birbaumer and his colleagues have

[3] A comprehensive survey of brain computer interface designs has been included in Chapter 2 of this dissertation, therefore, this part only provides a high-level literature review of the field.

shown that people can learn to control their SCPs (using SCP-based biofeedback) and thereby control the movement of an object on a computer screen (Birbaumer *et al* 1999, Birbaumer *et al* 2000). This is done with the help of visual, auditory or tactile feedbacks (Birbaumer *et al* 2000). This demonstration is the basis for a BCI referred to as 'thought translation device' (TTD). They used a language support program (Perelmouter and Birbaumer 2000) that enables the user to choose a letter or a letter combination by a series of two-choice selections. This system has been tested extensively on people with late-stage ALS and has proved to be able to supply basic communication capability (Birbaumer *et al* 2000). While the idea of the language support program has proved useful, an additional predictive algorithm that uses the first two letters of a word to select the most likely word from a lexicon that encompasses the user's vocabulary can markedly increase the communication speed.

Infrequent or particularly significant auditory, visual, or somatosensory stimuli, when interspersed with frequent or routine stimuli, typically evoke in the EEG over parietal cortex a positive peak at about 300 ms (after the presentation of the stimuli) named the P300 evoked potential (Donchin and Smith 1970). Donchin and his colleagues have used this 'P300', or 'oddball' response to build a brain computer interface (Donchin *et al* 2000, Farwell and Donchin 1988). In this system, the user faces a 6*6 matrix of letters, numbers, and/or other symbols or commands. Every 125 ms, a single row or column flashes; and, in a complete trial of 12 flashes, each row or column flashes twice. The user makes a selection by counting how many times the row or column containing the desired choice flashes. P300 is prominent only in the responses elicited by the desired choice, and the BCI uses this effect to determine the user's intent. In people with visual impairments, auditory or tactile stimuli might be used (Glover *et al* 1986, Roder *et al* 1996). In two recent studies Sellers et al. and Piccione et al. have shown that a P300-based brain computer interface could function as an alternative method of communication for paralyzed patients including spinal cord injured and ALS patients (Piccione *et al* 2006, Sellers and Donchin 2006). In related work, Bayliss and Ballard (Bayliss and Ballard 2000) recorded P300s in a virtual environment. Offline analyses suggested that single-trial P300 amplitudes could be used for environmental control.

Unlike a SCP-based brain computer interface, a P300-based BCI has an apparent advantage in that it requires no initial user training: P300 is a typical, or naive, response to a desired

choice. A P300 used in a brain computer interface is also likely to change over time. Studies to date have only reported short-term evaluations of the P300-based BCI systems. Thus, appropriate adaptation by the translation algorithm is likely to be important for this BCI in long-term application, as it is for other types of BCI systems.

In awake people, primary sensory or motor cortical areas often display 8–12 Hz (Mu rhythm) EEG activity when they are not engaged in processing sensory input or producing motor output (Niedermeyer and Lopes da Silva 1998). Analyses also show that the Mu-rhythm activity comprises a variety of different 8–12 Hz rhythms, distinguished from each other by location, frequency, and/or relationship to concurrent sensory input or motor output. These Mu rhythms are usually associated with 18–25 Hz Beta rhythms. While some Beta rhythms are harmonics of the Mu rhythms, some are separable from them by topography and/or timing, and thus are independent EEG features (McFarland *et al* 2000, Pfurtscheller and Berghold 1989, Pfurtscheller and Lopes da Silva 1999). Several factors suggest that the Mu and/or Beta rhythms could be good signal features for EEG-based communication. They are associated with those cortical areas most directly connected to the brain's normal motor output channels. Movement execution, preparation or even imagination (McFarland *et al* 2000, Pfurtscheller *et al* 1997) is typically accompanied by a decrease in the Mu and Beta rhythms, particularly contralateral to the movement. This decrease has been labeled 'event-related desynchronization' or ERD (Pfurtscheller and Lopes da Silva 1999). Its opposite, rhythm increase, or 'event-related synchronization' (ERS) occurs after movement and with relaxation (Pfurtscheller and Lopes da Silva 1999). Since the mid-1980s, several Mu/Beta rhythm based brain computer interfaces have been developed.

With the BCI system in (McFarland *et al* 1997, Wolpaw *et al* 1991, Wolpaw *et al* 2000), people with or without motor disabilities learn to control their Mu or Beta rhythm amplitude and use that control to move a cursor in one or two dimensions to targets on a computer screen. They participate in 2–3 40-minute sessions per week, and most (i.e. about 80%) acquire significant control within 2–3 weeks. With this control, users can move the cursor to answer spoken yes/no questions with accuracies of about 95% (Miner *et al* 1998, Wolpaw *et al* 1998). Research with this system has focused on defining the topographical, spectral, and temporal features of the Mu and Beta rhythm control, optimizing the mutually adaptive interactions between the user and the BCI system, and incorporating other EEG features into

this BCI (McFarland *et al* 1997, Ramoser *et al* 1997, Schalk *et al* 2000). Recent studies of this research group on ALS patients show usefulness of this brain computer interface for these patients (Kubler *et al* 2005).

The Graz BCI group has also developed a brain computer interface system based on the ERD and ERS of the Mu and Beta rhythms in the EEG over the sensorimotor cortex. Research to date has focused on distinguishing between the EEG associated with imagination of different simple motor actions, such as right or left hand or foot movement, and thereby enabling the user to control a cursor or an orthotic device that opens and closes a paralyzed hand (Neuper *et al* 1999, Pfurtscheller *et al* 1993, Pfurtscheller *et al* 2000). Over a period of 6–7 sessions and with two-choice trials (i.e. left hand vs. right hand imagery), users can reach accuracies over 90%. About 90% of people can use this system successfully. Current studies are seeking modifications that improve classification. Recently, this group has also started developing the so called self-paced brain computer interfaces (Scherer *et al* 2004, Townsend *et al* 2004). Unlike synchronized brain computer interfaces, self-paced brain computer interfaces enable users to control the system at any time they wish. Self-paced and synchronized brain computer interfaces will be discussed later in this section.

Penny et al. describe a BCI that also uses the EEG over sensorimotor cortex to control cursor movement (Penny *et al* 2000). They concentrate on detecting the EEG associated with imagery of actions like right or left hand movements, and/or tasks like simple calculations. Their translation algorithm uses Autoregressive parameters and a logistic regression model trained with a Bayesian evidence framework. They report user success in controlling one-dimensional cursor movement (Roberts and Penny 2003). Babiloni et al. (Babiloni *et al* 2000) are developing a Laplacian EEG analysis and a signal-space projection algorithm to detect imagined movements in the EEG over the sensorimotor cortex. Anderson et al. have also designed a multi-class brain computer interface that detects mental tasks such as solving a multiplication problem, imagining a 3D object, and mental counting using Autoregressive parameters of the EEG (Anderson *et al* 1998, Garrett *et al* 2003).

Levine et al. (Levine *et al* 2000) recorded electrocorticogram (EcoG) activity from 17 patients temporarily implanted with 16–126 subdural electrodes prior to epilepsy surgery. They found topographically focused potentials associated with specific movements and

vocalizations. Results of their analyses show that these potentials can provide the basis for a BCI with multiple control channels (Graimann *et al* 2004, Levine *et al* 2000). Two other studies have also reported the use of EcoG activity in a brain computer interface system for epileptic patients (Lal *et al* 2005, Leuthardt *et al* 2004). With these patients, it was possible in just one session to differentiate without any training imagination of hand-, tongue-, and mouth movement.

Several laboratories have used multielectrode arrays to record signals from single neurons in the motor cortex of monkeys or rats during learned movements (Chapin *et al* 1999, Donoghue 2002, Isaacs *et al* 2000, Liu *et al* 1999, Nicolelis 2001, Nicolelis 2003). These studies are aimed at reconstructing a movement from multielectrode recorded spike trains or synaptic field potentials. After extensive training and implementation of learning algorithms (for an exception, where animals learned rapidly, see (Serruya *et al* 2002)), monkeys move cursors on screens toward targets or move an artificial hand in four directions, clearly demonstrating the possibility of translating cellular activity into simple movements online. After extensive training, even complex movement patterns can be reconstructed from an astonishingly small number of cells located in the motor or parietal areas (Nicolelis 2001). Plasticity of cortical circuits allows learned control of movements directly from the cellular activity even outside the primary and secondary homuncular representations of the motor cortex (Schwartz *et al* 2001, Taylor *et al* 2002). The first multielectrode array was implanted in a quadriplegic patient's motor hand area in 2004 by Donoghue's group (Hochberg *et al* 2006). Within a few training sessions, the patient learnt to use his neuronal activity to move a computer cursor in several directions. While training has been limited due to recurring illness and medication effects, the results have been encouraging and suggest that more rapid and accurate control are possible in the future.

1.2.1. Self-Paced and Synchronized BCI Systems

As previously mentioned, many brain computer interface transducer designs have been proposed in the literature (for a review of the field, see (Mason *et al* 2007, Nicolelis 2003, Vaughan *et al* 2003, Wolpaw *et al* 2002). Few of them, however, have been designed specifically for self-paced control. The concept of self-paced control of brain computer interface systems was introduced in (Birch 1988, Mason and Birch 2000) and denoted as

"asynchronous control". In a self-paced brain computer interface the users affect the BCI transducer output whenever they want by intentionally changing their brain states (see Fig. 1.3(a)). Between periods of intentional control (IC), users are said to be in a no-control (NC) state - they may be idle, daydreaming, thinking about a problem or lunch, or performing any other action other than trying to control the BCI transducer. These BCI transducers are thus designed to respond only when there is an intentional user control. The appropriate BCI response to no-control (NC) would be a neutral or inactive output. We refer to this ability as **NC support**. NC support is necessary for most types of machine or device interactions where frequent intentional controls (IC) are spaced by periods of inaction. NC support must handle the diversity of activity and thoughts that make up the NC state and must operate effectively during such periods that range from a few seconds to a few hours depending on the type of application. *It is unlikely that one can model all possible NC states related to a target application.* In general, this problem can be constrained by including some mechanisms to turn the interface off when it is not in use and turn it on when a control action is desired. While this mechanism is a useful mode for avoiding false responses during long periods of NC states, it is not practical during periods of intended interaction which contain frequent short pauses containing other thoughts, composition, or response monitoring. *Therefore, having a mechanism that turns off the system is not sufficient for NC support. The BCI system should still be able to handle NC state while the system in on.*

In comparison to the self-paced BCIs, in most brain computer interface system evaluations reported in the literature, the allowable time periods for intentional user control are *restricted to periods defined by a computer* (as shown in Fig. 1.3(b)). In other words, these systems operate only during specific periods determined by the system (not the user). Thus, these systems have not been tested for general intermittent or self-paced operating paradigms. Since the user's input is synchronized with the external computer, this type of control has been termed "synchronized control" (Mason and Birch 2000). In these experimental systems, the BCI technology is tested only during those periods with intentional user control and *the response of the BCI transducer during the NC state is not tested.*

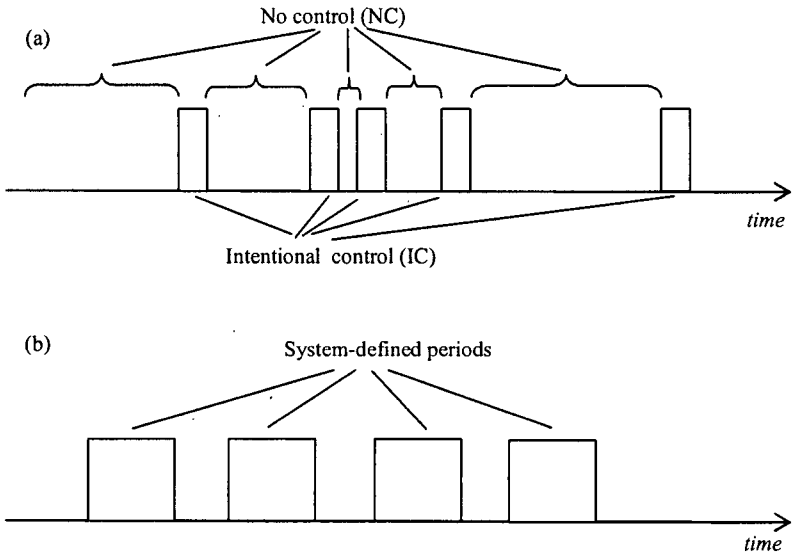

Figure 1.3 (a) Self-paced brain computer interface operating paradigm, (b) synchronized brain computer interface paradigm

The performance of a self-paced brain computer interface system that differentiates between NC and IC classes is evaluated by 1) the percentage of correct activations during IC states (true positives, TPs) and 2) the percentage of false output activations during NC states (false positives, FPs). A state is identified as true positive if the brain computer interface system is activated at least once in a time window around the actual intentional control state (Birch *et al* 1993, Graimann *et al* 2004, Scherer *et al* 2004, Townsend *et al* 2004, Yom-Tov and Inbar 2003). Any activation outside this window is considered a false positive. Ideally, one needs to design a system that has 100% true positive rate and 0% false positive rate.

Although self-paced control is the most natural mode of interaction, it has received less attention. Only a few BCI systems (Birch *et al* 1993, Graimann *et al* 2004, Mason and Birch 2000, Millan et al 2004, Scherer *et al* 2004, Townsend *et al* 2004, Yom-Tov and Inbar 2003) have been specifically designed and tested for self-paced control. As recognized by many researchers in brain computer interface field (e.g. Wolpaw *et al* 2002), self-paced BCI systems address a problem that is important for practical applications, i.e. detection of user commands without the timing cues provided by structured trials.

The self-paced BCI systems introduced in (Birch *et al* 1993, Graimann *et al* 2004, Mason and Birch 2000, Townsend *et al* 2004, Yom-Tov and Inbar 2003) attempt to detect a specific

intentional control state, e.g. imagined right hand movement, from the ongoing brain signal. As the output of these BCI systems can have two possible states, i.e. NC and IC states, these self-paced BCI systems are considered a 2-state self-paced BCIs.

Among all the self-paced BCI systems introduced in the literature, only two have attempted to increase the number of output states (Millan et al 2004, Scherer *et al* 2004).

The 3-state self-paced BCI implemented in (Scherer *et al* 2004) attempts to differentiate between right hand, left hand and foot movements in order to operate a virtual keyboard. Although this system is operated in a self-paced paradigm, its response during NC periods has not yet been studied and reported. *Therefore, the ability of this system to support NC state is not known.* In the experimental paradigm for which this system is tested, the user should *continuously engage* in operating the virtual keyboard without having the option to stay in a no-control state.

In the study of (Millan et al 2004) the subjects were asked to perform one of the following three actions: (1) imagine right hand movement, (2) imagine left hand movement, and (3) relax. A 3-state self-paced BCI was designed to navigate a mobile robot in an 80cm*60cm house-like environment by differentiating amongst these three states. The system generates 'unknown state output' when there is not enough confidence in choosing one of the three above mentioned mental tasks. The classifier of this system was *not explicitly* trained to recognize idle (NC) state (Millan et al 2004). According to the authors, it could process them adequately by responding 'unknown'. It was also reported that the task of steering the robot between rooms was so engaging that the two tested subjects preferred to emit continuously mental commands *rather than to go through NC (idle) state.* Therefore, the response of this system on NC (idle) state was evaluated on a dataset with limited amount of NC (idle) state. Moreover, having the choice of 'unknown state output' may represent some neutral output but it is not clear whether the unknown state output was caused by the actual idle (NC) state or by lack of confidence in detecting one of the three commands. Additionally, there is no evidence that the NC state will fall into the unknown state in these designs.

Although, the two 3-state self-paced BCI systems mentioned above (Millan et al 2004, Scherer *et al* 2004) can be used in some practical applications, *ideally* a self-paced BCI system should have three important capabilities as following:

(1) The system should be continuously available for control,

(2) The system should not require the user to constantly engage in control, and

(3) The system should support NC state as defined above.

The 3rd criterion actually implies the 2nd criterion, however, to emphasize its importance we have considered them as two separate criteria.

1.2.2. BCI Research at the Neil Squire Society (NSS) and the University of British Columbia (UBC)

BCI research at the NSS and UBC began 15 years ago with the development of the Outlier Processing Method (OPM) (Birch 1988, Mason *et al* 1991). Results from this work on the OPM were promising as hit rates (true positive rates) of greater than 90% were achieved on a thumb movement task. However, its relatively poor performance on spontaneous, idle EEG (yielding false positive rates ranging from 10% to 30%) restricted its use as a self-paced BCI system. During the past years, the Low Frequency-Asynchronous Switch Design (LF-ASD) was introduced as a brain computer interface for self-paced control applications (Mason and Birch, 2000). Figure 1.4 shows the high-level design of the LF-ASD. The original design of this brain computer interface (Mason and Birch 2000) was modified to reduce the processing delays (Lisogurski and Birch 1998) and improve the classification accuracies (Mason *et al* 2000). The most recent version of this brain computer interface seeks to recognize the movement related potentials (MRPs) in the EEG signal. The inputs to the LF-ASD are six bipolar EEG signals recorded over the supplementary motor area (SMA) and sensory-motor cortex (defined with reference to the International 10-20 System at F1-FC1, Fz-FCz, F2-FC2, FC1-C1, FCz-Cz, and FC2-C2) sampled at 128Hz. The switch (i.e. the BCI system) produces a single output every 1/16th of a second; this output is equivalent to a 2-position switch. Internally, features are extracted from the amplified, bipolar EEG signals and then classified as a class '1' (IC state) or class '0' (NC state). The feature extraction algorithm low-pass filters the signal to below 4Hz and then calculates a 6-dimensional feature vector using a feature extraction scheme designed to recognize the temporal patterns in a single-trial bipolar EEG related to voluntary movement. The feature vector is classified as either an IC or an NC state class using a one-nearest neighbor (1-NN) classifier. Reference vectors for

both NC and IC classes in the feature classifier are selected from the training data using learning vector quantization (LVQ) algorithm (Kohonen 1990).

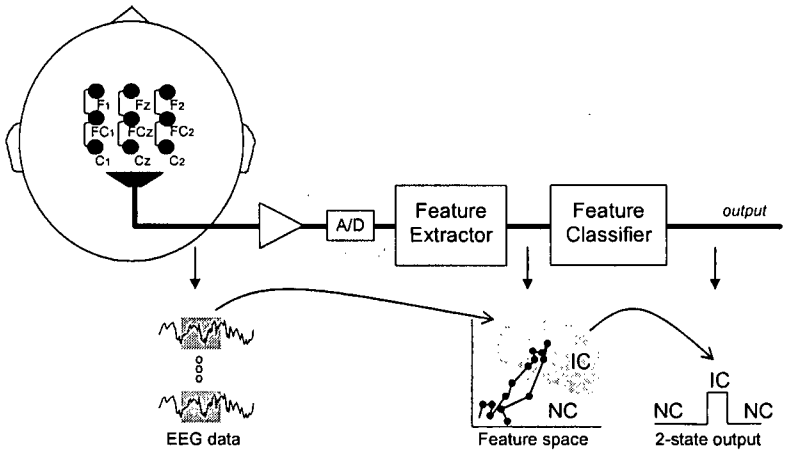

Figure 1.4 High-level design of LF-ASD brain computer interface. The 'Feature Classifier' continually monitors the 6-dimensional feature vectors and when a feature vector enters a pre-defined sub-space "IC", the output of the classifier is activated (IC state). Otherwise, the output state remains inactive (NC state).

In the latest study, before the start of this project on both able-bodied and disabled subjects, the subjects activated the brain computer interface with an imagined finger flexion to control a simple pong style video game at their own pace. Users would themselves report the system classification errors with a pneumatic sip and puff switch whenever an error occurred. During the game, if ocular artifact (OA) was detected (by using a customized threshold on the EOG signal), the input to the brain switch was ignored during the persistence of OA till for 0.5 seconds afterward. Evaluation results showed an average hit (true positive (TP)) rate of 51.3% and false positive (FP) rate of 2% (Borisoff *et al* 2002). Among the proposed self-paced BCI transducers whose offline performances have been reported in terms of true positives and false positives (Graimann *et al* 2004, Levine *et al* 2000, Townsend *et al* 2004, Yom-Tov and Inbar 2003), the LF-ASD has the advantage of *being capable* of generating low false positive rates. All these offline studies have reported average false positive rates in the range of 6% to 28% while the average true positive rates were between 73% and 94% (Graimann *et al* 2004, Levine *et al* 2000, Townsend *et al* 2004, Yom-Tov and Inbar 2003). It is difficult, however, to directly compare the results of different studies, as the recording equipment, recording and classification protocols, decision rate and time intervals during

which false positives could occur and mental tasks considered are different. In addition, the amount of data involved and the degree of training the subjects received before participating in the BCI experiments also vary between studies.

Although the evaluation of the LF-ASD had shown the potential capability of the system, the error rates of the system was still not suitable for real-world applications, therefore further improvements in the performance of the system was needed. On the other hand, the LF-ASD provided a 2-state (binary) output, i.e., NC and IC states. This output can be used as a single push button for example to select an object on the monitor or turn something on and off. Although this single function switch is very helpful for people with extreme disabilities, providing more options in controlling the output of the system is still desirable.

1.3. Objectives and Contributions

The goals of this thesis are to:

(a) Improve the performance of the Neil Squire Society's existing 2-state self-paced brain computer interface (BCI) system (the LF-ASD), and

(b) Design and investigate the feasibility of a 3-state self-paced BCI.

To our best knowledge, this is the first 3-state self-paced BCI system[4] that best satisfies the criteria mentioned in Section 1.2.1, i.e., *the system is continuously available for control, and the system is specifically designed to support the NC state.* This system continuously differentiates the predefined intended control states (i.e. right and the left hand extensions) from the NC state. As defined in Section 1.2.1, the NC state includes any brain activity other than the IC states. The two 3-state self-paced BCI systems introduced previously by Millan et al and Scherer et al (Millan et al 2004, Scherer *et al* 2004) differ from our proposed system in that they only partially satisfy the three criteria mentioned in Section 1.2.1.

As stated earlier, although the evaluation of the LF-ASD had shown the potential capability of the system, the error rates were still not suitable for real-world applications. For a real-world application, one needs to have a system with a very low false positive rate. A false

[4] A 4-state self-paced BCI has been introduced very recently (Scherer et al Aug 2007) just before the deadline for submitting this thesis to the library. This system generates mean true positive rate of 28.4% at the false positive rate of 16.9%. Results of the system introduced in this dissertation are compared with other BCI systems in Chapter 10.

positive rate of 2%, in the existing 2-state self-paced BCI, corresponded to two false activations every six seconds, which is not suitable for most practical applications. Therefore further improvements in the performance of the system were needed. Another reason for carrying out research towards improving the existing 2-state self-paced BCI was to build more knowledge to be able to design a 3-state self-paced BCI. In fact, the latest design of the 2-state system which we developed during the course of this project was directly used in the design of the 3-state self-paced BCI system.

Figure 1.5 shows samples of the outputs of 2-state and 3-state self-paced BCIs. A 2-state self-paced brain computer interface generates an output which corresponds to two different brain states. In the LF-ASD design, when the user intends control by imagining a finger flexion, the output switches from the NC state to the IC state. In fact, the user activates the output by imagining a finger flexion. On the other hand, a 3-state self-paced BCI would have a 3-state output corresponding to three different brain states. Generally, in such a system, the output of the BCI is in an inactive state, i.e. the NC state. The corresponding intended control states IC1 and IC2, will be activated when specific predefined brain states such as a right finger flexion and a left finger flexion is detected from the recorded brain signals.

While a 2-state self-paced BCI system that is based on movement related potentials can be used to determine whether or not a movement, e.g. right index finger flexion, is intended, a 3-state BCI aims at not only detecting the person's intention to move but also distinguishes between two movements, e.g. right/left finger movements. As a result, the 3-state BCI provides faster communication abilities and more flexibility in operating one or more devices. As a very simple example, for a wheelchair control application, while a 2-state BCI can provide the command for e.g. turning right, a 3-state BCI would provide both turn right and turn left options. In a more complicated control paradigm, 2-state and 3-state self-paced BCIs can for example be used to navigate through different menu items on a user display and select the desired tasks (refer to Section 10 for a more detailed application example of 2-state and 3-state self-paced BCIs).

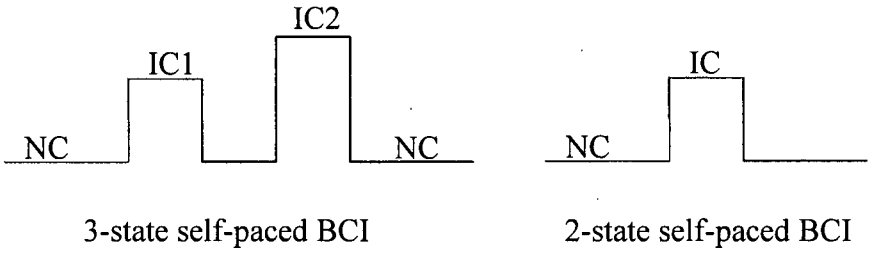

Figure 1.5 Sample outputs of the 2-state BCI (the LF-ASD) and proposed 3-state BCI

The main contributions of this thesis, achieved through the course of pursuing the above goals are the following:

1) A comprehensive survey of the brain computer interfaces conducted from the signal processing point of view,

2) Introduction of the design of a 3-state self-paced BCI,

3) Introduction of two new movements (neuromechanisms) to control a 3-state BCI,

4) Improvement in the performance of the 3-state BCI using different feature extraction and classification algorithms.

5) Introduction of alternative adaptive classification schemes for the existing 2-state BCI,

6) Introduction of training-data generation methods for self-paced brain computer interfaces,

7) Improvement in the design of the feature extraction block of the 2-state BCI by customizing the parameter values of this block for each user,

8) Introduction of a feature extraction algorithm that improves the 2-state BCI,

9) Evaluation of the performance of the 2-state BCI system on ocular artifact contaminated EEG data,

Although the contributions listed as 5 to 9 are directly attributed to improving the 2-state BCI system, the findings of these studies were directly incorporated in the design of the 3-state BCI system.

1.4. Thesis Scope and Organization

This dissertation focuses on improving the existing 2-state self-paced brain computer interface and an introducing the design of a 3-state self-paced brain computer interface. Both systems intend to detect movement(s) intentions from the EEG signal.

At first, a comprehensive survey of more than 300 refereed papers in the BCI field was carried out. The focus was on signal processing aspects of the different brain computer interfaces. The aims of this study were to perform a historical analysis of signal processing in this field, to identify the trends in signal processing of BCIs and the methods that have been used for different BCIs and to introduce a possible taxonomy of signal processing in BCI designs. Chapter 2 of this dissertation presents this comprehensive survey.

To improve the performance of the 2-state BCI, several studies focusing on improving the different building blocks of the current BCI system (as shown in Fig. 1.2) were conducted as follows:

To improve the performance of the existing 2-state BCI design, methods for the classification stage and for the dimensionality reduction of the feature space were implemented. Chapter 3 presents the details and findings of this study (Borisoff *et al* 2004).

Generating training-data for brain computer interfaces that aim at detecting intended tasks such as imagined finger flexions is challenging. In these systems, no external knowledge of the time of the actual performed task is known. Therefore, designing a BCI system without knowing the exact time that the user has performed the intended task is difficult. Chapter 4 presents and compares several methods of generating training-data for self-paced BCIs (Bashashati *et al* 2007a). These methods are specifically based on probability density estimation and clustering algorithms.

As the EEG characteristics during intended movements may vary from one subject to another, design parameters of a brain computer interface need to be customized for each subject. For the LF-ASD design, without such tuning, the system may detect non-MRP patterns in the ongoing EEG or its performance may not be optimal. Therefore, a method that customizes the parameter values of the feature extraction block of the current BCI system for each subject is proposed in Chapter 5 (Bashashati *et al* 2006a). The aim of this study is to

improve the performance of the BCI design and more importantly to ensure that the output is activated by movement attempts and not by other unwanted brain activity. Previously, these parameter values were determined based on the data of one subject and were then used for all subjects in the study.

In another study, we focused on the feature extraction of the current BCI. A novel pattern recognition approach that models the trajectory of feature vectors to detect intentional control commands (attempted finger movements) was proposed and implemented. This novel approach resulted in significant improvements in the 2-state BCI system (Bashashati *et al* 2006b). The details of this study are presented in Chapter 6 of this dissertation.

In the original design of the LF-ASD, the output of the system was blocked during the presence of ocular artifacts and the user could not control the output during these times. Analysis of the EEG data recorded in our BCI experiments show that an average of 22% of the data had contained ocular artifacts and the users were not able to control the output during these times. Therefore, a BCI system that does not block out ocular artifacts is desirable. What led us to believe that such a design is possible were the successful results obtained in Chapter 6 where the proposed design uses all past values of the features to determine whether or not a movement is performed. Therefore, in Chapter 7 the performance of the proposed system on ocular artifact contaminated data is evaluated (Bashashati *et al* 2007b). In addition, an evaluation method that can truly reflect and compare the performance of the BCI system with and without including ocular artifacts is introduced and discussed.

Several studies were also conducted to design a 3-state self-paced BCI:

As previously mentioned, there are several neurological mechanisms that can be used to build a BCI system. Movement related potentials (MRP) were used as the mechanism to activate the output of the existing 2-state BCI (the LF-ASD). In this specific design, attempted right index finger flexions were used. Evaluation results of the LF-ASD showed the potential ability of MRPs to activate the BCI. To operate a 3-state self-paced BCI system, two different neurological command sources for activating the output of the system are needed. We decided to use neuromechanisms related to movements as the source of controlling the new 3-state BCI. This is because of our previous experience in detecting movement patterns, the many scientific studies on movement related potentials, and the ease

of mapping and using this command source in real world applications. The first and the most important question was 'What are the optimal two movements that can be used to build a BCI?'. Based on the results of a survey conducted, the right hand and left hand extensions were likely to generate more differentiable patterns compared to other movements such as finger movements. A study involving human subjects was conducted to collect EEG data while the subjects were performing these two movements. A design of a 3-state BCI system which contains two major blocks is implemented. The first block (DET1) determines whether a movement is present or not. Once a movement is detected, the second block in the system (DET2) determines whether it is a right hand or a left hand extension. Two designs including the latest design of the LF-ASD were implemented and tested for DET1 which detects presence of movements. For DET2, a design that is based on selecting the most informative frequency components of the EEG and a linear classifier was implemented and tested. Chapter 8 of this dissertation presents the details of this study (Bashashati *et al* 2007c).

Chapter 9 explores possible improvements of the 3-state BCI system by employing different designs of DET1 and the use of other feature extraction methods. These designs utilize the history of the feature values and nonlinear classifiers to improve the performance of the 3-state self-paced BCI. Due to the modular design of the 3-state BCI, these algorithms are also directly useable in the designs of 2-state self-paced BCIs which detect the presence of an IC state in the ongoing EEG.

The thesis is concluded in Chapter 10 where a summary of the main contributions of this thesis is presented. Potential research topics that can immediately follow this research and an application example of 2-state and 3-state self-paced BCIs are also presented in this chapter.

Appendix A includes a copy of the approval from the University of British Columbia's behavioural research ethics board (BREB) to conduct this study. Appendix B presents expanded tables of Chapter 2 of this thesis and Appendix C includes details of the methods that have been used in different parts of this thesis.

Figure 1.6 provides a summary of the organization of this dissertation.

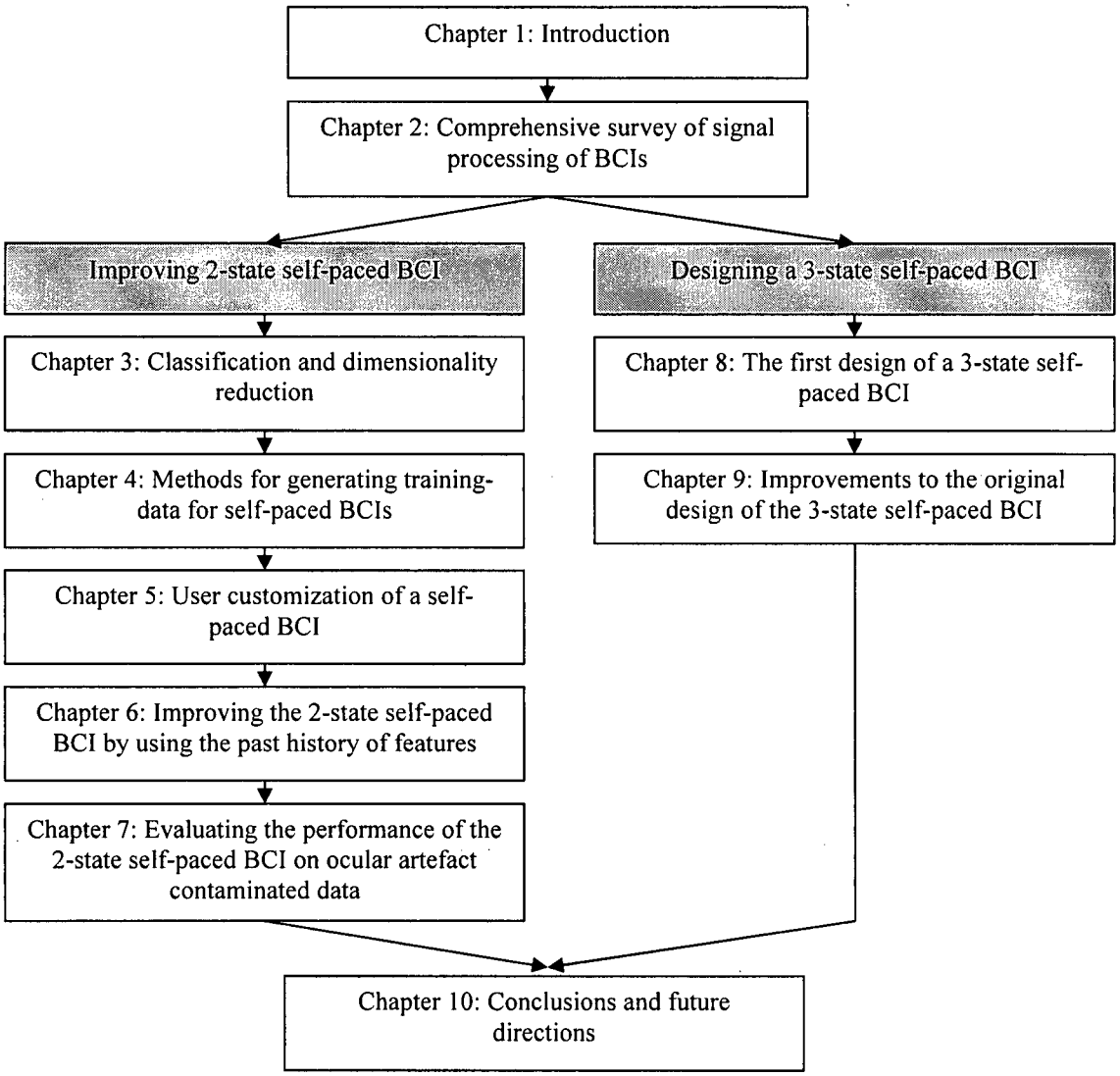

Figure 1.6 Organization of chapters

1.5. References

Anderson C W, Stolz E A and Shamsunder S 1998 Multivariate autoregressive models for classification of spontaneous electroencephalographic signals during mental tasks *IEEE Transactions on Biomedical Engineering* **45** 277-86

Babiloni F, Cincotti F, Lazzarini L, Millan J, Mourino J, Varsta M, Heikkonen J, Bianchi L and Marciani M G 2000 Linear classification of low-resolution EEG patterns produced by imagined hand movements *IEEE Transactions on Rehabilitation Engineering* **8** 186-8

Bashashati A, Fatourechi M, Ward R K and Birch G E 2006a User customization of the feature generator of an asynchronous brain interface *Annals of Biomedical Engineering* **34** 1051-60

Bashashati A, Mason S G, Borisoff J F, Ward R K and Birch GE 2007a A comparative study on generating training-data for self-paced brain interfaces *IEEE Transactions on Neural Systems and Rehabilitation Engineering* **15** 59-66

Bashashati A, Mason S, Ward R K and Birch G E 2006b An improved asynchronous brain interface: Making use of the temporal history of the LF-ASD feature vectors *J Neural Engineering* **3** 87-94

Bashashati A, Noureddin B, Ward R, Lawrence P and Birch G 2007b Effects of eye blinks on a self-paced brain interface *Clinical Neurophysiology* **118** 1639-47.

Bashashati A, Rabab Ward and Gary Birch 2007c Towards development of a 3-state self-paced brain interface based on hand extension movements *J Computational Intelligence & Neuroscience* In press

Bayliss J D and Ballard D H 2000 A virtual reality test bed for brain-computer interface research *IEEE Transactions on Rehabilitation Engineering* **8** 188-90

Birbaumer N, Ghanayim N, Hinterberger T, Iversen I, Kotchoubey B, Kubler A, Perelmouter J, Taub E and Flor H 1999 A spelling device for the paralysed *Nature* **398** 297-8

Birbaumer N, Kubler A, Ghanayim N, Hinterberger T, Perelmouter J, Kaiser J, Iversen I, Kotchoubey B, Neumann N and Flor H 2000 The thought translation device (TTD) for completely paralyzed patients *IEEE Transactions on Rehabilitation Engineering* **8** 190-3

Birch G E 1988 Single trial EEG signal analysis using outlier information PhD dissertation, University of Biritsh Columbia

Birch G E, Bozorgzadeh Z and Mason S G 2002 Initial on-line evaluations of the LF-ASD brain-computer interface with able-bodied and spinal-cord subjects using imagined voluntary motor potentials *IEEE Transactions on Neural Systems and Rehabilitation Engineering* **10** 219-24

Birch G E, Lawrence P D and Hare R D 1993 Single trial processing of event related potentials using outlier information *IEEE Transactions on Biomedical Engineering* **40** 59-73

Borisoff J F, Mason S G, Bashashati A and Birch G E 2004 Brain-computer interface design for asynchronous control applications: Improvements to the LF-ASD asynchronous brain switch *IEEE Transactions on Biomedical Engineering* **51** 985-92

Chapin J K, Moxon K A, Markowitz R S and Nicolelis M A 1999 Real-time control of a robot arm using simultaneously recorded neurons in the motor cortex *Nature neuroscience* **2** 664-70

Donchin E and Smith D B 1970 The contingent negative variation and the late positive wave of the average evoked potential *Electroencephalography and clinical neurophysiology* **29** 201-3

Donchin E, Spencer K M and Wijesinghe R 2000 The mental prosthesis: Assessing the speed of a P300-based brain-computer interface *IEEE Transactions on Rehabilitation Engineering* **8** 174-9

Donoghue J P 2002 Connecting cortex to machines: Recent advances in brain interfaces *Nature neuroscience* **5** 1085-8

Farwell L A and Donchin E 1988 Talking off the top of your head: Towards a mental prosthesis utilizing event-related brain potentials *Electroencephalography and clinical neurophysiology* **80** 510-23

Garrett D, Peterson D A, Anderson C W and Thaut M H 2003 Comparison of linear, nonlinear, and feature selection methods for EEG signal classification *IEEE Transactions on Neural Systems and Rehabilitation Engineering* **11** 141-4

Glover A A, Onofrj M C, Ghilardi M F and Bodis-Wollner I 1986 P300-like potentials in the normal monkey using classical conditioning and an auditory 'oddball' paradigm *Electroencephalography and clinical neurophysiology* **65** 231-5

Graimann B, Huggins J E, Levine S P and Pfurtscheller G 2004 Toward a direct brain interface based on human subdural recordings and wavelet-packet analysis *IEEE transactions on bio-medical engineering* **51** 954-62

Hochberg L R, Serruya M D, Friehs G M, Mukand J A, Saleh M, Caplan A H, Branner A, Chen D, Penn R D and Donoghue J P 2006 Neuronal ensemble control of prosthetic devices by a human with tetraplegia *Nature* **442** 164-71

Isaacs R E, Weber D J and Schwartz A B 2000 Work toward real-time control of a cortical neural prothesis *IEEE Transactions on Rehabilitation Engineering* **8** 196-8

Kohonen T 1990 Self-organizing map *Proceedings of IEEE* **78** 1464-80

Kubler A, Nijboer F, Mellinger J, Vaughan T M, Pawelzik H, Schalk G, McFarland D J, Birbaumer N and Wolpaw J R 2005 Patients with ALS can use sensorimotor rhythms to operate a brain-computer interface *Neurology* **64** 1775-7

Lal T N, Hinterberger T, Widman G, Schroder M, Hill N, Rosenstiel W, Elger C E, Scholkopf B and Birbaumer N 2005 Methods towards invasive human brain computer interfaces *Advances in Neural Information Processing Systems* **17** 737–44

Leuthardt E C, Schalk G, Wolpaw J R, Ojemann J G and Moran D W 2004 A brain-computer interface using electrocorticographic signals in humans **1** 63-71

Levine S P, Huggins J E, Bement S L, Kushwaha R K, Schuh L A, Rohde M M, Passaro E A, Ross D A, Elisevich K V and Smith B J 2000 A direct brain interface based on event-related potentials *IEEE Transactions on Rehabilitation Engineering* **8** 180-5

Lisogurski D and Birch G E 1998 Identification of finger flexions from continuous EEG as a brain computer interface *Proc. IEEE Engineering in Medicine and Biology Society Inter. Conf.* **20** 2004-7

Liu X, McCreery D B, Carter R R, Bullara L A, Yuen T G and Agnew W F 1999 Stability of the interface between neural tissue and chronically implanted intracortical microelectrodes *IEEE Transactions on Rehabilitation Engineering* **7** 315-26

Mason S G, Bashashati A, Fatourechi M, Navarro K F and Birch G E 2007 A comprehensive survey of brain interface technology designs *Annals of Biomedical Engineering* **35** 137-69

Mason S G and Birch G E 2000 A brain-controlled switch for asynchronous control applications *IEEE Transactions on Biomedical Engineering* **47** 1297-307

Mason S G and Birch G E 2003 A general framework for brain-computer interface design *IEEE Transactions on Neural Systems and Rehabilitation Engineering* **11** 70-85

Mason S G, Birch G E and Ito M R 1991 A modified algorithm for single-trial signal extraction of low SNR events *Proc. IASTED Inter. Conf. on Computers, Electronics, Communication and Control* 257-61

Mason S G, Bozorgzadeh Z and Birch G E 2000 The LF-ASD brain-computer interface: On-line identification of imagined finger flexions in subjects with spinal cord injuries *Proc. fourth Inter. ACM conf. on Assistive technologies* 109-13

Mason S G, Moore M M and Birch G E 2003 Designing pointing devices using brain-computer interface technology *Proc. IEEE 1st Inter. Conf. on Neural Engineering (Capri, Italy)* 610-3

McFarland D J, Miner L A, Vaughan T M and Wolpaw J R 2000 Mu and beta rhythm topographies during motor imagery and actual movements *Brain topography* **12** 177-86

McFarland D, Lefkowicz A and Wolpaw J 1997 Design and operation of an EEG-based brain—computer interface with digital signal processing technology *Behavior research methods, instruments & computers* **29** 337-45

Middendorf M, McMillan G, Calhoun G and Jones K S 2000 Brain-computer interfaces based on the steady-state visual-evoked response *IEEE Transactions on Rehabilitation Engineering* **8** 211-4

Millan J R, Renkens F, Mourino J and Gerstner W 2004 Noninvasive brain-actuated control of a mobile robot by human EEG *IEEE Trans. Biomed. Eng.* **51** 1026-33.

Miner L A, McFarland D and Wolpaw J R 1998 Answering questions with an electroencephalogram-based brain computer interface *Arch Phys Med Rehabil* **79** 1029-33

Neuper C, Schloegl A and Pfurtscheller G 1999 Enhancement of left-right sensorimotor EEG differences during feedback-regulated motor imagery *Journal of Clinical Neurophysiology* **16** 373-82

Nicolelis M A 2001 Actions from thoughts *Nature* **409** 403-7

Nicolelis M A 2003 Brain-machine interfaces to restore motor function and probe neural circuits *Nat Rev Neurosci* **4**(5) 417-22

Niedermeyer E and Lopes da Silva F 1998 Electroencephalography: Basic principles, clinical applications, and related fields Fourth Edition, ed C Mitchell. (Baltimore, Maryland USA: Lippincott Williams & Wilkins)

Penny W D, Roberts S J, Curran E A and Stokes M J 2000 EEG-based communication: A pattern recognition approach *IEEE Transactions on Rehabilitation Engineering* **8** 214-5

Perelmouter J and Birbaumer N 2000 A binary spelling interface with random errors *IEEE Transactions on Rehabilitation Engineering* **8** 227-32

Pfurtscheller G and Berghold A 1989 Patterns of cortical activation during planning of voluntary movement *Electroencephalography and clinical neurophysiology* **72** 250-8

Pfurtscheller G, Flotzinger D and Kalcher J 1993 Brain-computer interface - a new communication device for handicapped persons *J Microcomputer App.* **16** 293-9

Pfurtscheller G and Lopes da Silva F H 1999 Event-related EEG/MEG synchronization and desynchronization: Basic principles *Clinical Neurophysiology* **110** 1842-57

Pfurtscheller G, Neuper C, Flotzinger D and Pregenzer M 1997 EEG-based discrimination between imagination of right and left hand movement *Electroencephalography and Clinical Neurophysiology* **103** 642-51

Pfurtscheller G, Neuper C, Guger C, Harkam W, Ramoser H, Schlogl A, Obermaier B and Pregenzer M 2000 Current trends in Graz brain-computer interface (BCI) research *IEEE Transactions on Rehabilitation Engineering* **8** 216-9

Piccione F, Giorgi F, Tonin P, Priftis K, Giove S, Silvoni S, Palmas G and Beverina F 2006 P300-based brain computer interface: Reliability and performance in healthy and paralysed participants *Clinical Neurophysiology* **117** 531-7

Ramoser H, Wolpaw J R and Pfurtscheller G 1997 EEG-based communication: Evaluation of alternative signal prediction methods *Biomedizinische Technik* **42** 226-33

Roberts S J and Penny W 2003 Real-time brain-computer interfacing: A preliminary study using bayesian learning *Medical and Biological Engineering and Computing* **38** 56-61

Rockstroh B, Birbaumer N, Elbert T and Lutzenberger W 1984 Operant control of EEG and event-related and slow brain potentials *Biofeedback and Self-Regulation* **9** 139-60

Roder B, Rosler F, Hennighausen E and Nacker F 1996 Event-related potentials during auditory and somatosensory discrimination in sighted and blind human subjects *Brain Research Cognitive Brain Research* **4** 77-93

Schalk G, Wolpaw J R, McFarland D J and Pfurtscheller G 2000 EEG-based communication: Presence of an error potential *Electroencephalography and Clinical Neurophysiology* **111** 2138-44

Scherer R, Muller G R, Neuper C, Graimann B and Pfurtscheller G 2004 An asynchronously controlled EEG-based virtual keyboard: Improvement of the spelling rate *IEEE Transactions on Biomedical Engineering* **51** 979-84

Scherer R, Lee F, Schlogl A, Leeb R, Bischot H and Pfurtscheller G Aug2007 Towards Self-Paced Brain-Computer Communication: Navigation through Virtual Worlds *IEEE Transactions on Biomedical Engineering*, In press.

Schwartz A B, Taylor D M and Tillery S I 2001 Extraction algorithms for cortical control of arm prosthetics *Curr Opin Neurobiol* **11** 701-7

Sellers E W and Donchin E 2006 A P300-based brain-computer interface: Initial tests by ALS patients *Clinical Neurophysiology* **117** 538-48

Serruya M D, Hatsopoulos N G, Paninski L, Fellows M R and Donoghue J P 2002 Instant neural control of a movement signal *Nature* **416** 141-2

Sutter E 1984 The visual evoked response as a communication channel *Proceedings of the IEEE Symposium on Biosensors* 95-100

Sutter E 1992 The brain response interface: Communication through visually-induced electrical brain responses *J Micro Comp App* **15** 31-45

Taylor D M, Tillery S I and Schwartz A B 2002 Direct cortical control of 3D neuroprosthetic devices *Science* **296** 1829-32

Townsend G, Graimann B and Pfurtscheller G 2004 Continuous EEG classification during motor imagery--simulation of an asynchronous BCI *IEEE Transactions on Neural Systems and Rehabilitation Engineering* **12** 258-65

Vaughan T M, Heetderks W J, Trejo L J, Rymer W Z, Weinrich M, Moore M M, Kubler A, Dobkin B H, Birbaumer N, Donchin E, Wolpaw E W and Wolpaw J R 2003 Brain-computer interface technology: A review of the second international meeting *IEEE Transactions on Neural Systems and Rehabilitation Engineering* **11** 94-109

Vidal J 1977 Real-time detection of brain events in EEG *Proceedings of the IEEE* **65** 633-41

Wolpaw J R, Birbaumer N, McFarland D J, Pfurtscheller G and Vaughan T M 2002 Brain-computer interfaces for communication and control *Electroencephalography and Clinical Neurophysiology* **113** 767-91

Wolpaw J R, McFarland D, Neat G W and Forneris C A 1991 An EEG-based brain-computer interface for cursor control *Electroencephalography and Clinical Neurophysiology* **78** 252-9

Wolpaw J R, McFarland D and Pfurtscheller G 1998 EEG-based communication: Improved accuracy by response verification *IEEE Transactions on Rehabilitation Engineering* **6** 326-33

Wolpaw J R, McFarland D J and Vaughan T M 2000 Brain-computer interface research at the Wadsworth center *IEEE Transactions on Rehabilitation Engineering* **8** 222-6

Yom-Tov E and Inbar G F 2003 Detection of movement-related potentials from the electro-encephalogram for possible use in a brain-computer interface *Medical and Biological Engineering and Computing* **41** 85-93

Chapter 2 A Survey of Signal Processing Algorithms in Brain-Computer Interfaces Based on Electrical Brain Signals[5]

2.1. Introduction

The ultimate purpose of a direct brain computer interface (BCI) is to allow an individual with severe motor disabilities to have effective control over devices such as computers, speech synthesizers, assistive appliances, and neural prostheses. Such an interface would increase an individual's independence, leading to an improved quality of life and reduced social costs.

A BCI system detects the presence of specific patterns in a person's ongoing brain activity that relates to the person's intention to initiate control. The BCI system translates these patterns into meaningful control commands. To detect these patterns, various signal processing algorithms are employed. Signal processing forms an important part of a BCI design, since it is needed in extracting the meaningful information from the brain signal.

This paper summarizes the results of a comprehensive survey of different signal processing schemes that have been used in BCI systems. It specifically focuses on the following signal processing components of a BCI: the pre-processing stage (which we refer to as the signal-enhancement stage), the feature extraction stage and the feature translation stage. To address all related BCI research, we include all the approaches that use standard scalp-recorded EEG as well as those that use epidural, subdural, or intracortical recordings. The aims of this study are (a) to make it easy to identify the signal processing methods employed in different BCI systems, and consequently to identify the methods that have not yet been explored, (b) to form a historical reference for new researchers in this field, and (c) to introduce a possible taxonomy of signal processing methods in brain computer interfaces.

The organization of the paper is as follows: in Section 2.2, the general structure of a BCI system and the current neuromechanisms[6] in BCI systems are presented. Section 2.3 details

---

[5] A version of this chapter has been published: Bashashati A., Fatourechi M., Ward R.K., and Birch G.E. (2007) A Survey of Signal Processing Algorithms in Brain Computer Interfaces Based on Electrical Brain Signals *Journal of Neural engineering* **4**(2), R35-57.

This work has also been resulted in two other publications as follows:

Mason S.G., Bashashati A., Fatourechi M., Navarro K.F., and Birch G.E. (2007) A Comprehensive Survey of Brain Interface Technology Designs *Annals of Biomedical Engineering* **35** 137-69.

Fatourechi M., Bashashati A., Ward R.K., and Birch G.E. (2007) EMG and EOG Artifacts in Brain Interface Systems: A Survey *Clinical Neurophysiology* **118** 480-94.

the procedure we followed to conduct this study. Results, discussions, and conclusions are in Sections 2.4-6, respectively.

2.2. General Structure of a BCI System

Fig. 2.1 shows the functional model of a BCI system (Mason and Birch 2003). The figure depicts a generic BCI system in which a person controls a device in an operating environment (e.g., a powered wheelchair in a house) through a series of functional components. In this context, the user's brain activity is used to generate the control signals that operate the BCI system. The user monitors the state of the device to determine the result of his/her control efforts. In some systems, the user may also be presented with a control display, which displays the control signals generated by the BCI system from his/her brain activity.

The electrodes placed on the head of the user record the brain signal from the scalp, or the surface of the brain, or from the neural activity within the brain, and convert this brain activity to electrical signals. The 'artifact processor' block shown in Fig. 2.1, removes the artifacts from the electrical signal after it has been amplified. Note that many transducer designs do not include artifact processing. The 'feature generator' block transforms the resultant signals into feature values that correspond to the underlying neurological mechanism employed by the user for control. For example, if the user is to control the power of his/her Mu (8-12Hz) and Beta (18-25Hz) rhythms, the feature generator would continually generate features relating to the power-spectral estimates of the user's Mu and Beta rhythms. The feature generator generally can be a concatenation of three components, the 'signal-enhancement', the 'feature extraction', and the 'feature selection' components, as shown in Fig. 2.1.

In some BCI designs, pre-processing is performed on the brain signal prior to the extraction of features so as to increase the signal-to-noise ratio of the signal. In this paper, we use the more general term 'signal- enhancement' to refer to the pre-processing stage. A feature selection component is sometimes added to the BCI system after the feature extraction stage. The aim of feature selection is to reduce the number of features and/or channels used so that

[6] According to the Merriam-Webster Medical dictionary, a bodily regulatory mechanism based in the structure and functioning of the nervous system is called a *neuromechanism*.

very high dimensional and noisy data are excluded. Ideally, the features that are meaningful or useful in the classification stage are identified and chosen, while others (including outliers and artifacts) are omitted.

The 'feature translator' translates the features into logical (device-independent) control signals, such as a two-state discrete output. The translation algorithm uses linear classification methods (e.g., classical statistical analyses) or nonlinear ones (e.g., neural networks). According to the definition in (Mason and Birch 2003), the resultant logical output states are independent of any semantic knowledge about the device or how it is controlled. As shown in Fig. 2.1, a feature translator may consist of two components: 'feature classification' and 'post-processing'. The main aim of the feature classification component is to classify the features into logical control signals. Post-processing methods such as a moving average block may be used after feature classification to reduce the number of error activations of the system.

The control interface translates the logical control signals (from the feature translator) into semantic control signals that are appropriate for the particular type of device used. Finally, the device controller translates the semantic control signals into physical control signals that are used by the device. The device controller also controls the overall behavior of the device. For more detail refer to (Mason and Birch 2003).

Table 2.1 provides a simplified description of the BCI transducer components.

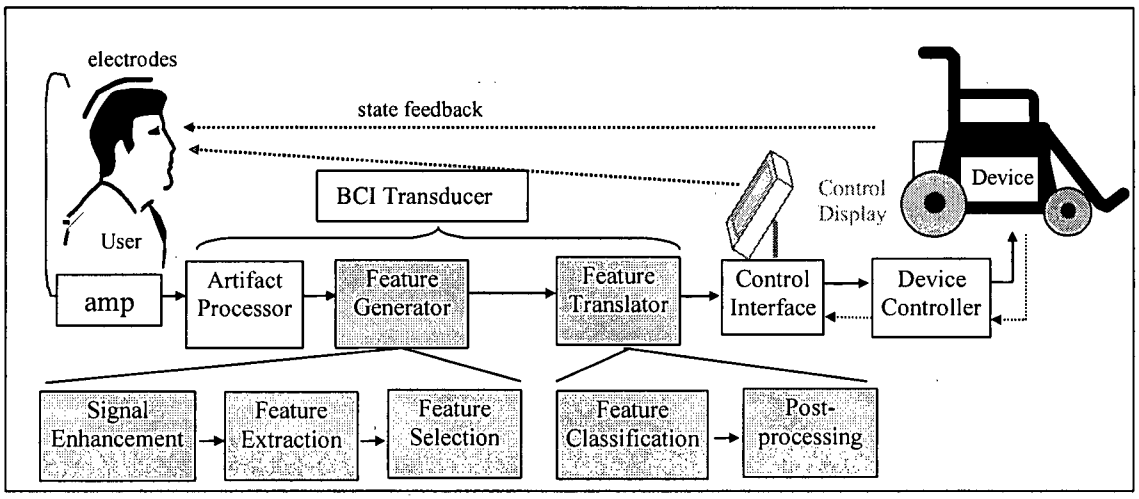

Figure 2.1 Functional model of a BCI system (Mason and Birch 2003). Note the control display is optional. This review focuses on the shaded components of BCI systems.

TABLE 2.1 TAXONOMY FOR BCI TRANSDUCER DESIGNS

Item	Terms		Definition
BCI	Artifact Processor		Removes artifact from the input signal
Transducer	Feature Generator	Signal Enhancement	(1) Enhances signal-to-noise ratio of the brain signal (2) The output of this block is a signal with the same nature of the input (i.e. the output like the input is in the temporal domain).
		Feature Extraction	Generates the feature vectors
		Feature Selection	Selects a subset of features
	Feature Translator	Feature Classification	Classifies the features into logical control signals
		Post-Processing	Increases the performance after feature classification e.g., by blocking activations with low certainty

2.2.1. Electrophysiological Sources of Control in Current BCIs

In BCI systems, electrophysiological sources refer to the neurological mechanisms or processes employed by a BCI user to generate control signals. Current BCIs fall into seven main categories, based on the *neuromechanisms* and *recording technology* they use. In (Wolpaw et al 2002) BCI systems are categorized as five major groups. These categories are sensorimotor activity, P300, VEP, SCP and activity of neural cell (ANC). In this paper, two other categories were added: "Response to Mental Tasks" and "Multiple Neuromechanisms". BCI systems that use non-movement mental tasks to control a BCI (e.g. (Anderson et al 1995b, Millan et al 1998)) assume that different mental tasks (e.g. solving a multiplication problem, imagining a 3D object, or mental counting) lead to distinct, task specific EEG patterns and aim to detect the patterns associated with these mental tasks from the EEG. BCI systems based on multiple neuromechanisms (e.g. (Gysels et al 2005)) use a combination of two or more of the above-mentioned neuromechanisms in a single design of a BCI system.

Table 2.2 shows these categories with a short description of each. Note that although the designs that use direct cortical recordings are included as a separate group, direct cortical recording is a recording technology and not a neuromechanism. As shown in Table 2.2, BCI designs that use sensorimotor activity as the neural source of control can be further divided into three sub-categories: those based on changes in brain rhythms (e.g. the Mu and Beta rhythms), those based on movement related potentials (MRP), and those based on other sensorimotor activity.

TABLE 2.2 ELECTROPHYSIOLOGICAL ACTIVITIES USED IN BCI DESIGNS AND THEIR DEFINITIONS

Neuromechanism		Short Description
Sensorimotor activity	**Changes in brain rhythms (Mu, Beta, and Gamma)**[7]	Mu rhythms in the range of 8-12 Hz and Beta rhythms in the range of 13-30 Hz both originate in the sensorimotor cortex and displayed when a person is not engaged in processing sensorimotor inputs or in producing motor outputs (Jasper and Penfield 1949). They are mostly prominent in frontal and parietal locations (Kozelka and Pedley 1990, Kubler *et al* 2001a, Niedermeyer and Lopes da Silva 1998). A voluntary movement results in a circumscribed desynchronization in the Mu and lower Beta bands (Pfurtscheller and Aranibar 1977). This desynchronization is called Event Related Desynchronization (ERD) and begins in the contralateral rolandic region about two seconds prior to the onset of a movement and becomes bilaterally symmetrical immediately before execution of movement (Pfurtscheller and Lopes da Silva 1999). After a voluntary movement, the power in the brain rhythms increases. This phenomenon, called Event Related Synchronization (ERS), is dominant over the contralateral sensorimotor area and reaches a maximum around 600 ms after movement offset (Pfurtscheller and Lopes da Silva 1999). Gamma rhythm is a high frequency rhythm in the EEG. Upon the occurrence of a movement, the amplitude of gamma rhythm increases. Gamma rhythms are usually more prominent in the primary sensory area.
	Movement-related potentials (MRPs)	MRPs are low-frequency potentials that start about 1-1.5 seconds before a movement. They have bilateral distribution and present maximum amplitude at the vertex. Close to the movement, they become contralaterally preponderant (Babiloni *et al* 2004, Deecke and Kornhuber 1976, Hallett 1994).
	Other sensorimotor activities	The sensorimotor activities that do not belong to any of the preceding categories are categorized as other sensorimotor activities. These activities are usually not restricted to a particular frequency band or scalp location and usually cover different frequency ranges. An example would be features extracted from an EEG signal filtered to frequencies below 30 Hz. Such a range covers different event-related potentials (ERPs) but no specific neuromechanism is used.

[7] In (Ramachandran and Histein 1998), references regarding the similarity between *attempted movements* and *real movements* in the ERD of Mu patterns are provided. An attempted movement occurs when a subject attempts to move some part of his/her body, but because of either a disability or the experiment control, the actual movement does not happen. Hence, all of the studies employing a specific brain rhythm as a source of control are associated with this category. Similarly, (Gevins *et al* 1989) has shown that imaginary (attempted) movements generate movement-related potentials (MRPs) similar to those generated by actual movements. Thus, neuromechanisms corresponding to attempted movements are grouped in the same category of real movement.

Neuromechanism	Short Description
Slow cortical potentials (SCPs)	SCPs are slow, non-movement potential changes generated by the subject. They reflect changes in cortical polarization of the EEG lasting from 300 ms up to several seconds. Functionally, a SCP reflects a threshold regularization mechanism for local excitory mobilization (Neumann *et al* 2003, Wolpaw *et al* 2002).
P300	Infrequent or particularly significant auditory, visual, or somatosensory stimuli, when interspersed with frequent or routine stimuli, typically evoke in the EEG over the parietal cortex a positive peak at about 300 ms after the stimulus is received. This peak is called P300 (Allison and Pineda 2003, Kubler *et al* 2001a).
Visual evoked potentials (VEP)	VEPs are small changes in the ongoing brain signal. They are generated in response to a visual stimulus such as flashing lights and their properties depend on the type of the visual stimulus (Kubler *et al* 2001a). These potentials are more prominent in the occipital area. If a visual stimulus is presented repetitively at a rate of 5-6 Hz or greater, a continuous oscillatory electrical response is elicited in the visual pathways. Such a response is termed steady-state visual evoked potentials (SSVEP). The distinction between VEP and SSVEP depends on the repetition rate of the stimulation (Gao *et al* 2003b).
Response to mental tasks	BCI systems based on non-movement mental tasks assume that different mental tasks (e.g., solving a multiplication problem, imagining a 3D object, and mental counting) lead to distinct, task-specific distributions of EEG frequency patterns over the scalp (Kubler *et al* 2001a).
Activity of neural cells (ANC)	It has been shown that the firing rates of neurons in the motor cortex are increased when movements are executed in the preferred direction of neurons. Once the movements are away from the preferred direction of neurons, the firing rate is decreased (Donoghue 2002, Olson *et al* 2005).
Multiple neuromechanisms (MNs)	BCI systems based on multiple neuromechanisms use a combination of two or more of the above-mentioned neuromechanisms.

2.3. Methods

The BCI designs selected for this review include every journal and conference paper that met the following criteria:

(1) One or more of the keywords BCI, BMI, DBI appeared in its title, abstract or keyword list;

(2) The work described one or more BCI designs (the minimum design content that met the criteria was a *BCI Transducer* as described in Section 2.2). There were a few papers that only reported pre-processing techniques specifically designed for brain computer interfaces that use neural cortical recordings. These papers were reported in the pre-processing techniques. Papers that presented tutorials, descriptions of electrode technology, neuroanatomy, and neurophysiology discussions that might serve as the basis for a BCI were not included;

(3) Only papers published in English and in refereed international journals and conference proceedings were included;

(4) Designs that use functional magnetic resonance imaging (fMRI) (Weiskopf *et al* 2003, Weiskopf *et al* 2004, Yoo *et al* 2004), magneto-encephalography (MEG) signals (Georgopoulos *et al* 2005), near infra red spectrum (NIRS), auditory evoked potentials (Hill *et al* 2004, Su Ryu *et al* 1999) and somatosensory evoked potentials (Yan Wang *et al* 2004) were not included in this paper; and

(5) Papers were published prior to January 2006.

Although no paper meeting the five criteria explained above was omitted from the analysis, some papers may have been missed unintentionally. The current work should thus be regarded as an initial step to build a public database that can be updated and evolved with time.

In Tables 2.3-8, we categorized the papers according to the signal processing methods used. For each of the design blocks of a BCI system shown in Fig. 2.1 (signal-enhancement, feature extraction, feature selection, feature classification, and post-processing), we created a table that reports the signal processing techniques used in that block. Since most of the BCI designs that use neural cortical recordings do not contain a feature extraction component, we generated a separate table (Table 2.7) to report the translation schemes used in these designs.

Feature extraction methods used in BCI systems are closely related to the specific neuromechanism(s) used by a BCI. For example, the feature extraction algorithms employed in VEP-based BCIs are used to detect the visual evoked potentials in the ongoing EEG. In BCI systems that operate on slow cortical potentials (SCP), the extracted features are mostly used for the purpose of identifying this specific phenomenon in the brain signal. Thus in Table 2.5, we categorize the feature extraction algorithms based on the seven neurological sources described in Table 2.2. For example, the methods used in VEP-based BCIs are assembled under a different category from those used in SCP-based BCIs. A more detailed version of Table 2.5 can be found in Table B.1 of Appendix B.

The different feature classification algorithms used in BCI systems are shown in Table 2.6. As feature classification algorithms are also closely related to the type of the features that they classify, the feature classification algorithms are also categorized based on the feature

extraction methods. This can be found in Table B.2 of Appendix B. Appendix B also contains a detailed version of Table 2.7 where the classification algorithms for BCIs that use cortical neural recordings are shown.

Categorizing the feature classification methods based on the feature extraction methods used does not necessarily limit the use of a specific feature classification to a specific feature extraction method. The same applies to the categorization of the feature extraction methods based on neuromechanisms used in BCI systems. The aim here is to provide as specific information as possible about signal processing in current BCI designs and the researchers can combine any feature extraction method and/or feature classification method from different categories if necessary.

Each table includes major classes corresponding to each design block. These classes were initially determined by our team and then refined after an initial pass through the selected papers. In some cases, each major class was further divided into more specific categories. The full classification template with all the major classes and sub-classes of each design component is listed in the left column of Tables 2.3, 2.4, 2.5 and 2.8, and in the left two major columns of Tables 2.6 and 2.7. Note that in this paper, major classes are written in bold type and sub-classes are represented in *bold-italic* type. For example, in Table 2.5 or Table B.1, SCP-based BCI designs that use some type of power spectral parameters of the EEG are categorized under the SCP-spectral parameters class, while a BCI design that is based on the movement-related potentials (MRP) and that uses the same method is categorized under the Sensorimtor Activity -PSD and Sensorimtor Activity-*MRP*-PSD classes in Table 2.5 and Appendix B, respectively. As an example from Table 2.6, BCI designs that use linear discriminant analysis (LDA) classifiers are categorized under LDA. Table B.2 which has a more detailed version of Table 2.6, categorizes BCI designs that use PSD features and LDA classifier under PSD-LDA class.

The category for each BCI design was determined by selecting the closest sub-class in the classification template. For the papers that reported multiple designs multiple classifications were recorded. The designs were categorized based only on what was reported in each paper. No personal knowledge of an authors' related work was used in the classification.

In some cases, it was difficult to differentiate between the signal-enhancement, feature selection, and feature extraction design components of a brain computer interface. Based on the definitions in Table 2.1, the methods that satisfied the following four criteria were considered to be signal-enhancement methods:

(1) The method was implemented to improve the signal-to-noise ratio of the brain signal.

(2) The output of the block had the same nature as the input brain signal (i.e. the output stayed in the temporal domain).

(3) The algorithm was directly performed on the brain signal and not on the features extracted from the brain signal.

(4) The method did not handle artifacts.

The common spatial patterns (CSP) method is an example of a method that satisfies the four above mentioned criteria and was thus categorized as a signal-enhancement method. Only designs that incorporated signal-enhancement algorithms other than the general band-pass filtering of the EEG, the power-line-effect rejection, and the traditional normalization of the signal were reported in the signal-enhancement section of this paper.

2.4. Results

The detailed classification results of the survey are summarized in Tables 2.3-8 (refer to tables B.1-3 in Appendix B for more detailed versions of tables 2.5-7). As mentioned in Section 2.3, these six tables address the signal-enhancement, feature selection, feature extraction, feature classification and post-processing methods used. The references listed for each sub-class entry represent all the papers that reported on designs related to that sub-class. As such, one can find all the designs that have specific attributes of interest. For example, if one is interested in all BCI technology designs that have used parametric modeling (and specifically extracted AR parameters of the signal) to detect the sensorimotor activity, then all the references to the relevant papers can be found in Table 2.5 under Sensorimotor Activity–Parametric modeling *(AR, AAR and ARX parameters)*. Alternatively, if one is looking for designs that do not have a feature extraction block but directly apply the support-vector-machine (SVM) classification method on the brain signal, then these papers can be easily located in the None-SVM class in Appendix C. Similarly, the designs that use the

SVM classification method, regardless of the feature extraction technique used, are categorized under the SVM class in Table 2.6.

To enhance the clarity of Tables 2.3-8, the following notations are used:

(a) BCI designs based on multiple neuromechanisms (as defined in Table 2.2) are presented in separate categories such as MN: Sensorimotor Activity + Response to Mental tasks, which show that the design is based on the sensorimotor activity and the response to mental tasks neuromechanisms.

(b) Two or more methods that are consecutively used in a design block are separated by "-". As an example, *CSP–log transformation* denotes a design that first applies common spatial patterns (CSP) on the signal and then applies a logarithmic function on the resulting time-series.

(c) Two methods that are applied simultaneously in a design component are separated by "+". For example, *AR parameters + PSD parameters* corresponds to a design that uses both autoregressive (AR) and power-spectral-density (PSD) features in the feature-extraction block.

(d) *LRP + {CSP – log-transformation}* denotes designs that use the two kinds of feature-extraction methods separated by "+". The first method is based on the extraction of lateralized readiness potentials (LRP), and the second feature extraction method is based on consecutively applying CSP followed by a logarithm function on the signals that are grouped in "{ }".

(e) To facilitate readability, we have provided an index of terms in Appendix A.

Table 2.3 Pre-processing (signal enhancement) methods in BCI designs

Pre-Processing method	Reference ID
Common average referencing (CAR)	(Cheng *et al* 2004, Fabiani *et al* 2004, Kubler *et al* 2005, Li *et al* 2004b, McFarland and Wolpaw 1998, McFarland *et al* 1997, McFarland *et al* 2003, Peters *et al* 2001, Ramoser *et al* 2000, Schalk *et al* 2000, Wolpaw *et al* 1997)
Surface Laplacian (SL)	(Babiloni *et al* 2000, Babiloni *et al* 2001b, Cincotti *et al* 2001, Cincotti *et al* 2003a, Dornhege *et al* 2004, Fabiani *et al* 2004, Gysels and Celka 2004, McFarland and Wolpaw 1998, McFarland *et al* 1997, McFarland *et al* 2003, McFarland *et al* 2005, Millan *et al* 2004a, Millan *et al* 2002a, Millan *et al* 2002b, Millan *et al* 1998, Millan *et al* 2000a, Millan 2004, Millan and Mourino 2003b, Millan *et al* 2004b, Muller *et al* 2003b, Peters *et al* 2001, Qin *et al* 2004b, Qin *et al* 2004a, Qin and He 2005, Qin *et al* 2005, Ramoser *et al* 2000, Schalk *et al* 2000, Wang *et al* 2004b, Wang *et al* 2004a, Wolpaw and McFarland 2004, Millan *et al* 2003a)
Independent component analysis (ICA)	(Bayliss and Ballard 1999, Bayliss and Ballard 2000a, Bayliss and Ballard 2000b, Erfanian and Erfani 2004, Gao Xiaorong *et al* 2004, Peterson *et al* 2005, Wu *et al* 2004, Serby *et al* 2005, Xu *et al* 2004a, Wang *et al* 2004c, Li *et al* 2004a)
Common spatial patterns (CSP)	(Blanchard and Blankertz 2004, Dornhege *et al* 2003, Dornhege *et al* 2004, Guger *et al* 2000b, Krauledat *et al* 2004, Krauledat *et al* 2004, Muller *et al* 2003b, Pfurtscheller *et al* 2000, Pfurtscheller and Neuper 2001, Pfurtscheller and Neuper 2001, Ramoser *et al* 2000, Townsend *et al* 2004, Xu *et al* 2004b)
Principal component analysis (PCA)	(Chapin *et al* 1999, Guan *et al* 2004, Hu *et al* 2004, Isaacs *et al* 2000, Lee and Choi 2002, Lee and Choi 2003, Thulasidas *et al* 2004, Xu *et al* 2004a, Yoon *et al* 2005, Li *et al* 2004a)
Combined CSP and PCA	(Xu *et al* 2004b)
Singular value decomposition (SVD)	(Trejo *et al* 2003)
Common spatio-spatial patterns (CSSP)	(Lemm *et al* 2005)
Frequency normalization (Freq-Norm)	(Bashashati *et al* 2005, Borisoff *et al* 2004, Fatourechi *et al* 2004, Fatourechi *et al* 2005, Yu *et al* 2002)
Local averaging technique (LAT)	(Peters *et al* 2001)
Robust Kalman filtering	(Bayliss and Ballard 1999, Bayliss and Ballard 2000a)
Common spatial subspace decomposition (CSSD)	(Cheng *et al* 2004, Li *et al* 2004b, Liu *et al* 2003, Wang *et al* 2004d)
Wiener filtering	(Vidal 1977)
Sparse component analysis	(Li *et al* 2004a)
Maximum noise fraction (MNF)	(Peterson *et al* 2005)
Spike detection methods	(Obeid and Wolf 2004)
Neuron ranking methods	(Sanchez *et al* 2004)

Table 2.4 Feature selection/dimensionality reduction methods in BCI designs

Feature selection/dimensionality reduction method	Reference ID
Genetic algorithm (GA)	(Flotzinger *et al* 1994, Garrett *et al* 2003, Graimann *et al* 2003a, Graimann *et al* 2004, Peterson *et al* 2005, Scherer *et al* 2004, Schroder *et al* 2003, Tavakolian *et al* 2004, Yom-Tov and Inbar 2001, Yom-Tov and Inbar 2002)
Principal component analysis (PCA)	(Anderson *et al* 1995a, Bashashati *et al* 2005, Borisoff *et al* 2004, Fatourechi *et al* 2004, Fatourechi *et al* 2005)
Distinctive sensitive learning vector quantization (DSLVQ)	(Flotzinger *et al* 1994, Neuper *et al* 2005, Pfurtscheller *et al* 1996, Pfurtscheller *et al* 1997, Pfurtscheller *et al* 1998, Pfurtscheller *et al* 2000, Pfurtscheller and Neuper 2001, Pregenzer and Pfurtscheller 1995, Pregenzer and Pfurtscheller 1999)
Sequential forward feature selection (SFFS)	(Fabiani *et al* 2004, Keirn and Aunon 1990)
Grid search method	(Glassman 2005)
Relief method (Kira and Rendell 1992)	(Millan *et al* 2002a)
Recursive feature/channel elimination (RFE)	(Lal *et al* 2004, Schröder *et al* 2005)
Support vector machine (SVM)-based recursive feature elimination	(Gysels *et al* 2005)
Stepwise discriminant procedure	(Vidal 1977)
Linear discriminant analysis (LDA)	(Graimann *et al* 2003b)
Fisher discriminant analysis (dimensionality reduction)	(Wang *et al* 2004d)
Fisher discriminant-based criterion (feature selection)	(Cheng *et al* 2004, Lal *et al* 2004)
Zero-Norm Optimization (*l*0-opt)	(Lal *et al* 2004)
Orthogonal Least Square (OLS1) based on radial basis function (RBF)	(Xu *et al* 2004b)

TABLE 2.5 FEATURE EXTRACTION METHODS IN BCI DESIGNS. REFER TO APPENDIX 2 FOR A MORE DETAILED VERSION OF THIS TABLE

Neurological phenomenon	Feature Extraction method	Reference ID
Sensorimotor Activity	**Spectral parameters**	(Babiloni *et al* 2000, Babiloni *et al* 2001a, Babiloni *et al* 2001b, Blanchard and Blankertz 2004, Boostani and Moradi 2004, Cho *et al* 2004, Cincotti *et al* 2001, Cincotti *et al* 2003a, Cincotti *et al* 2003b, Coyle *et al* 2005, Fabiani *et al* 2004, Flotzinger *et al* 1994, Garcia *et al* 2003b, Garrett *et al* 2003, Guger *et al* 2000b, Guger *et al* 2003a, Ivanova *et al* 1995, Kalcher *et al* 1992, Kalcher *et al* 1993, Kelly *et al* 2002b, Krauledat *et al* 2004, Krausz *et al* 2003, Kubler *et al* 2005, Lal *et al* 2004, Leeb and Pfurtscheller 2004, Lemm *et al* 2005, Mahmoudi and Erfanian 2002, Mason and Birch 2000, McFarland and Wolpaw 1998, McFarland *et al* 1997, McFarland *et al* 2003, McFarland *et al* 2005, Millan *et al* 2002a, Millan *et al* 2002b, Muller *et al* 2003c, Muller-Putz *et al* 2005b, Neuper *et al* 2003, Neuper *et al* 2005, Pfurtscheller *et al* 2005, Pfurtscheller *et al* 1993, Pfurtscheller *et al* 1994, Pfurtscheller *et al* 1996, Pfurtscheller *et al* 1997, Pfurtscheller *et al* 1998, Pfurtscheller *et al* 2000, Pfurtscheller and Neuper 2001, Pfurtscheller and Neuper 2001, Pfurtscheller and Neuper 2001, Pfurtscheller and Neuper 2001, Pfurtscheller *et al* 2003a, Pfurtscheller *et al* 2003b, Pineda *et al* 2003, Pregenzer and Pfurtscheller 1995, Pregenzer and Pfurtscheller 1999, Ramoser *et al* 2000, Schalk *et al* 2000, Scherer *et al* 2004, Sheikh *et al* 2003, Townsend *et al* 2004, Trejo *et al* 2003, Jia *et al* 2004, Wolpaw *et al* 1991, Wolpaw and McFarland 1994, Wolpaw *et al* 1997, Wolpaw *et al* 2000, Wolpaw *et al* 2003, Wolpaw and McFarland 2004, Li *et al* 2004a)
	Parametric modeling (AR, AAR & ARX parameters)	(Burke *et al* 2002, Burke *et al* 2005, Graimann *et al* 2003b, Guger *et al* 1999, Guger *et al* 2000a, Guger *et al* 2003a, Guger *et al* 2003b, Haselsteiner and Pfurtscheller 2000, Huggins *et al* 2003, Kelly *et al* 2002b, Kelly *et al* 2002a, Lal *et al* 2004, Neuper *et al* 1999, Obermaier *et al* 2001b, Obermaier *et al* 2001a, Peters *et al* 2001, Pfurtscheller *et al* 1998, Pfurtscheller and Guger 1999, Pfurtscheller *et al* 2000, Pfurtscheller and Neuper 2001, Schloegl *et al* 1997a, Schloegl *et al* 1997b, Schlogl *et al* 2003, Schröder *et al* 2005, Sykacek *et al* 2003, Yoon *et al* 2005)
	TFR method	(Bashashati *et al* 2005, Birch *et al* 2002, Birch *et al* 2003, Borisoff *et al* 2004, Bozorgzadeh *et al* 2000, Costa and Cabral 2000, Fatourechi *et al* 2004, Fatourechi *et al* 2005, Garcia *et al* 2003a, Garcia *et al* 2003b, Glassman 2005, Graimann *et al* 2003a, Graimann *et al* 2004, Huggins *et al* 2003, Lemm *et al* 2004, Lisogurski and Birch 1998, Mason and Birch 2000, Mason *et al* 2004, Pineda *et al* 2000, Qin *et al* 2004b, Qin and He 2005, Qin *et al* 2005, Yom-Tov and Inbar 2003)
	CCTM	(Balbale *et al* 1999, Graimann *et al* 2003b, Graimann *et al* 2004, Huggins *et al* 1999, Huggins *et al* 2003, Levine *et al* 1999, Levine *et al* 2000)
	Signal envelope – Cross-correlation	(Wang *et al* 2004b, Wang *et al* 2004a)
	Hjorth parameters	(Boostani and Moradi 2004, Lee and Choi 2002, Obermaier *et al* 2001a, Obermaier *et al* 2001c, Pfurtscheller and Neuper 2001)
	Signal complexity	(Boostani and Moradi 2004, Roberts *et al* 1999, Trejo *et al* 2003)
	Combination of different feature extraction methods	(Cheng *et al* 2004, Dornhege *et al* 2003, Dornhege *et al* 2004, Krauledat *et al* 2004, Mahmoudi and Erfanian 2002, Muller *et al* 2003b, Yom-Tov and Inbar 2001, Yom-Tov and Inbar 2002)
	LRP features	(Blankertz *et al* 2002a, Blankertz *et al* 2003, Krauledat *et al* 2004)

Neurological phenomenon	Feature Extraction method	Reference ID
	Other	(Coyle *et al* 2004, Huggins *et al* 2003, Hung *et al* 2005, LaCourse and Wilson 2003, Li *et al* 2004b, Liu *et al* 2003, Mason and Birch 2000, Pineda *et al* 2000, Qin *et al* 2004a, Qin *et al* 2005, Wang *et al* 2004d, Xu *et al* 2004b, Yom-Tov and Inbar 2003)
	None	(Barreto *et al* 1996a, Barreto *et al* 1996b, Blankertz *et al* 2002a, Lee and Choi 2002, Lee and Choi 2003, Mahmoudi and Erfanian 2002, Parra *et al* 2002, Parra *et al* 2003a, Schroder *et al* 2003, Trejo *et al* 2003)
SCP	**Calculation of SCP amplitude**	(Birbaumer *et al* 1999, Birbaumer *et al* 2000, Hinterberger *et al* 2003, Hinterberger *et al* 2004a, Hinterberger *et al* 2004b, Hinterberger *et al* 2005b, Hinterberger *et al* 2005a, Kaiser *et al* 2001, Kaiser *et al* 2002, Kubler *et al* 1999, Kubler *et al* 2001b, Kubler *et al* 1998, Neumann *et al* 2003, Neumann *et al* 2004)
	TFR method	(Bostanov 2004, Hinterberger *et al* 2003)
	Mixed filter	(Hinterberger *et al* 2003)
	None	(Hinterberger *et al* 2003, Schroder *et al* 2003)
P300	**Cross-correlation**	(Bayliss and Ballard 1999, Bayliss and Ballard 2000a, Bayliss and Ballard 2000b, Farwell and Donchin 1988)
	Stepwise discriminant analysis	(Donchin *et al* 2000, Farwell and Donchin 1988)
	Matched filtering	(Serby *et al* 2005)
	PPM	(Jansen *et al* 2004)
	TFR method	(Bostanov 2004, Donchin *et al* 2000, Fukada S *et al* 1998, Glassman 2005, Jansen *et al* 2004, Kawakami *et al* 1996)
	Peak picking	(Allison and Pineda 2003, Allison and Pineda 2005, Bayliss *et al* 2004, Farwell and Donchin 1988)
	Area calculation	(Farwell and Donchin 1988)
	Area and peak picking	(Kaper and Ritter 2004b, Xu *et al* 2004a)
	Not mentioned (calculated P300 but details not mentioned)	(Bayliss 2003, Polikoff *et al* 1995)
	None	(Guan *et al* 2004, Jansen *et al* 2004, Kaper and Ritter 2004a, Kaper and Ritter 2004b, Kaper *et al* 2004, Thulasidas *et al* 2004)
VEP	**Spectral parameters**	(Cheng Ming *et al* 2005, Cheng and Gao 1999, Cheng *et al* 2001, Cheng *et al* 2002, Gao *et al* 2003b, Kelly *et al* 2004, Kelly *et al* 2005c, Kelly *et al* 2005a, Kelly *et al* 2005b, Lalor *et al* 2005, Middendorf *et al* 2000, Muller-Putz *et al* 2005a, Wang *et al* 2005a, Wang *et al* 2004c)
	Lock-in amplifier	(Calhoun and McMillan 1996, McMillan and Calhoun 1995, Muller-Putz *et al* 2005a)
	Asymmetry ratio of different band powers	(Su Ryu *et al* 1999)
	Cross-correlation	(Sutter 1992)
	Amplitude between N2 and P2 peaks	(Lee *et al* 2005)

Neurological phenomenon	Feature Extraction method	Reference ID
Response to Mental tasks[8]	None	(Guan *et al* 2005, Vidal 1977)
	Spectral parameters	(Bashashati *et al* 2003, Keirn and Aunon 1990, Kostov and Polak 1997, Liu *et al* 2005, Millan *et al* 1998, Palaniappan *et al* 2002, Palaniappan 2005, Peterson *et al* 2005, Polak and Kostov 1997, Polak and Kostov 1998, Wang *et al* 2005a)
	Parametric modeling (AR & AAR parameters)	(Anderson *et al* 1995b, Anderson *et al* 1998, Garrett *et al* 2003, Huan and Palaniappan 2004, Keirn and Aunon 1990, Kostov and Polak 2000, Huan and Palaniappan 2005, Polak and Kostov 1998, Polak and Kostov 1999, Sykacek *et al* 2003)
	Signal Complexity	(Bashashati *et al* 2003, Tavakolian *et al* 2004)
	Eigen values of correlation matrix	(Anderson *et al* 1998)
	LPC using Burg's method	(Kostov and Polak 1997)
ANC	None	(Anderson *et al* 1995a, Panuccio *et al* 2002)
	Cross-covariance - PCA	(Isaacs *et al* 2000)
	LBG vector quantization (VQ)	(Darmanjian *et al* 2003)
	Filtering – Rectification - Thresholding	(Karniel *et al* 2002, Kositsky *et al* 2003, Reger *et al* 2000a, Reger *et al* 2000b)
	Averaging	(Laubach *et al* 2000, Otto *et al* 2003, Vetter *et al* 2003)
	TFR methods	(Laubach *et al* 2000, Musallam *et al* 2004)
	None (Most of these designs model the relationship between neural firing rates and 'position and/or velocity and/or acceleration' of hand)	(Black *et al* 2003, Byron *et al* 2005, Carmena *et al* 2003, Carmena *et al* 2005, Chapin *et al* 1999, Gao *et al* 2002, Gao *et al* 2003a, Hatsopoulos *et al* 2004, Hu *et al* 2004, Karniel *et al* 2002, Kemere *et al* 2004, Kennedy *et al* 2000, Kim *et al* 2005a, Kim *et al* 2005b, Lebedev *et al* 2005, Olson *et al* 2005, Patil *et al* 2004, Rao *et al* 2005, Roushe *et al* 2003, Sanchez *et al* 2002a, Sanchez *et al* 2002b, Sanchez *et al* 2003, Serruya *et al* 2003, Serruya *et al* 2002, Taylor *et al* 2002, Taylor *et al* 2003, Wessberg *et al* 2000, Wu *et al* 2002a, Wu *et al* 2002b)
MN: Sensorimotor Activity + Response to Mental Tasks	Spectral parameters	(Gysels and Celka 2004, Gysels *et al* 2005, Millan *et al* 2004a, Millan *et al* 2002b, Millan *et al* 2000a, Millan *et al* 2000b, Millan 2004, Millan and Mourino 2003b, Millan *et al* 2004b, Obermaier *et al* 2001d, Varsta *et al* 2000, Millan *et al* 2003a)
	Parametric modeling	(Curran *et al* 2004, Penny *et al* 2000, Roberts and Penny 2003, Sykacek *et al* 2004, Varsta *et al* 2000)
	TFR method	(Garcia and Ebrahimi 2002, Garcia *et al* 2002, Garcia *et al* 2003c, Molina *et al* 2003, Varsta *et al* 2000)

[8] Designs that differentiate between relaxed state and movement tasks are considered in "Sensorimotor activity + Response to Mental Tasks" category.

Neurological phenomenon	Feature Extraction method	Reference ID
	Combination of different features	(Erfanian and Erfani 2004)
	PLV	(Gysels and Celka 2004, Gysels *et al* 2005)
	Mean spectral coherence	(Gysels and Celka 2004)
	None	(Mourino *et al* 2002, Rezek *et al* 2003)
MN: SCP + other brain rhythms	**SCP calculation + Power spectral parameters**	(Hinterberger and Baier 2005Mensh *et al* 2004)

TABLE 2.6 FEATURE CLASSIFICATION METHODS IN BCI DESIGNS THAT USE EEG AND ECOG RECORDING TECHNOLOGY

Feature translation method		Reference ID
Neural Networks (NN)	***MLP***	(Anderson *et al* 1995b, Anderson *et al* 1995a, Anderson *et al* 1998, Costa and Cabral 2000, Erfanian and Erfani 2004, Fukada S *et al* 1998, Garrett *et al* 2003, Haselsteiner and Pfurtscheller 2000, Huan and Palaniappan 2004, Hung *et al* 2005, Ivanova *et al* 1995, Mahmoudi and Erfanian 2002, Huan and Palaniappan 2005, Palaniappan 2005, Su Ryu *et al* 1999, Tavakolian *et al* 2004)
	Committee of MLP NN	(Millan *et al* 2002b, Millan *et al* 2000b, Varsta *et al* 2000)
	FIR- MLP NN	(Haselsteiner and Pfurtscheller 2000)
	Committee of Plat's RAN algorithm (Platt 1991)	(Millan *et al* 1998)
	Committee of NNs trained with Adaboost	(Boostani and Moradi 2004)
	Committee of single Perceptrons with no hidden layers	(Peters *et al* 2001)
	TBNN	(Ivanova *et al* 1995)
	TDNN	(Barreto *et al* 1996a, Barreto *et al* 1996b)
	LVQ	(Flotzinger *et al* 1994, Ivanova *et al* 1995, Kalcher *et al* 1992, Kalcher *et al* 1993, Pfurtscheller *et al* 1993, Pfurtscheller *et al* 1994, Pfurtscheller *et al* 1996, Pfurtscheller *et al* 1997, Pfurtscheller *et al* 1998, Pfurtscheller *et al* 2000, Pfurtscheller and Neuper 2001, Pregenzer and Pfurtscheller 1999)
	kMeans – LVQ	(Bashashati *et al* 2005, Birch *et al* 2002, Birch *et al* 2003, Borisoff *et al* 2004, Bozorgzadeh *et al* 2000, Fatourechi *et al* 2004, Fatourechi *et al* 2005, Lisogurski and Birch 1998, Mason and Birch 2000, Mason *et al* 2004, Yom-Tov and Inbar 2003)
	fART – LVQ	(Borisoff *et al* 2004)
	DSLVQ	(Muller-Putz *et al* 2005a, Neuper *et al* 2005, Pregenzer and Pfurtscheller 1995, Pregenzer and Pfurtscheller 1999)
	Growing Hierachical SOM	(Liu *et al* 2005)
	ALN	(Kostov and Polak 1997, Polak and Kostov 1998, Polak and Kostov 1999, Kostov and Polak 2000)
	ANN	(Cincotti *et al* 2003b)
	Custom designed local NN	(Mourino *et al* 2002, Millan *et al* 2002b, Millan *et al* 2000a, Millan and Mourino 2003b)
	Fuzzy ARTMAP	(Palaniappan *et al* 2002)
	Single layer NN	(Garcia *et al* 2002)
	RBF-NN	(Hung *et al* 2005)
	Static neural classifier (Adaline)	(Barreto *et al* 1996a, Barreto *et al* 1996b)
	Gamma NN	(Barreto *et al* 1996a, Barreto *et al* 1996b)

Feature translation method		Reference ID
(R)LDA[9]		(Boostani and Moradi 2004, Bostanov 2004, Burke *et al* 2002, Burke *et al* 2005, Coyle *et al* 2005, Coyle *et al* 2004, Dornhege *et al* 2003, Dornhege *et al* 2004, Fabiani *et al* 2004, Fukada S *et al* 1998, Garcia *et al* 2003b, Garrett *et al* 2003, Guger *et al* 2000b, Guger *et al* 2003a, Guger *et al* 2003b, Hinterberger *et al* 2003, Huan and Palaniappan 2004, Huggins *et al* 2003, Kelly *et al* 2002b, Kelly *et al* 2002a, Kelly *et al* 2004, Kelly *et al* 2005c, Kelly *et al* 2005a, Krauledat *et al* 2004, Krausz *et al* 2003, Lalor *et al* 2005, Leeb and Pfurtscheller 2004, Lemm *et al* 2005, Mensh *et al* 2004, Muller *et al* 2003c, Muller-Putz *et al* 2005a, Muller-Putz *et al* 2005b, Muller *et al* 2003b, Neuper *et al* 1999, Neuper *et al* 2003, Obermaier *et al* 2001b, Pfurtscheller *et al* 1998, Pfurtscheller and Guger 1999, Pfurtscheller *et al* 2000, Pfurtscheller and Neuper 2001, Pfurtscheller *et al* 2003b, Schloegl *et al* 1997a, Schloegl *et al* 1997b, Townsend *et al* 2004, Jia *et al* 2004)
(R)FLD		(Babiloni *et al* 2001b, Blanchard and Blankertz 2004, Blankertz *et al* 2002a, Blankertz *et al* 2003, Cincotti *et al* 2001, Cincotti *et al* 2003a, Guger *et al* 1999, Guger *et al* 2000a, Hung *et al* 2005, Obermaier *et al* 2001a, Pfurtscheller *et al* 2003a, Scherer *et al* 2004, Li *et al* 2004a)
Sparse FLD		(Blankertz *et al* 2002a)
MD-based classifier		(Babiloni *et al* 2001a, Cincotti *et al* 2003a, Cincotti *et al* 2003b, Garcia and Ebrahimi 2002, Molina *et al* 2003)
Nonlinear discriminant function		(Fabiani *et al* 2004)
Bayes quadratic classifier		(Keirn and Aunon 1990)
Bayesian classifier (linear classifier)		(Curran *et al* 2004, Lemm *et al* 2004, Penny *et al* 2000, Roberts and Penny 2003)
Linear Bayesian decision rule		(Vidal 1977)
Linear classifier based on time-warping		(Mason and Birch 2000)
Logistic regression		(Parra *et al* 2002, Parra *et al* 2003a)
Linear classifier (no details)		(Ramoser *et al* 2000)
Single layer Perceptron model (a linear classifier)		(Li *et al* 2004b, Wang *et al* 2004d)
2-dimensional linear classifier trained by a non-enumerative search procedure		(Cheng *et al* 2004)
ZDA		(Hinterberger *et al* 2003)
LDS		(Lee and Choi 2002)
Gaussian classifier		(Millan *et al* 2004a, Millan 2004, Millan *et al* 2004b , Millan *et al* 2003a)
SSP		(Babiloni *et al* 2000, Babiloni *et al* 2001a, Babiloni *et al* 2001b, Cincotti *et al* 2001, Cincotti *et al* 2003a, Millan *et al* 2002b, Millan *et al* 2000b)
SOM-based SSP		(Millan *et al* 2002b, Millan *et al* 2000b)
HMM Based techniques	***CHMM***	(Rezek *et al* 2003)
	AR HMM	(Panuccio *et al* 2002)
	HMM + SVM	(Lee and Choi 2002, Lee and Choi 2003)

[9] Regularization may be applied before LDA classification scheme.

Feature translation method	Reference ID
HMM	(Cincotti *et al* 2003b, Lee and Choi 2003, Liu *et al* 2003, Obermaier *et al* 2001a, Obermaier *et al* 2001c, Obermaier *et al* 2001d, Pfurtscheller and Neuper 2001, Sykacek *et al* 2003)
SVM	(Blankertz *et al* 2002a, Guan *et al* 2004, Garcia *et al* 2003a, Garcia *et al* 2003b, Garcia *et al* 2003c, Garrett *et al* 2003, Glassman 2005, Gysels and Celka 2004, Gysels *et al* 2005, Hung *et al* 2005, Guan *et al* 2005, Kaper and Ritter 2004a, Kaper and Ritter 2004b, Kaper *et al* 2004, Lal *et al* 2004, Peterson *et al* 2005, Schroder *et al* 2003, Schröder *et al* 2005, Thulasidas *et al* 2004, Trejo *et al* 2003, Xu *et al* 2004b, Yom-Tov and Inbar 2001, Yom-Tov and Inbar 2002, Yom-Tov and Inbar 2003, Yoon *et al* 2005)
NID3	(Ivanova *et al* 1995)
CN2	(Ivanova *et al* 1995)
C4.5	(Ivanova *et al* 1995, Millan *et al* 2002a)
k-NN	(Blankertz *et al* 2002a, Pineda *et al* 2000, Pregenzer and Pfurtscheller 1999)
Threshold detector	(Allison and Pineda 2003, Balbale *et al* 1999, Bayliss and Ballard 1999, Bayliss and Ballard 2000a, Bayliss and Ballard 2000b, Bayliss 2003, Bayliss *et al* 2004, Calhoun and McMillan 1996, Cheng Ming *et al* 2005, Cheng and Gao 1999, Cheng *et al* 2001, Cheng *et al* 2002, Donchin *et al* 2000, Farwell and Donchin 1988, Gao *et al* 2003b, Graimann *et al* 2003a, Graimann *et al* 2003b, Graimann *et al* 2004, Hinterberger *et al* 2003, Huggins *et al* 1999, Huggins *et al* 2003, Jansen *et al* 2004, Kawakami *et al* 1996, Kelly *et al* 2005b, Kostov and Polak 1997, Lee *et al* 2005, Levine *et al* 1999, Levine *et al* 2000, McMillan and Calhoun 1995, Middendorf *et al* 2000, Pfurtscheller *et al* 2005, Pineda *et al* 2003, Polak and Kostov 1997, Polikoff *et al* 1995, Qin *et al* 2004a, Qin *et al* 2004b, Qin and He 2005, Roberts *et al* 1999, Serby *et al* 2005, Sutter 1992, Wang *et al* 2004b, Wang *et al* 2004a, Xu *et al* 2004a, Yom-Tov and Inbar 2003)
Linear combination - Threshold detector	(Townsend *et al* 2004)
Continuous feedback + Threshold detector	(Birbaumer *et al* 1999, Birbaumer *et al* 2000, Hinterberger *et al* 2003, Hinterberger *et al* 2004a, Hinterberger *et al* 2004b, Hinterberger *et al* 2005b, Hinterberger *et al* 2005a, Kaiser *et al* 2001, Kaiser *et al* 2002, Kubler *et al* 1999, Kubler *et al* 2001b, Kubler *et al* 1998, Neumann *et al* 2003, Neumann *et al* 2004)
Linear combination - Continuous feedback	(Fabiani *et al* 2004, Krausz *et al* 2003, Kubler *et al* 2005, McFarland and Wolpaw 1998, McFarland *et al* 1997, McFarland *et al* 2003, McFarland *et al* 2005, Schalk *et al* 2000, Sheikh *et al* 2003, Wolpaw and McFarland 1994, Wolpaw *et al* 1997, Wolpaw *et al* 2000, Wolpaw *et al* 2003, Wolpaw and McFarland 2004)
Continuous feedback	(Bashashati *et al* 2003, Cho *et al* 2004, LaCourse and Wilson 2003, Middendorf *et al* 2000, Trejo *et al* 2003, Wolpaw *et al* 1991)
Continuous feedback using MD	(Schlogl *et al* 2003)
Continuous audio feedback	(Hinterberger and Baier 2005)
Variatioanal Kalman filter	(Sykacek *et al* 2004)
Static classifier that is inferred with sequential variational inference	(Curran *et al* 2004, Sykacek *et al* 2004)
Random forest algorithm	(Neuper *et al* 1999)

TABLE 2.7 FEATURE CLASSIFICATION METHODS IN BCI DESIGNS THAT ARE BASED ON NEURAL CORTICAL RECORDINGS

Feature Classification		Reference ID
Neural Networks	***Recurrent MLP Neural network (RNN)***	(Sanchez *et al* 2002a, Sanchez *et al* 2002b, Sanchez *et al* 2003)
	MLP	(Kim *et al* 2005b)
	Feed-forward ANN	(Patil *et al* 2004)
	ANN recurrent dynamic back-propagation	(Chapin *et al* 1999)
	ANN model	(Hatsopoulos *et al* 2004, Wessberg *et al* 2000)
	LVQ	(Laubach *et al* 2000)
	Other	(Karniel *et al* 2002)
Support vector machine regression (SVR) model		(Kim *et al* 2005b)
Cosine tuning model (a linear model)		(Black *et al* 2003, Kemere *et al* 2004, Taylor *et al* 2002, Taylor *et al* 2003)
Linear Gaussian models (LGM) implemented by Kalman filter		(Black *et al* 2003, Gao *et al* 2003a, Patil *et al* 2004, Sanchez *et al* 2002a, Wu *et al* 2002a, Wu *et al* 2002b)
Generalized linear models (GLA)		(Black *et al* 2003, Gao *et al* 2003a)
Generalized additive models (GAM)		(Black *et al* 2003, Gao *et al* 2003a)
Weighted linear combination of neuronal activity (Wiener filter: a linear model)		(Carmena *et al* 2005, Hatsopoulos *et al* 2004, Kim *et al* 2005a, Kim *et al* 2005b, Lebedev *et al* 2005, Patil *et al* 2004, Sanchez *et al* 2002b, Serruya *et al* 2003, Serruya *et al* 2002)
Gamma filter (a linear model)		(Sanchez *et al* 2002b)
Mixture of multiple models based on NMF (non-negative matrix factorization)		(Kim *et al* 2005a)
Echo State Networks (ESN) - Optimal sparse linear mapping		(Rao *et al* 2005)
Linear model (no details mentioned)		(Carmena *et al* 2003, Wessberg *et al* 2000)
Threshold detector		(Otto *et al* 2003, Roushe *et al* 2003, Vetter *et al* 2003)
SVM		(Byron *et al* 2005, Hu *et al* 2004, Olson *et al* 2005)
Bayesian classifier		(Gao *et al* 2002, Hu *et al* 2004, Musallam *et al* 2004)
Maximum likelihood-based model		(Hatsopoulos *et al* 2004, Kemere *et al* 2004, Serruya *et al* 2003)
LPF (continuous signal)		(Karniel *et al* 2002, Kositsky *et al* 2003, Reger *et al* 2000a, Reger *et al* 2000b)
Direct translation of firing rate to cursor movement (continuous signal)		(Kennedy *et al* 2000)
k-NN		(Isaacs *et al* 2000)
HMM		(Darmanjian *et al* 2003)

TABLE 2.8 POST PROCESSING METHODS IN BCI DESIGNS

Post processing	Reference ID
ERN (event-related negativity)-based error correction	(Bayliss *et al* 2004, Blankertz *et al* 2002b, Blankertz *et al* 2003, Parra *et al* 2003b, Schalk *et al* 2000)
Successive averaging and/or rejection option for 'moderated' posterior probabilities (choice of "unknown" output state) (SA-UK)	(Anderson *et al* 1995a, Bashashati *et al* 2005, Birch *et al* 2002, Borisoff *et al* 2004, Fatourechi *et al* 2004, Fatourechi *et al* 2005, Gysels and Celka 2004, Millan *et al* 1998, Millan 2004, Millan and Mourino 2003b, Millan *et al* 2004b, Muller-Putz *et al* 2005b, Penny *et al* 2000, Roberts and Penny 2003, Townsend *et al* 2004, Vidal 1977, Millan *et al* 2003a)
Debounce (considering refractory period)	(Bashashati *et al* 2005, Borisoff *et al* 2004, Fatourechi *et al* 2004, Fatourechi *et al* 2005, Muller-Putz *et al* 2005b, Obeid and Wolf 2004, Pfurtscheller *et al* 2005, Townsend *et al* 2004)

2.5. Discussion

Several points raised in the previous section deserve further comment. Fig. 2.2 summarizes the information in Tables 2.3, 2.4, and 2.8, which respectively address signal-enhancement, feature selection and post-processing algorithms in BCI designs. Specifically, this figure shows the number of BCI designs that use specific signal-enhancement, feature selection, and post-processing techniques.

In the remainder of this section we highlight the top 3 or 4 methods that have been used in the signal processing blocks of BCI systems (as introduced in Section 2.2).

Of the 96 BCI designs that employ signal-enhancement techniques before extracting the features from the signal, 32% use surface Laplacian (SL), 22% use either principal component analysis (PCA) or independent component analysis (ICA), 14% use common spatial patterns (CSP) and 11% use common average referencing (CAR) techniques. 38 of the reported BCI designs employ feature-selection algorithms; 26% of these 38 designs use genetic algorithms (GA), 24% use distinctive sensitive learning vector quantization (DSLVQ), and 13% use PCA.

Of the 30 BCI designs that use post-processing algorithms to reduce the amount of error in the output of the BCI system, 57% use averaging techniques and consider rejecting activations that have low certainty, 27% consider using the debounce block (or refractory period) to deactivate the output for a short period of time when a false activation is detected, and 16% use event-related negativity (ERN) signals to detect error activations.

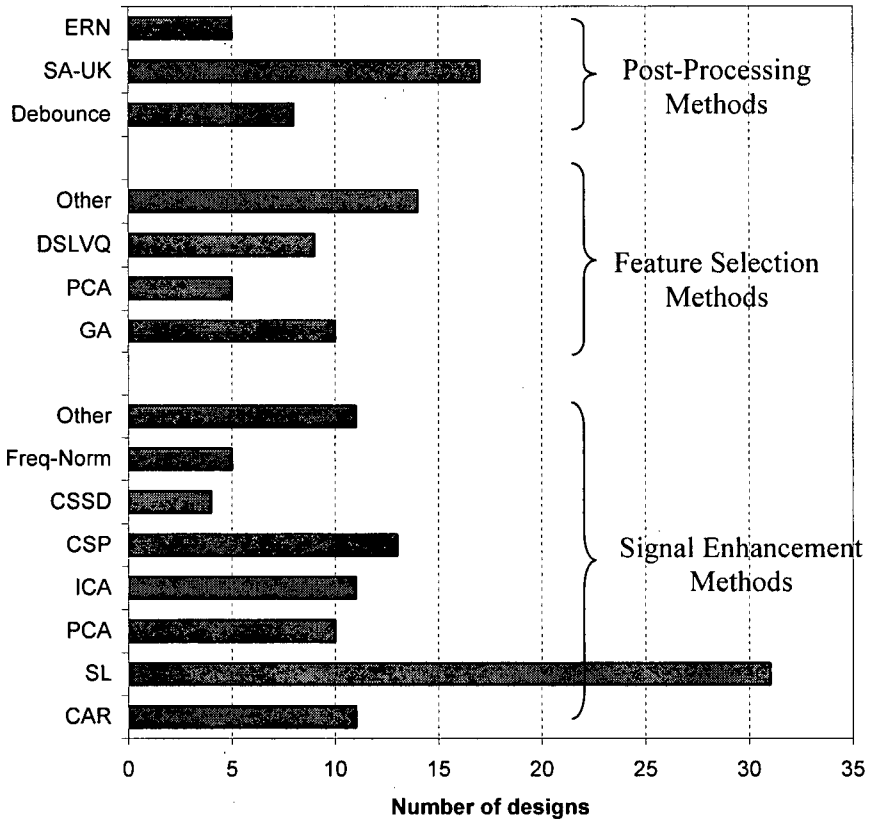

Figure 2.2 Signal-enhancement, feature selection and post-processing methods in BCI designs

Fig. 2.3 summarizes the results presented in Table 2.5, and shows the number of BCI designs that are based on sensorimotor activity, SCP, VEP, P300, activity of neural cells, and 'response to mental tasks' and use different feature extraction techniques.

Based on the results of Fig. 2.3, 41% of the BCIs that are based on the sensorimotor activity use power-spectral-density features, 16% rely on parametric modeling of the data, 13% use time-frequency representation (TFR) methods, and 6% do not employ any feature extraction methods. 74% of the SCP-based BCI designs calculate SCP signals using low-pass filtering methods, and 64% of the VEP-based BCIs use power-spectral features at specific frequencies. 26% of the BCIs based on P300 calculate the peaks of the signal in a specific time window to detect the P300 component of the EEG; 22% use TFR-based methods, 22% use no feature extraction method, and 15% use cross-correlation with a specific template. 41% of the BCI designs that use mental tasks to control a BCI use power-spectral features

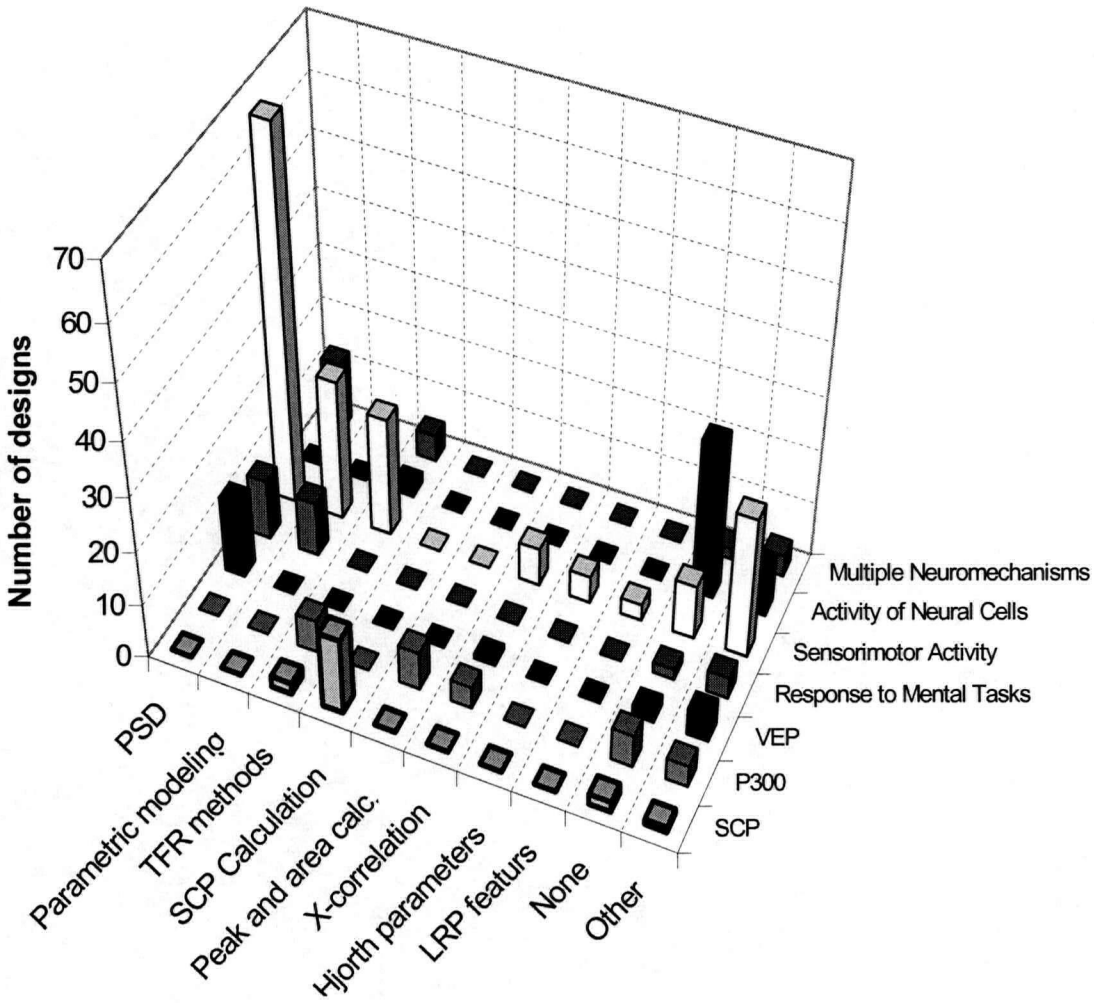

Figure 2.3 Feature extraction methods in BCI designs based on Sensorimotor Activity, VEP, P300, SCP, Response to Mental Tasks, Activity of Neural Cells, and Multiple Neuromechanisms

and 37% use parametric modeling of the input signal. As most of the BCI designs that are based on neural cortical recordings mainly try to model the direct relationship between the neural cortical recordings and movements, they do not use a feature-extraction algorithm. 45% of the BCI designs that are based on multiple neuromechanisms rely on power spectral features, 17% use parametric modeling, and 17% use time-frequency representation (TFR) methods.

Summarizing Tables 2.6 and 2.7, the number of BCI designs that use different feature classification algorithms are shown in Fig. 2.4. About 75% of the BCI designs use classification schemes that are *not* based on neural networks (NN). These are composed of

those methods that use threshold detectors as the feature classifier or as part of the feature classification scheme (27%), linear discriminant (either LDA or FLD) classifiers (26%), those that show continuous feedback of the extracted features (16%), and those that use support-vector-machines (SVM) (11%). 27% of the neural-network-based classifiers are based on the multi-layer perceptrons (MLP) neural network and 39% are based on learning-vector-quantization (LVQ) classification scheme.

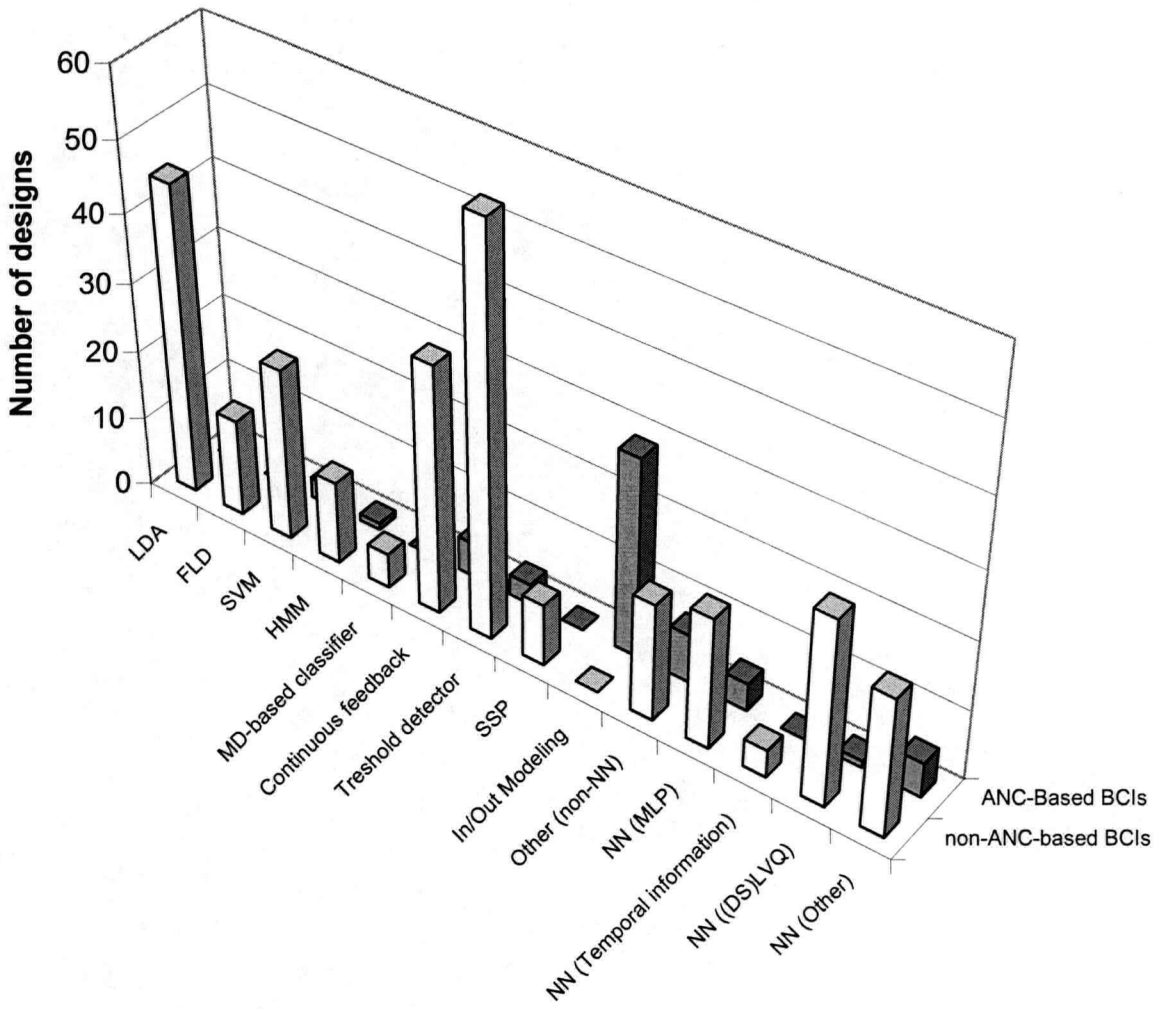

Figure 2.4 Feature classification methods in BCI designs. 'In/Out Modeling' refers to those ANC-based BCIs that directly map the input neural recordings to the output without using a feature extraction technique.

During our analysis of the literature, a number of salient points about the signal processing methods emerged. We think that some of these points are worth sharing with the BCI research community. In the following sections we summarize some of them. Note that these observations are based on comments made by the researchers in their published papers and are also based on the trends in the literature; they do not cover all the methods reported in the literature.

2.5.1. Signal Enhancement

Signal-enhancement (pre-processing) algorithms have been used for brain computer interfaces that are based on the EEG and the activity of the neural cells (ANC), but no signal-enhancement algorithms have been applied on electrocorticogram (ECoG)-based brain computer interfaces. Given the huge difference in the characteristics of EEG and ANC, the signal-enhancement algorithms used in EEG-based and ANC-based BCIs have very little overlap; only PCA has been used in both groups. While ANC-based BCIs mostly aim at spike detection, ranking, and sorting neuron activities, EEG-based ones mostly transform or select EEG channels that yield better performance. Overall, the use of a pre-processing stage before feature extraction (if applied) has been proven to be useful. The choice of a suitable pre-processing technique however is dependent on several factors such as the recording technology, number of electrodes, and neuromechanism of the BCI. Next, we discuss some of the techniques used in signal-enhancement in EEG-based BCI systems. Specifically, a discussion of spatial filtering including referencing methods and common spatial patterns (CSP) is presented. Since these methods are among the most used techniques that have become increasingly popular in BCI studies.

2.5.1.1. Referencing methods

Referencing methods are considered as spatial filters. The proper selection of a spatial filter for any BCI is determined by the location and extent of the control signal (e.g., the Mu rhythm) and of the various sources of EEG or non-EEG noise. The latter two are not completely defined and presumably vary considerably between different studies and both across and within individuals (McFarland *et al* 1997).

For BCIs that use the Mu and Beta rhythms, the common average referencing (CAR) and Laplacian methods are superior to the ear reference method. This may be because these

methods use high-pass spatial filters and enhance the focal activity from the local sources (e.g., the Mu and the Beta rhythms) and reduce the widely distributed activity, including that resulting from distant sources (e.g. EMG, eye movements and blinks, visual alpha rhythm). Comparing the two variations of the Laplacian filtering methods (the large Laplacian and the small Laplacian), it is shown that the large Laplacian method is superior to the small Laplacian method in BCI systems that use the Mu rhythm (McFarland *et al* 1997).

Although an accurate Laplacian estimate from raw potentials requires many electrodes, one study showed that the recognition rates were increased by using a small number of electrodes only (Cincotti *et al* 2003a). In this case, the linear combination of channels implementing the Laplacian estimation was likely to have caused a favorable transformation of the signals to recognize different patterns in the ongoing EEG.

2.5.1.2. Common spatial patterns (CSP)

CSP is a signal-enhancement method that detects patterns in the EEG by incorporating the spatial information of the EEG signal. Some of its features and limitations include the following:

CSP is a signal-enhancement method that detects patterns in the EEG by incorporating the spatial information of the EEG signal. An advantage of the CSP method is that it does not require the a-priori selection of subject-specific frequency bands. Knowledge of these bands, however, is necessary for the band-power and frequency-estimation methods (Guger *et al* 2000b). One disadvantage of the CSP method is that it requires the use of many electrodes. However, the inconvenience of applying more electrodes can be rationalized by improved performance (Guger *et al* 2000b, Pfurtscheller *et al* 2000). The major problem in the application of CSP is its sensitivity to artifacts in the EEG. Since the covariance matrices are used as the basis for calculating the spatial filters, and are estimated with a comparatively small number of examples, a single trial contaminated with artifacts can unfortunately cause extreme changes to the filters (Guger *et al* 2000b, Ramoser *et al* 2000). Since, the CSP method detects spatial patterns in the EEG, any change in the electrode positions may render the improvements in the classification accuracy gained by this method useless. Therefore, this method requires almost identical electrode positions for all trials and sessions which may be difficult to accomplish (Ramoser *et al* 2000).

2.5.2. Feature Extraction

In this section we discuss some of the feature extraction techniques that have received more attention in BCI systems. Specifically, time and/or frequency representation methods, parametric modeling, and specific techniques of modeling neural cortical recordings are discussed.

2.5.2.1. Time and/or Frequency Methods

A signal, as a function of time, may be considered as a representation with perfect temporal resolution. The magnitude of the Fourier transform (FT) of the signal may be considered as a representation with perfect spectral resolution but with no temporal information. Frequency-based features have been widely used in signal processing because of their ease of application, computational speed, and direct interpretation of the results. Specifically, about $1/3^{rd}$ of BCI designs have used power-spectral features. Due to the non-stationary nature of the EEG signals, these features do not provide any time domain information. Thus, mixed time-frequency representations (TFRs) that map a one-dimensional signal into a two-dimensional function of time and frequency are used to analyze the time-varying spectral content of the signals. It has been shown that TFR methods may yield performance improvements comparing to the traditional FT-based methods (e.g. (Qin *et al* 2005, Lemm *at al* 2003, Bostanov 2004)). Most of the designs that employ TFR methods use wavelet-based feature-extraction algorithms. The choice of the particular wavelet used is a crucial factor in gaining useful information from wavelet analysis. Prior knowledge of the physiological activity in the brain can be useful in determining the appropriate wavelet function.

Correlative TFR (CTFR) is another time-frequency representation method that, besides the spectral information, provides information about the time-frequency interactions between the components of the input signal. Thus, with the CTFR the EEG data samples are not independently analyzed (as in the Fourier transform case) but their relationship is also taken into account. One drawback of the CTFR resides in its relative high sensitivity to noise. Consequently, the most important values of the CTFR, in terms of classification must be selected (Garcia *et al* 2003a, b).

2.5.2.2. Parametric Modeling

Parametric approaches assume the time series under analysis to be the output of a given linear mathematical model. They require an a-priori choice of the structure and order of the signal generation mechanism model (Weitkunat 1991). The optimum model order is best estimated not only by maximizing the fitness but also by limiting the model's complexity. For noisy signals, if the model's order is too high, spurious peaks in the spectra will result. On the other hand, if the order is too low, smooth spectra are obtained (Kelly *et al* 2002a, Polak and Kostov 1998, Weitkunat 1991).

For short EEG segments, parametric modeling results in better frequency resolution and a good spectral estimate. Note that parametric modeling may yield poor estimates if the length of the EEG segments processed is too short (Birch 1988). For such modeling, there is no need for a-priori information about potential frequency bands, and there is no need to window the data in order to decrease the spectral leakage. Also, the frequency resolution does not depend on the number of data points (Guger *et al* 2003a, Polak and Kostov 1998, Weitkunat 1991). Estimating these parameters, however, is very sensitive to artifacts (Birch 1988, Guger *et al* 2003a).

Special attention should be paid to the choice of the sampling rate in parametric modeling (Weitkunat 1991), since severely oversampled signals tend to show only very small amplitude differences between successive samples. Hence, low-order models produce small prediction errors, giving the false illusion that an adequate model has been obtained. The sampling rates dictated by the Nyquist criterion are recommended.

2.5.2.3. Modeling the Neural Firing Rates

Extraction algorithms for motor control operate on spike trains, recorded from a population of cortical units, mostly with the purpose of predicting arm trajectories. Several extraction methods such as linear filtering methods and neural networks have been used to determine arm movement trajectories from neural firing rates. We summarize below a few important issues in modeling the neural firing rates. A more detailed critical discussion of extraction algorithms for cortical control of arm prosthetics can be found in (Schwartz *et al* 2001).

One limitation of linear filter methods is that they rely on an a-priori model of movement-related neuronal responses. Artificial neural network (ANN) solutions can optimize each cell's contribution to the population prediction (Schwartz *et al* 2001).

Several of the algorithms used are based on the position of the moving limb. In the primary motor cortex at least, this parameter is more poorly represented than the velocity during movement. With most algorithms, the different sources of variability need to be specified explicitly because some sort of optimal function is being modeled to the cell response (Schwartz *et al* 2001).

The performance of the modeling techniques is constrained by their training sets and may be limited, both in terms of extrapolation beyond and interpolation within the training set when new data are applied. The success of the linear filters is due to the underlying linearity of the relationship between firing rate and movement direction. These filters are limited by the conditions used to fit their coefficients and may suffer from the same training constraints as ANNs (Schwartz *et al* 2001).

2.5.3. Feature Selection

Feature selection algorithms are used in BCI designs to find the most informative features for classification. This is especially useful for BCI designs with high dimensional input data, as it reduces the dimension of the feature space. Since the feature selection block reduces the complexity of the classification problem, higher classification accuracies might be achieved. The experiments carried out in (Flotzinger *et al* 1994, Pregenzer and Pfurtscheller 1999) show that when feature selection is used, the classification accuracy is better than when all the features are used.

Principal component analysis (PCA) and genetic algorithms (GA) are among the mostly used feature selection and/or dimensionality reduction methods in BCIs. PCA has also been widely used in pre-processing stage of BCI designs. PCA is a linear transformation that can be used for dimensionality reduction in a dataset while retaining those characteristics of the dataset that contribute most to its variance, by keeping lower-order principal components and ignoring higher-order ones. Such low-order components often contain the "most important" aspects of the data. PCA has the distinction of being the optimal linear transformation for keeping the subspace that has largest variance. PCA only finds linear subspaces, works best

if the individual components have Gaussian distributtions, and is not optimized for class separability. One other possible application area of PCA is in classification stage, in which, PCA is applied for weighting input features. While a standard neural network, like the multi-layer pereceptrons (MLP) can do the necessary classification itself, in some cases doing a PCA in parallel and weighting input features can give better results as it simplifies the training of the rest of the system.

Unlike PCA, GAs are heuristic search techniques in the problem space. GAs typically maintain a constant-sized population of individuals which represent samples of the space to be searched. Each individual is evaluated on the basis of its overall fitness with respect to the given application domain. New individuals (samples of the search space) are produced by selecting high performing individuals to produce "offspring" which retain many of the features of their "parents". This eventually leads to a population that has improved fitness with respect to the given goal. Genetic algorithms have demonstrated substantial improvement over a variety of random and local search methods (De Jong 1975). This is accomplished by their ability to exploit accumulating information about an initially unknown search space in order to bias subsequent search into promising subspaces. Since GAs are basically a domain independent search technique, they are ideal for applications where domain knowledge and theory is difficult or impossible to provide (De Jong 1975). An important step in developing a GA-based search is defining a suitable fitness function. An ideal fitness function correlates closely with the algorithm's goal, and yet may be computed quickly. Speed of execution is very important, as a typical genetic algorithm must be iterated many, many times in order to produce a usable result for a non-trivial problem. Definition of the fitness function is not strightforward in many cases and often is performed iteratively if the fittest solutions produced by a GA are not what is desired.

2.5.4. Feature Classification

Linear classifiers are generally more robust than nonlinear ones. This is because linear classifiers have fewer free parameters to tune, and are thus less prone to over-fitting (Muller *et al* 2003a). In the presence of strong noise and outliers, even linear systems can fail. One way of overcoming this problem is to use regularization. Regularization helps limit (a) the

influence of outliers and strong noise, (b) the complexity of the classifier, and (c) the raggedness of the decision surface (Muller *et al* 2003a).

It is always desirable to avoid reliance on nonlinear classification methods, if possible, because these methods often involve a number of parameters whose values must be chosen appropriately. However, when there are large amounts of data and limited knowledge of the data, nonlinear methods are better suited in finding the potentially more complex structure in the data. In particular, when the source of the data to be classified is not well understood, using methods that are good at finding nonlinear transformation of the data is suggested. In these cases, kernel-based and neural-networks-based methods can be used to determine the transformations. Kernel-based classifiers are classification methods that apply a linear classification in some appropriate (kernel) feature space. Thus, all the beneficial properties of linear classification are maintained, but at the same time, the overall classification is nonlinear. Examples of such kernel-based classification methods are support-vector-machines (SVMs) and kernel Fisher discriminant (KFD) (Muller *et al* 2003a). For a more detailed critical discussion regarding linear and nonlinear classifiers in brain computer interfaces, refer to (Muller *et al* 2003a).

Some BCI designs have used classification algorithms such as FIR-MLP and TBNN that utilize temporal information of the input data (Haselsteiner and Pfurtscheller 2000, Ivanova *et al* 1995). The motivation for using such classifiers is that the patterns to be recognized are not static data but time series. Thus, the temporal information of the input data can be used to improve the classification results (Haselsteiner and Pfurtscheller 2000). Utilizing the temporal information of features is not necessarily performed directly in the classification stage, and can be done with a static classifier like MLP and a mapping of the temporal input data to static data. However, using classifiers such as FIR-MLP and TBNN that directly utilize temporal information may yield better performances as they are much better suited for exploiting temporal information contained in the time series to be classified. Regardless of the method that is used for exploiting temporal information, these approaches are preferred over static classification as they may increase the performance of BCI systems.

Using a group (committee) of classifiers rather than using a single classifier might also yield to better performances of BCI systems. Only a few BCI designs have employed such an

approach in classifying features and achieved performance improvements (Millan *et al* 2002b, Millan *et al* 2000b, Peters *et al* 2001, Varsta *et al* 2000). The classification accuracy of the committee depends on how much unique information each committee member contributes to classification. A committee of classifiers usually yields better classification accuracy than any individual classifier could provide, and can be used to combine information from several channels, i.e., from different spatial regions (Peters *et al* 2001).

As the number of epochs available for evaluating a BCI system is small, using a technique that reduces the bias of the estimated performance on a specific data set is highly recommended. This is especially important when different architectures of a certain design are being compared. K-fold cross-validation and statistical significance tests are especially useful for these cases (e.g. refer to (Anderson *et al* 1998, Kelly *et al* 2002b, Lalor *et al* 2005, Obermaier *et al* 2001d, Peterson *et al* 2005)). K-fold cross-validation can be used simply to estimate the generalization error of a given model, or it can be used for model selection by choosing one of several models that has the smallest estimated generalization error but it is not suitable for online evaluations. A value of 5 to 10 for K is recommended for estimating the generalization error. For an insightful discussion of the limitations of cross-validatory choice among several learning methods, see (Stone 1977).

2.5.5. Post-Processing

Post-processing techniques can be utilized in most of the BCI designs to decrease the error rates. Some post-processing techniques can be designed specifically for a target application. For example, when a BCI system is used to activate a spelling device, some letters can be omitted without losing information. The system can also take into consideration the conditional probabilities of letters provided by one or two preceding letters and make corresponding suggestions to the patient (Kubler *et al* 1999). Such techniques may also be feasible for other applications and consequently increase the performance of the BCI systems.

There is a possibility that just after the end of a trial, some features of the brain signal reveal whether or not the trial was successful (that is, whether the outcome was or was not what the subject desired). These features are referred to as error potentials and can be used to detect errors in a BCI system and void the outcome. This error detection approach was encouraged

by evidence that errors in conventional motor performances have detectable effects on the EEG recorded just after the error occurs (Falkenstein *et al* 1995, Falkenstein *et al* 2001, Gehring *et al* 1995). Whatever the nature of the error potential, the central decision for a BCI is how useful the error potential can be in detecting errors in single trials, and thereby improving accuracy. While its signal-to-noise ratio (SNR) is low, the error potential can improve the performance of a BCI system. In the meantime, better methods for recognizing and measuring the error potential could substantially improve its SNR, and thereby increase its impact on accuracy of a BCI system. Such error potentials have been used in a few BCI systems to increase the performance (Bayliss *et al* 2004, Blankertz *et al* 2002b, Blankertz *et al* 2003, Parra *et al* 2003b, Schalk *et al* 2000).

Another useful technique in decreasing false activations of BCI systems is to consider a measure of confidence in classification. In such case, the output of the system can only be activated when the probability of the output being in an active state is greater than a given probability threshold or some criterion. Otherwise, the response of the BCI is considered "unknown" and rejected to avoid making risky decisions. This is a useful way of reducing false decisions of the system (e.g., (Cincotti et al 2003b, Millan et al 1998, Penny et al 2000)) and might be used in any BCI design.

Considering mechanisms like debouncing the output of BCI designs also can reduce the number of false activations (Bashashati *et al* 2005, Borisoff *et al* 2004, Fatourechi *et al* 2004, Fatourechi *et al* 2005, Muller-Putz *et al* 2005b, Obeid and Wolf 2004, Pfurtscheller *et al* 2005, Townsend *et al* 2004). These methods are specifically useful for so called asynchronous (self-paced) BCIs. Since false positives could happen in periods longer than just a few samples, using debouncing technique in a manner similar to the debouncing of physical switches is expected to improve false activation rates (but with a cost in decreased re-activation time). The debounce component continuously monitors the output of the classifier. After an activation is detected (e.g., a change in logical state from '0' to '1' in a binary classifier), the output is activated for one time sample, then the output is forced to an inactive state for Td-1 time samples, where Td is the debounce time period in samples. In some studies this time period is referred to as refractory period. As the debounce period is increased, the false activation rate is decreased for a given true positive rate. However, with

increasing this time period, the re-activation time of the BCI system is impacted. The trade-off is clear and one needs to consider this for a given application.

2.6. Conclusions

We have completed the first comprehensive survey of signal processing methods used in BCI studies and published prior to January 2006. The results of this survey form a valuable and historical cross-reference for methods used in the following signal processing components of a BCI design: (1) pre-processing (signal-enhancement), (2) feature selection, (3) feature extraction, (4) feature classification, and (5) post-processing methods. This survey shows which signal-processing techniques have received more attention and which have not. This information is also valuable for newcomers to the field, as they can now find out which signal-processing methods have been used for a certain type of a BCI system.

Many signal processing methods have been proposed and implemented in various brain computer interfaces and comparison of these methods for different BCI applications would be a useful task. However, at this point we cannot perform this task given the diversity of brain computer interface systems from different aspects such as target application, neurological phenomena used, amount of data tested, number of subjects and the amount of training they have received, recording systems, and experimental paradigms. Also acknowledged in (McFarland *et al* 2006), we think that comparison of methods would be possible in well-designed systematic studies (Jackson *et al* 2006) and on established datasets like the BCI Competition datasets (Blankertz *et al* 2004, Blankertz *et al* 2006). We believe that, for a fair comparison of methods, more data would be needed as comparing methods with the data of one or two subjects does not necessarily guarantee the same findings on a larger subject pool. (Jackson *et al* 2006) has provided a step towards this goal by proposing some ways to establish a systematic study both in design and reporting the results and we think that this task would only be possible with the collective help of all the researchers in this field.

We hope that this study will spawn further discussion of signal processing schemes for BCI designs. The proposed taxonomy and classes defined in Tables 2.3-8, represent a proposed set of subcategories, not a final one, and we encourage others to revise or expand upon this initial set. Our direction in the future is to establish an online public-accessible database

where research groups will be able to submit their signal processing designs as well as propose revisions/expansions of the proposed definitions and categories presented in this paper.

2.7. References

Allison B Z and Pineda J A 2003 ERPs evoked by different matrix sizes: Implications for a brain computer interface (BCI) system *IEEE Trans. Neural Syst. Rehabil. Eng.* **11** 110-3

Allison B Z and Pineda J A 2005 Effects of SOA and flash pattern manipulations on ERPs, performance, and preference: Implications for a BCI system *Int J Psychophysiol* **59** 127-40

Anderson C W, Devulapalli S V and Stolz E A 1995a Signal classification with different signal representations *Proc. IEEE Workshop on Neural Networks for Signal Processing* 475-83

Anderson C W, Stolz E A and Shamsunder S 1995b Discriminating mental tasks using EEG represented by AR models *Proc. 17th Annual Int. Conf. of the IEEE Engineering in Medicine and Biology Society (Montreal)* pp 875-6

Anderson C W, Stolz E A and Shamsunder S 1998 Multivariate autoregressive models for classification of spontaneous electroencephalographic signals during mental tasks *IEEE Trans. Biomed. Eng.* **45** 277-86

Babiloni F, Cincotti F, Lazzarini L, Millan J, Mourino J, Varsta M, Heikkonen J, Bianchi L and Marciani M G 2000 Linear classification of low-resolution EEG patterns produced by imagined hand movements *IEEE Trans. Rehabil. Eng.* **8** 186-8

Babiloni F, Bianchi L, Semeraro F, Millan J R, Mourino J, Cattini A, Salinari S, Marciani M G and Cincotti F 2001a Mahalanobis distance-based classifiers are able to recognize EEG patterns by using few EEG electrodes *Proc. 23rd Annual Int. Conf. of the IEEE Engineering in Medicine and Biology Society (Istanbul)* pp 651-4

Babiloni C, Babiloni F, Carducci F, Cappa S F, Cincotti F, Del Percio C, Miniussi C, Moretti D V, Rossi S, Sosta K and Rossini P M 2004 Human cortical responses during one-bit short-term memory. A high-resolution EEG study on delayed choice reaction time tasks *Clin. Neurophysiol.* **115** 161-70

Babiloni F, Cincotti F, Bianchi L, Pirri G, Millan J R, Mourino J, Salinari S and Marciani M G 2001b Recognition of imagined hand movements with low resolution surface laplacian and linear classifiers *Med. Eng. Phys.* **23** 323-8

Balbale U H, Higgins J E, Bement S L and Levine S P 1999 Multi-channel analysis of human event-related cortical potentials for the development of a direct brain interface *Proc. 21st Annual Int. Conf. of the IEEE Engineering in Medicine and Biology Society & Annual Fall meeting of the Biomedical Engineering Society (Atlanta, GA)* p 447

Barreto A B, Taberner A M and Vicente L M 1996a Classification of spatio-temporal EEG readiness potentials towards the development of a brain-computer interface *Proc. IEEE Southeast Conf. (Raleigh, NC)* pp 99-102

Barreto A B, Taberner A M and Vicente L M 1996b Neural network classification of spatio-temporal EEG readiness potentials *Proc. IEEE 15th Southern Biomedical Engineering Conf. (Dayton, OH)* pp 73-6

Bashashati A, Ward R K and Birch G E 2005 A new design of the asynchronous brain computer interface using the knowledge of the path of features *Proc. 2nd IEEE-EMBS Conf. on Neural Engineering (Arlington, VA)* pp 101-4

Bashashati A, Ward R K, Birch G E, Hashemi M R and Khalilzadeh M A 2003 Fractal dimension-based EEG biofeedback system *Proc. 25th Annual Int. Conf. of the IEEE Engineering in Medicine and Biology Society (Cancun, Mexico)* pp 2220-3

Bayliss J D 2003 Use of the evoked potential P3 component for control in a virtual apartment *IEEE Trans Neural Syst Rehabil Eng* **11** 113-6

Bayliss J D and Ballard D H 1999 Single trial P300 recognition in a virtual environment *Proc. Int. ICSC Symp. on Soft Computing in Biomedicine (Genova, Italy)*

Bayliss J D and Ballard D H 2000a Recognizing evoked potentials in a virtual environment *Advances in Neural Information Processing Systems* vol 12, eds S A Solla, T K Leen and K R Müller (Cambridge, MA: MIT Press) pp 3–9

Bayliss J D and Ballard D H 2000b A virtual reality testbed for brain-computer interface research *IEEE Trans Rehabil. Eng.* **8** 188-90

Bayliss J D, Inverso S A and Tentler A 2004 Changing the P300 brain computer interface *Cyberpsychol. Behav.* **7** 694-704

Birbaumer N, Ghanayim N, Hinterberger T, Iversen I, Kotchoubey B, Kubler A, Perelmouter J, Taub E and Flor H 1999 A spelling device for the paralysed *Nature* **398** 297-8

Birbaumer N, Kubler A, Ghanayim N, Hinterberger T, Perelmouter J, Kaiser J, Iversen I, Kotchoubey B, Neumann N and Flor H 2000 The thought translation device (TTD) for completely paralyzed patients *IEEE Trans Rehabil Eng* **8** 190-3

Birch G E 1988 *Single trial EEG signal analysis using outlier information* PhD Thesis (Vancouver, Canada: The University of British Columbia)

Birch G E, Bozorgzadeh Z and Mason S G 2002 Initial on-line evaluations of the LF-ASD brain-computer interface with able-bodied and spinal-cord subjects using imagined voluntary motor potentials *IEEE Trans Neural Syst. Rehabil. Eng.* **10** 219-24

Birch G E, Mason S G and Borisoff J F 2003 Current trends in brain-computer interface research at the neil squire foundation *IEEE Trans. Neural Syst. Rehabil. Eng.* **11** 123-6

Black M J, Bienenstock E, Donoghue J P, Wu W and Gao Y 2003 Connecting brains with machines: The neural control of 2D cursor movement *Proc. 2nd IEEE-EMBS Conf. on Neural Engineering (Arlington, VA)* pp 580-3

Blanchard G and Blankertz B 2004 BCI competition 2003--data set IIa: Spatial patterns of self-controlled brain rhythm modulations *IEEE Trans. Biomed. Eng.* **51** 1062-6

Blankertz B, Curio G and Muller K R 2002a Classifying single trial EEG: Towards brain computer interfacing *Advances in Neural Information Processing Systems* vol 14, eds. T G Dietterich, S Becker and Z Ghahramani (Cambridge, MA: MIT Press) pp 157-64.

Blankertz B, Dornhege G, Sch├ñfer C, Krepki R, Kolmorgen J, Muller K R, Kunzmann V, Losch F and Curio G 2003 Boosting bit rates and error detection for the classification of fast-paced motor commands based on single-trial EEG analysis *IEEE Trans. Neural Syst. Rehabil. Eng.* **11** 127-31

Blankertz B, Muller K R, Curio G, Vaughan T M, Schalk G, Wolpaw J R, Schlogl A, Neuper C, Pfurtscheller G, Hinterberger T, Schroder M and Birbaumer N 2004 The BCI competition

2003: Progress and perspectives in detection and discrimination of EEG single trials *IEEE Trans. Biomed. Eng.* **51** 1044-51

Blankertz B, Muller K R, Krusienski D J, Schalk G, Wolpaw J R, Schlogl A, Pfurtscheller G, Millan Jdel R, Schroder M and Birbaumer N 2006 The BCI competition. III: Validating alternative approaches to actual BCI problems *IEEE Trans. Neural Syst. Rehabil. Eng.* **14** 153-9

Blankertz B, Sch ├ñfer C, Dornhege G and Curio G 2002b Single trial detection of EEG error potentials: A tool for increasing BCI transmission rates *Proc. Int. Conf. on Artificial Neural Networks (Madrid, Spain)* pp 1137-43

Boostani R and Moradi M H 2004 A new approach in the BCI research based on fractal dimension as feature and adaboost as classifier *J. Neural Eng.* **1** 212-7

Borisoff J F, Mason S G, Bashashati A and Birch G E 2004 Brain-computer interface design for asynchronous control applications: Improvements to the LF-ASD asynchronous brain switch *IEEE Trans. Biomed. Eng.* **51** 985-92

Bostanov V 2004 BCI competition 2003--data sets ib and IIb: Feature extraction from event-related brain potentials with the continuous wavelet transform and the t-value scalogram *IEEE Trans. Biomed. Eng.* **51** 1057-61

Bozorgzadeh Z, Birch G E and Mason S G 2000 The LF-ASD BCI: On-line identification of imagined finger movements in spontaneous EEG with able-bodied subjects *Proc. IEEE Int. Conf. on Acoustics, Speech and Signal Processing (Istanbul, Turkey)* pp 109-13

Burke D, Kelly S, Chazal P d and Reilly R 2002 A simultaneous filtering and feature extraction strategy for direct brain interfacing *Proc. 24th Annual Int. Conf. of the IEEE Engineering in Medicine and Biology Society (Houston, TX)* pp 279-80

Burke D P, Kelly S P, de Chazal P, Reilly R B and Finucane C 2005 A parametric feature extraction and classification strategy for brain-computer interfacing *IEEE Trans. Neural Syst. Rehabil. Eng.* **13** 12-7

Byron O, He J P, Hu J and Si J 2005 A conceptual brain machine interface system *Proc. 1st Int. Conf. on Neural Interface and Control (Wuhan, ,China)* pp 40-44

Calhoun G L and McMillan G R 1996 EEG-based control for human-computer interaction *Proc. 3rd Symp. On Human Interaction with Complex Systems (Dayton, OH)* pp 4-9

Carmena J M, Lebedev M A, Crist R E, O'Doherty J E, Santucci D M, Dimitrov D F, Patil P G, Henriquez C S and Nicolelis M A 2003 Learning to control a brain-machine interface for reaching and grasping by primates *Plos Biol* **1** 193-208

Carmena J M, Lebedev M A, Henriquez C S and Nicolelis M A 2005 Stable ensemble performance with single-neuron variability during reaching movements in primates *J Neurosci* **25** 10712-6

Chapin J K, Moxon K A, Markowitz R S and Nicolelis M A 1999 Real-time control of a robot arm using simultaneously recorded neurons in the motor cortex *Nat. Neurosci.* **2** 664-70

Cheng M and Gao S 1999 An EEG-based cursor control system Proc. 21st Annual Int. Conf. of the IEEE Engineering in Medicine and Biology Society & Annual Fall meeting of the Biomedical Engineering Society (Atlanta, GA) p 669

Cheng M, Gao X, Gao S and Wang B 2005 Stimulation frequency extraction in SSVEP-based brain-computer interface *Proc. 1st Int. Conf. on Neural Interface and Control (Wuhan, China)* pp 64-7

Cheng M, Gao X, Gao S and Xu D 2002 Design and implementation of a brain-computer interface with high transfer rates *IEEE Trans. Biomed. Eng.* **49** 1181-6

Cheng M, Jia W, Gao X, Gao S and Yang F 2004 Mu rhythm-based cursor control: An offline analysis *Clin. Neurophysiol.* **115** 745-51

Cheng M, Xu D, Gao X and Gao S 2001 Brain-computer interface with high transfer rates *Proc. 8th Int. Conf. on Neural Information Processing (Shanghai, China)*

Cho B H, Kim S, Shin D I, Lee J H, Lee S M, Kim I Y and Kim S I 2004 Neurofeedback training with virtual reality for inattention and impulsiveness *Cyberpsychol Behav.* **7** 519-26

Cincotti F, Bianchi L, Millan J, Mourino J, Salinari S, Marciani M G and Babiloni F 2001 Brain computer interface: The use of low resolution surface laplacian and linear classifiers

for the recognition of imagined hand movements *Proc. 23rd Annual Int. Conf. of the IEEE Engineering in Medicine and Biology Society (Istanbul)* pp 655-8

Cincotti F, Mattia D, Babiloni C, Carducci F, Salinari S, Bianchi L, Marciani M G and Babiloni F 2003a The use of EEG modifications due to motor imagery for brain-computer interfaces *IEEE Trans. Neural Syst. Rehabil. Eng.* **11** 131-3

Cincotti F, Scipione A, Timperi A, Mattia D, Marciani M G, Millan J, Salinari S, Bianchi L and Babiloni F 2003b Comparison of different feature classifiers for brain computer interfaces *Proc. 25th Annual Int. Conf. of the IEEE Engineering in Medicine and Biology Society (Cancun, Mexico)* pp 645-7

Costa E J and Cabral E F 2000 EEG-based discrimination between imagination of left and right hand movements using adaptive gaussian representation *Med. Eng. Phys.* **22** 345-8

Coyle D, Prasad G and McGinnity T M 2004 Extracting features for a brain-computer interface by self-organising fuzzy neural network-based time series prediction *Proc. 26th Annual Int. Conf. of the IEEE Engineering in Medicine and Biology Society (San Francisco, CA)* pp 4371-4

Coyle D, Prasad G and McGinnity T M 2005 A time-frequency approach to feature extraction for a brain-computer interface with a comparative analysis of performance measures *EURASIP J. Appl. Signal Processing* **2005** 3141-51

Curran E, Sykacek P, Stokes M, Roberts S J, Penny W, Johnsrude I and Owen A M 2004 Cognitive tasks for driving a brain-computer interfacing system: A pilot study *IEEE Trans Neural Syst Rehabil Eng* **12** 48-54

Darmanjian S, Kim S P, Nechbya M C, Morrison S, Principe J, Wessberg J and Nicolelis M A 2003 Bimodal brain-machine interface for motor control of robotic prosthetic *Proc. IEEE/RSJ Int. Conf. on Intelligent Robots and Systems (Las Vegas, NV)* pp 3612-7

De Jong K A 1975 *An analysis of the behaviour of a class of genetic adaptive systems* PhD thesis (Ann Arbor, MI: University of Michigan) Diss. Abstr. Int. 36(10), 5140B, University Microfilms No. 76--9381. 44.

Deecke L and Kornhuber H 1976 Voluntary finger movement in man: Cerebral potentials and theory *Biol. Cybern.* **23** 99-119

Donchin E, Spencer K M and Wijesinghe R 2000 The mental prosthesis: Assessing the speed of a P300-based brain-computer interface *IEEE Trans Rehabil Eng* **8** 174-9

Donoghue J P 2002 Connecting cortex to machines: Recent advances in brain interfaces *Nat. Neurosci.* **5** 1085-8

Dornhege G, Blankertz B and Curio G 2003 Speeding up classification of multi-channel brain-computer interfaces: Common spatial patterns for slow cortical potentials *Proc. 2nd IEEE-EMBS Conf. on Neural Engineering (Arlington, VA)* pp 595-8

Dornhege G, Blankertz B, Curio G and Muller K R 2004 Boosting bit rates in noninvasive EEG single-trial classifications by feature combination and multiclass paradigms *IEEE Trans. Biomed. Eng.* **51** 993-1002

Erfanian A and Erfani A2004 ICA-based classification scheme for EEG-based brain-computer interface: The role of mental practice and concentration skills *Proc. 26th Annual Int. Conf. of the IEEE Engineering in Medicine and Biology Society (San Francisco, CA)* pp 235-8

Fabiani G E, McFarland D J, Wolpaw J R and Pfurtscheller G 2004 Conversion of EEG activity into cursor movement by a brain-computer interface (BCI) *IEEE Trans. Neural Syst. Rehabil. Eng.* **12** 331-8

Falkenstein M, Hielscher H, Dziobek I, Schwarzenau P, Hoormann J, Sunderman B and Hohnsbein J 2001 Action monitoring, error detection, and the basal ganglia: an ERP study *Neuroreport* **12** 157–61

Falkenstein M, Hohnsbein J and Hoormann J 1995 Event-related potential correlates of errors in reaction tasks *Perspectives of event-related brain potentials research* ed Karmos *et al* (Amsterdam: Elsevier) pp 287-296

Farwell L A and Donchin E 1988 Talking off the top of your head: Towards a mental prosthesis utilizing event-related brain potentials *Electroencephalogr Clin Neurophysiol* **80** 510-23

Fatourechi M, Bashashati A, Borisoff J F, Birch G E and Ward R K 2004 Improving the performance of the LF-ASD brain computer interface by means of genetic algorithm *Proc. IEEE Symposium on Signal Processing and Information Technology (Rome, Italy)* pp 38-41

Fatourechi M, Bashashati A, Ward R K and Birch G E 2005 A hybrid genetic algorithm approach for improving the performance of the LF-ASD brain computer interface *Proc. IEEE Int. Conf. on Acoustics, Speech and Signal Processing (Philadelphia, PA)* pp 345-8

Flotzinger D, Pregenzer M and Pfurtscheller G 1994 Feature selection with distinction sensitive learning vector quantisation and genetic algorithms *Proc. IEEE Int. Conf. On Neural Networks (Orlando, FL)* pp 3448-51

Fukada S, Tatsumi D, Tsujimoto H and Inokuchi S 1998 Studies of input speed of word inputting system using event-related potential *Proc. 20th Annual Int. Conf. of the IEEE Engineering in Medicine and Biology Society (Hong Kong)* pp 1458-60

Gao Y, Black M J, Bienenstock E, Shoham S and Donoghue J P 2002 Probabilistic inference of hand motion from neural activity in motor cortex *Advances in Neural Information Processing Systems* vol 14, eds. T G Dietterich, S Becker and Z Ghahramani (Cambridge, MA: MIT Press) pp 213-20

Gao Y, Black M J, Bienenstock E, Wu W and Donoghue J P 2003a A quantitative comparison of linear and non-linear models of motor cortical activity for the encoding and decoding of arm motions *Proc. 25th Annual Int. Conf. of the IEEE Engineering in Medicine and Biology Society (Hong Kong)* pp 189-92

Gao X, Xu D, Cheng M and Gao S 2003b A BCI-based environmental controller for the motion-disabled *IEEE Trans. Neural Syst. Rehabil. Eng.* **11** 137-40

Gao X, Xu N, Hong B, Gao S and Yang F 2004 Optimal selection of independent components for event-related brain electrical potential enhancement *Proc. IEEE Int. Workshop on Biomedical Circuits and Systems (Singapore)* pp S3/5/INV-S3/5/1-4

Garcia G and Ebrahimi T 2002 Time-frequency-space kernel for single EEG-trial classification *Presented at the 5th Nordic Signal Processing Symp. (Norway)*

Garcia G, Ebrahimi T and Vesin J M 2002 Classification of EEG signals in the ambiguity domain for brain computer interface applications *Proc. IEEE 14th Int. Conf. on Digital Signal Processing (Santorini, Greece)* pp 301-305

Garcia G, Ebrahimi T and Vesin J M 2003a Correlative exploration of EEG signals for direct brain-computer communications *Proc. IEEE Int. Conf. on Acoustics, Speech, and Signal Processing (Hong Kong)* pp 816-9

Garcia G, Ebrahimi T and Vesin J M 2003b Support vector EEG classification in the fourier and time-frequency correlation domains *Proc. 1st IEEE-EMBS Conf. on Neural Engineering (Capri Island, Italy)* pp 591-4

Garcia G N, Ebrahimi T, Vesin J M and Villca A 2003c Direct brain-computer communication with user rewarding mechanism *Proc. IEEE Int. Symp. in Information Theory (Yokohama, Japan)* pp 221.

Garrett D, Peterson D A, Anderson C W and Thaut M H 2003 Comparison of linear, nonlinear, and feature selection methods for EEG signal *IEEE Trans. Neural Syst. Rehabil. Eng.* **11** 141-4

Gehring W J, Coles M G H, Meyer D E, Donchin E 1995 A brain potential manifestation of error-related processing," In: Perspectives of event-related brain potentials research *EEG Suppl 44* ed Karmos *et al* (Amsterdam: Elsevier) pp 261-72

Georgopoulos A P, Langheim F J, Leuthold A C and Merkle A N 2005 Magnetoencephalographic signals predict movement trajectory in space *Exp. Brain Res.* **167** 132-5

Gevins A, Bressler S L, Morgan N H, Cutillo B A, White R M, Greer D S and Illes J 1989 Event-related covariances during a bimanual visuomotor taks. I. methods and analysis of stimulus- and response-locked data *Electroencephalogr Clin Neurophysiol* **74** 58-75

Glassman E L 2005 A wavelet-like filter based on neuron action potentials for analysis of human scalp electroencephalographs *IEEE Trans. Biomed. Eng.* **52** 1851-62

Graimann B, Huggins J E, Levine S P and Pfurtscheller G 2003a Detection of ERP and ERD/ERS patterns in single ECoG channels *Proc. 1st IEEE-EMBS Conf. on Neural Engineering (Capri Island, Italy)* pp 614-7

Graimann B, Huggins J E, Levine S P and Pfurtscheller G 2004 Toward a direct brain interface based on human subdural recordings and wavelet-packet analysis *IEEE Trans. Biomed. Eng.* **51** 954-62

Graimann B, Huggins J E, Schlogl A, Levine S P and Pfurtscheller G 2003b Detection of movement-related desynchronization patterns in ongoing single-channel electrocorticogram *IEEE Trans. Neural Syst. Rehabil. Eng.* **11** 276-81

Guan C, Thulasidas M and Wu J 2004 High performance P300 speller for brain-computer interface *Proc. IEEE Int. Workshop on Biomedical Circuits and Systems (Singapore)* pp S3/5/INV-S3/13-16

Guger C, Edlinger G, Harkam W, Niedermayer I and Pfurtscheller G 2003a How many people are able to operate an EEG-based brain-computer interface (BCI)? *IEEE Trans. Neural Syst. Rehabil. Eng.* **11** 145-7

Guger C, Edlinger G and Pfurtscheller G2003b How many people are able to operate an EEG-based brain-computer interface (BCI)? *Presented at the 2nd Int. Meeting on Brain-Computer Interfaces for Communication and Control (Albany, NY)*

Guger C, Muller G, Neuper C, Krausz G, Niedermayer I and Pfurtscheller G 2000a Brain-computer communication system: The EEG-based control of a hand orthesis in a quadriplegic patient *Presented at the Int. Conf. on Computers Helping People with Special Needs (Karlsruhe, Germany)*

Guger C, Ramoser H and Pfurtscheller G 2000b Real-time EEG analysis with subject-specific spatial patterns for a brain-computer interface (BCI) *IEEE Trans. Rehabil. Eng.* **8** 447-56

Guger C, Schloegl A, Walterspacher D and Pfurtscheller G 1999 Design of an EEG-based brain-computer interface (BCI) from standard components running in real-time under windows *Biomed Tech (Berl)* **44** 12-6

Gysels E and Celka P 2004 Phase synchronization for the recognition of mental tasks in a brain-computer interface *IEEE Trans. Neural Syst. Rehabil. Eng.* **12** 406-15

Gysels E, Renevey P and Celka P 2005 SVM-based recursive feature elimination to compare phase synchronization computed from broadband and narrowband EEG signals in brain-computer interfaces *Signal Process.* **85** 2178-89

Guan J, Chen Y, Lin J, YunYuan and Huang M 2005 N2 components as features for brain computer interface *Proc. 1st Int. Conf. on Neural Interface and Control (Wuhan, ,China)* pp 45-9

Hallett M 1994 Movement-related cortical potentials *Electromyogr. Clin. Neurophysiol.* **34** 5-13

Haselsteiner E and Pfurtscheller G 2000 Using time-dependent neural networks for EEG classification *IEEE Trans. Rehabil. Eng.* **8** 457-63

Hatsopoulos N, Joshi J and O'Leary J G 2004 Decoding continuous and discrete motor behaviors using motor and premotor cortical ensembles *J Neurophysiol.* **92** 1165-74

Hill N J, Lal T N, Bierig K, Birbaumer N and Scholkopf B 2004 Attention modulation of auditory event-related potentials in a brain-computer interface *Proc. IEEE Int. Workshop on Biomedical Circuits and Systems (Singapore)* pp S3/5/INV-S3/17-20

Hinterberger T and Baier G 2005 Parametric orchestral sonification of EEG in real time *IEEE Multimedia* **12** 70-9

Hinterberger T, Kubler A, Kaiser J, Neumann N and Birbaumer N 2003 A brain-computer interface (BCI) for the locked-in: Comparison of different EEG classifications for the thought translation device *Electroencephalogr Clin Neurophysiol* **114** 416-25

Hinterberger T, Neumann N, Pham M, Kubler A, Grether A, Hofmayer N, Wilhelm B, Flor H and Birbaumer N 2004a A multimodal brain-based feedback and communication system *Exp Brain Res* **154** 521-6

Hinterberger T, Veit R, Wilhelm B, Weiskopf N, Vatine J J and Birbaumer N 2005a Neuronal mechanisms underlying control of a brain-computer interface *Eur. J. Neurosci.* **21** 3169-81

Hinterberger T, Weiskopf N, Veit R, Wilhelm B, Betta E and Birbaumer N 2004b An EEG-driven brain-computer interface combined with functional magnetic resonance imaging (fMRI) *IEEE Trans. Biomed. Eng.* **51** 971-4

Hinterberger T, Wilhelm B, Mellinger J, Kotchoubey B and Birbaumer N 2005b A device for the detection of cognitive brain functions in completely paralyzed or unresponsive patients *IEEE Trans. Biomed. Eng.* **52** 211-20

Hu J, Si J, Olson B P and He J 2004 Principle component feature detector for motor cortical control *Proc. 26th Annual Int. Conf. of the IEEE Engineering in Medicine and Biology Society (San Francisco, CA)* pp 4021-4

Huan N J and Palaniappan R 2004 Neural network classification of autoregressive features from electroencephalogram signals for brain-computer interface design *J. Neural Eng.* **1** 142-50

Huggins J E, Levine S P, Bement S L, Kushwaha R K, Schuh L A, Passaro E A, Rohde M M, Ross D A, Elisevich K V and Smith B J 1999 Detection of event-related potentials for development of a direct brain interface *J Clin Neurophysiol* **16** 448-55

Huggins J E, Levine S P, Fessler J A, Sowers W M, Pfurtscheller G, Graimann B, Schloegl A, Minecan D N, Kushwaha R K, Bement S L, Sagher O and Schuh L A 2003 Electrocorticogram as the basis for a direct brain interface: Opportunities for improved detection accuracy *Proc. 1st IEEE-EMBS Conf. on Neural Engineering (Capri Island, Italy)* pp 587-90

Hung C I, Lee P L, Wu Y T, Chen L F, Yeh T C and Hsieh J C 2005 Recognition of motor imagery electroencephalography using independent component analysis and machine classifiers *Ann. Biomed. Eng.* **33** 1053-70

Isaacs R E, Weber D J and Schwartz A B 2000 Work toward real-time control of a cortical neural prothesis *IEEE Trans Rehabil. Eng.* **8** 196-8

Ivanova I, Pfurtscheller G and Andrew C 1995 AI-based classification of single-trial EEG data *Proc. 17th Annual Int. Conf. of the IEEE Engineering in Medicine and Biology Society (Montreal, Canada)* pp 703-4

Jackson M M, Mason S G and Birch G E 2006 Analyzing trends in brain interface technology: A method to compare studies *Ann. Biomed. Eng.* **34** 859-78

Jansen B H, Allam A, Kota P, Lachance K, Osho A and Sundaresan K 2004 An exploratory study of factors affecting single trial P300 detection *IEEE Trans. Biomed. Eng.* **51** 975-8

Jasper H and Penfield W 1949 Electrocortiograms in man: Effect of voluntary movement upon the electrical activity of the precentral gyrus *Arch. Psychiat. Nervenkr.* **183** 163-74

Jia W, Zhao X, Liu H, Gao X, Gao S and Yang F 2004 Classification of single trial EEG during motor imagery based on ERD *Proc. 26th Annual Int. Conf. of the IEEE Engineering in Medicine and Biology Society (San Francisco, CA)* pp 5-8

Kaiser J, Kubler A, Hinterberger T, Neumann N and Birbaumer N 2002 A non-invasive communication device for the paralyzed *Minim Invasive Neurosurg* **45** 19-23

Kaiser J, Perelmouter J, Iversen I H, Neumann N, Ghanayim N, Hinterberger T, Kubler A, Kotchoubey B and Birbaumer N 2001 Self-initiation of EEG-based communication in paralyzed patients *Electroencephalogr Clin Neurophysiol* **112** 551-4

Kalcher J, Flotzinger D and Pfurtscheller G 1992 A new approach to a brain-computer-interface (BCI) based on learning vector quantization (LVQ3) *Proc. 14th Annual Int. Conf. of the IEEE Engineering in Medicine and Biology Society (Paris, France)* pp 1658-9

Kalcher J, Flotzinger D and Pfurtscheller G 1993 Graz brain-computer interface: An EEG-based cursor control system *Proc. 15th Annual Int. Conf. of the IEEE Engineering in Medicine and Biology Society (San Diego, CA)* pp 1264-5

Kaper M, Meinicke P, Grossekathoefer U, Lingner T and Ritter H 2004 BCI competition 2003--data set IIb: Support vector machines for the P300 speller paradigm *IEEE Trans. Biomed. Eng.* **51** 1073-6

Kaper M and Ritter H 2004a Generalizing to new subjects in brain-computer interfacing Proc. 26th Annual Int. Conf. of the IEEE Engineering in Medicine and Biology Society (San Francisco, CA) pp 4363-6

Kaper M and Ritter H 2004b Progress in P300-based brain-computer interfacing *Proc. IEEE Int. Workshop on Biomedical Circuits and Systems (Singapore)* pp S3/5/INV-S3/59-12

Karniel A, Fleming K M, Sanguineti V, Alford S and Mussa-Ivaldi F A 2002 Dynamic properties of the lamprey's neuronal circuits as it drives a two-wheeled robot *Proc. SAB'2002 Workshop on Motor Control in Humans and Robots: On the Interplay of Real Brains and Artificial Devices (Edinburgh, Scotland)* pp 29–36

Kawakami T, Inoue M, Kobayashi Y and Nakashima K 1996 Application of event related potentials to communication aids *Proc. 18th Annual Int. Conf. of the IEEE Engineering in Medicine and Biology Society (Amsterdam, Holland)* pp 2229-31

Keirn Z A and Aunon J I 1990 A new mode of communication between man and his surroundings *IEEE Trans. Biomed. Eng* **37** 1209-14

Kelly S, Burke D, Chazal P d and Reilly R 2002a Parametric models and classification for direct brain interfaces *Proc. Irish Signal and Systems Conf. (Cork, Ireland)* pp 25-26

Kelly S, Burke D, Chazal P d and Reilly R 2002b Parametric models and spectral analysis for classification in brain-computer interfaces *Proc. 14th IEEE International Conf. on Digital Signal Proceesing (Santorini, Greece)* pp 307-10

Kelly S P, Lalor E, Finucane C and Reilly R B 2004 A comparison of covert and overt attention as a control option in a steady-state visual evoked potential-based brain computer interface *Proc. 26th Annual Int. Conf. of the IEEE Engineering in Medicine and Biology Society (San Francisco, CA)* pp 4725-8

Kelly S P, Lalor E, Reilly R B and Foxe J J 2005a Independent brain computer interface control using visual spatial attention-dependent modulations of parieto-occipital alpha *Proc. IEEE-EMBS Conf. on Neural Engineering (Arlington, VA)* pp 667-70

Kelly S P, Lalor E C, Finucane C, McDarby G and Reilly R B 2005b Visual spatial attention control in an independent brain-computer interface *IEEE Trans. Biomed. Eng* **52** 1588-96

Kelly S P, Lalor E C, Reilly R B and Foxe J J 2005c Visual spatial attention tracking using high-density SSVEP data for independent brain-computer communication *IEEE Trans. Neural Syst Rehabil Eng* **13** 172-8

Kemere C, Shenoy K V and Meng T H 2004 Model-based neural decoding of reaching movements: A maximum likelihood approach *IEEE Trans Biomed Eng* **51** 925-32

Kennedy P R, Bakay R A, Moore M M, Adams K and Goldwaithe J 2000 Direct control of a computer from the human central nervous system *IEEE Trans Rehabil Eng* **8** 198-202

Kim K H, Kim S S and Kim S J 2005a Superiority of nonlinear mapping in decoding multiple single-unit neuronal spike trains: A simulation study *J Neurosci Methods* **150** 202-11

Kim S P, Rao Y N, Erdogmus D, Sanchez J C, Nicolelis M A L and Principe J C 2005b Determining patterns in neural activity for reaching movements using nonnegative matrix factorization *EURASIP J Appl Signal Processing* **19** 3113-21

Kira K and Rendell L A 1992 The feature selection problem: Traditional methods and a new algorithm *Proc. of the 10th National Conf. on Artificial Intelligence (San Jose, CA)* pp 129-34

Kositsky M, Karniel A, Alford S, Fleming K M and Mussa-Ivaldi F A 2003 Dynamical dimension of a hybrid neurorobotic system *IEEE Trans Neural Syst Rehabil Eng* **11** 155-9

Kostov A and Polak M 1997 Prospects of computer access using voluntary modulated EEG signal *Proc. ECPD Symposium on Brain & Consciousness (Belgrade, Yugoslavia)* pp 233-6

Kostov A and Polak M 2000 Parallel man-machine training in development of EEG-based cursor control *IEEE Trans Rehabil Eng* **8** 203-5

Kozelka J W and Pedley T A 1990 Beta and mu rhythms *J. Clin. Neurophysiol.* **7** 191-207

Krauledat M, Dornhege G, Blankertz B, Losch F, Curio G and Muller K 2004 Improving speed and accuracy of brain-computer interfaces using readiness potential features *Proc. 26th Annual Int. Conf. of the IEEE Engineering in Medicine and Biology Society (San Francisco, CA)* pp 4511-5

Krausz G, Scherer R, Korisek G and Pfurtscheller G 2003 Critical decision-speed and information transfer in the "graz brain-computer interface" *Appl.Psychophysiol.Biofeedback* **28** 233-40

Kubler A, Kotchoubey B, Hinterberger T, Ghanayim N, Perelmouter J, Schauer M, Fritsch C, Taub E and Birbaumer N 1999 The thought translation device: A neurophysiological approach to communication in total motor paralysis *Exp Brain Res* **124** 223-2

Kubler A, Kotchoubey B, Kaiser J, Wolpaw J R and Birbaumer N 2001a Brain-computer communication: Unlocking the locked in *Psychol Bull* **127** 358-75

Kubler A, Kotchoubey B, Salzmann H P, Ghanayim N, Perelmouter J, Homberg V and Birbaumer N 1998 Self-regulation of slow cortical potentials in completely paralyzed human patients *Neurosci Lett* **252** 171-4

Kubler A, Neumann N, Kaiser J, Kotchoubey B, Hinterberger T and Birbaumer N P 2001b Brain-computer communication: Self-regulation of slow cortical potentials for verbal communication *Arch Phys Med Rehabil* **82** 1533-9

Kubler A, Nijboer F, Mellinger J, Vaughan T M, Pawelzik H, Schalk G, McFarland D J, Birbaumer N and Wolpaw J R 2005 Patients with ALS can use sensorimotor rhythms to operate a brain-computer interface *Neurology* **64** 1775-7

LaCourse J R and Wilson E 2003 Brainiac: A brain computer link *Proc. IEEE Instrumentation and Measurement Technology Conf (Vail, CO)* pp 587-92

Lal T N, Schroder M, Hinterberger T, Weston J, Bogdan M, Birbaumer N and Scholkopf B 2004 Support vector channel selection in BCI *IEEE Trans. Biomed. Eng* **51** 1003-10

Lalor E, Kelly S, Finucane C, Burke R, Smith R, Reilly R and McDarby G 2005 Steady-state VEP-based brain computer interface control in an immersive 3-D gaming environment *EURASIP J. Appl. Signal Processing* **19** 3156-64

Laubach M, Wessberg J and Nicolelis M A 2000 Cortical ensemble activity increasingly predicts behaviour outcomes during learning of a motor task *Nature* **405** 567-71

Lebedev M A, Carmena J M, O'Doherty J E, Zacksenhouse M, Henriquez C S, Principe J C and Nicolelis M A 2005 Cortical ensemble adaptation to represent velocity of an artificial actuator controlled by a brain-machine interface *J Neurosci* **25** 4681-93

Lee H and Choi S 2002 PCA-based linear dynamical systems for multichannel EEG classification *Proc. 9th Int Conf on Neural Information Processing (Singapore)* pp 745-9

Lee H and Choi S 2003 PCA+HMM+SVM for EEG pattern classification Proc. IEEE 7th Int. Symp. on Signal Processing and Its Applications (Paris, France) pp 541-4

Lee P L, Wu C H, Hsieh J C and Wu Y T 2005 Visual evoked potential actuated brain computer interface: A brain-actuated cursor system *Electronics Letters* **41** 832-4

Leeb R and Pfurtscheller G 2004 Walking through a virtual city by thought Proc. 26th Annual Int. Conf. of the IEEE Engineering in Medicine and Biology Society (San Francisco, CA) pp 4503-6

Lemm S, Blankertz B, Curio G and Muller K R 2005 Spatio-spectral filters for improving the classification of single trial EEG *IEEE Trans. Biomed. Eng* **52** 1541-8

Lemm S, Schafer C and Curio G 2004 BCI competition 2003--data set III: Probabilistic modeling of sensorimotor mu rhythms for classification of imaginary hand movements *IEEE Trans. Biomed. Eng* **51** 1077-80

Levine S P, Huggins J E, Bement S L, Kushwaha R K, Schuh L A, Passaro E A, Rohde M M and Ross D A 1999 Identification of electrocorticogram patterns as the basis for a direct brain interface *J Clin Neurophysiol* **16** 439-47

Levine S P, Huggins J E, Bement S L, Kushwaha R K, Schuh L A, Rohde M M, Passaro E A, Ross D A, Elisevich K V and Smith B J 2000 A direct brain interface based on event-related potentials *IEEE Trans Rehabil Eng* **8** 180-185

Li Y, Cichocki A, Guan C and Qin J 2004a Sparse factorization preprocessing-based offline analysis for a cursor control experiment *Proc. IEEE Int. Workshop on Biomedical Circuits and Systems (Singapore)* pp S3/5/INV-S3/5/5-8

Li Y, Gao X, Liu H and Gao S 2004b Classification of single-trial electroencephalogram during finger movement *IEEE Trans. Biomed. Eng* **51** 1019-25

Lisogurski D and Birch G E 1998 Identification of finger flexions from continuous EEG as a brain computer interface *Proc. 20th Annual Int. Conf. of the IEEE Engineering in Medicine and Biology Society (Hong Kong)* **pp** 2004-7

Liu H, Wang J and Zheng C 2005 Mental tasks classification and their EEG structures analysis by using the growing hierarchical self-organizing map *Proc. 1st Int. Conf. on Neural Interface and Control (Wuhan, China)* pp 115-8

Liu H S, Gao X, Yang F and Gao S 2003 Imagined hand movement identification based on spatio-temporal pattern recognition of EEG *Proc. IEEE-EMBS Conf. on Neural Engineering (Capri Island, Italy)* pp 599-602

Mahmoudi B and Erfanian A 2002 Single-channel EEG-based prosthetic hand grasp control for amputee subjects *Proc. 24th Annual Int. Conf. of the IEEE Engineering in Medicine and Biology Society (Houston, TX)* pp 2406-7

Mason S G and Birch G E 2000 A brain-controlled switch for asynchronous control applications *IEEE Trans. Biomed. Eng* **47** 1297-307

Mason S G and Birch G E 2003 A general framework for brain-computer interface design *IEEE Trans. Neural Syst. Rehabil. Eng* **11** 70-85

Mason S G, Bohringer R, Borisoff J F and Birch G E 2004 Real-time control of a video game with a direct brain--computer interface *J. Clin. Neurophysiol* **21** 404-8

McFarland D and Wolpaw J R 1998 EEG-based communication and control: Short-term role of feedback *IEEE Trans. Rehabil. Eng* **6** 7-11

McFarland D J, Anderson C W, Muller K R, Schlogl A and Krusienski D J 2006 BCI meeting 2005--workshop on BCI signal processing: Feature extraction and translation *IEEE Trans. Neural Syst. Rehabil. Eng* **14** 135-8

McFarland D J, McCane L M, David S V and Wolpaw J R 1997 Spatial filter selection for EEG-based communication *Electroencephalogr. Clin. Neurophysiol* **103** 386-94

McFarland D J, Sarnacki W A, Vaughan T M and Wolpaw J R 2005 Brain-computer interface (BCI) operation: Signal and noise during early training sessions *Clin. Neurophysiol* **116** 56-62

McFarland D J, Sarnacki W A and Wolpaw J R 2003 Brain-computer interface (BCI) operation: Optimizing information transfer rates *Biol. Psychol* **63** 237-51

McMillan G R and Calhoun G L 1995 Direct brain interface utilizing self-regulation of steady-state visual evoked response (SSVER) *Proc. RESNA '95 Annual Conference (Vancouver, BC)* pp 693-5

Mensh B D, Werfel J and Seung H S 2004 BCI competition 2003--data set ia: Combining gamma-band power with slow cortical potentials to improve single-trial classification of electroencephalographic signals *IEEE Trans. Biomed. Eng* **51** 1052-6

Middendorf M, McMillan G, Calhoun G and Jones K S 2000 Brain-computer interfaces based on the steady-state visual-evoked response *IEEE Trans Rehabil Eng* **8** 211-4

Millan Jdel R, Renkens F, Mourino J and Gerstner W 2004a Noninvasive brain-actuated control of a mobile robot by human EEG *IEEE Trans. Biomed. Eng* **51** 1026-33

Millan J R, Renkens F, Mourino J and Gerstner W 2003a Non-invasive brain-actuated control of a mobile robot *Proc. 18th International Joint Conference on Artificial Intelligence (Acapulco, Mexico)* pp 1121-6

Millán J R, Renkens F, Mouriño J and Gerstner W 2004b Brain-actuated interaction *Artificial Intelligence* **159** 241-59.

Millan J, Franze M, Mourino J, Cincotti F and Babiloni F 2002a Relevant EEG features for the classification of spontaneous motor-related tasks *Biol. Cybern* **86** 89-95

Millan J, Mourino J, Franze M, Cincotti F, Varsta M, Heikkonen J and Babiloni F 2002b A local neural classifier for the recognition of EEG patterns associated to mental tasks *IEEE Trans. Neural Net* **13** 678-86

Millan J R 2004 On the need for on-line learning in brain-computer interfaces *Proc. Annual Inter. Joint Conf. on Neural Networks (Budapest, Hungary)*

Millan J R, Mourino J, Babiloni F, Cincotti F, Varsta M and Heikkonen J 2000a Local neural classifier for EEG-based recognition of mental tasks *Proc. IEEE-INNS-ENNS Inter. Joint Conf. on Neural Networks (Como, Italy)* pp 632-6

Millan J R, Mourino J, Cincotti F, Varsta M, Heikkonen J, Topani F, Marciani M G, Kaski K and Babiloni F 2000b Neural networks for robust classification of mental tasks *Proc. 22nd Annual Int. Conf. of the IEEE Engineering in Medicine and Biology Society (Chicago, IL)* pp 1380-2

Millan J R, Mourino J, Marciani M G, Babiloni F, Topani F, Canale I, Heikkonen J and Kaski K 1998 Adaptive brain interfaces for physically-disabled people *Proc. 20th Annual Int. Conf. of the IEEE Engineering in Medicine and Biology Society (Hong Kong)* **pp** 2008-11

Millan J R and Mourino J 2003b Asynchronous BCI and local neural classifiers: An overview of the adaptive brain interface project *IEEE Trans. Neural Syst. Rehabil. Eng* **11** 159-61

Molina G G, Ebrahimi T and Vesin J M 2003 Joint time-frequency-space classification of EEG in a brain-computer interface application *EURASIP J. Applied Signal Processing* **7** 713-29

Mourino J, Chiappa S, Jane R and Millan J R 2002 Evolution of the mental states operating a brain-computer interface *Proc. of the Inter. Federation for Medical and Biological Engineering (Vienna, Austria)* **pp** 600-1

Muller K R, Anderson C W and Birch G E 2003a Linear and nonlinear methods for brain-computer interfaces *IEEE Trans. Neural Syst. Rehabil. Eng* **11** 165-9

Muller K R, Curio G, Blankertz B and Dornhege G 2003b Combining features for BCI *Advances in Neural Information Processing Systems (NIPS02)*, vol. 15, eds S Becker, S Thrun and K Obermayer, pp 1115–22.

Muller G R, Neuper C and Pfurtscheller G 2003c Implementation of a telemonitoring system for the control of an EEG-based brain-computer interface *IEEE Trans. Neural Syst. Rehabil. Eng* **11** 54-9

Muller-Putz G R, Scherer R, Brauneis C and Pfurtscheller G 2005a Steady-state visual evoked potential (SSVEP)-based communication: Impact of harmonic frequency components *J neural engineering* **2** 123-30

Muller-Putz G R, Scherer R, Pfurtscheller G and Rupp R 2005b EEG-based neuroprosthesis control: A step towards clinical practice *Neurosci. Lett* **382** 169-74

Musallam S, Cornell B D, Greger B, Scherberger H and Andersen R A 2004 Cognitive control signals for neural prosthetics *Science* **305** 258-62

Huan N J and Palaniappan R 2005 Classification of mental tasks using fixed and adaptive autoregressive models of EEG signals *Proc. 27th Annual Int. Conf. of the IEEE Engineering in Medicine and Biology Society (Shanghai, China)* pp 633-6

Neumann N, Hinterberger T, Kaiser J, Leins U, Birbaumer N and Kubler A 2004 Automatic processing of self-regulation of slow cortical potentials: Evidence from brain-computer communication in paralysed patients *Electroencephalogr Clin Neurophysiol* **115** 628-35

Neumann N, Kubler A, Kaiser J, Hinterberger T and Birbaumer N 2003 Conscious perception of brain states: Mental strategies for brain-computer communication *Neuropsychologia* **41** 1028-36

Neuper C, Muller G R, Kubler A, Birbaumer N and Pfurtscheller G 2003 Clinical application of an EEG-based brain-computer interface: A case study in a patient with severe motor impairment *Clin Neurophysiol* **114** 399-409

Neuper C, Scherer R, Reiner M and Pfurtscheller G 2005 Imagery of motor actions: Differential effects of kinesthetic and visual-motor mode of imagery in single-trial EEG *Brain Res. Cogn. Brain Res* **25** 668-77

Neuper C, Schloegl A and Pfurtscheller G 1999 Enhancement of left-right sensorimotor EEG differences during feedback-regulated motor imagery *J. of Clin Neurophysiol* **16** 373-82

Niedermeyer E and Lopes da Silva F 1998 *Electroencephalography: Basic Principles, Clinical Applications, and Related Fields* Fourth Edition ed C Mitchell (Baltimore, Maryland USA: Lippincott Williams & Wilkins)

Obeid I and Wolf P D 2004 Evaluation of spike-detection algorithms for a brain-machine interface application *IEEE Trans. Biomed. Eng* **51** 905-11

Obermaier B, Guger C, Neuper C and Pfurtscheller G 2001a Hidden markov models for online classification of single trial EEG data *Pattern Recognition Letters* **22** 1299-309

Obermaier B, Muller G R and Pfurtscheller G 2001b "Virtual keyboard" controlled by spontaneous EEG activity *IEEE Trans. Neural Syst. Rehabil. Eng* **11** 636-41

Obermaier B, Munteanu C, Rosa A and Pfurtscheller G 2001c Asymmetric hemisphere modeling in an offline brain-computer interface *IEEE Trans Syst Man Cybern* **31** 536-40

Obermaier B, Neuper C, Guger C and Pfurtscheller G 2001d Information transfer rate in a five-classes brain-computer interface *IEEE Trans Neural Syst. Rehabil. Eng* **9** 283-8

Olson B P, Si J, Hu J and He J 2005 Closed-loop cortical control of direction using support vector machines *IEEE Trans. Neural Syst. Rehabil. Eng* **13** 72-80

Otto K J, Vetter R J, Marzullo T C and Kipke D R 2003 Brain-machine interfaces in rat motor cortex: Implications of adaptive decoding algorithms *Proc. IEEE-EMBS Conf. on Neural Engineering (Capri Island, Italy)* pp 100-3

Palaniappan R 2005 Brain computer interface design using band powers extracted during mental tasks *Proc. IEEE-EMBS Conf. on Neural Engineering (Arlington, VA)* pp 321-324

Palaniappan R, Paramesran R, Nishida S and Saiwaki N 2002 A new brain-computer interface design using fuzzy ARTMAP *IEEE Trans Neural Syst Rehabil Eng* **10** 140-8

Panuccio A, Bicego M and Murino V 2002 A hidden markov model-based approach to sequential data clustering *Proc. Joint IAPR Inter. Workshop on Structural, Syntactic, and Statistical Pattern Recognition (Windsor, Canada)* pp 734-42

Parra L, Alvino C, Tang A, Pearlmutter B, Yeung N, Osman A and Sajda P 2002 Linear spatial integration for single-trial detection in encephalography *Neuroimage* **17** 223-30

Parra L, Alvino C, Tang A, Pearlmutter B, Yeung N, Osman A and Sajda P 2003a Single-trial detection in EEG and MEG: Keeping it linear *Neurocomputing* **52-54** 177-83

Parra L C, Spence C D, Gerson A D and Sajda P 2003b Response error correction--a demonstration of improved human-machine performance using real-time EEG monitoring *IEEE Trans. Neural Syst. Rehabil. Eng* **11** 173-7

Patil P G, Carmena J M, Nicolelis M A and Turner D A 2004 Ensemble recordings of human subcortical neurons as a source of motor control signals for a brain-machine interface *Neurosurgery* **55** 27-35

Penny W D, Roberts S J, Curran E A and Stokes M J 2000 EEG-based communication: A pattern recognition approach *IEEE Trans. Rehabil. Eng* **8** 214-5

Peters B O, Pfurtscheller G and Flyvbjerg H 2001 Automatic differentiation of multichannel EEG signals *IEEE Trans. Biomed. Eng* **48** 111-6

Peterson D A, Knight J N, Kirby M J, Anderson C W and Thaut M H 2005 Feature selection and blind source separation in an EEG-based brain-computer interface *EURASIP J. Appl. Signal Processing* **19** 3128-40

Pfurtscheller G and Aranibar A 1977 Event-related cortical desynchronization detected by power measurements of scalp EEG *Electroencephalogr. Clin. Neurophysiol* **42** 817-26

Pfurtscheller G, Flotzinger D and Kalcher J 1993 Brain-computer interface - a new communication device for handicapped persons *J Microcomputer Applications* **16** 293-9

Pfurtscheller G, Flotzinger D and Neuper C 1994 Differentiation between finger, toe and tongue movement in man based on 40-hz EEG *Electroencephalogr Clin Neurophysiol* **90** 456-60

Pfurtscheller G and Guger C 1999 Brain-computer communication system: EEG-based control of hand orthesis in a tetraplegic patient *Acta Chir. Austriaca* **31** 23-5

Pfurtscheller G, Kalcher J, Neuper C, Flotzinger D and Pregenzer M 1996 On-line EEG classification during externally-paced hand movements using a neural network-based classifier *Electroencephalogr Clin Neurophysiol* **99** 416-25

Pfurtscheller G and Lopes da Silva F H 1999 Event-related EEG/MEG synchronization and desynchronization: Basic principles *Clin. Neurophysiol* **110** 1842-57

Pfurtscheller G, Muller G R, Pfurtscheller J, Gerner H J and Rupp R 2003a 'Thought'--control of functional electrical stimulation to restore hand grasp in a patient with tetraplegia *Neurosci. Lett* **351** 33-6

Pfurtscheller G, Muller-Putz G R, Pfurtscheller J and Rupp R 2005 EEG-based asynchronous BCI controls functional electrical stimulation in a tetraplegic patient *EURASIP J. Appl. Signal Processing* **19** 3152-5

Pfurtscheller G and Neuper C 2001 Motor imagery and direct brain-computer communication *Proc. IEEE* **89** 1123-34

Pfurtscheller G, Neuper C, Flotzinger D and Pregenzer M 1997 EEG-based discrimination between imagination of right and left hand movement *Electroencephalogr Clin Neurophysiol* **103** 642-51

Pfurtscheller G, Neuper C, Guger C, Harkam W, Ramoser H, Schlogl A, Obermaier B and Pregenzer M 2000 Current trends in graz brain-computer interface (BCI) research *IEEE Trans. Rehabil. Eng* **8** 216-9

Pfurtscheller G, Neuper C, Muller G R, Obermaier B, Krausz G, Schlogl A, Scherer R, Graimann B, Keinrath C, Skliris D, Wortz M, Supp G and Schrank C 2003b Graz-BCI: State of the art and clinical applications *IEEE Trans Neural Syst. Rehabil. Eng* **11** 177-80

Pfurtscheller G, Neuper C, Schlogl A and Lugger K 1998 Separability of EEG signals recorded during right and left motor imagery using adaptive autoregressive parameters *IEEE Trans. Rehabil. Eng* **6** 316-25

Pineda J A, Allison B Z and Vankov A 2000 The effects of self-movement, observation, and imagination on mu rhythms and readiness potentials (RP's): Toward a brain-computer interface (BCI) *IEEE Trans Rehabil Eng* **8** 219-22

Pineda J A, Silverman D S, Vankov A and Hestenes J 2003 Learning to control brain rhythms: Making a brain-computer interface possible *IEEE Trans. Neural Syst. Rehabil. Eng* **11** 181-4

Platt J 1991 A resource-allocating network for function interpolation *Neural Comput* **3** 213-25

Polak M and Kostov A 1997 Development of brain-computer interface: Preliminary results Proc. 19th Annual Int. Conf. of the IEEE Engineering in Medicine and Biology Society (Chicago, IL) pp 1543-6

Polak M and Kostov A 1998 Feature extraction in development of brain-computer interface: A case study *Proc. 20th Annual Int. Conf. of the IEEE Engineering in Medicine and Biology Society (Hong Kong)* pp 2058-61

Polak M and Kostov A 1999 Training setup for control of neural prosthesis using brain-computer interface Proc. 21st Annual Int. Conf. of the IEEE Engineering in Medicine and Biology Society & Annual Fall meeting of the Biomedical Engineering Society (Atlanta, GA) p 446

Polikoff J B, Bunnell H T and Borkowski W 1995 Toward a P300-based computer interface *Proc. RESNA'95 Annual Conf. (Vancouver, Canada)* pp 178-80

Pregenzer M and Pfurtscheller G 1995 Distinction sensitive learning vector quantization (DSLVQ) - application as a classifier based feature selection method for a brain computer interface *Proc. 4th Int. Conf. on Artificial Neural Networks (Cambridge, UK)* pp 433-6

Pregenzer M and Pfurtscheller G 1999 Frequency component selection for an EEG-based brain to computer interface *IEEE Trans. Rehabil. Eng* **7** 413-9

Qin L, Deng J, Ding L and He B 2004a Motor imagery classification by means of source analysis methods *Proc. 26th Annual Int. Conf. of the IEEE Engineering in Medicine and Biology Society (San Francisco, CA)* pp 4356-8

Qin L, Ding L and He B 2004b Motor imagery classification by means of source analysis for brain-computer interface applications *J. Neural Eng* **1** 135-41

Qin L and He B 2005 A wavelet-based time-frequency analysis approach for classification of motor imagery for brain-computer interface applications *J. Neural Eng* **2** 65-72

Qin L, Kamousi B, Liu Z M, Ding L and He B 2005 Classification of motor imagery tasks by means of time-frequency-spatial analysis for brain-computer interface applications *Proc. IEEE-EMBS Conf. on Neural Engineering (Arlington, VA)* pp 374-6

Ramachandran V S and Histein W 1998 The perception of phantom limbs *Brain* **121** 1603-30

Ramoser H, Muller-Gerking J and Pfurtscheller G 2000 Optimal spatial filtering of single trial EEG during imagined hand movement *IEEE Trans. Rehabil. Eng* **8** 441-6

Rao Y N, Kim S -, Sanchez J C, Erdogmus D, Principe J C, Carmena J M, Lebedev M A and Nicolelis M A 2005 Learning mappings in brain machine interfaces with echo state networks *Proc. IEEE Inter. Conf. on Acoustics, Speech and Signal Processing (Philadelphia, PA)* pp v/233-v/236

Reger B D, Fleming K M, Sanguineti V, Alford S and Mussa-Ivaldi F A 2000a Connecting brains to robots: The development of a hybrid system for the study of learning in neural tissues *Proc. VIIth Inter.Conf. on Artificial Life (Portland, OR)* pp 263-72

Reger B D, Fleming K M, Sanguineti V, Alford S and Mussa-Ivaldi F A 2000b Connecting brains to robots: An artificial body for studying the computational properties of neural tissues *Artif Life* **6** 307-24

Rezek I, Roberts S and Sykacek P 2003 Ensemble coupled hidden markov models for joint characterization of dynamic signals *Proc. 9th Int. Workshop on Artificial Intelligence and Statistics (Key West, Florida)* ed C M Bishop and B J Frey

Roberts S J and Penny W 2003 Real-time brain-computer interfacing: A preliminary study using bayesian learning *Med Biol Eng Comput* **38** 56-61

Roberts S J, Penny W and Rezek I 1999 Temporal and spatial complexity measures for electroencephalogram based brain-computer interfacing *Med Biol Eng Comput* **37** 93-8

Roushe P, Clement R, Visser C, Cruz J and Si J 2003 "Neurabotics": An integration of neurons, rats and robots for advanced studies of brain-computer interface systems *Proc. IEEE-EMBS Conf. on Neural Engineering (Capri Island, Italy)* pp 462-465

Sanchez J C, Carmena J M, Lebedev M A, Nicolelis M A, Harris J G and Principe J C 2004 Ascertaining the importance of neurons to develop better brain-machine interfaces *IEEE Trans. Biomed. Eng* **51** 943-53

Sanchez J C, Erdogmus D, Rao Y N, Principe J and Nicolelis M A 2002a A comparison between nonlinear mappings and linear state estimation to model the relation from motor cortical neuronal firing to hand movements *Proc. SAB Workshop on Motor Control in Humans and Robots (Edinburgh, Scotland)* pp 59-65

Sanchez J C, Erdogmus D, Rao Y N, Principe J, Nicolelis M A and Wessberg J 2003 Learning the contributions of the motor, premotor, and posterior parietal cortices for hand trajectory reconstruction in a brain machine interface *Proc. IEEE-EMBS Conf. on Neural Engineering (Capri Island, Italy)* pp 59-62

Sanchez J C, Kim S P, Erdogmus D, Rao Y N, Principe J, Wessing J and Nicolelis M A 2002b Input-output mapping performance of linear and nonlinear models for estimating hand trajectories from cortical neuronal firing patterns *Proc. IEEE Workshop on Neural Networks and Signal Processing (Martigny, Switzerland)* pp 139-48.

Schalk G, Wolpaw J R, McFarland D J and Pfurtscheller G 2000 EEG-based communication: Presence of an error potential *Clin. Neurophysiol* **111** 2138-44

Scherer R, Muller G R, Neuper C, Graimann B and Pfurtscheller G 2004 An asynchronously controlled EEG-based virtual keyboard: Improvement of the spelling rate *IEEE Trans. Biomed. Eng* **51** 979-84

Schloegl A, Lugger K and Pfurtscheller G 1997a Using adaptive autoregressive parameters for a brain-computer-interface experiment *Proc. 19th Annual Int. Conf. of the IEEE Engineering in Medicine and Biology Society (Chicago, IL)* pp 1533-5

Schloegl A, Neuper C and Pfurtscheller G 1997b Subject specific EEG patterns during motor imaginary *Proc. 19th Annual Int. Conf. of the IEEE Engineering in Medicine and Biology Society (Chicago, IL)* pp 1530-2

Schlogl A, Keinrath C, Scherer R and Pfurtscheller G 2003 Information transfer of an EEG-based brain computer interface *Proc. IEEE-EMBS Conf. on Neural Engineering (Capri Island, Italy)* pp 641-4

Schröder M, Lal T N, Hinterberger T, Bogdan M, Hill N J, Birbaumer N, Rosenstiel W and Schölkopf B 2005 Robust EEG channel selection across subjects for brain-computer interfaces *EURASIP J. Appl. Signal Processing* **19** 3103-12

Schroder M, Bogdan M, Rosenstiel W, Hinterberger T and Birbaumer N 2003 Automated EEG feature selection for brain computer interfaces *Proc. IEEE-EMBS Conf. on Neural Engineering (Capri Island, Italy)* pp 626-9

Schwartz A B, Taylor D M and Tillery S I 2001 Extraction algorithms for cortical control of arm prosthetics *Curr Opin Neurobiol* **11** 701-7

Serby H, Yom-Tov E and Inbar G F 2005 An improved P300-based brain-computer interface *IEEE Trans. Neural Syst. Rehabil. Eng* **13** 89-98

Serruya M, Hatsopoulos N, Fellows M, Paninski L and Donoghue J 2003 Robustness of neuroprosthetic decoding algorithms *Biol cybern* **88** 219-28

Serruya M D, Hatsopoulos N G, Paninski L, Fellows M R and Donoghue J P 2002 Instant neural control of a movement signal *Nature* **416** 141-2

Sheikh H, McFarland D J, Sarnacki W A and Wolpaw J R 2003 Electroencephalographic(EEG)-based communication: EEG control versus system performance in humans *Neurosci. Lett* **345** 89-92

Stone M 1977 Asymptotics for and against cross-validation *Biometrika* **64** 29-35

Su Ryu C, Song Y, Yoo D S, Choi S, Moon S S and Sohn J H 1999 EEG-based discrimination between yes and no Proc. 21st Annual Int. Conf. of the IEEE Engineering in Medicine and Biology Society & Annual Fall meeting of the Biomedical Engineering Society (Atlanta, GA) p 444

Sutter E E 1992 The brain response interface: Communication through visually-induced electrical brain responses *J Micro Comp App* **15** 31-45

Sykacek P, Roberts S, Stokes M, Curran E, Gibbs M and Pickup L 2003 Probabilistic methods in BCI research *IEEE Trans Neural Syst Rehabil Eng* **11** 192-5

Sykacek P, Roberts S J and Stokes M 2004 Adaptive BCI based on variational bayesian kalman filtering: An empirical evaluation *IEEE Trans. Biomed. Eng* **51** 719-27

Tavakolian K, Nasrabadi A M and Rezaei S 2004 Selecting better EEG channels for classification of mental tasks *Proc. IEEE Inter. Symp. on Circuits and Systems* pp 537-40

Taylor D M, Tillery S I and Schwartz A B 2002 Direct cortical control of 3D neuroprosthetic devices *Science* **296** 1829-32

Taylor D M, Tillery S I H and Schwartz A B 2003 Information conveyed through brain-control: Cursor versus robot *IEEE Trans Neural Syst Rehabil Eng* **11** 195-9

Thulasidas M, Guan C, Ranganatha S, Wu J K, Zhu X and Xu W 2004 Effect of ocular artifact removal in brain computer interface accuracy *Proc. 26th Annual Int. Conf. of the IEEE Engineering in Medicine and Biology Society (San Francisco, CA)* pp 4385-8

Townsend G, Graimann B and Pfurtscheller G 2004 Continuous EEG classification during motor imagery--simulation of an asynchronous BCI *IEEE Trans. Neural Syst. Rehabil. Eng* **12** 258-65

Trejo L J, Wheeler K R, Jorgensen C C, Rosipal R, Clanton S T, Matthews B, Hibbs A D, Matthews R and Krupka M 2003 Multimodal neuroelectric interface development *IEEE Trans Neural Syst. Rehabil. Eng* **11** 199-204

Varsta M, Heikkonen J, Millan J d R and Mourino J 2000 Evaluating the performance of three feature sets for brain-computer interfaces with an early stopping MLP commitee *Inter. Conf. on Pattern Recognition (Barcelona, Spain)* pp 907-10

Vetter R J, Otto K J, Marzullo T C and Kipke D R 2003 Brain machine interfaces in rat motor cortex: Neuronal operant conditioning to perform a sensory detection task *Proc. IEEE-EMBS Conf. on Neural Engineering (Capri Island, Italy)* pp 637-40

Vidal J J 1977 Real-time detection of brain events in EEG *Proc. IEEE* **65** 633-41

Wang D, Kochiyama T, Lu S and Wu J 2005a Measurement and analysis of electroencephalogram (EEG) using directional visual stimuli for brain computer interface *Proc. Inter. Conf. on Active Media Technology (Takamatsu, Japan)* pp 34-9

Wang T, Deng J and He B 2004a Classifying EEG-based motor imagery tasks by means of time-frequency synthesized spatial patterns *Clin. Neurophysiol* **115** 2744-53

Wang T, Deng J and He B 2004b Classification of motor imagery EEG patterns and their topographic representation *Proc. 26th Annual Int. Conf. of the IEEE Engineering in Medicine and Biology Society (San Francisco, CA)* pp 4359-62

Wang Y, Wang R, Gao X and Gao S 2005b Brain-computer interface based on the high-frequency steady-state visual evoked potential *Proc. 1st Inter. Conf. on Neural Interface and Control (Wuhan, China)* pp 37-9

Wang Y, Zhang Z, Gao X and Gao S 2004c Lead selection for SSVEP-based brain-computer interface *Proc. 26th Annual Int. Conf. of the IEEE Engineering in Medicine and Biology Society (San Francisco, CA)* pp 4507-10

Wang Y, Zhang Z, Li Y, Gao X, Gao S and Yang F 2004d BCI competition 2003--data set IV: An algorithm based on CSSD and FDA for classifying single-trial EEG *IEEE Trans. Biomed. Eng* **51** 1081-6

Weiskopf N, Mathiak K, Bock S W, Scharnowski F, Veit R, Grodd W, Goebel R and Birbaumer N 2004 Principles of a brain-computer interface (BCI) based on real-time functional magnetic resonance imaging (fMRI) *IEEE Trans. Biomed. Eng* **51** 966-70

Weiskopf N, Veit R, Erb M, Mathiak K, Grodd W, Goebel R and Birbaumer N 2003 Physiological self-regulation of regional brain activity using real-time functional magnetic resonance imaging (fMRI): Methodology and exemplary data *Neuroimage* **19** 577-86

Weitkunat R 1991 *Digital Biosignal Processing* (New York: Elsevier Science)

Wessberg J, Stambaugh C R, Kralik J D, Beck P D, Laubach M, Chapin J K, Kim J, Biggs S J, Srinivasan M A and Nicolelis M A 2000 Real-time prediction of hand trajectory by ensembles of cortical neurons in primates *Nature* **408** 361-5

Wolpaw J R, Birbaumer N, McFarland D J, Pfurtscheller G and Vaughan T M 2002 Brain-computer interfaces for communication and control *Clin. Neurophysiol* **113** 767-91

Wolpaw J R, Flotzinger D, Pfurtscheller G and McFarland D J 1997 Timing of EEG-based cursor control *J. Clin. Neurophysiol* **14** 529-38

Wolpaw J R, McFarland D, Neat G W and Forneris C A 1991 An EEG-based brain-computer interface for cursor control *Electroencephalogr Clin Neurophysiol* **78** 252-9

Wolpaw J R and McFarland D J 1994 Multichannel EEG-based brain-computer communication *Electroencephalogr Clin Neurophysiol* **90** 444-9

Wolpaw J R and McFarland D J 2004 Control of a two-dimensional movement signal by a noninvasive brain-computer interface in humans *Proc. Natl. Acad. Sci. U. S. A.* **101** 17849-54

Wolpaw J R, McFarland D J and Vaughan T M 2000 Brain-computer interface research at the wadsworth center *IEEE Trans. Rehabil. Eng* **8** 222-6

Wolpaw J R, McFarland D J, Vaughan T M and Schalk G 2003 The wadsworth center brain-computer interface (BCI) research and revelopment program *IEEE Trans Neural Syst. Rehabil. Eng* **11** 204-7

Wu W, Black M J, Gao Y, Bienenstock E, Serruya M D and Donoghue J P 2002a Inferring hand motion from multi-cell recordings in motor cortex using a kalman filter *Proc. SAB Workshop on Motor Control in Humans and Robots (Edinburgh, Scotland)* pp 66-73

Wu W, Black M J, Gao Y, Bienenstock E, Shaikhounix A and Donoghue J P 2002b Neural decoding of cursor motion using a kalman filter *Advances in Neural Information Processing Systems* **15** 133–40

Wu R C, Liang S F, Lin C T and Hsu C F 2004 Applications of event-related-potential-based brain computer interface to intelligent transportation systems *Proc. IEEE Inter. Conf. on Networking, Sensing and Control (Taipei, Taiwan)* pp 813-8

Xu N, Gao X, Hong B, Miao X, Gao S and Yang F 2004a BCI competition 2003--data set IIb: Enhancing P300 wave detection using ICA-based subspace projections for BCI applications *IEEE Trans. Biomed. Eng* **51** 1067-72

Xu W, Guan C, Siong C E, Ranganatha S, Thulasidas M and Wu J 2004b High accuracy classification of EEG signal *Proc. 17th Inter. Conf. on Pattern Recognition (Cambridge, UK)* pp 391-4

Yan Wang, Sutherland M T, Sanfratello L L and Tang A C 2004 Single-trial classification of ERPS using second-order blind identification (SOBI) *Proc. IEEE Inter. Conf. on Machine Learning and Cybernetics (Shanghai, China)* pp 4246-51

Yom-Tov E and Inbar G F 2001 Selection of relevant features for classification of movements from single movement-related potentials using a genetic algorithm *Proc. 23rd Annual Int. Conf. of the IEEE Engineering in Medicine and Biology Society (Istanbul, Turkey)* pp 1364-6

Yom-Tov E and Inbar G F 2002 Feature selection for the classification of movements from single movement-related potentials *IEEE Trans Neural Syst. Rehabil. Eng* **10** 170-7

Yom-Tov E and Inbar G F 2003 Detection of movement-related potentials from the electro-encephalogram for possible use in a brain-computer interface *Med Biol Eng Comput* **41** 85-93

Yoo S S, Fairneny T, Chen N K, Choo S E, Panych L P, Park H, Lee S Y and Jolesz F A 2004 Brain-computer interface using fMRI: Spatial navigation by thoughts *Neuroreport* **15** 1591-5

Yoon H, Yang K and Shahabi C 2005 Feature subset selection and feature ranking for multivariate time series *IEEE Trans. on Knowledge and Data Engineering* **17** 1186-98

Yu Z, Mason S G and Birch G E 2002 Enhancing the performance of the LF-ASD brain-computer interface *Proc. 24th Annual Int. Conf. of the IEEE Engineering in Medicine and Biology Society (Houston, TX)* pp 2443-4

2.8. Appendix A. Index of Terms

TABLE 2.9 INDEX OF TERMS

Index term	Description
AAR	Adaptive auto-regressive
AEP	Auditory evoked potential
AGR	Adaptive Gaussian representation
ALN	Adaptive logic network
ANC	Activity of neural cells
ANN	Artificial neural networks
AR	Auto-regressive
ARTMAP	Adaptive resonance theory MAP
ARX	Autoregressive with exogenous input
BPF	Band-pass filter
C4.5	-
CAR	Common average referencing
CBR	Changes in brain rhythms
CCTM	Cross-Correlation based template matching
CER	Coarse-grained entropy rate
CHMM	Coupled hidden markov model
CN2	-
CSP	Common Spatial Patterns
CSSD	Common spatial subspace decomposition
CSSP	Common spatio-spectral patterns
CTFR	Correlative time-frequency representation
CTFSR	Correlative time-frequency-space representation
DFT	Discrete Fourier transform
DSLVQ	Distinctive sensitive learning vector quantization
ERD	Event related desynchronization
ERN	Event related negativity
ERS	Event related synchronization
FLD	Fisher's linear discriminat
FFT	Fast Fourier transform
Freq-Norm	Frequency normalization
GA	Genetic algorithm
GAM	Generalized additive models
GLA	Generalized linear models
GPER	Gaussian process entropy rates
HMM	Hidden Markov Model
ICA	Independent component analysis
IFFT	Inverse fast Fourier transform
k-NN	k-nearest neighbour
LDA	Linear Discriminant Analysis
LDS	Linear dynamical system
LGM	Linear Gaussian models implemented by Kalman filter

Index term	Description
LMS	Least mean square
LPC	Linear predictive coding
LPF	Low pass filter
LRP	Lateralized readiness potential
LVQ	Learning vector quantization
MD	Mahalanobis distance
MLP	Multi-Layer perceptron neural networks
MN	Multiple neuro-mechanisms
MNF	Maximum noise fraction
MRA	Movement related activity
NID3	-
NMF	Non-negative matrix factorization
NN	Neural networks
OLS1	Orthogonal least square
OPM	Outlier processing method
PCA	Principal Component Analysis (a.k.a. Karhounen Loeve Transform)
PLV	Phase locking values
PPM	Piecewise Prony method
PSD	Power spectral density
RBF	Radial basis function
RFE	Recursive feature/channel elimination
RNN	Recurrent neural network
SA-UK	Successive averaging and/or considering choice of unknown
SCP	Slow cortical potentials
SE	spectral entropy
SFFS	Sequential forward feature selection
SL	Surface Laplacian
SOFNN	Self organizing feature neural network
SOM	Self organizing map
SSEP	Somatosensory evoked potential
SSP	Signal space projection
SSVEP	Steady state visual evoked potential
STD	Standard Deviation
SVD	Singular value decomposition
SVM	Support vector machine
SVR	Support vector machine regression
SWDA	Stepwise discriminant analysis
TBNN	Tree-based neural network
TFR	Time-frequency representation
VEFD	Variable epoch frequency decomposition
VEP	Visual evoked potential
WE	Wavelet entropy
WK	Wiener-Khinchine
ZDA	Z-scale based discriminant analysis

Chapter 3 Brain Computer Interface (BCI) Design for Asynchronous Control Applications: Improvements to the LF-ASD Asynchronous Brain Switch [10]

3.1. Introduction

Over the past 15 years, several research groups throughout the world have developed direct brain-computer interface (BCI[11]) devices as possible alternative communication and control solutions for individuals with severe disabilities. For a review of the field, see (Mason and Birch 2003, Nicolelis 2003, Wolpaw *et al* 2000, Wolpaw *et al* 2002). BCI technology functions by mapping a user's cortical activity associated with an intentional BCI control paradigm (such as attempted finger movements) directly to application-specific control signals. Thus, control of various devices such as neural prostheses is possible by thinking alone, bypassing traditional interface pathways unusable by individuals with severe disabilities.

Several different approaches to the design of BCI technology based on signals from scalp electrodes (i.e. electroencephalograms, EEG) or implanted electrodes have been reported for various communications and control applications. All these systems can be represented by the common functional model presented in Fig. 3.1 (Mason and Birch 2003) (or a variant of this model (Mason *et al* 2003)). In this model, the User desires to control a Device (via the Device's control hardware, termed the Device Controller) through a series of components. These components can collectively be called a BCI Interface Device (conceptually similar to a keyboard, mouse or joystick). To aid the discussion below, the BCI Interface Device can be divided into two parts. The components between User and Control Interface can be treated as a single component, a BCI Transducer[12], which functions in a manner similar to a physical transducer like a dial or switch. The role of the BCI Transducer is to translate the

[10] A version of this chapter has been published. © 2004 IEEE. Reprinted, with permission, from (Borrisof J., Mason S., Bashashati A., and Birch G. (2004) Brain Computer Interface (BCI) Design for Asynchronous Control Applications: Improvements to the LF-ASD Asynchronous Brain Switch *IEEE Trans. Biomed. Eng.* **51** 985-92)

[11] Also known as Brain-Machine Interface (BMI), Direct Brain Interface (DBI) or Adaptive Brain Interface (ABI) technology. The term BCI will be used in this paper.

[12] The term BCI Transducer introduced in (Mason *et al* 2003) is synonymous to the term BCI Control originally proposed by Mason and Birch (Mason and Birch 2003). The former is chosen because of the functional similarity to physical transducers.

User's brain activity into logical (or device-independent) control signals. The role of the Control Interface is to translate the logical control signals into semantically meaningful information or commands. It may do this over time providing feedback through a Control Display.

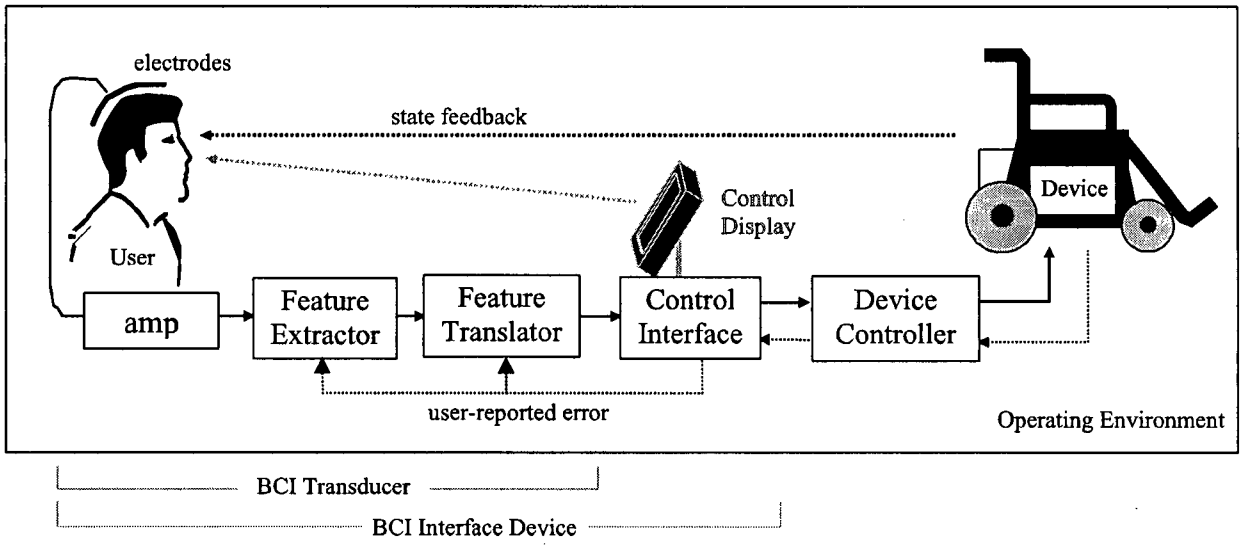

Figure 3.1 Functional model of a BCI System depicting the principle functional components (Mason and Birch 2003, Mason *et al* 2003). Note the Control Display is optional.

There are many BCI Transducer designs presented in the literature. However few have been designed specifically for asynchronous control. The concept of asynchronous control for BCI Systems was introduced in (Mason and Birch 2000). As a brief review, BCI Systems are designed to operate in the following general control paradigm. From an OFF state, a BCI System is turned ON using some mechanism. (At this point in the development of BCI systems, an attendant is needed to turn all existing BCI Systems ON)[13]. With the system turned ON, the User controls the system for a period of time, and then the system is turned OFF using a command or some other mechanism. This sequence is shown in Fig. 3.2. For an asynchronous BCI system, once the system is ON, the User affects the BCI Transducer output when they want by intentionally changing their brain state. In between periods of this

[13] Developing an automated switch to turn the system on is recognized as a difficult problem similar to the open microphone problem with speech recognition. Such a switch has to differentiate between all possible innate brain states and the system ON state. In practical terms, the mechanism will probably be implemented in the future as a sequence of commands, where each step in the sequence confirms the User's intent to turn the system ON.

Intentional Control (IC) the User is in a No Control (NC) state [14] – they may be idle, daydreaming, thinking about a problem or lunch, or performing some other action, but they are not trying to control the BCI Transducer. This form of intermittent control has been termed asynchronous control (Mason and Birch 2000). To operate in this paradigm, BCI Transducers are designed to respond only when there is intentional User control and maintain an inactive state output during times when the User is in a NC state. The performance of a User operating a two-state asynchronous BCI Transducer can be measured in percentage successful switch activations during the IC state (i.e., True Positive error rate) and percentage false switch activation during the NC state (False Positive error rate). (Note, in most BCI System evaluations reported in the literature, the allowable times for intentional User control are restricted to periods defined by a computer. Thus these evaluations have not tested their BCI technology for general intermittent or asynchronous operating paradigms. Since the User's input is synchronized with the external computer, this type of control has been termed synchronous control (Mason and Birch 2000). In these experimental systems the BCI technology is tested only during intentional User control. The response of the BCI Transducer during the NC state is not tested.)

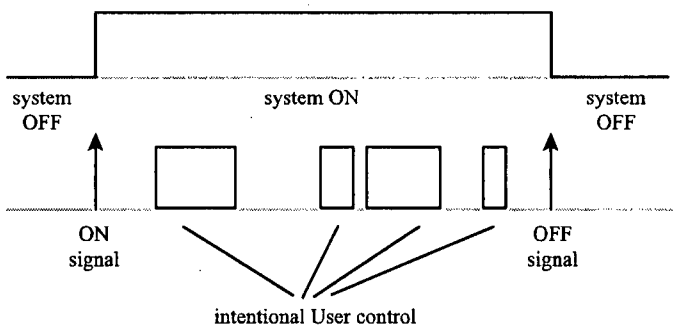

Figure 3.2 General asynchronous system control sequence.

Even though asynchronous (or intermittent) control is the most natural mode of interaction, it has received relatively little attention in the field. As recognized in (Wolpaw *et al* 2002), this is an important problem that requires more attention. Only a few BCI Transducers (Birch *et al* 1993, Levine *et al* 2000, Mason and Birch 2000, Millan and Mourino 2003 Yom-Tov and Inbar 2003) have been specifically designed (and tested) for asynchronous control. Each of

[14] The IC and NC states have also been referred to as "active" and "idle" states [6].

the proposed transducers produces a two-state discrete output and as such will be referred to as an Asynchronous Brain Switch (ABS) in the remainder of this paper.

Recent on-line studies with the Low-Frequency Asynchronous Switch Design (LF-ASD) have demonstrated total mean classification accuracies over 96% with spinal cord-injured and able-bodied subjects (Birch *et al* 2002a,b). Despite these encouraging results, our experience to date indicates that these error rates are too high for individuals with spinal cord injuries (our target population) in most practical asynchronous control applications. For practical applications, one needs to focus on low false positive rates. From our experience, false positive rates above 2% cause excess frustration and distraction in subjects (Birch *et al* 2002a).

This paper presents the results of an off-line study to evaluate four new design implementations of the LF-ASD transducer. The new designs incorporated combinations of EEG energy normalization, feature space dimensionality reduction, and an alternative classification scheme. EEG recordings of attempted finger movements were collected from our target population of individuals with spinal cord injuries (SCI subjects) as well as able-bodied (AB) subjects.

3.2. New Asynchronous Brain Switch Designs

The four new ABS designs tested in this study were variations of the original LF-ASD transducer design (Mason and Birch 2000). The new designs were named nLF-ASD- (A,B,C and D) as they were based on a set of normalized-energy, low-frequency features. Fig. 3.3 presents a block diagram with original components shown in white and the new components shown in gray. The four designs use various configurations of the new components and codebook generation methods as summarized in Table 2.1.

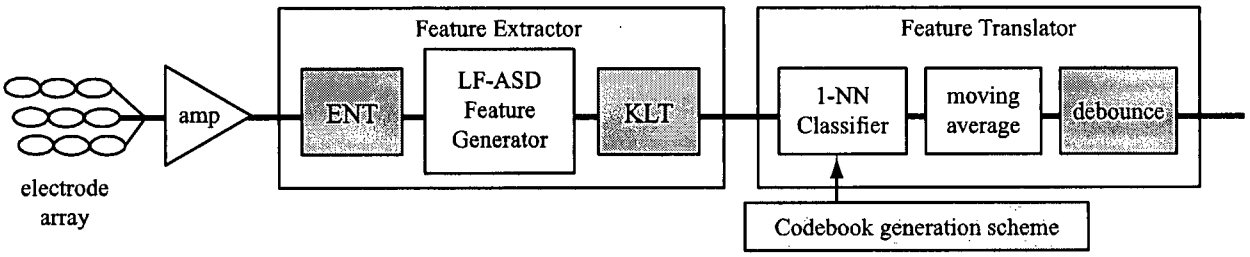

Figure 3.3 Components of nLF-ASD transducers with new components shown in gray, where ENT = Energy Normalization Transform, KLT = Karhunen-Loève Transform, and 1-NN = 1-Nearest Neighbor.

TABLE 3.1 CONFIGURATIONS OF THE NEW ASYNCHRONOUS BRAIN SWITCH DESIGNS, WHERE NLF-ASD = NORMALIZED-LOW-FREQUENCY ASYNCHRONOUS SWITCH DESIGN, ENT = ENERGY NORMALIZATION TRANSFORM, KLT = KARHUNEN-LOÈVE TRANSFORM, FUZZY ART = FUZZY ADAPTIVE RESONANCE THEORY, LVQ3 = LEARNING VECTOR QUANTIZATION.

Design Name	ENT	KLT	Debounce	Codebook Generation
NLF-ASD-A	X		X	K-MEANS + LVQ3
NLF-ASD-B	X		X	FUZZY ART + LVQ3
NLF-ASD-C	X	X	X	K-MEANS + LVQ3
NLF-ASD-D	X	X	X	FUZZY ART + LVQ3

3.3. Description of New Components and Methods

The Energy Normalization Transform (ENT) component, introduced in (Yu *et al* 2002), demonstrated that normalizing input energy results in greater class separation between IC and NC periods of movement and reduces system sensitivity to variations in EEG energy. The output of the transform, *y(n)*, is calculated from the input, *x(n)*, using

$$y(n) = \frac{x(n)}{\sqrt{w_N \Big/ \sum_{s=-(w_N-1)/2}^{s=(w_N-1)/2} x(n-s)^2}}$$

where w_N is the size of the input data window. For this work, the optimal w_N was 51 as determined by previous work (Yu *et al* 2002).

The Karhunen-Loève Transform (KLT) component was used to reduce the 6-dimensional feature space produced by the LF-ASD Feature Generator to a 2-dimensional space using the KLT algorithm (Jayant 1984). This component was added to test if a reduction in feature space could be accomplished without performance degradation. A reduced feature space potentially offers greater insight and hence improved customization of a particular individual's system parameters.

The Debounce component was introduced to reduce the number of false switch activations. Observations from previous studies (Birch et al 2002a, Lisogurski and Birch 1998) indicated that switch activations were multiple samples long and false positives occurred in clusters. Statistical analysis of the activation lengths and inter-activation periods, shown as L_i and P_j in Fig. 3.4A, confirmed these initial informal observations. Debouncing the switch output in a

manner similar to the debouncing of physical switches was expected to improve false activation rates (but with a cost in decreased re-activation time). The debounce component continuously monitors the output of the moving average block. After an activation is detected (i.e., a change in state from 0 to 1), the output is set to the logical state 1 for one sample then the output is forced to an inactive state 0 for $T_{db} - 1$ samples, where T_{db} is the debounce time period in samples. In this study various T_{db} values were evaluated.

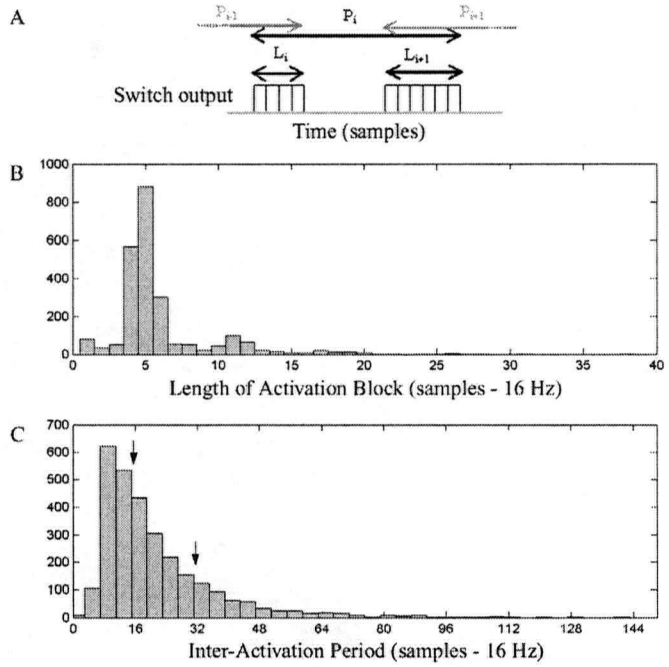

Figure 3.4 Distribution of false switch activations. A. Schematic diagram showing the metrics used to characterize false switch activations: L_i = length of the *i*th switch activation block (i.e. the number of activations that occur in consecutive sample times); and P_i = the *i*th inter-activation period (i.e. the distance from start of the *i*th activation block to the end of the *ith*+1 block). B. Histogram of switch activation block length (L_i values). C. Histogram of inter-activation period (P_i values). The arrows indicate the primary debounce values used in evaluation of the new ABS designs.

Two Codebook Generation Methods were used to generate a codebook for the 1-NN classifier from training data. The first method was that employed by Mason and Birch (Mason and Birch 2000). In this method, the k-means algorithm (Kohonen 1990) with 3 vectors per class was used to generate initial clustering of the two data sets. This was followed by Learning Vector Quantization (LVQ3) (Kohonen 1990) to generate the final codebook. The second method used a self-organizing neural model called fuzzy adaptive resonance theory (fuzzyART) (Carpenter *et al* 1991) to perform independent data clustering

of the two data sets. The fuzzyART algorithm provides a data-driven selection of the number of code vectors in the codebook which is an advantage over the original k-means (which uses a static number of code vectors). This neural network accepts analog inputs one at a time and develops an adaptive categorization of the input data based on the user defined degree of similarity of patterns in clusters. Familiar inputs activate their category, whereas unfamiliar inputs trigger either adaptive learning by an existing category, or commitment of a new category. The algorithm has one parameter, the vigilance parameter, which was set to between 0.45 and 0.6 in order to constrain the total number of codebook vectors for both IC states and NC states to be less than nine. The means of the resulting clusters were fed to LVQ3 to generate the final codebook.

3.4. Evaluation Methods

For this study the new designs were evaluated off-line and the performance of the new ABS designs were summarized in receiver operating characteristic (ROC) curves. These results were compared to the performance of the original LF-ASD design.

The data used in this evaluation was collected from subjects positioned 150 cm in front of a computer monitor. EEG was recorded from six bi-polar electrode pairs positioned over the supplementary motor area and the primary motor cortex (defined with reference to the International 10-20 System at F_1-FC_1, F_z-FC_z, F_2-FC_2, FC_1-C_1, FC_z-C_z, and FC_2-C_2). Electro-oculographic (EOG) activity was measured as the potential difference between two electrodes, placed to the corner and below the right eye. Ocular artifact was considered present when the difference between the EOG electrodes exceeded ±25 μV. All signals were sampled at 128 Hz (see (Birch *et al* 2002a) for details).

The subjects used in this study were four subjects with a high-level SCI and four able-bodied subjects. SCI subjects (all males and right handed) were between 33 and 56 years old. All SCI subjects had no residual sensation or motor function in the hands (spinal cord injuries between C3-C4 and C5-C6) and no other compounding physical or emotional conditions that may have interfered with the study (e.g. none were ventilator dependent). AB subjects (3 males and 1 female) were all right handed and between 31 and 57 years old.

Data was collected from the subjects performing a guided task. At random intervals (mean 7 seconds), a 2cm white circle was displayed on the subject's monitor for ¼ second, cuing

them to attempt a movement. In response to the cue, subjects tried to activate the brain switch by attempting to move their right index finger 1 second after the cue appeared[15]. (The 1 second delay was used to avoid visual evoked potential effects from the cue.) To train the subjects for appropriate response timing, a yellow dot was flashed 1 second after the white circle in order to provide a timing cue. After 5 to 15 minutes of practice, this cue was only provided once every 4-8 attempts as a reference for the subject to self check their timing. Data collected when a yellow dot was displayed was not used for the codebook training phase or performance evaluation of this study. The period between trials was varied; however, subjects attempted an average of 15 switch activations in approximately 2 minutes of recording. For each subject, an average of 10 such recordings was collected every day for 6 days. The first days' recordings were used to compute the codebooks for the subsequent 5 days of evaluation.

The ability of subjects to control the ABS designs was evaluated with percentage of correct activations during IC states (true positives, TPs) and percentage of false switch activations during NC states (false positives, FPs). A TP was identified if the ABS was activated at least once in the window 0.5 seconds before and 1 second after the time of expected movement, a method similar to that employed by others (Levine *et al* 2000, Yom-Tov and Inbar 2003). Multiple activations in this window were considered as a single activation. FPs were assessed in the periods before the appearance of a white circle and after the end of the activation window. Periods during which ocular artifact occurred were not evaluated.

3.5. Results and Discussion

3.5.1. Debounce Analysis

The previous observations and the results of the distribution analysis of switch activations necessitated an investigation into the impact of debounce on the various switch designs. As an example, the ROC curve for subject SC2 is shown in Fig. 3.5A. Also shown is an expanded view of the ROC curve (Fig. 3.5B) to emphasize the performance characteristics of the switch at FP rates below 8%. (To improve the presentation of the results, only FP rates below 8% will be displayed in further ROC curves.) Table 3.2 shows mean TP rate for all

[15]Both subject groups used the same neurological mechanism to drive the brain switch: an attempted finger flexion. This resulted in no movement in SCI subjects, and an actual finger flexion in AB subjects.

eight subjects processed with the nLF-ASD-A and interpolated for the given FP rate of 2% for eight different values of debounce.

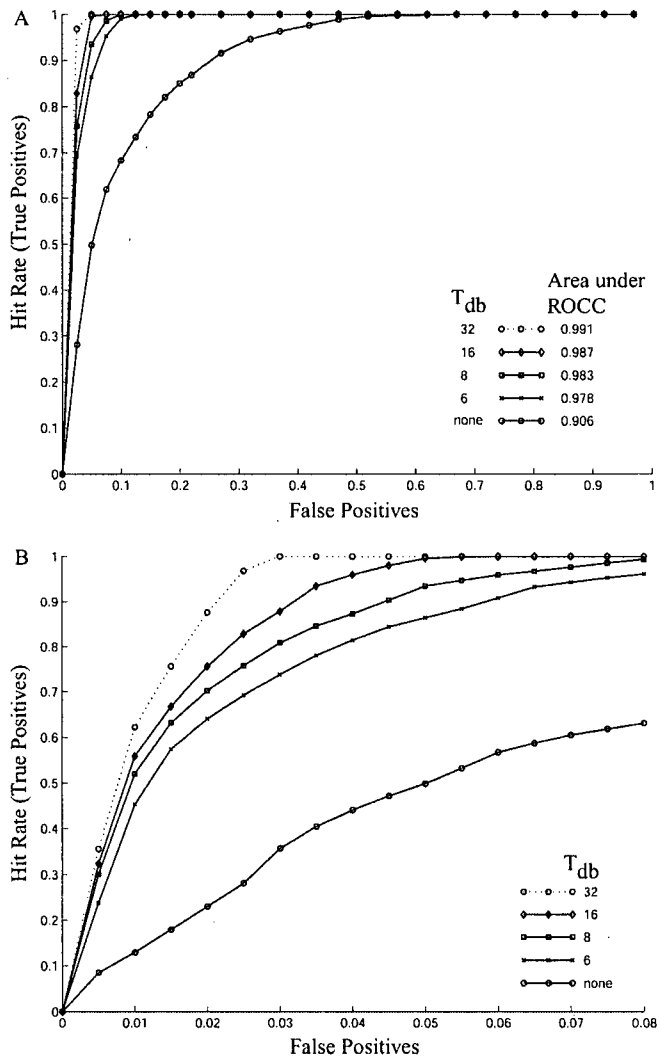

Figure 3.5 ROC curves for Subject SC2 using system design nLF-ASD-A. A. Analysis of the 8 different values of debounce (T_{db}) used in this study with corresponding Areas under the ROC curve to indicate overall system performance. B. An expanded view of A. Only those values of false positives below 8% are shown for clarity.

TABLE 3.2 MEAN TRUE POSITIVE RATES FOR ALL SUBJECTS WITH DIFFERENT DEBOUNCE VALUES, WHERE NLF-ASD = NORMALIZED-LOW-FREQUENCY ASYNCHRONOUS SWITCH DESIGN, STD = STANDARD DEVIATION OF TRUE POSITIVE RATES, S = SECONDS, TDB.= DEBOUNCE PERIOD. NOTE: ALL FALSE POSITIVE RATES = 2%.

	Debounce (T_{DB}) in Samples (and Time)									
	none (0 sec)		6 (0.38 s)		8 (0.5 s)		16 (1.0 s)		32 (2.0 s)	
Design Name	mean	STD	mean	STD	mean	STD	mean	STD	mean	STD
LF-ASD	0.13	0.09	0.36	0.14	0.44	0.15	0.51	0.15	0.70	0.11
NLF-ASD-A	0.21	0.05	0.54	0.10	0.61	0.10	0.68	0.10	0.83	0.06
NLF-ASD-B	0.21	0.05	0.55	0.09	0.62	0.09	0.68	0.09	0.83	0.05
NLF-ASD-C	0.19	0.05	0.53	0.09	0.61	0.09	0.66	0.09	0.82	0.06
NLF-ASD-D	0.20	0.05	0.53	0.09	0.60	0.09	0.66	0.09	0.81	0.06

As the debounce period increased, the FP rate decreased for a given TP rate. These results are in line with the application of debounce in other physical transducer designs. As the length of the debounce period increased the re-activation time of a BCI transducer is impacted. The tradeoff is clear and one needs to consider this for a given application. For the remainder of the results reported here, the debounce period of 16 samples (1 second) was chosen for data presentation because it provides a practical minimum re-activation time while rejecting the majority of the clustered FP activations (see arrow in Fig. 3.4C).

3.5.2. New vs. Old Transducer Designs

The performance of the new switch design methods with the previous design (LF-ASD) at fixed debounce periods was compared. The results of all five processing methods for subject SC2 are shown in Fig. 3.6. The TP rates at 2% FP for all eight subjects are shown in Table 3.3. The results show that all four new nLF-ASD-*X* variants performed similarly with no statistically significant differences. No differences were detected between codebooks generated using k-means or fuzzyART. As well, no differences were detected with data transformed to 2-dimensional feature vectors. Because performance is not worsened with lower dimensional data, the Feature Extractors with KLT will probably be preferred in future studies because of the benefits of a lower feature space dimensionality, i.e., easier interpretation of feature space characteristics which can facilitate and guide classifier design choices. The fact that no differences were shown with the different schemes suggests alternate approaches need to be explored to achieve performance improvements. Such

approaches may include 1) more complex classifiers such as support vector machines (SVM) (Burges 1998) or fuzzy ARTMAP (Carpenter 1992); 2) customization of the LF-ASD Feature Generator parameters to individual subjects (which to date has not been done in this or any previous study); and/or 3) the exploration of different EEG features.

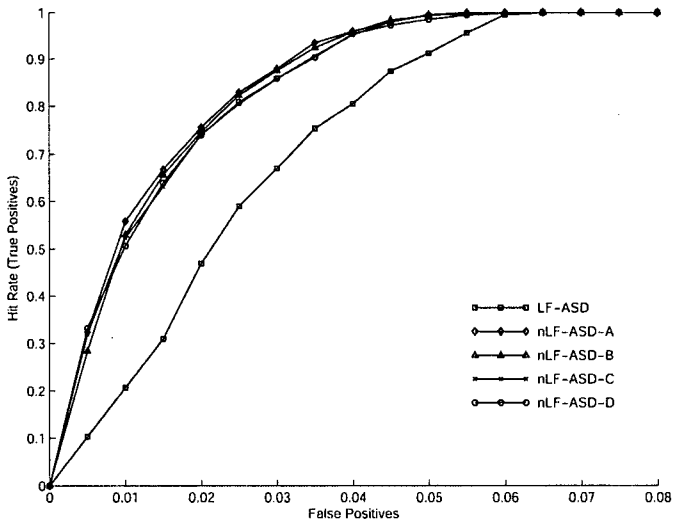

Figure 3.6 ROC curves for Subject SC2 with debounce set to 16 samples. Analysis of the five different processing methods used in this study. Only those values of false positives below 8% are shown for clarity.

All four new transducer designs performed better than the previous LF-ASD transducer. This is most likely due to the presence of the ENT block in the processing path which increases the separation between IC and NC feature vectors and stabilizes the scale of input signals to the LF-ASD processor (Yu *et al* 2002). The mean ROC curves for all eight subjects are shown in Fig. 3.7. The nLF-ASD-A system was used to compare the new methods with the previous LF-ASD because of its relative computational simplicity and the fact that the previous (LF-ASD) codebooks were generated with this method. The nLF-ASD-A system performed significantly better than the previous design, as seen with a mean TP rate increase of 33% for a FP rate of 2% (from 51% to 68%; $p < 0.05$, 2-way analysis of variance). Performance improvements can also be seen in individual subjects (Table 3.3) when ENT processing was used (for instance with subject SC1, TP rate improved from 45% to 71%), although for three able-bodied subjects (AB2-4) the improvements were minimal. It should

also be noted that the TP performance results presented in Table 3.3 represent total system classification accuracies greater than 97%. This is due to the fact that the LF-ASD is continually classifying inputs every 16^{th} of a second and the fact that the majority of User's time is spent in an NC state which for a 2% FP rate represents an accuracy of 98% during this state alone.

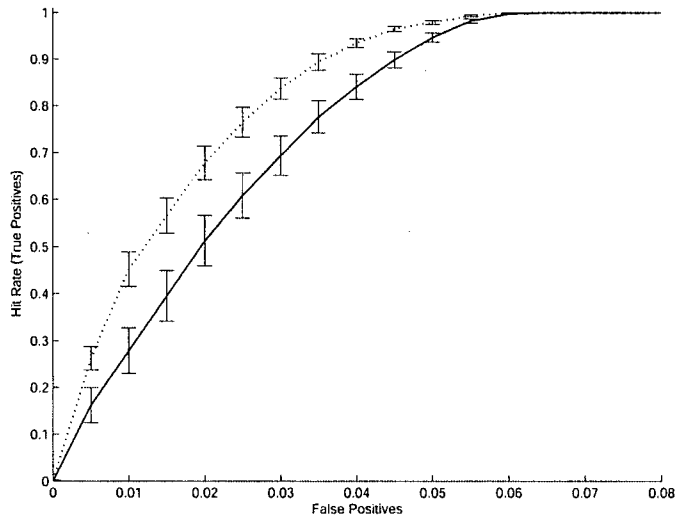

Figure 3.7 ROC curve of the true positive rate means for all 8 subjects (depicted with standard error of the mean error bars) with debounce set to 16 samples. Solid line = LF-ASD. Dashed line = nLF-ASD-A. The difference is significant ($p < 0.05$, 2-way ANOVA). Only those values of false positives below 8% are shown for clarity.

TABLE 3.3 TRUE POSITIVE RATES FOR INDIVIDUAL SUBJECTS. NOTE: ALL FALSE POSITIVE RATES = 2%. DEBOUNCE VALUES OF 16 ARE SHOWN.

	Subject							
Design Name	SC1	SC2	SC3	SC4	AB1	AB2	AB3	AB4
LF-ASD	0.45	0.47	0.46	0.35	0.32	0.73	0.65	0.67
NLF-ASD-A	0.71	0.76	0.47	0.63	0.72	0.81	0.67	0.66
NLF-ASD-B	0.72	0.75	0.50	0.63	0.67	0.79	0.69	0.66
NLF-ASD-C	0.67	0.74	0.49	0.59	0.68	0.78	0.68	0.65
NLF-ASD-D	0.67	0.74	0.50	0.56	0.69	0.79	0.68	0.66

3.5.3. Spinal Cord-Injured Subjects vs. Able-Bodied Subjects

The performances of spinal cord-injured subjects versus able-bodied subjects were compared with the original LF-ASD and the new nLF-ASD-A system design (Fig. 3.8). For the new system designs, little or no differences between SCI subjects and AB subjects were detected (Fig. 3.8A, Table 3.3). Interestingly, AB subjects performed better than SCI subjects on the LF-ASD system (Fig. 3.8B), although these results were not statistically significant ($p > 0.05$, 2-way ANOVA). Differences between SCI subjects and AB subjects are readily evident from Table 3.3. For example, three SCI subjects showed major improvements with ENT processing compared to only one AB subject. The differences in performance between SCI subjects and AB subjects using the older LF-ASD may reflect differences in EEG energy levels during attempted motor movements by the SCI subjects compared to AB subjects, although the ensemble average movement related potentials (MRP) for these groups of subjects are similar (Birch *et al* 2002a,b). Because SCI subjects are able to operate the LF-ASD, which is presumed to be activated by MRPs (Mason and Birch 2000), (Birch *et al* 2002a,b), it seems likely that SCI subjects produce similar MRPs to those of AB subjects. Others have suggested the same (Decety and Biosson 1990, Green *et al* 1998, Green *et al* 1999), although there is some disagreement in the field (Levy *et al* 1990, Levt *et al* 1991, Streletz *et al* 1995). The results presented here suggest it is possible that SCI subjects have only differences in relative EEG signal energy levels, an issue mitigated with the use of an energy normalization transform. Thus, the similarity of SCI subjects and AB subjects suggest that the LF-ASD with energy normalization may be a viable BCI for individuals with a disability.

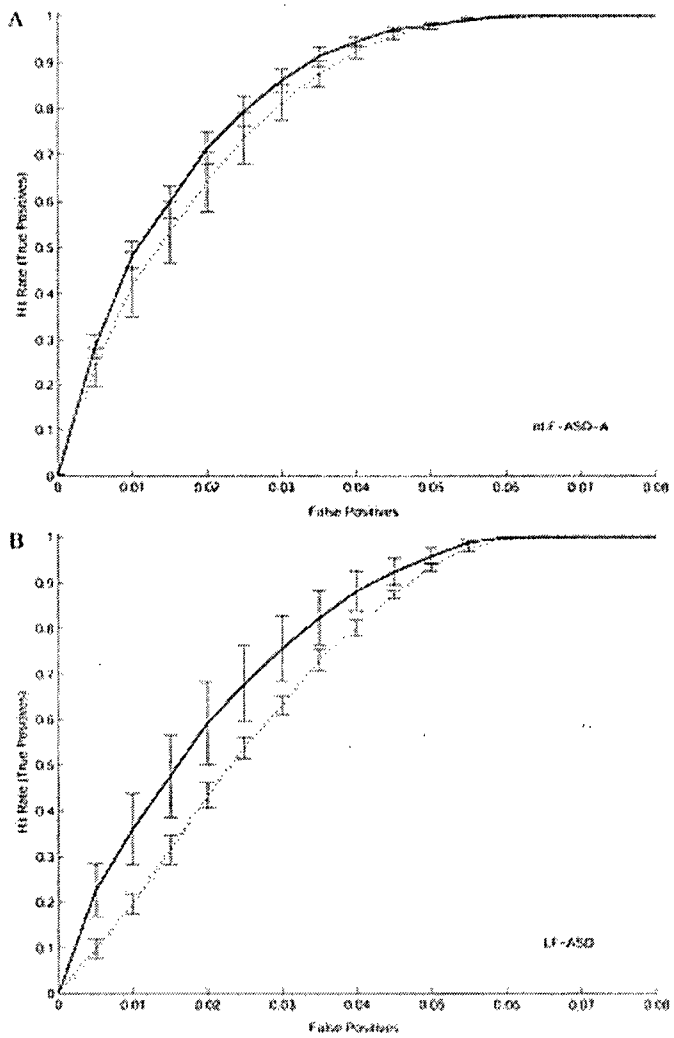

Figure 3.8 ROC curve of the mean true positive rates for AB subjects vs. SCI subjects (depicted with standard error of the mean error bars) with debounce set to 16 samples. Solid line = able-bodied subjects. Dashed line = spinal cord-injured subjects. A. System design nLF-ASD-A. B. System design LF-ASD.

3.6. Conclusion

In conclusion, the error characteristics of the new asynchronous brain switch designs were significantly better than the LF-ASD design with true positive rate increases of approximately 33% for false positive rates in the range of 1-2%. The improvement was attributed to the addition of an energy normalization transform (ENT). The most significant improvements with ENT were found in spinal cord-injured subjects, indicating possible energy differences in EEG recorded from SCI and AB subjects. One of the next steps is to evaluate these new designs in an on-line study.

The four new nLF-ASD designs had no significant performance differences between them. The main conclusion from this finding is that we can use a two-dimensional feature space without performance degradation. This may improve our ability to understand the feature space and thus select better classifier designs. This finding also suggests that the 1-NN classification algorithm was not sensitive to the codebook generation method.

This work has succeeded in decreasing the error rates of our ABS designs. Although this decrease in error rate is encouraging, practical experience indicates that further improvements are needed. Thus, our future work will explore the use of self-learning classification schemes like SVM or fuzzy ARTMAP instead of the 1-NN classifier. We will also explore customization of the LF-ASD Feature Generator parameters (which have never been adjusted for individual subjects) or develop different feature extraction methods.

An exciting finding of this study, which confirms the findings of (Birch *et al* 2002a), was that spinal cord-injured subjects can operate these new ABS designs to the same ability as able-bodied subjects. Both populations are achieving promising control accuracies with current technology. Thus, AB subjects using a finger movement are good predictors of the controllability of the nLF-ASD technologies by SCI subjects using an attempted finger movement. This evidence supports our use of able-bodied subjects as proxies for our target population in future development efforts. The results of this study support our belief that ABS technology will dramatically increase the level of independence for individuals with high level spinal cord injuries in the foreseeable future.

3.7. References

Birch G E, Bozorgzadeh Z and Mason S G 2002a Initial on-line evaluation of the LF-ASD brain-computer interface with able-bodied and spinal-cord subjects using imagined voluntary motor potentials *IEEE Trans. Neural Syst. Rehabil. Eng* **10** 219.

Birch G E, Lawrence P D and Hare R D 1993 Single trial processing of event related potentials using outlier information *IEEE Trans Biomed Eng* **40** 59-73.

Birch G E, Mason S G and Borisoff J F 2002b Current Trend in Brain-Computer Interface Research at the Neil Squire Foundation *IEEE Trans. Neural Syst. Rehabil. Eng* **11** 123-6.

Burges C J C 1998 A Tutorial on Support Vector Machines for Pattern Recognition *Data Mining and Knowledge Discovery* **2** 121-67.

Carpenter G A, Grossberg S, Markuzon N, Reynolds J H and Rosen D B 1992 Fuzzy ARTMAP: A neural network architecture for incremental supervised learning of analog multidimensional maps *IEEE Trans.on Neural Networks* **3** 698-713.

Carpenter G A, Grossberg S and Rosen D B 1991 Fuzzy ART: an adaptive resonance algorithm for rapid, stable classification of analog patterns *Proc. Inter. Joint Conf. on Neural Networks (Seattle, USA)* pp 411-6.

Decety J and Boisson D 1990 Effect of brain and spinal cord injuries on motor imagery *European Archives of Clinical Neuroscience* **240** 39-43.

Green J B, Sora E, Bialy Y, Ricamato A and Thatcher R W 1998 Cortical sensorimotor reorganization after spinal cord injury: an electroencephalographic study *Neurology* **50** 1115-21.

Green J B, Sora E, Bialy Y, Ricamato A and Thatcher R W 1999 Cortical sensorimotor reorganization after paraplegia: an EEG study *Neurology* **53** 736-43.

Jayant N S and Noll P 1984 Digital Coding of Waveforms (NJ: Prentice Hall).

Kohonen T 1990 The Self-Organizing Map *Proc IEEE* **78** 1464-80.

Levine S P, Huggins J E, Bement S L, Kushwaha R, Schuh L A, Rohde M M, Passaro E A, Ross D A, Elisevich K V and Smith R J 2000 A Direct Brain Interface Based on Event-Related Potentials *IEEE Trans Reh Eng* **8** 180-5.

Levy W G J, Amassian V E, Schmid U D and Jungreis C 1991 Mapping of motor cortex gyral sites non-invasively by transcranial magnetic stimulation in normal subjects and patients *Electroencephalography and Clinical Neurophysiology* **43** 51-75.

Levy W G J, Amassian V E, Traad M and Cadwell J 1990 Focal magnetic coil stimulation reveals motor cortical system reorganized in humans after traumatic quadriplegia *Brain Research* **510** 130-4.

Lisogurski D and Birch G E 1998 Identification of finger flexions from continuous EEG as a brain computer interface *Proc. 20th Annual Inter. Conf. IEEE Engineering in Medicine and Biology Society (Hong Kong)*

Mason S G and Birch G E 2000 A brain-controlled switch for asynchronous control applications *IEEE Trans. Biomed. Eng* **47** 1297-307.

Mason S G and Birch G E 2003 A general framework for brain-computer interface design *IEEE Trans. Neural Syst. Rehabil. Eng* **11** 70-85.

Mason S G, Moore M M and Birch G E 2003 Designing Pointing Devices using Brain-Computer Interface Technology *Proc. 1st Int. IEEE EMBS Conf. on Neural Engineering (Capri, Italy)* pp 26-3.

Millan J R and Mourino J 2003 Asynchronous BCI and local neural classifiers: an overview of the Adaptive Brain Interface project *IEEE Trans. Neural Syst. Rehabil. Eng* **11** 159-61.

Nicolelis M A 2003 Brain-machine interfaces to restore motor function and probe neural circuits *Nat. Rev. Neurosci.* **4** 417-22.

Streletz L J, Belevich J K, Jones S M, Bhushan A, Shah S H and Herbison G J 1995 Transcranial magnetic stimulation: cortical motor maps in acute spinal cord injury *Brain Topography* **7** 245-50.

Wolpaw J R, Birbaumer N, Heetderks W J, McFarland D J, Peckham P H, Schalk G, Donchin E, Quatrano L A, Robinson C J and Vaughan T M 2000 Brain-computer interface technology: a review of the first international meeting *IEEE Trans. Rehabil. Eng* **8** 164-73.

Wolpaw J R, Birbaumer N, McFarland D J, Pfurtscheller G and Vaughan T M 2002 Brain-computer interfaces for communication and control *Clin.Neurophysiol.* **113** 767-91.

Yom-Tov E and Inbar G F 2003 Detection of movement-related potentials from the electro-encephalogram for possible use in a brain-computer interface *Med. Biol. Eng Comput.* **41** 85-93.

Yu Z, Mason S G and Birch G E 2002 Enhancing the Performance of the LF-ASD Brain-Computer Interface *Proc. IEEE 2nd Joint EMBS-BMES Conf. (Houston, TX)*

Chapter 4 A Comparative Study on Generating Training-Data for Self-Paced Brain Interfaces [16]

4.1. Introduction

Direct Brain Interface (BI) systems provide an alternative communication and control solution for individuals with severe motor disabilities, bypassing impaired interface pathways. In a BI system, the cortical activity associated with an intentional control command is mapped directly to application-specific control signals. Various devices, such as neural prostheses, can then be controlled by cognitive processes alone. For a review of the field, see (Mason and Birch 2003, Mason *et al* 2006, Nicolelis 2003, Vaughan *et al* 2003, Woplaw *et al* 2002).

Many BI transducer designs have been presented in the literature. Few of them, however, have been designed specifically for asynchronous or self-paced control. The concept of self-paced control of BI systems was introduced in (Mason and Birch 2000) as "asynchronous control". In a self-paced BI, the users affect the BI transducer output whenever they want by intentionally changing their brain state. Between periods of intentional control (IC), users are said to be in a no-control (NC) state - they may be idle, daydreaming, thinking about a problem or lunch, or performing any other action, but they are not trying to control the BI transducer. To operate in this paradigm, BI transducers are designed to respond only when there is intentional user control and to remain inactive when the user is in an NC state. In contrast, most BIs operate only during specific periods determined by the system (not the user). The latter operating paradigm is referred to as synchronous or synchronized control (Mason and Birch 2000, Mason and Birch 2005). Although self-paced control is the most natural mode of interaction, it has received relatively little attention. Only a few BI transducers (Birch *et al* 1993, Borisoff *et al* 2004, Levine *et al* 2000, Graimann *et al* 2004, Mason and Birch 2000, Millan and Mourino 2003, Yom-Tov and Inbar 2003, Scherer *et al* 2004, Townsend *et al* 2004) have been specifically designed and tested for self-paced

[16] A version of this chapter has been published. © 2007 IEEE. Reprinted, with permission, from (Bashashati A., Mason S.G., Borisoff J., Ward R.K., and Birch G. (2007) A Comparative Study on Generating Training-Data for Self-Paced Brain Interfaces *IEEE Trans. Neural Systems and Rehabilitation* **15** 59-66)

control. As recognized in (Wolpaw *et al* 2002), it is an important issue that deserves more attention from the research community.

Like any control system dependent on pattern recognition or machine learning, before a user can operate the system, the system needs to be trained. System training typically refers to training the classifier component of the system, a process that requires well-defined training-data that includes representative samples of each class of data. For self-paced BI systems, generation of the training-data is especially challenging. As an example, consider designing a BI system that is activated by the user attempting or imagining a specific movement. Furthermore, consider that most BI systems are designed for use by individuals with severe motor disabilities. With these individuals, there is no observable indicator of their intent. With no indication of intent, the exact time that the person actually imagined or intended to perform the movements is not known. Thus, little or no knowledge is available to label the training-data for the intentional control data class. In contrast, an able-bodied subject can perform the desired movements and one can observe his/her movement as the indicator of intent. Even for able-bodied individuals, when the BI system aims at detecting imagined mental tasks (e.g. imagined movement), no indication of intent is available. In such cases, generating training-data for such a system is also problematic. With the lack of an observable indication of intent, one possibility is to use the time that the intentional control (IC) task such as an imagined movement is expected to be performed. However, since the actual time of IC is not precisely known, the use of the expected time of IC can result in poor training-data and consequently worse system performance.

This problem is also observed in other research fields such as the cases when satellite images need to be classified but no knowledge of the ground-truth is available. In such cases, the expert's interpretation of satellite images is used to generate training-data (Chia-Tang *et al* 2003) or unsupervised signal processing methods are employed to detect specific objects in the image (Kersten *et al* 2005). Because the signal-to-noise ratio of the brain signal is very low and the EEG patterns associated with different brain states are not visually differentiable in a single trial basis, these approaches are not useful in generating training-data for BI systems.

This paper introduces and then evaluates three methods to generate system training-data for self-paced BI systems. These methods rely on the external knowledge of the 'approximate' time of the intended control (IC), i.e. the time of expected attempted movement. In such cases, the exact time of the IC state is not known. Thus the extracted features around the approximate time of IC could belong to the NC or IC class. Comparing the statistical likelihood of mixed NC and IC class features to NC class features, the proposed methods estimate which class each feature belongs to and labels them accordingly in order to tune the various system components such as the classifier.

In Section 4.4, the performance of the proposed methods is compared to four other methods of generating training-data. These four methods are simply based on the expected time of the IC. To compare the performance of the proposed methods, the methods are applied to the EEG data of four able-bodied and four spinal-cord-injured (SCI) subjects which were previously recorded in self-paced BI experiments at the Neil Squire Brain Interface Lab, Vancouver, Canada. We compare the performance of these methods on the classifier of a specific self-paced brain interface, named the LF-ASD, as a representative example of self-paced BIs in the literature (Mason and Birch 2000).

4.2. Data Generation Methods

In the following subsections, we introduce the proposed methods for generating training-data for self-paced brain interfaces. These methods are based on an experimental protocol where several attempts at intentional control (IC) are measured assuming the trial structure shown in Fig. 4.1. For each trial, the experimental system provides a timing cue. The subjects are instructed to attempt intentional control in response to this cue[17]. The cue determines the "*time of the expected IC*" or TEIC which is when the subjects are instructed to attempt intentional control. A time window that spans T seconds before to T seconds after this time is called the '*expected response window*' or ERW. The purpose of the proposed methods is to extract the most likely feature (or features) that corresponds to IC, of all those mixed IC and NC features that occurred during the ERW. These extracted IC features are then used as training-data for the BI system.

[17] Cues can be offset by T_{Cue} from actual TEIC to avoid stimulus-related artifacts.

The proposed methods require approximately four minutes of EEG data related to the no control (NC) class. These data can be extracted from the interval times between IC trials (as shown in Fig. 4.1) or separately during any time interval when the subject does not intend issuing control.

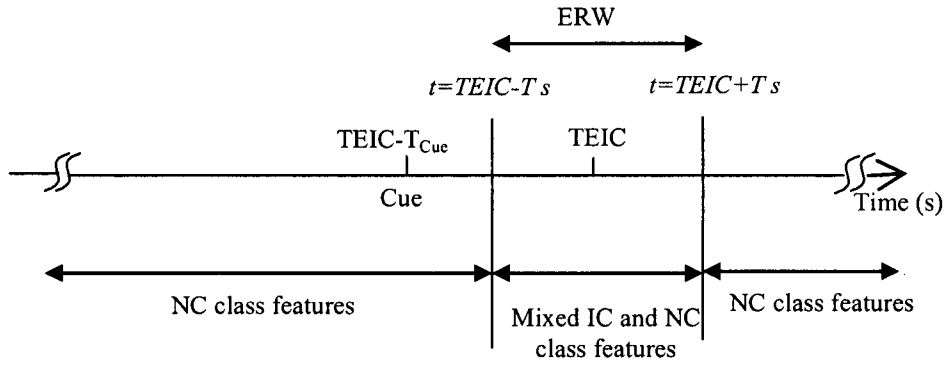

Figure 4.1 Structure of an IC trial, where TEIC: time of the expected IC, ERW: expected response window, IC: intended control, NC: no control, T_{Cue}: time of the cue appearance.

4.2.1. Parzen-Based Training-Data Generation (TR_Gen1)

The first method, named TR_Gen1 generates the probability density function (PDF) of the known samples which lie outside the ERW. Since these samples are known to be of the NC type, the resulting PDF is denoted by $f_{NC}(x)$. $f_{NC}(x)$ is then used to rank the samples within the ERW such that the feature vectors that have higher probability of belonging to the NC class are ranked lower than those feature vectors that have a low probability of belonging to the NC class. In fact, the higher ranked features would most likely belong to the IC class rather than the NC class.

Details of the procedure for generating the training-data with TR_Gen1 method is shown in Fig. 4.2. This procedure has two main stages:

In the first stage, the PDF of the NC features ($f_{NC}(x)$) is estimated using the Parzen's probability density estimation method (Cacoullos 1966, Parzen 1962). The Parzen method yields accurate results when a large population of data is available. For the problem at hand, because of the availability of a large population of NC state features (Cacoullos 1966, Parzen

1962) and because of the findings in (Glavinovic 1996) that shows Parzen density estimation outperforms frequency histogram estimation, the estimation of the probability density distribution using the Parzen method should yield more accurate results than those given by other probability density estimation methods. The kernel function and the kernel size are the two important parameters of the Parzen's probability density estimation method. A Gaussian kernel with kernel size of $N^{-k/n}$ as recommended in (Cacoullos 1966) was used, where N is the number of available data, n is the dimension of the data, and k is chosen as a number between 0 and 1. To obtain k, we used simulated Gaussian distributed data and obtained the best estimated PDF results with k=0.15 and used this value in our method.

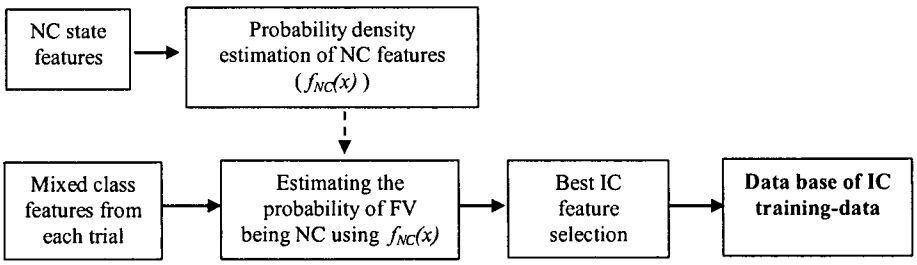

Figure 4.2 IC state training-data generation using TR_Gen1 method, IC: intended control, NC: no control, FV: feature vector, $f_{NC}(x)$: probability density function of NC features.

In the second stage, we consider the features extracted from the ERW time duration. The class to which each of these features belongs is not known. These features are processed with the goal of selecting amongst them the best representative features of the IC class. The probability density distribution of the NC feature vectors computed in the previous step is used to estimate the probability of each of these features belonging to the NC class. For each ERW, the top ranked feature (the feature that is least likely to belong to the NC class) is selected as an IC class feature. This procedure is repeated for each ERW. The resulting set of IC class features are selected as IC training-data. To select the features of the NC training-data, the features from outside the ERW are considered and the probabilities of these features belonging to NC class are calculated separately for each feature. Then, the top H=75% of NC class features that has the highest probability of being NC are selected as NC class training-data.

4.2.2. kMeans-Based Training-Data Generation (TR_Gen2)

The second method, called TR_Gen2, separates IC from NC features in the ERW based on their initial clustering. As this clustering method only separates the features into two classes and does not provide the label of the resulting clusters, the probability density function of the NC class features ($f_{NC}(x)$) is used to label the resulting clusters as NC or IC class. The same procedure as described in Section 4.2.1 is used to estimate the probability density function ($f_{NC}(x)$) of the NC class.

As Fig. 4.3 shows, the ERW features are fed into the k-Means clustering algorithm (Kohonen 1990) using k=2, i.e. two feature clusters. Using $f_{NC}(x)$, each of the two resulting clusters is labeled as an NC or IC class. The method that labels the clusters is as follows: the average of each of the features of the two resulting clusters is calculated. Using $f_{NC}(x)$, the features of the cluster whose average has less probability of being an NC class is considered as the IC class cluster and the other cluster is considered as the NC class cluster. This procedure is repeated for each ERW and all features belonging to all the IC clusters form the set of IC class features to be used as the IC training-data. To generate the NC class training-data, the same procedure as described for the TR_Gen1 method is used.

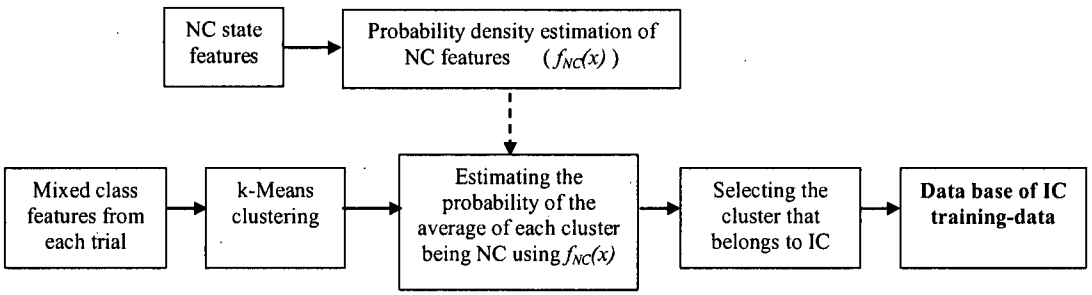

Figure 4.3 IC state training-data generation using TR_Gen2 method, IC: intended control, NC: no control, $f_{NC}(x)$: probability density function of NC features.

4.2.3. Averaged kMeans-Based Training-Data Generation (TR_Gen3)

The third method, named TR_Gen3, is also based on the initial kMeans clustering of the ERW features, as explained in Section 4.2.2. After clustering the ERW features and labeling them, the average feature of all IC features in the cluster is calculated and used as the representative IC class feature for that ERW. This procedure is repeated for each ERW

resulting in a set of IC class features for the training set. The rationale behind using the average (and not all the features) of the IC cluster is as follows: when all the features in the IC cluster are used, there might be some features that are very close to the NC class but they were considered as IC class features. By averaging the features of the IC cluster, the effect of such features is hopefully reduced.

4.3. Evaluation

The proposed training-data generation schemes were evaluated on data previously recorded for self-paced BI experiments at the Neil Squire Society, Vancouver, Canada. The proposed methods were used to train the feature classifier of the LF-ASD brain switch (Mason and Birch 2000). The results are evaluated with standard performance metrics and are presented in Section 4.4.

Fig. 4.4 shows the block diagram of the latest LF-ASD design. Using a custom-designed template matching algorithm, the features from each of the six incoming bipolar channels are calculated. Overall, six feature values corresponding to each of the six bipolar channels are generated. Then, the Karhunen-Loeve transform (i.e. Principal Component Analysis) is used to reduce the dimensions of the resultant features from six two. Every $1/16^{th}$ of a second, a 1-nearest neighbor (1-NN) feature classifier classifies each feature to either the IC or NC class. A moving average and a debounce block are then used to further improve the classification accuracy of the system by reducing the number of false switch activations. Specific details on the latest design and implementation of the LF-ASD can be found in (Borisoff *et al* 2004). To generate the codebooks for the 1-NN classifier, the k-means algorithm (Kohonen 1990) with three vectors per class state is followed by Learning Vector Quantization (LVQ3) (Kohonen 1990) to find the final codebook in the feature space. In the LVQ algorithm, the learning rate, α, is set to 15/(length of training data) and ε to 0.25. The algorithm is stopped after it runs 2000 times or if the template does not change significantly according to a predefined threshold.

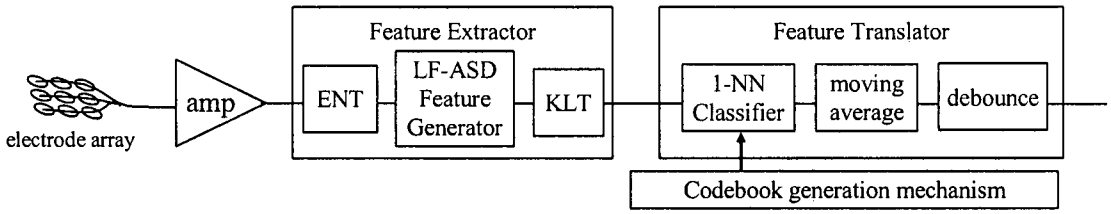

Figure 4.4 Components of the Low Frequency Asynchronous Switch Design (the LF-ASD) (from (Borisoff *et al* 2004)). ENT: energy normalization transform, KLT: Karhounen-Loéve transform, 1-NN: one nearest neighbour

4.3.1. Experimental Data

The subjects consisted of four subjects with a high-level spinal cord injury (SCI) (level of injury between C3-4 and C5-6) and four able-bodied subjects. All subjects were male except for one female subject. They were all right handed and between 31 and 57 years old. All SCI subjects had no residual sensation or motor function in the hands. All the subjects had signed the consent form required by the Behavioral Research Ethics Board (BREB) of the University of British Columbia.

The EEG data were collected from subjects positioned 150 cm in front of a computer monitor. The EEG signal was recorded from six bipolar electrode pairs positioned over the supplementary motor area and the primary motor cortex (defined with reference to the International 10-20 System at F1-FC1, Fz-FCz, F2-FC2, FC1-C1, FCz-Cz, and FC2-C2). Electro-oculographic (EOG) activity was measured as the potential difference between two electrodes, placed at the corner and below the right eye. An eye-blink artifact was considered present when the difference between the EOG electrodes exceeded ±25 μV. All signals were amplified, then filtered by a 0.1 to 30Hz band-pass filter and then sampled at 128Hz by a PC equipped with a 12-bit analog to digital converter.

The data were collected from the subjects while performing a guided task, in 2-minute sub-sessions, over a session period of 1.5 hours. The sub-sessions contained both the NC and IC state periods as shown in Fig. 4.1 where T_{Cue}=1s, T=0.5s and TEIC corresponds to time of attempted movement. At random intervals of 5.6 to 7.0 seconds (mean of 6.7 seconds), a 2cm white circle cue was displayed on the subject's monitor for ¼ second, prompting them to attempt a movement. In response to this cue, the subject tried to activate the brain switch by

attempting to move the right index finger one second (T_{Cue}) after the cue appeared. The one-second delay (T_{Cue}) was used to avoid the visual evoked potential effects from the activity. The time, one second after the cue, is called "time of *expected* (attempted) intended control (TEIC)". As the time to perform the movement attempt depended on a user's response, the movement attempt was not necessarily performed at TEIC and would be different from subject to subject and attempt to attempt. Both subject groups used the same neurological mechanism to drive the brain switch: an attempted right index finger flexion. This resulted in no movement in subjects with high level SCI, and an actual finger flexion in able-bodied subjects. For each subject, an average of 80 trials was collected every day for 6 days.

Besides recording the EEG data during movement attempts, in each session, the EEG data were also recorded for several 2-minutes periods while the person was in a specific no control (NC) state. The sub-sessions that only contained NC state EEG data were gathered while subject was in different NC states such as attentive eyes opened while looking at a picture on the monitor, doing a search task, attentive eyes closed etc. The reason this type of data was recorded was to evaluate the performance of the BI design in different NC state periods.

4.3.2 Method of Evaluation

The proposed training-data generation schemes were evaluated on all available data, i.e., the sub-sessions that contained mixed NC and IC state data and the sub-sessions that included only NC state periods. Specifically, the sub-sessions that contained only NC state EEG data were used to generate the probability density distribution of NC class features (f_{NC}) as explained in Section 4.2. In this experiment we chose H=75% and T=0.5s (for more details refer to Section 4.2).

The ability of the subjects to control the LF-ASD BI switch was evaluated by 1) the percentage of correct activations during ERWs (referred to as true positives, TPs) and 2) the percentage of false switch activations during NC states (false positives, FPs). A TP was identified if the BI system was activated at least once in a window spanning 0.5 seconds before to 1 second after the time of the expected IC (TEIC). This method is similar to that employed previously (Borisoff *et al* 2004, Graimann *et al* 2004, Levine *et al* 2000, Mason and Birch 2000, Yom-Tov and Inbar 2003). FPs were assessed in the periods before the

appearance of a white circle and after the end of the activation window. Periods during which ocular artifacts occurred were blocked by the system and not included in the evaluation.

To assess the performance of the LF-ASD system, a method based on 5-fold stratified cross-validation is used. In this approach, the trials are randomly divided into five groups of equal trial numbers. Then the classifier is trained using the data of one of the five groups and the system's performance is evaluated using the data of the remaining groups. As shown in (Bashashati *et al* 2006), for this specific BI system, evaluating the performance of the system on one cross-validation set provides an accurate measure of performance without having to repeat this procedure for each of the five cross-validation sets. Details of the evaluation method and the procedure detailing how the trials are randomly picked from continuous EEG are found in (Bashashati *et al* 2006).

The above three proposed methods for generating the training-data were compared to the following four other schemes used to generate the training-data for the IC class: (1) the single feature specifically at TEIC are picked from each ERW (referred to as TR_TEIC), (2) three features around TEIC are picked from each ERW (TR_3TEIC), (3) all the features in ERW are picked from each trial (TR_All), and (4) one feature is randomly picked in the ERWs (TR_Ran). To generate the NC class training-data, the same procedure as described for TR_Gen1 method which selects the top **H**=75% of features that belong to the NC state is used.

The 1-NN classifier of the LF-ASD design was trained seven separate times using training–data generated by each of the seven methods. Receiver operating characteristic (ROC) curves were generated for the BI system associated with each of the training-data generation methods. Then, for each subject, the area under the specific region of interest of the ROC curves (AROI-ROCC) was used to compare the performance of each method. For practical applications, one needs to focus on low FP rates. From our experience, FP rates above 2% cause subjects excess frustration and distraction in subjects (Birch *et al* 2002). Thus, AROI_ROCC for FPs less than 2% are calculated and used for comparison. Note that we have not measured frustration in a systematic way; our knowledge is based on informal subject interviews conducted at the end of the study.

To assess the statistical significance of the results, for each subject, the algorithms were repeated 10 times, each time with a random set of trials as training and test data.

4.4. Results

Table 4.1 shows the area under ROC curves (AROI_ROCC) for FP<2% for the BI system associated with the seven above mentioned training-data generation methods averaged across the 10 runs of the algorithms for each subjects.

TABLE 4.1 AREA UNDER ROC CURVE (FOR FP<2%) AVERAGED OVER 10 RUNS OF THE ALGORITHMS FOR EACH SUBJECT FOR DIFFERENT TRAINING-DATA GENERATION METHODS

Subject	Area under specific region of ROC curve (for FP<2%) *10^4						
	TR_Gen1	TR_Gen2	TR_Gen3	TR_TEIC	TR_3TEIC	TR_All	TR_Ran
AB1	**80.89**	72.67	**79.08**	67.04	62.70	69.63	55.58
AB2	**90.64**	77.09	**91.13**	53.13	45.49	61.65	54.12
AB3	**70.45**	52.12	**71.78**	59.89	60.75	70.76	71.01
AB4	**82.57**	66.32	**83.58**	45.96	60.19	81.39	59.20
SCI1	**52.22**	44.36	**49.27**	48.52	51.14	50.61	49.53
SCI2	**76.37**	69.16	**76.85**	56.90	59.76	78.12	53.62
SCI3	**34.22**	32.47	**35.56**	39.63	35.74	36.57	43.41
SCI4	**79.34**	75.85	**82.82**	53.21	70.66	72.88	56.64
Average	**70.84**	61.25	**71.26**	53.04	55.80	65.20	55.39

Table 4.2 shows the results of the paired T-test to examine the hypotheses whether each of TR_Gen1, TR_Gen2 and TR_Gen3 generate significantly better results than the other alternative methods stated in Section 4.3.2. As shown in Tables 4.1 and 4.2, the performances of two of the three proposed methods (TR_Gen1 and TR_Gen3) are better than the four other methods. These two methods generate almost the same performance results. Results of the significance tests also show that these two methods generated significantly higher AROI-ROCC than other methods ($p<<0.003$). Table 4.3 shows the averaged true positive (TP) rates (across the eight subjects) at fixed false positive (FP) rates of 1% and 2%. Fig. 4.5 also shows the average ROC curves of the eight subjects for each of the seven methods of training-data generation. As this figure shows, the TR_Gen1 and TR_Gen3 methods generate higher true positives (TP) for each level of false positives (FP). For example, at the FP rate of 1% as shown in Table 4.3, two of the proposed methods increase the TP rates from 27.3-34.2% to 37.1-37.6% which correspond to 2.9-10.3% improvement. At FP rate of 2%, the proposed

methods increase the TP rate from 50.8-58.4% to 61.9-62.2% which corresponds to 3.5-11.4% improvement. Comparing TR_Gen3 with the best performing alternative method, TR_All, the TP rates increase 3.4% and 3.5% at FP rates of 1% and 2%, respectively.

TABLE 4.2 OVERALL SIGNIFICANCE LEVEL (P-VALUE) OF *IMPROVEMENTS* AND PERCENTAGE OF IMPROVEMENTS (IN PARENTHESES) OF THE AREA UNDER ROC CURVE (FOR FP<2%) WHEN USING THE PROPOSED TRAINING-DATA GENERATION METHOD. ITEMS THAT HAS '-' INDICATE PERFORMANCE DECREASE AND THUS NO VALUES IS REPORTED.

	Significance level (p-value) using "paired T-test" and percentage of improvements (in parentheses)						
	TR_Gen1	**TR_Gen2**	**TR_Gen3**	**TR_TEIC**	**TR_3TEIC**	**TR_All**	**TR_Ran**
TR_Gen1	-	p<<0.003 (15.7%)	-	p<<0.003 (33.6%)	p<<0.003 (27.0%)	p<0.003 (8.7%)	p<<0.003 (27.9%)
TR_Gen2	-	-	-	p<0.003 (15.5%)	p<0.08 (9.8%)	-	p<0.08 (10.6%)
TR_Gen3	p>0.08 (0.6%)	p<<0.003 (16.3%)	-	p<<0.003 (34.4%)	p<<0.003 (27.7%)	p<0.003 (9.3%)	p<<0.003 (28.7%)

TABLE 4.3 AVERAGE TRUE POSITIVE RATES (ACROSS EIGHT SUBJECTS) AT FIXED FALSE POSITIVE RATES OF 1% AND 2% FOR THE TRAINING-DATA GENERATION METHODS

Training-data generation method	**TR_Gen1**	**TR_Gen2**	**TR_Gen3**	**TR_TEIC**	**TR_3TEIC**	**TR_All**	**TR_Ran**
Average TP rate (%) at fixed FP=1%	**37.1**	31.9	**37.6**	27.3	28.0	34.2	28.2
Average TP rate (%) at fixed FP=2%	**62.2**	53.6	**61.9**	50.8	53.7	58.4	52.3

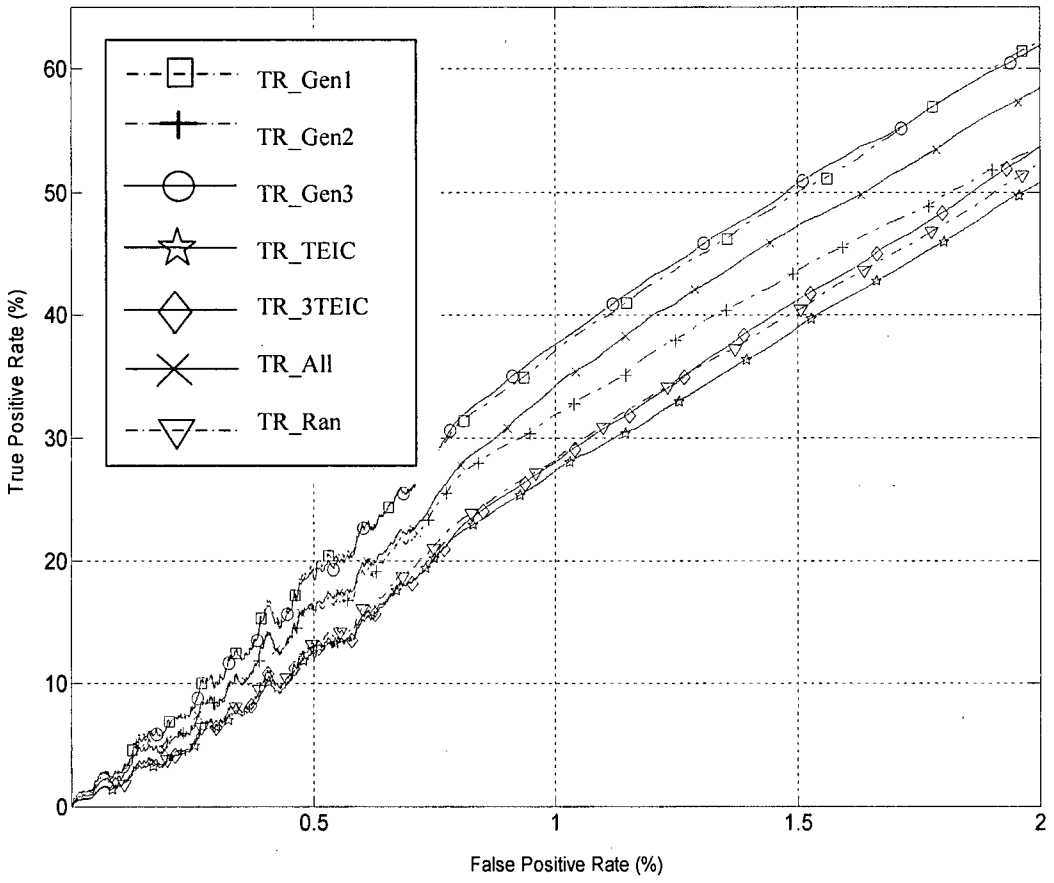

Figure 4.5 Average ROC curves (for false positives less than 2%, as we are interested in false positives less than 2%) across eight subjects for the seven training-data generation methods (TR_Gen1 (dashed line with rectangles), TR_Gen2 (dashed line with plus signs), TR_Gen3 (solid line with circles), TR_TEIC (solid line with stars), TR_3TEIC (solid line with lozenges), TR_All (solid line with crosses), TR_Ran (dashed line with triangles))

4.5. Discussion

Methods that generate training-data for self-paced brain interfaces are proposed and evaluated. Experimental results from this study on eight subjects show that the training-data generated by two of the proposed methods yield 9.3-34.4% larger AROI-ROCC than alternative methods which use time of the expected intended control (TEIC) as a time reference to generate the training-data. Comparing the TP rates, the proposed methods improve the average performance from 50.8%-58.4% to about 62% at FP rate of 2%.

As shown in Table 4.1, the two of three proposed methods resulted in significantly better performances than the other alternative methods of training-data generation for all subjects except for SCI3. For this specific subject, our three proposed methods yielded slightly less performance, although the performance was not significantly different than the four alternate methods.

Based on the results shown in Table 4.1, TR_Gen2 generated better results than the TR_TEIC, TR_3TEIC, TR_Ran. methods. However, this method did not perform as well as TR_Gen1 and TR_Gen3 methods. As mentioned before, the TR_Gen3 method uses the average of the features in the IC cluster as the representative feature of the IC class. However, TR_Gen2 uses all the features in the IC cluster as IC training-data. Thus, one reason for TR_Gen2 having lower performance than TR_Gen3 could have resulted from it containing more features that are less likely to belong to the IC class and thus this may have shifted the decision boundary of the classifier towards the NC class. To test whether the use of more IC class features can result in lower system performance, we also applied a method similar to the TR_Gen1 method, except that the three features that are more likely to belong to the IC class are chosen from each trial as IC training-data instead of the single best feature. Using this training-data resulted in slightly worse performance than TR_Gen1.

In three of the eight tested subjects, the performance of the system significantly improves by using the proposed methods. According to the results of the eight tested subjects, if such methods are used, we believe that the performance of the system will not decrease compared to other alternative methods, and in some subjects significant improvements may be achieved.

The proposed training-data generation methods were evaluated on the LF-ASD's 1-NN classifier which was trained by LVQ. They yielded superior results than the four alternative methods of training-data generation. As the comparison was evaluated on the same systems with only training-data being different, this clearly indicated that the quality of the training-data significantly affects system performance. This leads us to believe that the proposed algorithms would also generate superior quality training-data when other classifiers are used, although this will have to be properly verified in a future study.

As mentioned in Section 4.2, before applying our algorithms, two requirements must be satisfied: (1) the use of an ERW (expected response window) is needed, and (2) a large set of features for the NC class (approximately 4 minutes of NC state data) is needed to accurately estimate the probability density distribution of NC features. The NC class data can be collected in separate sub-sessions or from the periods between the IC trials. As such, these two requirements do not significantly constrain most approaches to system training.

We used the top **H**=75% of NC class features as the NC class training-data. It should be noted that we tried the **H**=50% and **H**=25% and the results did not change significantly in our experiments. However, a value of **H**=75% is more desirable as it would represent the more variability in the NC class features (if any) and enable the classifier to handle this variability. The reason for introducing a variable H in our algorithm was to eliminate the features that are less likely related to the NC class and might be related to artifacts or other brain states.

As shown in Table 4.1 and Fig. 4.5, the training-data generation methods that select the most probable IC feature in the ERW result in better performance of the BI system than the ones that select or use the features around the TEIC such as TR_TEIC or TR_3TEIC. This implies that the TEIC is not the exact time of an actual imagined movement which is usually true as confirmed in (Bashashati *et al* 2004). One may suggest using a synchronized paradigm to train and set up a self-paced BI system in which TEIC may be known quite accurately. Although TEIC might be known more accurately, but there still is variability in TEIC in response to cue, and synchronizing cues may introduce different brain states (evoked or otherwise) that would not translate well when used in a self-paced setting.

It should be noted that the system generates almost 100% true positive rates at higher false positive rates, e.g. FP>4%. However in our experience, relatively high false positive rates cause excessive frustration in subjects. On the other hand, if we fix the false positive rate at 1%, true positive rates drop to less than 40%. This true positive rate is slightly better than 1 successful attempt out of every 3 attempts, a level that may or may not be usable given the application. For example, a continuous cursor control application may cause less frustration with low true positive rates compared to a menu-driven control application. For cursor control, the subject simply needs to attempt three successive commands to move a certain direction and error correction is a natural part of the control paradigm. However, with a

menu-driven system, a repetitive series of erroneous commands may be unduly frustrating while waiting for the correct window of opportunity to re-present.

The proposed methods basically generate higher quality training-data from a population of available fuzzy training-data. In other words, these methods select a subset of training-data that has a higher probability of being real events. As such, the proposed methods are directly applicable to other BI designs, including synchronized BIs and other neuroscience applications where covert tasks (e.g. imagined movements) are involved. In a recent study (Bashashati *et al* 2004), one of these proposed methods was used to generate higher quality ensemble averages of movement-related potentials related to attempted (or imagined) movements of people with SCI.

The methods introduced here were tested on a 2-class brain interface. However, the methods can be expanded to more classes of IC. In the meantime, this study was performed offline; thus, an online study is needed to confirm the results in a more real-world application simulation.

4.6. References

Bashashati A, Fatourechi M, Ward R and Birch G 2006 User Customization of the Feature Generator of an asynchronous Brain Interface *Annals of Biomedical Engineering* **34** 1051-60.

Bashashati A, Mason S, Ward R and Birch G 2004 An Automatic Method to Generate Ensemble Averages of Movement-Related Potentials for Individuals with Spinal Cord Injuries *Proc. of the 26th Inter. Conf. of the IEEE Eng. in Medicine and Biology Science (San Francisco: USA)* pp. 4529-4532.

Birch G E, Bozorgzadeh Z and Mason S G 2002 Initial on-line evaluation of the LF-ASD brain-computer interface with able-bodied and spinal-cord subjects using imagined voluntary motor potentials *IEEE Trans. Neural Sci. Rehab. Eng.* **11 219**.

Birch G E, Lawrence P D and Hare R D 1993 Single trial processing of event related potentials using outlier information *IEEE Trans. Biomed. Eng.* **40** 59–73.

Borisoff J F, Mason S G, Bashashati A and Birch G E 2004 Brain Computer Interface (BCI) Design for Asynchronous Control Applications: Improvements to the LF-ASD Asynchronous Brain Switch *IEEE Trans. Biomed. Eng.* **51** 985-92.

Chia-Tang C, Kun-Shan C, Jong-Sen L 2003 The use of fully polarimetric information for the fuzzy neural classification of SAR images IEEE Trans Geoscience and Remote Sensing **41** 2089-100.

Cacoullos T 1966 Estimation of a multivariate density *Annals of the Institute of Statistical Math.* **18** 179-89.

Glavinovic M I 1996 Comparison of parzen density and frequency histogram as estimators of probability density functions *Pflugers Arch* **433** 174-9.

Graimann B, Huggins J E, Levine S P and Pfurtscheller G 2004 Toward a direct brain interface based on human subdural recordings and wavelet-packet analysis *IEEE Trans Biomed. Eng.* **51** 954-62.

Kersten P R, Lee J S, Ainsworth T L 2005 Unsupervised classification of polarimetric synthetic aperture Radar images using fuzzy clustering and EM clustering *IEEE Trans Geoscience and Remote Sensing* **43** 519-27.

Kohonen T 1990 The self-organizing map *Proc. of IEEE* **78** 1464-80.

Levine S P, Huggins J E, Bement S L, Kushwaha R, Schuh L A, Rohde M M, Passaro E A, Ross D A, Elisevich K V, and Smith R J 2000 A direct brain interface based on event-related potentials *IEEE Trans. Rehabil. Eng.* **8** 180–5.

Mason S G, Bashashati A, Fatourechi M and Birch G E Developing a Framework for Brain-Interface Technology Design," available online at *http://www.braininterface.org/.*

Mason S G and Birch G E 2000 A brain-controlled switch for asynchronous control applications *IEEE Trans. Biomed. Eng.* **47** 1297-307.

Mason S G and Birch G E 2003 A general framework for brain-computer interface design *IEEE Trans. Neural Syst. Rehabil. Eng.* **11** 70–85.

Mason S G and Birch G E 2005 Temporal Control Paradigms for Direct Brain Interfaces - Rethinking the Definition of Asynchronous and Synchronous *Proc. HCI Inter. Conf. (Las Vegas, USA).*

Millan J R and Mourino J 2003 Asynchronous BCI and local neural classifiers: An overview of the adaptive brain interface project *IEEE Trans. Neural Syst. Rehabil. Eng.* **11** 159–61.

Nicolelis M A 2003 Brain-machine interfaces to restore motor function and probe neural circuits *Nat. Rev. Neurosci.* **4** 417– 22.

Parzen E 1962 On estimation of a probability density function and mode *Annals Math. Statistics* **33** 1065-76.

Scherer R, Muller G R, Neuper C, Graimann B, Pfurtscheller G 2004 An asynchronously controlled EEG-based virtual keyboard: improvement of the spelling rate *IEEE Trans. Biomed. Eng.* **51** 979-84.

Townsend G, Graimann B, Pfurtscheller G 2004 Continuous EEG classification during motor imagery--simulation of an asynchronous BCI *IEEE Trans. Neural Syst. Rehabil. Eng.* **12** 258-65.

Vaughan T M et al. 2003 Guest editorial brain-computer interface technology: a review of the second international meeting *IEEE Trans. Neural Syst. and Rehabil. Eng.* **11** 94-109.

Wolpaw J R, Birbaumer N, McFarland D J, Pfurtscheller G and Vaughan T M 2002 Brain-computer interfaces for communication and control *Clin. Neurophysiol.* **113** 767-91.

Yom-Tov E and Inbar G F 2003 Detection of movement-related potentials from the electro-encephalogram for possible use in a brain-computer interface *Med. Biol. Eng. Comput.* **41** 85–93.

Chapter 5 User Customization of the Feature Generator of an Asynchronous Brain Interface [18]

5.1. Introduction

Direct Brain Interface (BI) systems provide an alternative communication and control solution for individuals with severe motor disabilities, bypassing impaired interface pathways. Cortical activity associated with an intentional control command is mapped directly to application-specific control signals. Various devices, such as neural prostheses, can then be controlled by cognitive processes only. For a review of the field, see (Mason and Birch 2003, Nicolelis 2003, Vaughan *et al* 2003, Woplaw *et al* 2002).

There are many BI transducer designs presented in the literature. However, few have been designed specifically for asynchronous control. The concept of asynchronous control of BI systems was introduced in (Mason and Birch 2000). Once the system is on, in an asynchronous BI the users affect the BI transducer output when they want by intentionally changing their brain state. Between periods of intentional control (IC), the user is in a no-control (NC) state - they may be idle, daydreaming, thinking about a problem or lunch, or performing some other action, but they are not trying to control the BI transducer. This form of intermittent control has been termed "asynchronous control" (Mason and Birch 2000). To operate in this paradigm, BI transducers are designed to respond only when there is intentional user control and to remain inactive when the user is in an NC state. By contrast, synchronous BIs are operational only during specific periods determined by the system (not the user).

Although asynchronous (or intermittent) control is the most natural mode of interaction, it has received relatively little attention; recognized in (Woplaw *et al* 2002), it deserves more. Only a few BI transducers (Birch *et al* 1993, Levine *et al* 2000, Mason and Birch 2000, Millan and Mourino 2003, Scherer *et al* 2004, Townsend *et al* 2004, Yom-Tov and Inbar

[18] A version of this chapter has been published. Bashashati A., Fatourechi M., Ward R., and Birch G. (2006) User Customization of the Feature Generator of an asynchronous Brain Interface *Annals of Biomedical Engineering* **34** 1051-60.

This work has also been resulted to another publication: Fatourechi M., Bashashati A., Birch G.E., and Ward R.K. (2006) The Design of an Automatically User Customized Asynchronous Brain Interface System *IEE Journal of Medical & Biological Engineering and Computing* **44** 1093-104.

2003) have been specifically designed and tested for asynchronous control. Each produces a multi-state discrete output, and as such will be referred to as "asynchronous brain switches" in the remainder of this paper.

The Low Frequency-Asynchronous Switch Design (LF-ASD) was first introduced as a two-state BI system for asynchronous control applications (Mason and Birch 2000). It recognizes scalp potentials related to single-trial Movement Related Potentials (MRPs) in the EEG signal. The feature generator of the LF-ASD generates six-dimensional features from six bipolar EEG channels to detect MRPs in the ongoing EEG signal (Mason and Birch 2000). However, to detect the desired MRP pattern in the EEG, design parameters of the feature generator need to be properly adjusted. These parameters were originally chosen based on the EEG data of one subject and since then have been used for all subjects (Mason and Birch 2000). As the EEG characteristics during intended movements may vary from one subject to another, design parameters need to be customized for each subject. Without such tuning, the system may detect non-MRP patterns in the ongoing EEG.

Although there are few user-customized BI systems, customization of BI systems has been reported in several recent papers. These studies focused on user customization of common spatial patterns (CSPs) of the Mu/Beta rhythms of EEG (Blanchard and Blankertz 2004), user-customization of band pass filters to select the proper frequency band (Pregenzer and Pfurtscheller 1999, Xu *et al* 2004), channel selection using support vector machines (Lal *et al* 2004), automatic selection of power-band features for each subject using a genetic algorithm (GA) (Scherer *et al* 2004), and adjusting the parameters of the energy normalization block of the LF-ASD (Fatourechi *et al* 2005). These papers established that customization of the parameters of a BI system may lead to performance improvements in *some* subjects.

In (Fatourechi *et al* 2005), we showed improvements in the system's performance for the two able-bodied subjects studied. This improvement motivated us to further pursue customization of the feature generator's parameters for each subject. Eight subjects were studied, four of whom were disabled. To customize parameters for each subject, the desired pattern associated with a specific movement was first determined through ensemble averaging of the EEG data related to the movement. The parameters of the feature generator were then

manually estimated. The feature generator's output and the performance of the customized BI are compared to those associated with the original design.

We also show that huge variations in performance result when the classifier was trained on trials from different sessions (refer to Section 5.4.2). We use an off-line method of evaluation of the LF-ASD based on the stratified cross-validation approach (Witten and Frank 2000) to reduce huge variations in system performance across the cross-validation sets. We have shown that a robust performance measure of the system can only be obtained by evaluating its performance on one cross-validation set instead of evaluating the performance of the system on all the cross-validation sets.

5.2. Background

Customizing the feature generator of the LF-ASD requires detailed knowledge of the LF-ASD's design (Mason and Birch 2000), which is briefly reviewed in this section.

Fig. 5.1 shows the block diagram of the most recent version of the Low Frequency Asynchronous Switch Design (the LF-ASD) (Borisoff *et al* 2004). This design uses features extracted from six bipolar EEG channels (defined with reference to the International 10-20 System at F1-FC1, Fz-FCz, F2-FC2, FC1-C1, FCz-Cz, and FC2-C2). After amplification, all six EEG channels are normalized with an Energy Normalization Transform (ENT) (Yu *et al* 2002). A wavelet-like function is applied as the feature generator. The Karhunen-Loève Transform (KLT) maps the six-dimensional feature space produced by the Feature Generator to a two-dimensional space. A one-nearest neighbor (1-NN) classifier is used as the feature classifier. The system's classification accuracy is further improved by using a moving average and a debounce block to reduce the number of false switch activations (for details, see (Mason and Birch 2000) (Borisoff *et al* 2004, Mason and Birch 2000)). Overall, the system classifies input patterns as either No Control (NC) or Intentional Control (IC).

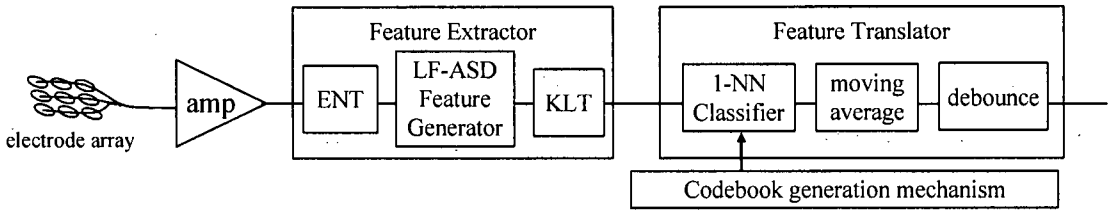

Figure 5.1 Components of the Low Frequency Asynchronous Switch Design (the LF-ASD) (from (Borisoff *et al* 2004)).ENT: energy normalization transform, KLT: Karhounen-Loéve transform, 1-NN: one nearest neighbor

5.2.1. LF-ASD Feature Generator

The desired bipolar EEG pattern associated with the MRPs is similar to that shown in Fig. 5.2 (Mason and Birch 2000), where the approximate time of the attempted movement is $t=n$. The feature extractor of the LF-ASD is designed to generate large feature values when such patterns exist in the EEG.

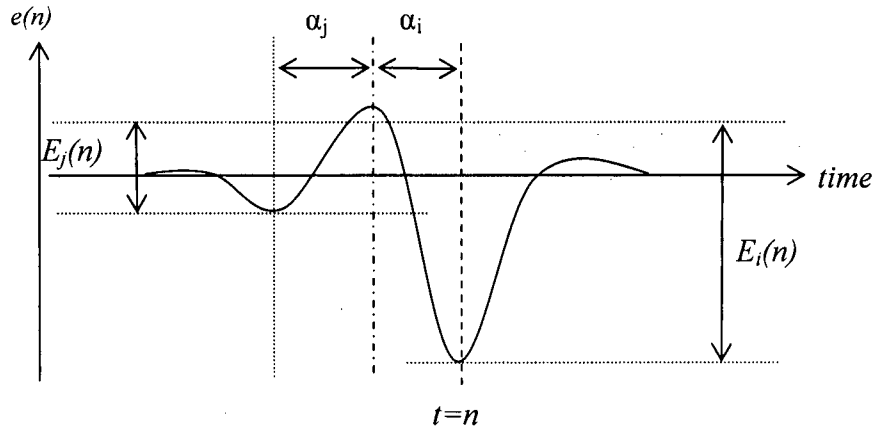

Figure 5.2 Desired pattern of the bipolar EEG during movement. $E_i(n)$: amplitude difference between local maximum before the movement and local minimum after the movement, $E_j(n)$: amplitude difference between local maximum before the movement and local minimum before the movement

As Fig. 5.2 shows, the elemental features $E_i(n)$ and $E_j(n)$ are defined as the difference of a filtered signal ($e(n)$) at two points in time, and are calculated in equations (1) and (2) (respectively for more details see (Mason and Birch 2000)). The filtered signal is measured from a pair of bipolar electrodes and is filtered at 1-4 Hz using a finite impulse response (FIR) filter based on a Hamming window. There are six such pairs and six such signals.

$$E_i(n) = e(n-\alpha_i) - e(n) \quad (1)$$

$$E_j(n) = e(n-\alpha_i) - e(n-\alpha_i-\alpha_j) \quad (2)$$

In the rest of this paper, we use the general term "delay parameters" of the feature generator when referring to α_i and α_j in equations (1) and (2). The delay terms are initially estimated from the ensemble averages based on the minimum peak near the trigger (at time $t=n$ in Fig. 5.2), the first local maximum, and the local minimum before the trigger as illustrated in Fig. 5.2. The trigger point is defined as the point around which the movement is performed.

Compound features are defined in equation (3) by pairing elemental features (E_i, E_j) to emphasize the samples in which two large elemental features appear concurrently.

$$\begin{aligned} g_{ij}(n) &= E_i(n) \times E_j(n) \qquad \text{if} \quad E_i(n) \times E_j(n) \geq 0 \\ &= 0 \qquad\qquad\qquad \text{otherwise} \end{aligned} \quad (3)$$

For robustness, the compound features are maximized over a window as follows.

$$G_{ij}(n) = \max\{g_{ij}(n-8), g_{ij}(n-7), \ldots, g_{ij}(n-1), g_{ij}(n)\} \quad (4)$$

This procedure is repeated for each channel. The resulting feature vector is an equally weighted six-dimensional vector, with each dimension reflecting the value of the feature $(G_{ij}(n))$ in each channel.

5.3. Data Recording

The off-line data used in this study were collected from subjects positioned 150 cm in front of a computer monitor. The EEG signal was recorded from six bipolar electrode pairs positioned over the supplementary motor area and the primary motor cortex, as stated in Section 5.2. Electro-oculographic (EOG) activity was measured as the potential difference between two electrodes, placed at the corner of and below the right eye. The ocular artifact was considered present when the potential difference between the EOG electrodes exceeded ±25 μV. All signals were sampled at 128 Hz.

The subjects used in this study consisted of four men with high-level spinal cord injuries (SCI) and three able-bodied men and one able-bodied female (subject AB3). Each of the subjects gave written consent prior to participating, according to the guidelines of the

Behavioral Research Ethics Board (BREB) of the University of British Columbia. All subjects were right handed and between 31 and 57 years of age. None of the SCI subjects had residual sensation or motor function in their hands.

Data were collected while the subjects performed a guided task. At random intervals of 5.6 to 7.0 seconds (mean of 6.7 seconds), a 2 cm white circle was displayed on the subject's monitor for ¼ second. The subject was asked to attempt to move his right index finger one second after the cue appeared. The one-second delay was used to avoid visually evoked potential effects from the cue. The one second time after the cue is denoted by "time of the expected attempted movement" (TEM). Note that this is the time when the subject is expected to attempt the movement, but this time may vary from subject to subject and from trial to trial. Both subject groups used the same neurological mechanism to drive the brain switch: an attempted finger flexion. This resulted in attempted (i.e., no physical) finger movements in subjects with high-level SCI and actual finger flexion in able-bodied subjects (see (Birch *et al* 2002) for more details). For each subject, an average of 80 trials was conducted every day for six days.

5.4. Methods

5.4.1. Delay Parameter Customization

To determine the desired bipolar pattern associated with the movement for each subject, the signals (within a window centered at TEM) for each of the six bipolar EEG channels were ensemble averaged. Ensemble averaging enhances the signal-to-noise ratio, and the resulting waveform exhibits the desired pattern that the LF-ASD aims to detect. After the ensemble averages of each subject were generated, the delay parameters were measured manually from the EEG averages. For example, the waveform of the ensemble average of the EEG for subject AB2 in bipolar channel F2-FC2 was generated as shown in Fig. 5.3. As our goal is to detect a pattern similar to the average waveform shown in Fig. 5.2, we choose the delay parameters based on the minimum peak "right after TEM", a maximum peak "before TEM" and a minimum peak "before the location of the chosen maximum peak" from the ensemble average waveform. Based on the location of the peaks (minimum peak at $t=0.43$s (Min1), maximum peak at $t=1.32$s (Max1), and minimum peak right after TEM at $t=1.97$s (Min2)), the delay parameters are calculated as $\alpha_i=Min2-Max1=0.65$s and $\alpha_j=Max1-Min1=0.89$s.

Note that the attempted movement is performed around *t=1.8*s. As shown in Fig. 5.3, there are several local minimum peaks (e.g., at *t=0.15*s or *t=1.13*s) just before the maximum peak at *t=1.32*s. We evaluated the system's performance considering these mentioned local minimum peaks. The best performance, however, was achieved at a chosen local minimum of *t=0.43*s.

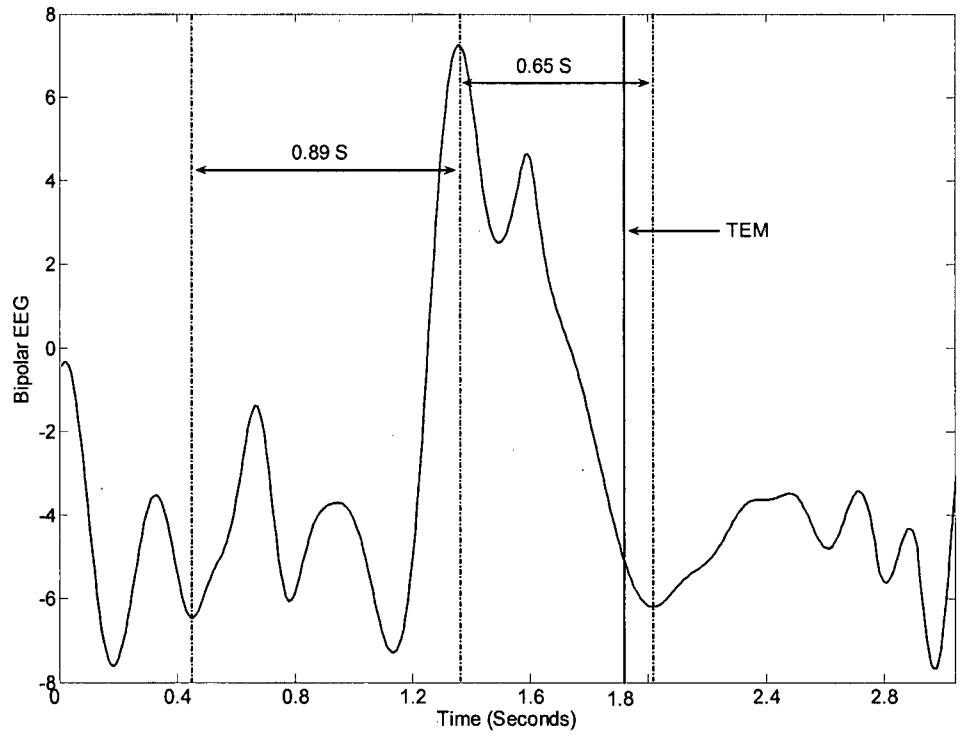

Figure 5.3 The ensemble averages of the normalized EEG in bipolar channel F2-FC2 for subject AB2. Time of the expected movement (TEM) is at t=1.8 s.

For simplicity (and given that the ensemble average patterns, time-locked to TEM, are relatively the same for all six channels), equal delay parameters were used for all six bipolar EEG channels. It should be emphasized that our main goal in this paper is to show that the delay parameter customization for each subject is useful.

Ensemble averages of the EEG for each subject were generated from the training data, excluding the EOG contaminated trials. The delay parameters were then calculated manually (see Table 5.1 for values). For the subjects whose ensemble average waveforms showed

several minimum and maximum peaks, the same procedure as explained for subject AB2 was performed. Delays resulting in the best performance are reported in Table 5.1.

TABLE 5.1 DELAY PARAMETERS (MEASURED IN SECONDS) ESTIMATED FROM THE ENSEMBLE AVERAGES OF THE BIPOLAR EEG SIGNALS (F2-FC2) GENERATED FROM THE TRAINING DATA SET. NOTE THAT THE SAME DELAY PARAMETERS ARE USED FOR ALL SIX BIPOLAR CHANNELS.

Subject	α_i	α_j
AB1	0.74	0.68
AB2	0.65	0.89
AB3	0.29	0.16
AB4	1	0.34
SCI1	0.88	0.77
SCI2	0.74	0.41
SCI3	0.30	0.5
SCI4	0.70	0.54

5.4.2. Cross-validation and Stratified Cross-validation

As mentioned in Section 5.3, the data from each subject were collected over six days, i.e., six sessions. In our previous work (Birch *et al* 2002, Borisoff *et al* 2004, Mason and Birch 2000), the first day's EEG recordings were used to train the classifier, and data from the subsequent five days were used to evaluate the BI system. However, to determine whether the first session's data is representative of future data, we carried out the following tests.

To assess the sensitivity of the classifier's performance to different training sets, we tested the system's performance using different training and test sets. Specifically, the classifier was trained based on the data of one of the days (sessions) and the system's performance was evaluated based on the data of the remaining sessions. This process was repeated for every session and averaged over the six values, in a procedure known as cross-validation (Witten

and Frank 2000). Table 5.2 shows the results of this analysis for all subjects. In Table 5.2, TS_i represents the case in which the data of the i^{th} session were used for training and the data of the other sessions for testing.

TABLE 5.2 TRUE POSITIVE (TP) RATES (%) AT FALSE POSITIVES (FP) OF 2% FOR DIFFERENT TRAINING AND TEST SETS. TS_I REPRESENTS THE CASE IN WHICH THE DATA OF THE I^{TH} SESSION WERE USED FOR TRAINING AND THE OTHER SESSIONS FOR TESTING.

Subject	Performance (TP(%) when FP=2%)							
	TS_1	TS_2	TS_3	TS_4	TS_5	TS_6	*Average*	*Standard deviation*
AB1	69.7	64.4	46.7	73.9	45.5	82.9	63.9	15.0
AB2	75.5	68.5	57.1	74.5	62.5	82.9	70.2	9.4
AB3	68.3	68.9	65.2	72.0	77.8	53.9	67.6	7.3
AB4	77.0	78.6	73.3	87.2	85.1	75.0	89.5	5.1
SCI1	67.3	70.9	55.8	66.0	56.8	65.8	63.7	5.5
SCI2	65.6	47.7	42.6	49.0	46.8	72.7	54.4	11.1
SCI3	49.9	75.8	75.0	69.1	57.1	65.2	66.0	9.5
SCI4	59.8	54.8	51.0	41.2	51.2	57.1	53.0	6.1

As Table 5.2 shows, the system's performance varies widely depending on which session was used for training the classifier. Specifically, the average true positives rates varied with standard deviations from 5.1% to 15% across subjects.

Using the data of the first session to train the classifier and then testing it on data collected subsequently is more suitable for real-world applications. However, our analysis showed that the system's performance depends highly on the quality of first session's data. We were therefore motivated to find a way of reducing the dependency of the system's performance on the training set.

In this paper, an *N*-fold *stratified* cross-validation is used for evaluating the system's performance (Witten and Frank 2000). In *stratified* cross-validation, the trials are randomly divided into *N* groups of equal trial numbers, with approximately the same frequency of classes. As in conventional cross-validation schemes, the classifier is trained based on the data of one of the N groups and the system's performance is evaluated based on the data of the remaining groups. This process is repeated for each group. The average of these N performance measures gives the overall performance of the system. In this study we used a five-fold stratified cross-validation. To randomly pick each cross-validation set, we divided

the EEG into 7s adjacent windows around each trial. Each 7s window of EEG contained an attempted movement trial as well as periods of No Control (NC) state. Finally, cross-validation sets were generated by randomly dividing the total available 7s windows into five equal groups. The classifier was then trained based on the data of one of the five groups and the system's performance evaluated based on the data of the remaining groups. This process was repeated for every group, resulting in five performance measures. The average of these five measures represents the performance of the system.

5.5. Results

In Figs. 4 and 5, the waveforms of the two-dimensional output of the feature generator and the waveforms of the ensemble averages centered at TEM are shown for one subject for the two cases: (a) our proposed customized delay parameters of the feature generator and (b) the original setting of the delay parameters. As Fig. 5.4 shows, the new delay parameters generated stronger feature values at times when we expected them to be high, i.e., the time of the attempted movement (TEM). This time is represented in these figures by the vertical line at $t=1.8$s. The feature values around the TEM were maximum in value compared to feature values at other times, when there was no movement, or an attempted one. Notice that the original settings of the delay parameters generated features at TEM that were not significantly different from the features at other times. For example, in Fig. 5.5 the features around $t=1.9$s and $t=0.9$s were not very different, while the features around $t=1.9$s were associated with movement. These observations suggest that with the new delay parameter settings of the feature generator, the system can generate more robust features and can better detect the desired MRP pattern. This is not the case with the original parameter settings.

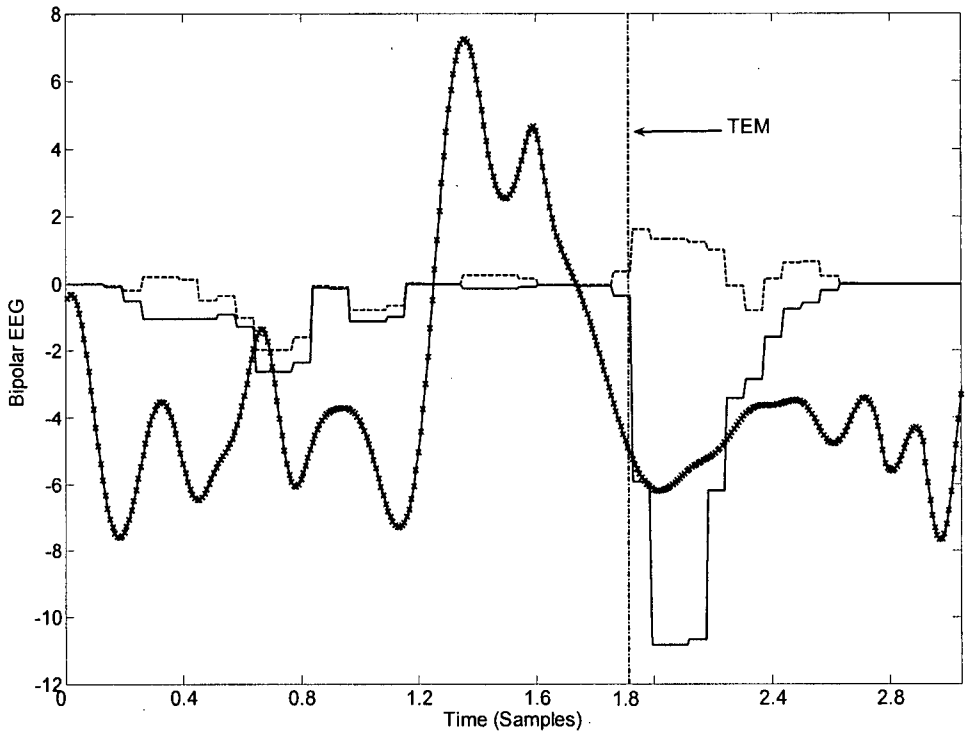

Figure 5.4 2-dimensional output of the feature generator for normalized bipolar EEG channel F2-FC2 for subject AB2 for the customized delay parameters (solid line: feature values of the first dimension, dashed line: feature values of the second dimension, and solid line with cross: bipolar EEG). Note that the vertical line at t=1.8 s corresponds to the time of the attempted movement (TEM).

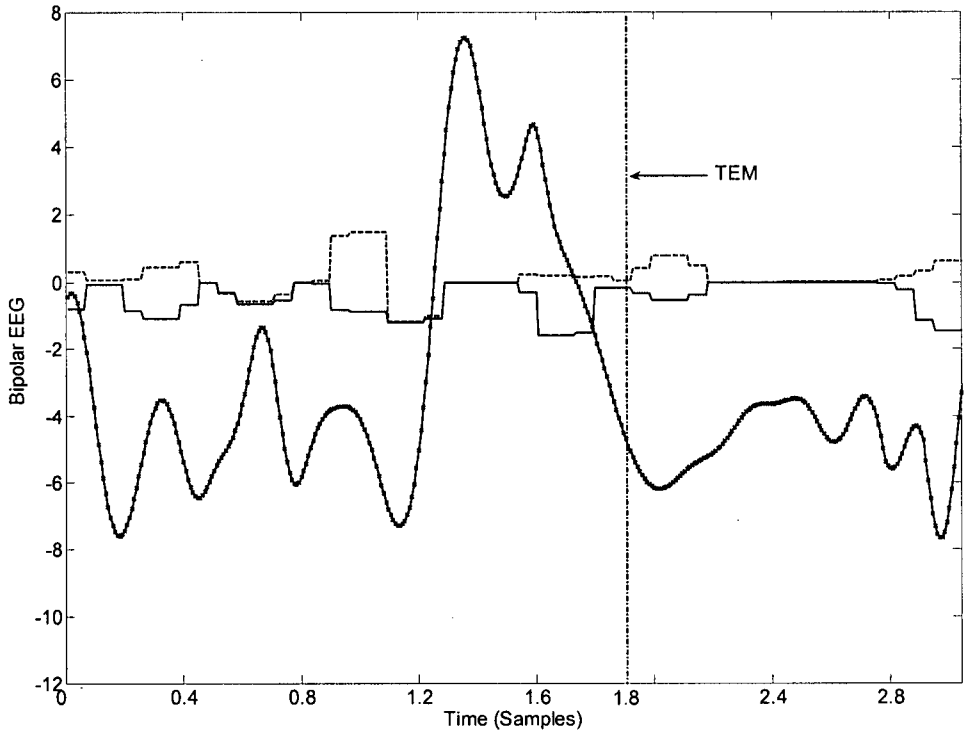

Figure 5.5 2-dimensional output of the feature generator for normalized bipolar EEG channel F2-FC2 for subject AB2 for the original delay parameters (solid line: feature values of the first dimension, dashed line: feature values of the second dimension, and solid line with cross: bipolar EEG). Note that the vertical line at t=1.8 s corresponds to the time of the attempted movement (TEM).

The performance of a two-state asynchronous BI system can be evaluated using two measures: (1) the percentage of correct activations during IC states (true positives, or "TPs") and (2) the percentage of false switch activations during NC states (false positives, or "FPs"). A TP was identified if the BI system was activated at any time within a window of 0.5 seconds before to 1 second after the TEM, called the "TP window". This method is similar to those used by others (Levine *et al* 2000, Townsend *et al* 2004, Yom-Tov and Inbar 2003). False positives were assessed in the periods before the system cued subjects to perform the movement and after subjects were expected to perform it (see (Borisoff *et al* 2004) for more details). We did not evaluate the period during which ocular artifacts occurred.

For all subjects, the five-fold *stratified* cross-validation algorithm was run ten times for each delay parameter set. Adjusting the parameters of the feature generator improved the system's

performance in four subjects, from whom three were able-bodied. However, for the rest of the subjects, the performance of the system did not improve with the use of customized delay parameters. Table 5.3 shows: (1) the average true positive rates (at fixed false positive rates of 2%), with standard deviations across the 10 runs for both original and customized delay settings for the subjects, and (2) the significance of the improvements using 'two sample T-test' with significance level of Alpha=0.1.

TABLE 5.3 PERFORMANCE OF THE LF-ASD TOGETHER WITH STANDARD DEVIATIONS ACROSS 10 RUNS OF STRATIFIED CROSS-VALIDATION WITH ORIGINAL AND NEW DELAY PARAMETERS.

Subject	Performance (TP (%) in FP=2%)			
	Original parameters	Customized parameters	Improvement	Significance level of improvement
AB1	65.0 ± 1.4	67.8 ± 1.4	+2.8	$p<0.005$
AB2	67.2 ± 1.6	74.0 ± 1.7	+6.8	$p<0.005$
AB3	62.0 ± 1.9	64.0 ± 1.3	+2.0	$p<0.03$
AB4	76.5 ± 1.5	73.1 ± 1.8	-	-
SCI1	61.1 ± 2.2	63.5 ± 1.9	+2.4	$p<0.08$
SCI2	71.2 ± 2.2	68.0 ± 2.7	-	-
SCI3	52.6 ± 2.3	52.8 ± 2.4	+0.2	-
SCI4	55.9 ± 3.0	52.9 ± 3.1	-	-

Table 5.4 shows the average standard deviations (STDs) across the five cross-validation sets to be low compared to values associated with the evaluation procedure (as shown in Table 5.2). The low STD (~0.5%) of performance across the five cross-validation sets implies that the TP rate for all five cross-validation sets is relatively the same. Consequently, the TP rate for one cross-validation set could show the overall TP rate of the system.

TABLE 5.4. AVERAGE STANDARD DEVIATION (STD) OF TP RATES (AT FIXED FP=2%) ACROSS EACH CROSS-VALIDATION SET.

Subject	AB1	AB2	AB3	AB4	SCI1	SCI2	SCI3	SCI4
Average standard deviation (%)	0.54	0.55	0.42	0.53	0.57	0.66	0.50	1.28

Figs. 6-9 show the ROC (receiver operating characteristic) curves for four of the subjects (subjects AB1, AB2, AB3, SCI1) for the two designs using (1) the original delay parameter values and (2) the new customized delay values for the feature generator. As Figs. 6-9 show, the new method generated a better TP rate at most of the FP rates.

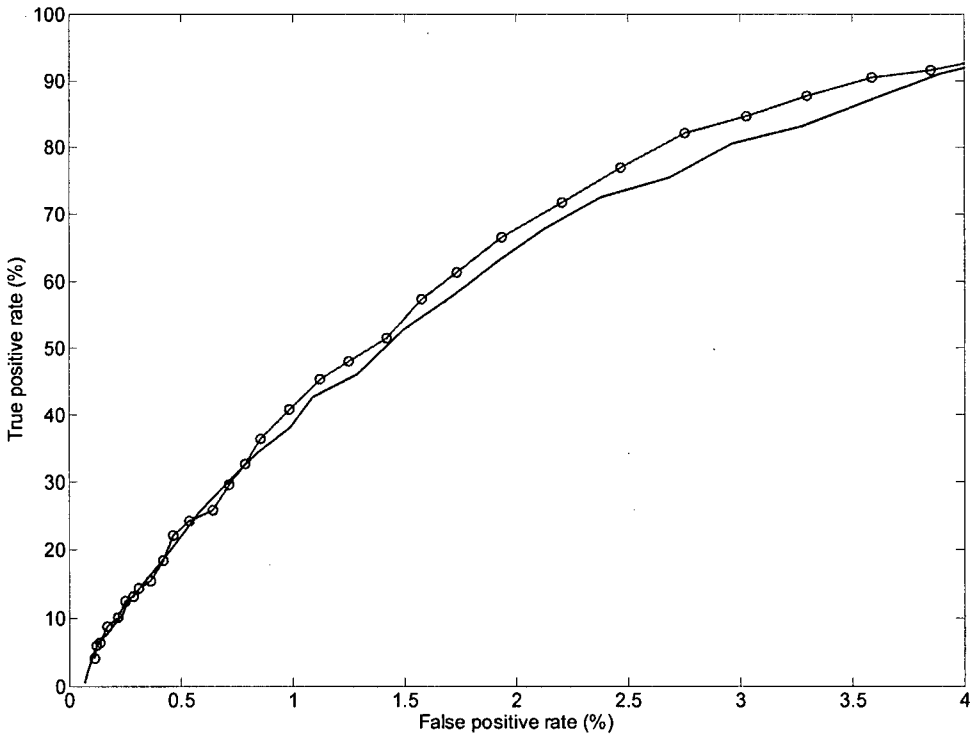

Figure 5.6 ROC curve for subject AB1 (solid line with circles: ROC curve for the customized BI system, solid line: ROC curve for the original BI system). Note that, for clarity, only false positives below 4% are shown.

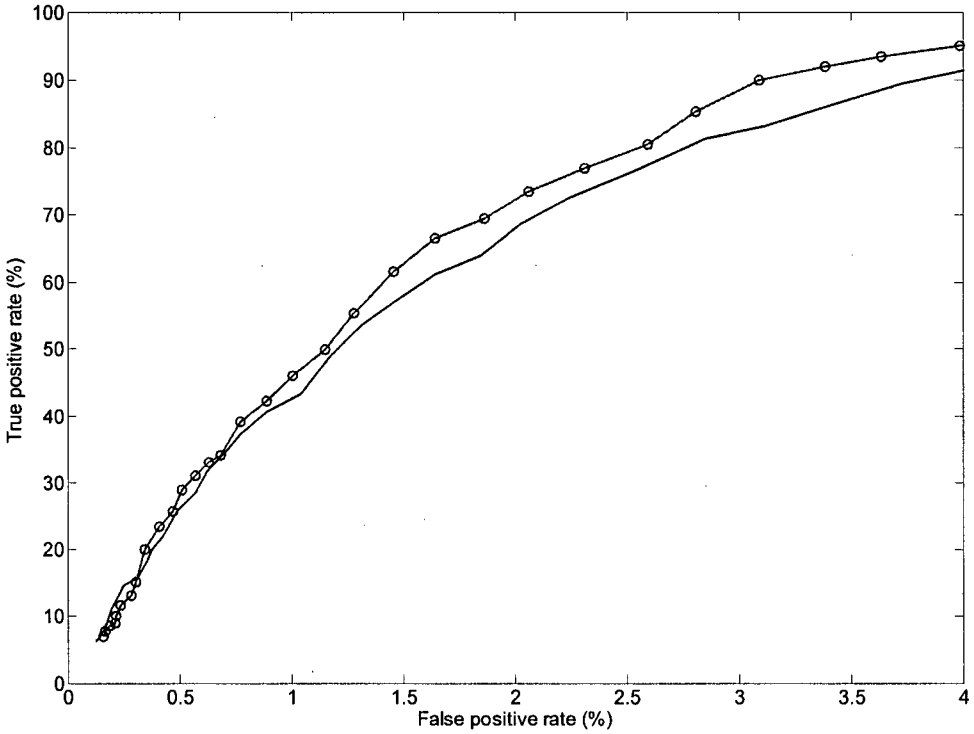

Figure 5.7 ROC curve for subject AB2 (solid line with circles: ROC curve for the customized BI system, solid line: ROC curve for the original BI system). Note that, for clarity, only false positives below 4% are shown.

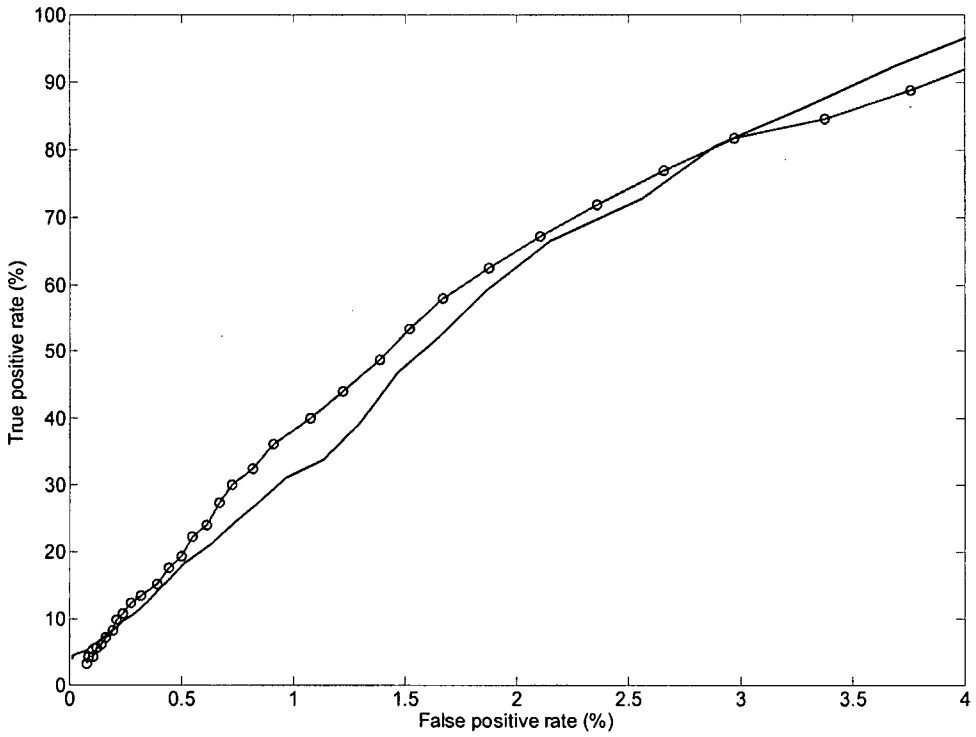

Figure 5.8 ROC curve for subject AB3 (solid line with circles: ROC curve for the customized BI system, solid line: ROC curve for the original BI system). Note that, for clarity, only false positives below 4% are shown.

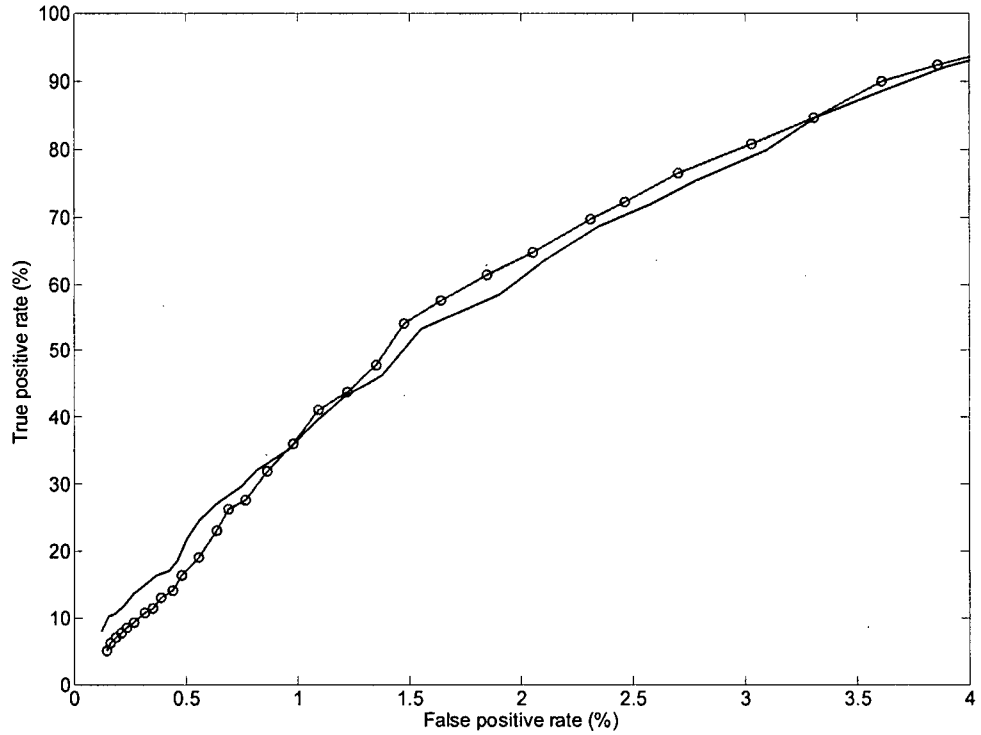

Figure 5.9 ROC curve for subject SCI1 (solid line with circles: ROC curve for the customized BI system, solid line: ROC curve for the original BI system). Note that, for clarity, only false positives below 4% are shown.

5.6. Conclusions

In this paper, we presented a method for estimating the parameters of the feature generator of our current asynchronous BI system, the LF-ASD. The error characteristics of the new design were shown to be better than those of the original design for four subjects. For these subjects, the true positive rates increased by 2% to 6.8% at false positive rates of 2%. We attribute the improvements to the adjusted delay parameters of the feature generator block. It is highly important to point out that with the new customized parameters, the system detected the desired subject-specific MRP pattern associated with movement. This was achieved by choosing a suitable set of delay parameters to result in more consistent and stronger feature values during movement.

Although the system's performance for four subjects did not increase, the system did detect the desired bipolar MRP pattern, which may not be the case with the original setting. In a BI system, it is very important to ensure that 'only' specific predefined movement attempts

activate the output and not any other mental activity. Although the performance of the system with the original delay parameters was slightly higher than that of the customized one, we believe that some patterns had been activating our original BI that were not related to the subject-specific bipolar MRP pattern we were interested in. In Fig. 5.4, which shows the ensemble averages of the EEG of subject AB2, the old delay setting generated features around movement that were not very different from feature values at other times; this may have caused performance decrease of the system in subject AB2. The opposite can also happen, i.e., some features can be generated in the TP window that activate the output but may not be related to movement. In such a case, the system is activated by EEG patterns that may not be attributed to the desired bipolar MRP pattern. Since the system aims at detecting movements from spontaneous EEG, we cannot determine whether the activations of the system are related to movement attempts or to other brain activity. With the new delay parameter values, one can expect activations of the BI system that are more likely due to movement attempts than other patterns in the EEG. A good original delay parameter value or poor manual customization might also account for the system's performance not improving.

These results are not surprising, as other studies have reported performance degradation after customizing their BI system for some subjects. For example, in (Blanchard and Blankertz 2004) the error rate of one of the three subjects decreased more than 11% after customization of the CSP patterns. In (Pregenzer and Pfurtscheller 1999) selection of subject-specific frequency components of the EEG for a BI system is reported. Although the results for two subjects improved when using the DSLVQ (distinctive sensitive LVQ) classifier, the performance of the third subject degraded after customization. However, it should be mentioned that it is difficult to directly compare the results from our study and these studies, as the recording equipment, recording and classification protocols, and mental tasks considered are different. In addition, the amount of data involved and the degree of training the subjects received before participating in the BI experiments varies for different studies. Compared to the results of our previous study (Fatourechi *et al* 2005), which customized the normalization block of our BI design, it appears that customization of the feature generator yielded less improvements than customization of the normalization block did for two of the tested subjects (AB2 and AB3) in (Fatourechi *et al* 2005). However, the results cannot be

generalized at this stage as the study reported in (Fatourechi *et al* 2005) was only performed for two of the subjects.

Despite the need to verify the results on a larger subject pool, current study yielded performance improvements in most of the able-bodied subjects rather than in the SCI subjects. Since estimating delay parameters from ensemble averages for SCI subjects proved to be difficult, we might not have been able to estimate a suitable delay setting for these subjects. However, we believe that the new customized system detects the MRP pattern in the EEG, which may not be the case for the original design.

The results of the stratified cross-validation showed that the standard deviation of the performances across cross-validation sets was low (as shown in Table 5.4). This implies that there is no need to repeat the analysis for each of the five cross-validation sets. Instead, by randomly choosing a set of trials for training, and evaluating the system on the rest of trials, a robust performance measure of the system can be obtained. Evaluating the performance of our system for a set of parameters using five-fold stratified cross-validation takes about 10 minutes on a Pentium 2.8GHz computer; with the new method, only $1/5^{th}$ of this time is needed. This new analysis procedure mostly benefits an automated parameter customization method. Using such method, the system's performance must be evaluated (for different parameter settings) hundreds of times. Thus, choosing a robust and time-efficient method for evaluating the system is desirable.

The study successfully detected the desired MRP pattern and decreased the error rates of our BI design for 50% of tested subjects. This decreased error rate demonstrates the need for a method that automatically adjusts the delay parameters for each subject. As mentioned in Section 5.4.1, manually estimating the delay parameter values may not yield better performances when there are several minimum or maximum peaks around TEM in the EEG ensemble averages. In such cases, it may be necessary to choose several delay settings and select the one that yields better performance. Using an automated method of adjusting the delay parameters may result in the best delay setting, further increase the system's performance, and remove the subjective bias in delay parameter adjustments. Our future work will specifically explore customization of the LF-ASD parameters in an automated framework.

5.7. References

Birch G E, Bozorgzadeh Z and Mason S G 2002 Initial on-line evaluation of the LF-ASD brain-computer interface with able-bodied and spinal-cord subjects using imagined voluntary motor potentials *Trans. Neural Syst. Rehabil. Eng.* **11** 219-24.

Birch G E, Lawrence P D and Hare R D 1993 Single trial processing of event related potentials using outlier information *IEEE Trans. Biomed. Eng.* **40** 59–73.

Blanchard G, Blankertz B 2004 BCI Competition 2003, Dataset IIa: spatial patterns of self-controlled brain rhythm modulations *IEEE Trans. Biomed. Eng.* **51** 1062 –6.

Borisoff J F, Mason S G, Bashashati A and Birch G E 2004 Brain Computer Interface (BCI) Design for Asynchronous Control Applications: Improvements to the LF-ASD Asynchronous Brain Switch *IEEE Trans. Biomed. Eng.* **51** 985-92.

Fatourechi M, Bashashati A, Ward R K and Birch G E 2005 A Hybrid Genetic Algorithm Approach for Improving the Performance of the LF-ASD Brain Computer Interface *Proc. of the IEEE Int. Conf. on Acoustics, Speech, and Signal Processing (Philadelphia, USA)* pp 345–8.

Levine S P, Huggins J E, Bement S L, Kushwaha R, Schuh L A, Rohde M M, Passaro E A, Ross D A, Elisevich K V and Smith R J 2000 A direct brain interface based on event-related potentials *IEEE Trans. Rehabil. Eng.* **8** 180–5.

Mason S G and Birch G E 2000 A brain-controlled switch for asynchronous control applications *IEEE Trans. Biomed. Eng.* **47** 1297-307.

Mason S G and Birch G E 2003 A general framework for brain-computer interface design *IEEE Trans. Neural Syst. Rehabil. Eng.* **11** 70–85.

Millan J R and Mourino J 2003 Asynchronous BCI and local neural classifiers: An overview of the adaptive brain interface project *IEEE Trans. Neural Syst. Rehabil. Eng.* **11** 159-61.

Lal T N, Schroder M, Hinterberger T, Weston J, Bogden M, Birbaumer N and Scholkpof B 2004 Support vector channel selection in BCI *IEEE Trans. Biomed. Eng.* **51** 1003-10.

Nicolelis M A 2003 Brain-machine interfaces to restore motor function and probe neural circuits *Nat. Rev. Neurosci.* **4** 417– 22.

Pregenzer M and Pfurtscheller G 1999 Frequency component selection for an EEG-based brain to computer interface *IEEE Trans. Rehabil. Eng.* **7** 413-9.

Scherer R, Muller G R, Neuper C, Graimann B and Pfurtscheller G, "An asynchronously controlled EEG-based virtual keyboard: improvement of the spelling rate *IEEE Trans. Biomed. Eng.* **51** 1979-84.

Townsend G, Graimann B and Pfurtscheller G 2004 Continuous EEG classification during motor imagery--simulation of an asynchronous BCI *IEEE Trans. Neural Syst. Rehabil. Eng.* **12** 258-65.

Vaughan T M et al. 2003 Guest editorial brain-computer interface technology: a review of the second international meeting *IEEE Trans. Neural Syst. and Rehabil. Eng.* **11** 94-109.
Witten I H and Frank E 2000 Data Mining (San Diego, CA: Academic Press).

Wolpaw J R, Birbaumer N, McFarland D J, Pfurtscheller G and Vaughan T M 2002 Brain-computer interfaces for communication and control *Clin. Neurophysiol.* **113** 767-91.

Xu W, Guan C, Siong C E, Ranganatha S, Thulasidas M and Jiankand W 2004 High accuracy classification of EEG signal *Proc. of the IEEE Inter. Conf. on Pattern Recognition (Cambridge, UK)* pp 391-4.

Yom-Tov E and Inbar G F 2003 Detection of movement-related potentials from the electro-encephalogram for possible use in a brain-computer interface *Med. Biol. Eng. Comput.* **41** 85–93.

Yu Z, Mason S G and Birch G E 2002 Enhancing the performance of the LF-ASD brain-computer interface *Proc. of the 24th Annual Conf. and the Annual Fall Meeting of the Biomed. Eng. Society (Houston, TX, USA)* pp 2443–4.

Chapter 6 An Improved Asynchronous Brain Interface: Making Use of the Temporal History of the LF-ASD Feature Vectors [19]

6.1. Introduction

Over the past decade, several research groups have developed direct brain interface (BI) systems as possible alternative communication and control solutions for individuals with severe disabilities. For a review of the field see (Mason and Birch 2002, Nicolelis 2003, Vaughan et al 2003, Wolpaw et al 2002). BI technology aims at mapping the user's cortical activity associated with an intentional control (such as imagined finger movements) directly to application-specific control signals. Thus, control of various devices such as neural prosthetics is made possible by cognitive processes only. In other words, BI systems bypass traditional interface pathways which cannot be used by individuals with severe disabilities. Several different approaches to the design of BI technology based on signals from scalp electrodes, i.e., electroencephalograms (EEG), or implanted electrodes have been reported for various communications and control applications. All these systems can be represented by the common functional model presented in Fig. 6.1 (Mason and Birch 2003, Mason et al 2003, mason et al 2005). The components between user and assistive device can be treated as a single component, a BI transducer, which functions in a manner similar to a physical transducer like a dial or switch. The role of the BI transducer is to translate the user's brain activity into reliable control signals.

There are many BI transducer designs presented in the literature. However, few have been designed specifically for asynchronous control as defined in (Mason and Birch 2000). In general, BI systems are designed to operate in either asynchronous or synchronous control paradigms. For an asynchronous BI system, when the system is ON, the user affects the BI transducer output when they want by intentionally changing their brain state. In between periods of this intentional control (IC) the user is in a no control (NC) state —they may be idle, daydreaming, thinking about a problem or lunch, or performing some other action, but they are not trying to control the BI transducer. To operate in the asynchronous paradigm, BI

[19] A version of this chapter has been published. Bashashati A., Mason S.G., Ward R.K., and Birch G. (2006) An Improved Asynchronous Brain Interface: Making Use of the Temporal History of the LF-ASD Feature Vectors *Journal of Neural Engineering* **3**(2) 87-94 *(Invited paper)*.

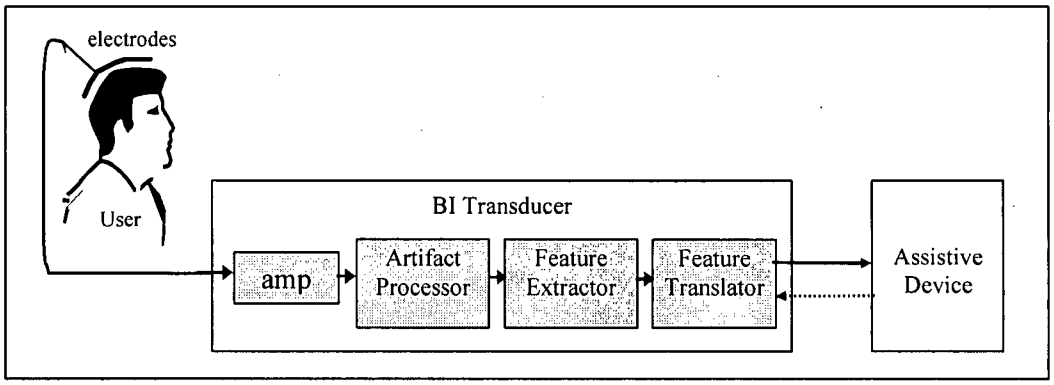

Figure 6.1 Functional model of a BI system depicting the principle functional components. More details can be found in (Mason and Birch 2003).

transducers are designed to respond only when there is intentional user control and maintain an inactive state output during times when the user is in a NC state. On the other hand, in a synchronous BI system, the allowable times for intentional user control are restricted to periods defined by the system. Thus, in synchronous systems, the BI technology is tested only during intentional user control and the response of the BI system during NC state is not tested.

Even though asynchronous (or intermittent) control is the most natural mode of interaction, it has received relatively little attention in the field. As recognized in (Wolpaw et al 2002), this is an important problem that requires more attention. Only a few BI transducers (Birch et al 1993, Graimann et al 2004, Levine et al 2000, Mason and Birch 2000, Millan and Mourino 2003, Scherer et al 2004, Townsend et al 2004, Yom-Tov and Inbar 2003) have been specifically designed (and tested) for asynchronous control. Each of the proposed transducers produces a multi-state discrete output and as such will be referred to as an asynchronous brain switch in the remainder of this paper.

In developing a non-invasive BI system, the Low Frequency-Asynchronous Switch Design (LF-ASD) was first introduced as a BI for asynchronous control applications (Mason and Birch 2000). The LF-ASD seeks to recognize the movement related potentials (MRPs) in the EEG signal. Recent studies with the latest design of the LF-ASD have demonstrated an average true positive (TP) rate of 64.7% for false positive (FP) rates of 2% (Borisoff et al 2004). To aid the presentation, the latest design of the LF-ASD (Borisoff et al 2004) will be referred as LF-ASD-V4 in the remainder of the paper. Among the proposed asynchronous BI

transducers whose offline performances have been reported in terms of true positives and false positives, (Graimann et al 2004, Levine et al 2000, Townsend et al 2004, Yom-Tov and Inbar 2003), the LF-ASD generates less false positives than others. All these offline studies reported average false positive rates in the range 6% and 28% while the average true positive rates were between 73% and 94% (Graimann et al 2004, Levine et al 2000, Townsend et al 2004, Yom-Tov and Inbar 2003). However, it should be mentioned that it is difficult to directly compare the results from our study and these studies, as the recording equipment, recording and classification protocols, and mental tasks considered are different. In addition, the amount of data involved and the degree of training the subjects received before participating in the BI experiments varies for different studies. Our experience to date indicates that the error rates of our design are still too high for individuals with high-level spinal cord injuries (our target population) in most practical asynchronous control applications. For practical applications, one needs to focus on low FP rates. From our experience, FP rates above 2% cause excess frustration and distraction in subjects (Birch et al 2002).

In the LF-ASD-V4 design, the output state of the system at time t_1, $O(t_1)$, is determined by the values of the feature vectors at time t_1, $FV_{V4}(t_1)$. In other words, the output of the system, at time t_1 is a function of the feature vector value at time t_1, i.e., $O(t_1) = f(FV_{V4}(t_1))$, where $f(.)$ is a function that maps the feature values to the output of the system. The assumption that the output state at time t_1, depends only on the value of the features at that time may not be realistic. This is because a movement, however short in duration, would take more than an instant of time. Moreover, this dependency on the exact instant in time makes the system more vulnerable to EEG signal artifacts. Thus, artifacts may easily trigger the output of the system and cause false activations of the output. Artifacts can also mask the features associated with a movement, thus causing the system not to detect such movement attempts. This would consequently decrease the true activation rate.

To study this dependency between the output, $O(t)$, and feature values, $FV_{V4}(t)$, we analyzed the ensemble averages of the movement related potentials (MRP). As these ensemble averages contain movement related information, we found that during a movement preparation and its execution the vector of the features extracted from the EEG ensemble

averages move on a path with a specific, subject-dependent shape. As an example, Fig. 6.2a shows the ensemble averages of the EEG of a subject for a time span of over three seconds. Fig. 6.2b shows the path of the 2-dimensional feature vector associated with the ensemble averages of the EEG signal centered to the finger switch activations. Fig. 6.2b shows that feature vectors move on a specific path during the movement (movement is attempted at $t=1.875s$). This path is different from that of which there was no movement ($t<1.2s$).

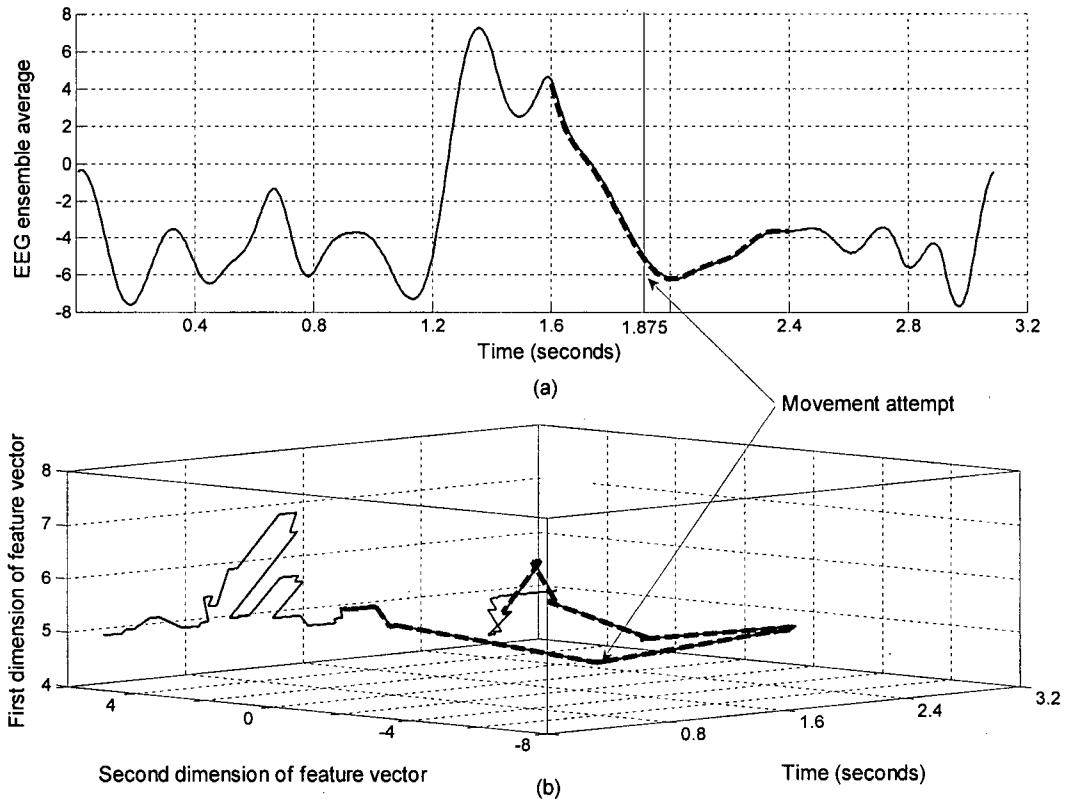

Figure 6.2 (a) Ensemble averages of the EEG of subject ID and (b) the corresponding feature vectors over time. The attempted movement is at t=1.875s.

This phenomenon implied that the past values of the features provided more knowledge about the actual movement attempt than that provided by the value of the features at one time instant. Thus, it was hypothesized that including the past information of the feature vector would improve the switch's error rates and robustness to artifacts.

In this paper, we present a method that models the path that the feature vector traverses during specific movement attempts (IC state) as well as the paths traversed during the No Control (NC) state. The specific path shapes (path templates) are used to identify the specific MRP patterns in the ongoing EEG signal and to trigger the output of the BI system. The performance of the modified design, named LF-ASD-V5, is evaluated using EEG recordings of attempted finger movements of individuals with spinal cord injuries (SCI) subjects as well as able-bodied subjects.

In Sections 6.2 of this paper, the proposed design of the modified LF-ASD design is presented. Section 6.3 presents the evaluation method used in this study. The results and conclusions are followed in Sections 6.4 and 6.5, respectively.

6.2. Proposed design of the LF-ASD-V5

In the design of the LF-ASD-V5, we aim at incorporating the history of the feature path where the features move in the multidimensional space during both IC states (attempted movement) and NC states. In other words, we want to find a relation between the output of the system and its input as written in equations (1) and (2):

$$O(t_1) = g(FV_{V5}(t_1)) \quad (1)$$

$$FV_{V5}(t_1) = [FV_{V4}(t_1 - L) \quad ... \quad FV_{V4}(t_1 - 1) \quad FV_{V4}(t_1)] \quad (2)$$

where $FV_{V5}(t_1)$ is the feature matrix at time t_1, $O(t_1)$ is the output at time t_1, $[FV_{V4}(t_1 - L) \quad ... \quad FV_{V4}(t_1 - 1) \quad FV_{V4}(t_1)]$are the values of the original features of the LF-ASD-V4 in the 'time window' of $t = t_1 - L$ to $t = t_1$, L is the length of the window, and $g(.)$ is the function that maps the feature values to the output of the system. Note that the feature matrix $FV_{V5}(t_1)$represents the path that the original feature vectors traverse during time. Basically, the new feature space captures the paths of the feature vectors and was referred to as "*path space*" in this study.

Our goal is to find the representative paths of feature vectors FV_{V4}, that correspond to IC or NC states. Conceptually these representative paths of feature vectors represent the paths that the features move through during NC and IC states. These representative paths of both state classes form the "*path templates*".

Fig. 6.3 shows the design of the LF-ASD-V5. LF_ASD-V5 has the same overall structure of the LF-ASD-V4 design except that now the feature extraction block contains an additional buffer. This block generates the new features, FV_{V5}, as described in equations (1) and (2). As the MRP pattern of each subject may vary in duration, the buffer length (L) is defined separately for each subject.

Like the LF-ASD-V4, this design uses features extracted from the 0-4Hz band in six bipolar EEG channels. After amplification, all six EEG channels are normalized with an Energy Normalization Transform (ENT). Then a low-pass-filter is used to decrease the interference with the features in the high-frequency band. A wavelet-like function is applied as the feature generator to each of the six bipolar EEG channels (For more details see (Mason and Birch 2000)). The resulting feature vector is a six-dimensional vector, with each dimension reflecting the value of the feature in each channel. The Karhunen-Loève Transform (KLT) component is used to reduce the 6-dimensional feature vector to a 2-dimensional feature vector (FV_{V4}, as shown in Fig. 6.3). A 1-NN classifier is used as the feature classifier. Finally, a moving average and a debounce block are used to further improve the classification accuracy of the system by reducing the number of false switch activations (for details, see (Mason and Birch 2000, Borisoff et al 2004). The system classifies the input patterns, at every 1/16th of a second, to one of the two classes, No Control (NC) or Intentional Control (IC) brain states.

6.2.1. Path Template Generation

The procedure used to find the specific *path templates* related to the movement (IC) and no movement (NC) states is shown in Fig. 6.4. These path templates are generated using the training data. To generate these *path templates* which form the *codebooks* in the new feature space, the k-means algorithm (Kohonen 1990) with three vectors per class state is used to generate initial clustering of each class separately. This is followed by Learning Vector Quantization (LVQ3) (Kohonen 1990) to find the final codebook (*path template*) in the path space. In the LVQ algorithm, the learning rate, α, is set to 15/(length of training data) and ε to 0.25. The algorithm is stopped after it runs 2000 times or if the template does not change significantly according to a predefined threshold. To generate the training data for the IC state, a window of feature vectors (FV_{V4}) is selected around the time of expected (attempted)

movement, TEM. (Note, details about TEM are given in Section 6.3). In other words, for each attempted movement, one feature vector at $t=TEM$ is picked for the training set. To generate the training data for the NC state, we randomly picked features in the path space ($FV_{V5}(t)$) from the first session's data corresponding to a NC state that did not contain any eye-blink artifacts.

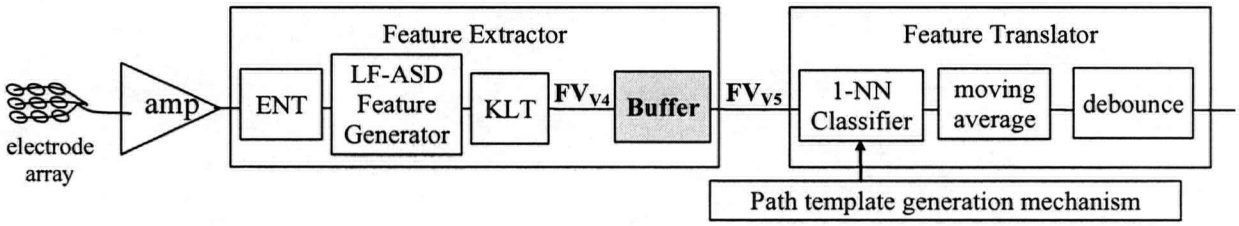

Figure 6.3 Components of the LF-ASD-V5 transducer, where ENT = Energy Normalization Transform, KLT = Karhunen-Loève Transform, and 1-NN = 1-Nearest Neighbour.

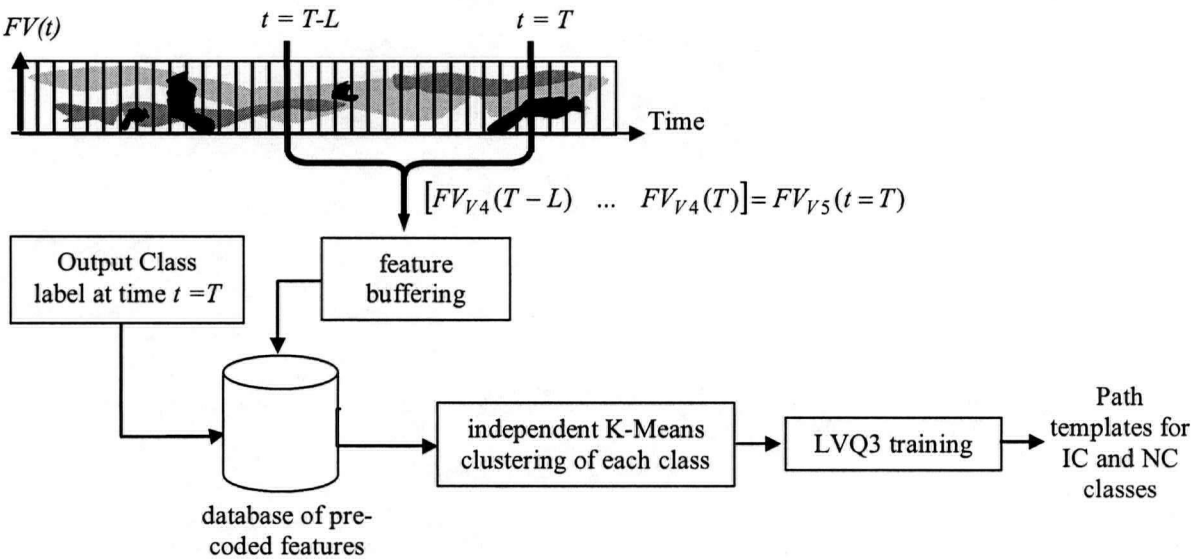

Figure 6.4 Path template generation procedure (also known as classifier training)

6.3. Evaluation Method

The data used in this study were collected from subjects positioned 150 cm in front of a computer monitor. The EEG signal was recorded from six bipolar electrode pairs positioned

over the supplementary motor area and the primary motor cortex (defined with reference to the International 10-20 System at F1-FC1, Fz-FCz, F2-FC2, FC1-C1, FCz-Cz, and FC2-C2). Electro-oculographic (EOG) activity was measured as the potential difference between two electrodes, placed at the corner and below the right eye. Eye-blink artifacts were considered present when the difference between the EOG electrodes exceeded ±25 μV. All signals were amplified by a Grass Model 8-18C EEG amplifier, filtered to a pass-band between 0.1 to 30Hz and sampled at 128Hz by a PC equipped with a 12-bit analog to digital converter embedded on a Data Translation 2801A data acquisition board.

The subjects participated in this study consisted of four subjects with a high-level spinal cord injury (SCI) and four able-bodied subjects. All subjects were male (except subject KT), right handed between 31 and 57 years old. All SCI subjects had no residual sensation or motor function in the hands. All the subjects were given written consent according to the Behavioral Research Ethics Board (BREB) of the University of British Columbia.

The data were collected from the subjects while performing a guided task in 2-minute sub-sessions. These sub-sessions contain both the NC and IC state periods as shown in Fig. 6.5. At random intervals of 5.6 to 7.0 seconds (mean of 6.7 seconds), a 2cm white circle was displayed on the subject's monitor for ¼ second, prompting them to attempt a movement. In response to this cue, the subject tried to activate the brain switch by attempting to move his right index finger one second after the cue appeared. The one-second delay was used to avoid visual evoked potential effects from the activity. The time, one second after the cue, is called "time of *expected* (attempted) movement (TEM)". As the time to perform the movement attempt depends on a user's response, the movement attempt is not necessarily performed at TEM and may change from subject to subject and attempt to attempt. Both subject groups used the same neurological mechanism to drive the brain switch: an attempted right index finger flexion. This resulted in no movement in subjects with high level SCI, and an actual finger flexion in able-bodied subjects. For each subject, an average of 80 trials was collected every day for 6 days.

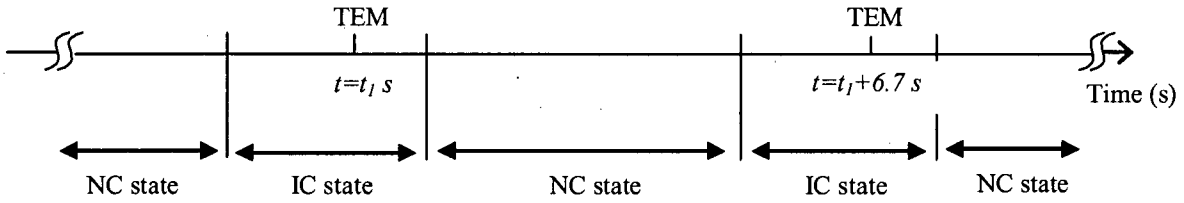

Figure 6.5 Structure of each 2-minute sub-session of EEG recording, where TEM=time of the expected (attempted) movement

Besides recording the EEG data during movement attempts, in each session, the EEG data were also recorded for several 2-minutes periods while the person was in a specific no control (NC) state. The sub-sessions that contain only NC state EEG data are gathered in different NC states such as attentive eyes opened while looking at a picture on the monitor or doing a search task, and attentive eyes closed. The reason to record this type of data was to evaluate the performance of the BI design in different NC state periods.

The proposed design is evaluated on all the available data, i.e., the sub-sessions that contain mixed NC and IC state data and the sub-sessions that include only NC state periods. The EEG data of the mixed NC and IC states contain movement attempts approximately every 6.7 seconds separated by periods of NC state. The reasons behind the addition of the periods of pure NC state data were to: 1) more thoroughly evaluate the performance of the system on different types of NC state data, and 2) approach the real-world paradigm where a person performs control with longer periods of NC state.

The ability of the subjects to control the BI system was evaluated by 1) percentage of correct activations during IC states (true positives, TPs) and 2) percentage of false switch activations during NC states (false positives, FPs). A TP was identified if the BI system was activated at least once in a window 0.5 seconds before and 1 second after the time of the expected movement (TEM), a method similar to that employed by others (Graimann et al 2004, Levine et al 2000, Townsend et al 2004, Yom-Tov and Inbar 2003). FPs were assessed in the periods before the appearance of a white circle and after the end of the activation window.

The testing system employed was the same as was used by (Mason and Birch 2000, Borisoff et al 2004]. This system automatically detected eye-blinks and blocked the output of the system during these times. Table 6.1 details the percentage of the recorded data of the

evaluation set that were blocked by the system for each subject. From the numbers in Table 6.1, an average of 22% of the EEG data contained eye-blinks and 7.4% of the trials of the test set are blocked by the system due to the presence of eye-blinks.

The first day's recordings were used to train the classifier and those from the subsequent 5 days were used for evaluation.

TABLE 6.1. DETAILS OF THE EEG DATA OF THE EVALUATION SET THAT WERE BLOCKED BY THE TEST SYSTEM DUE TO EYE-BLINK

Subject	ID	CB	CS	KT	AJ	LB	BK	RT
Total duration of recorded EEG (minutes)	66	77	61	87	63	81	64	79
Percentage of data with eye-blinks (%)	17	19	15	28	34	22	19	23
Total number of movement attempts	320	411	294	397	324	415	356	322
Number of movement attempts blocked by the test system due to eye-blink.	21	16	12	4	43	25	76	10
Percentage of movement attempts blocked by the test system due to eye-blink.	6.6	3.9	4.1	1.0	13.3	6.0	21.4	3.1

6.4. Results

The performance of the LF_ASD-V5 design is summarized via the receiver operating characteristic (ROC) curves. These results are compared to the performance of the latest LF-ASD design (LF-ASD-V4) (Borisoff et al 2004).

For each subject, different buffer lengths (L's) were used to build the classifier and the buffer length that resulted in the best performance is reported here. Specifically, we tried buffer lengths of 1, 3, 5, 7, 9 and 11. Buffer length of one corresponds to the design of previous system, LF-ASD-V4.

Figs. 6 and 7 show the *path templates* of the feature vectors that the classifier generates for the two cases 1) Intentional Control (IC) state, and 2) No Control (NC) state. In these figures, the path templates for each class are shown for subjects LB and ID. These templates correspond to the buffer lengths that resulted in the best performance for these subjects. As the figures show, the path templates of the IC state (the paths that the FV_{V4} features move on during movement attempts) are quite different from those of the NC state path templates. In most cases, the path templates during NC states were templates with small amplitudes. This coincides with the rationale of the original feature extractor design. The original feature

extractor of the LF-ASD was designed to produce features with large values when specific movements were performed and features with small values when the subject was in the NC state. As mentioned in Section 6.2, the algorithm was designed to generate three path templates per class. In some cases, like the one shown in Fig. 6.6 for NC state path templates, the three templates estimates for the NC class were very similar, thus when they are plotted they appear as one template in this figure. The reason is that the data of that class could be represented with less (than three) path templates

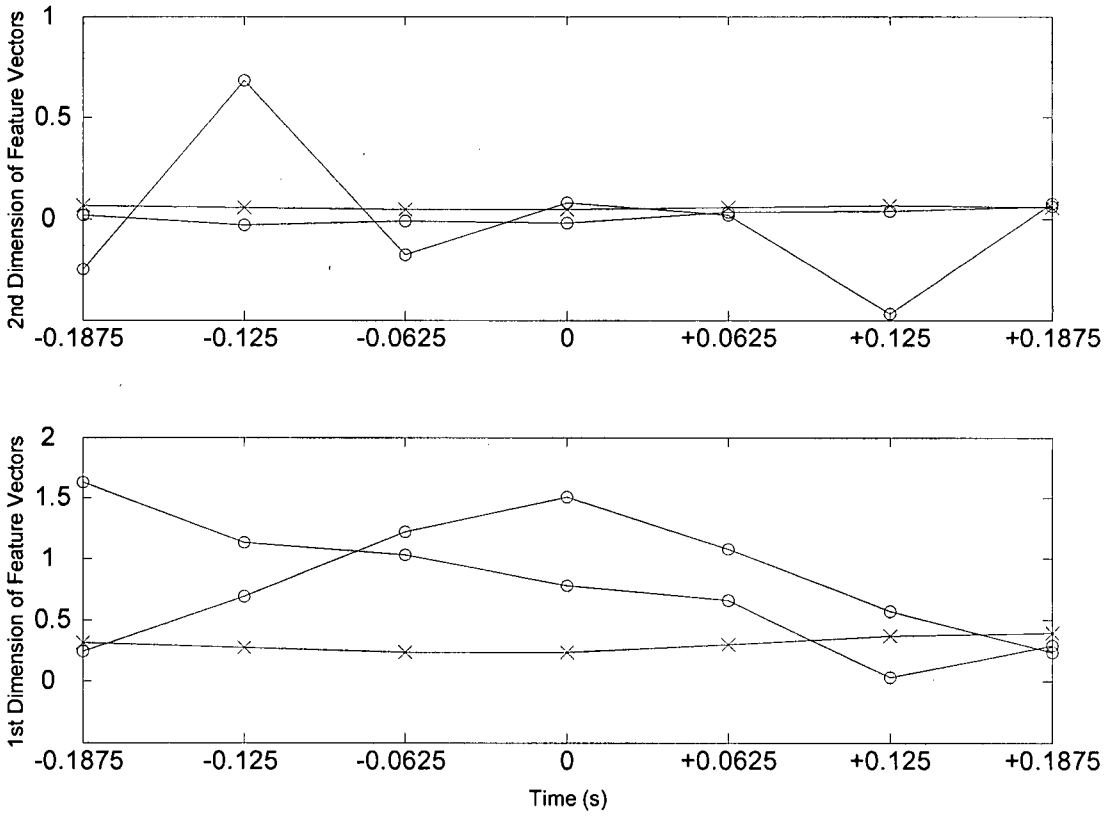

Figure 6.6 *Path templates* for subject LB for the two cases 1) movement (IC) state (lines with circles) and 2) no movement (NC) state (lines with crosses). Time=0 corresponds to the time of the expected (attempted) movement (TEM). Note that the algorithm estimates three path templates per class. However, as can be seen in this figure, the three path templates of the NC state

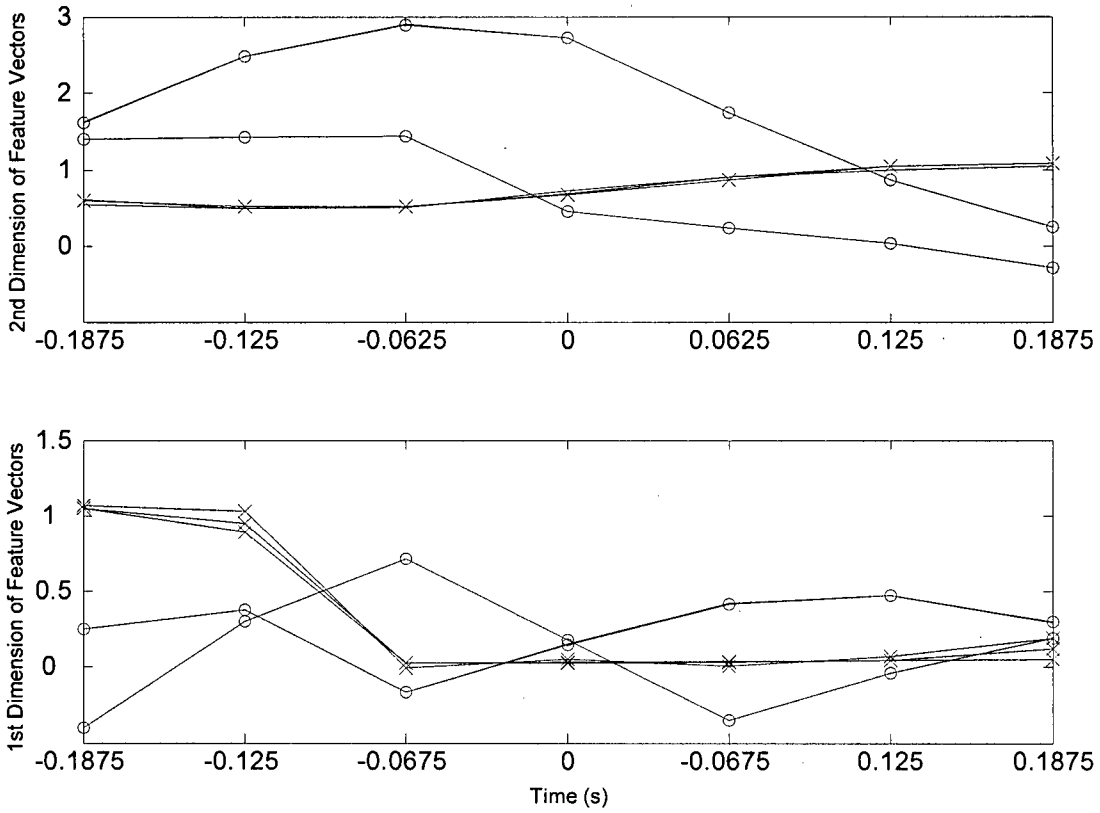

Figure 6.7 *Path templates* for subject ID for the two cases 1) movement (IC) state (lines with circles) and 2) no movement (NC) state (lines with crosses). Time=0 corresponds to the time of the expected (attempted) movement (TEM). Note that the algorithm estimates three path templates per class. However, as can be seen in this figure, two of the three path templates of the IC state were very similar and are seen as one template. This is also can be seen for NC state path templates.

The performance of the LF-ASD-V5 was compared to the LF-ASD-V4 design for a debounce period of 16 (as used in previous study (Borisoff et al 2004)). In Tables 6.2 and 6.3, we show the TP rates at fixed FP rates of 1% and 2% for able-bodied and SCI subjects. The results showed that the best performance improvement of 50% was achieved for subject BK when the modified BI system (LF-ASD-V5) was used. For able-bodied subjects, the average performance of LF-ASD-V5 was approximately 6.5% better than LF-ASD-V4 in the false positive ranges of 1% to 2%. On the other hand, LF-ASD-V5 improved the detection of attempted movements of spinal cord injured subjects by an average of 25% in the false positive ranges of 1% to 2%.The hypothesis that the performances of LF-ASD-V4 and LF-ASD-V5, operating at false positive level of 2%, had equal means (against the alternate

hypothesis that LF-ASD-V5 had higher average performance than LF-ASD-V4) was rejected at significance level of $p<0.01$ using paired T-test.

The results in Tables 6.2 & 6.3 show that the average true positive rates for SCI subjects are 3.2-6.7% lower than the able-bodied subjects. Using the new design, the average true positive rate differences between the two subject groups drop to the 1-3.4% range.

TABLE 6.2 TRUE POSITIVE (TP) RATES AT FIXED FALSE POSITIVE (FP) RATES OF 1% AND 2% FOR ABLE-BODIED SUBJECTS.

Subject	Buffer length (L)	LF-ASD-V4		LF-ASD-V5		Absolute TP Improvement at		Percentage of TP Improvement at	
		TP (%) at FP=1 %	TP (%) at FP=2%	TP (%) at FP=1%	TP (%) at FP=2%	FP=1%	FP=2%	FP=1%	FP=2%
ID	7	41.1	64.6	47.6	69.2	+6.5	+4.6	+16%	+7%
CB	5	44.5	66.0	42.7	68.2	-1.8	+2.2	-4%	+3
CS	1	45.8	67.6	45.8	67.6	0	0	0%	0%
KT	9	23.6	48.5	28.3	54.0	+4.7	+5.5	+20%	+11%
Average		**38.8**	**61.7**	**41.1**	**64.8**	**+2.3**	**+3.1**	**+8%**	**+5%**

TABLE 6.3 TRUE POSITIVE (TP) RATES AT FIXED FALSE POSITIVE (FP) RATES OF 1% AND 2% FOR SCI SUBJECTS.

Subject	Buffer length (L)	LF-ASD-V4		LF-ASD-V5		Absolute TP Improvement at		Percentage of TP Improvement at	
		TP (%) at FP=1 %	TP (%) at FP=2%	TP (%) at FP=1%	TP (%) at FP=2%	FP=1%	FP=2%	FP=1%	FP=2%
AJ	5	31.7	61.0	43.7	71.1	+12.0	+10.1	+38%	+17%
LB	7	39.3	64.5	44.7	69.9	+5.5	+5.4	+14	+8%
BK	9	28.6	53.5	42.9	68.5	+14.3	+15.0	+50%	+28%
RT	5	28.7	55.0	36.9	63.1	+8.2	+8.1	+29%	+15%
Average		**32.1**	**58.5**	**42.1**	**68.2**	**+10.0**	**+9.7**	**+33%**	**+17%**

Truncated ROC curves for two SCI subjects (BK and RT) are shown in Figs. 8 and 9 for both LF-ASD-V4 and our proposed LF-ASD-V5 design. As we are interested in lower FP rate levels, only those values of FPs below 5% are shown in the ROC curves. As the figures show, for most of the FP rate levels, LF-ASD-V5 generated a better TP rate than LF-ASD-V4.

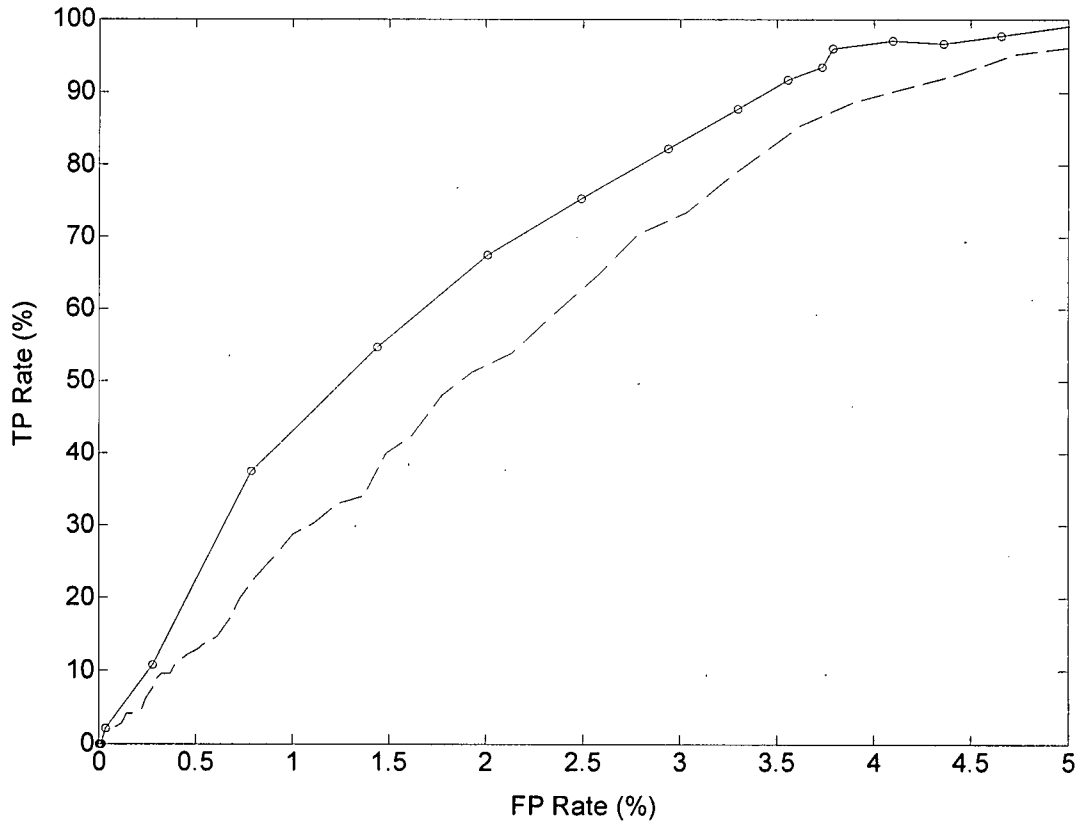

Figure 6.8 Truncated ROC curves for SCI subject BK for LF-ASD-V4 system (Dashed line) and our proposed LF-ASD-V5 design (Solid line with circles).

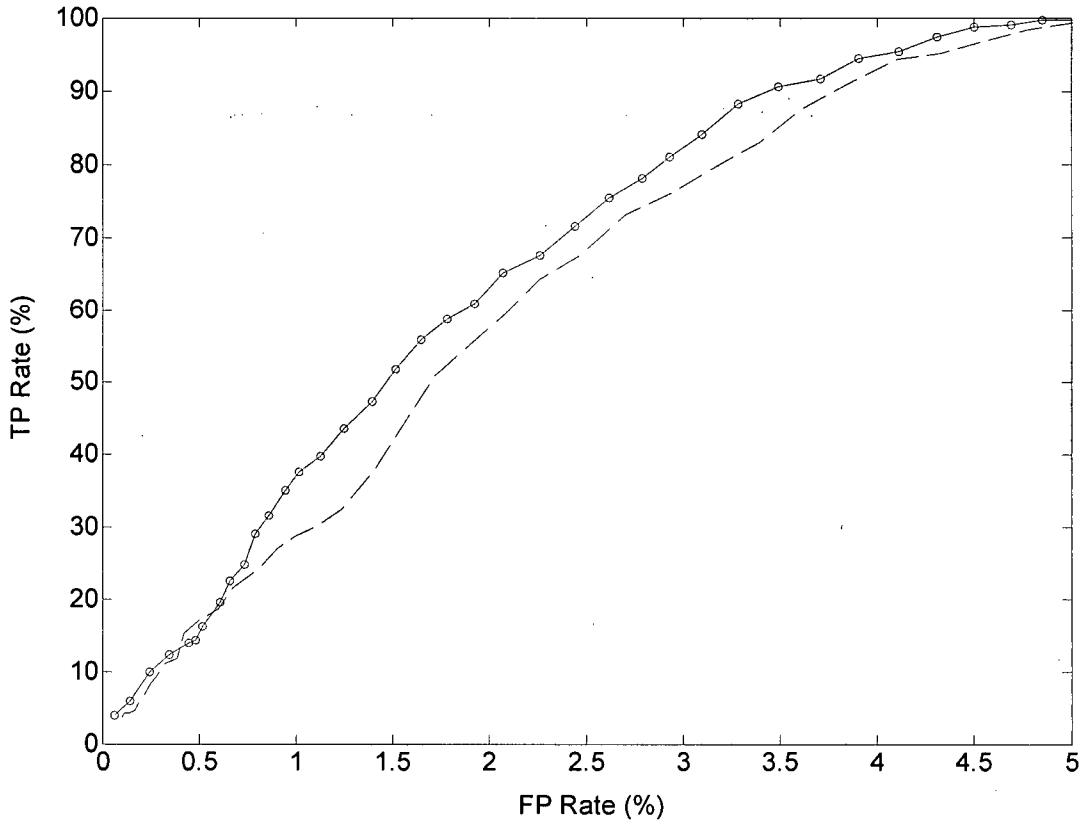

Figure 6.9 Truncated ROC curves for SCI subject RT for LF-ASD-V4 system (Dashed line) and our proposed LF-ASD-V5 design (Solid line with circles).

6.5. Conclusions

We have introduced a new design of an asynchronous BI by utilizing the history of feature vectors in time. The error characteristics of the proposed LF-ASD-V5 design were better than the previous design (LF-ASD-V4) with true positive rates increases of up to 50% for false positive rates in the 1-2% range. We have demonstrated that utilizing the knowledge of the path of feature vectors improved the performance of the LF-ASD, but this idea may be useful for other BI transducer designs and pattern recognition problems.

Results showed that the performances of the SCI subjects were improved by approximately 25% on average, while the average improvements for able-bodied subjects were 6.5%. These results demonstrated that the proposed method mostly benefited the SCI subjects rather than the able-bodied ones. One reason behind the higher improvements for SCI subjects might be that the able-bodied subjects generated MRP patterns with large amplitudes and thus the

previous design could detect them without considering the path of features. One of our recent studies (Mason et al 2004) showed that SCI subjects generated bipolar MRP patterns whose amplitudes were smaller than the ones of able-bodied subjects. As in the new design, the paths of the features are taken into account, we are incorporating more information during the movement and thus the trials that were missing before can be detected and the improvements are higher for SCI subjects.

While the performance of the subjects does differ significantly between LF-ASD-V4 and LF-ASD-V5, it does not differ between able-bodied and disabled subjects in LF-ASD-V5. This suggests LF-ASD-V5 gives consistent results for both subject groups unlike LF-ASD-V4, in which able-bodied subjects performed better than SCI subjects. This is an important point that needs to be verified statistically with more subjects.

In summary, this work has succeeded in decreasing the error rates of our current BI design. Although this forms a substantial decrease in the error rate, practical experience indicates that further system improvements are still desirable.

Several ideas emerged from the results that may be studied in future investigations. For example, as mentioned in Section 6.3, the exact time that a subject attempted the movement was not known accurately. As this time was user dependent, the subject did not necessarily attempt the movement at TEM which is one second after the cue. In this study to train the classifier, the features in the path space at the TEM were selected even though this time may not have been the actual time of the attempted movements. Thus, these features may not have been good representatives of the actual movement attempt. We observed that using these features resulted in no improvement for subject CS. Thus, we carried out another approach to generate the training data to train the classifier. As mentioned in Section 6.2.1, to generate the training data for the IC state, the features at the TEM were picked. In the new procedure, we picked more features around TEM for training the classifier. Specifically, we picked the features at $t=TEM-1$, TEM, and $TEM+1$ and then trained the classifier with the new training set for subject CS. The results showed true positive percentage improvement of approximately 5%. We also applied the same procedure for subject ID, but the results did not improve. Statistical classifiers are dependent for their accuracy on the quality of the training data as much as on the algorithm used for classification. For useful results to be obtained, the

training data set must be representative of the whole area to be classified. This preliminary analysis on the data of two subjects implies the need for a method that selects the most suitable training data to train the classifier. We will look into this issue in our future research.

In this study, the output of the system was blocked when the eye-blinks were present. Utilizing the path of the features may nullify our need for an eye-blink detector in our BI system. Thus, our future work will explore the system performance and robustness when the output of the system is not blocked due to eye-blinks. This study was an offline evaluation of the proposed LF-ASD-V5 design; however, online feedback experiments are also needed to confirm the findings of this study.

The use of different feature extraction methods, self-learning classification schemes and customization of the LF-ASD Feature Generator parameters are in the scope of our future directions as well.

6.6. References

Birch G E, Bozorgzadeh Z and Mason S G 2002 Initial on-line evaluation of the LF-ASD brain-computer interface with able-bodied and spinal-cord subjects using imagined voluntary motor potentials *IEEE Trans. Neural Syst. Rehab. Eng.* **10** 219-224.

Birch G E, Lawrence P D and Hare R D 1993 Single trial processing of event related potentials using outlier information *IEEE Trans. Biomed. Eng.* **40** 59–73.

Borisoff J F, Mason S G, Bashashati A and Birch G E 2004 Brain Computer Interface (BCI) Design for Asynchronous Control Applications: Improvements to the LF-ASD Asynchronous Brain Switch *IEEE Trans. Biomed. Eng.* **51** 985-92.

Graimann B, Huggins J E, Levine S P and Pfurtscheller G 2004 Toward a direct brain interface based on human subdural recordings and wavelet-packet analysis *IEEE Trans. Biomed. Eng.* **51** 954-62.

Kohonen T 1990 The self-organizing map *Proc. of IEEE* **78** 1464-1480.

Levine S P, Huggins J E, Bement S L, Kushwaha R, Schuh L A, Rohde M M, Passaro E A, Ross D A, Elisevich K V and R. J. Smith 2000 A direct brain interface based on event-related potentials *IEEE Trans. Rehab. Eng.* **8** 180–5.

Mason S G, Bashashati A, Fatourechi M and Birch G E Developing a Framework for Brain-Interface Technology Design *available online at http://www.braininterface.org/.*

Mason S G and Birch G E 2000 A Brain-Controlled Switch for Asynchronous Control Applications *IEEE Trans. Biomed. Eng.* **47** 1297-307.

Mason S G and Birch G E 2003 A general framework for brain-computer interface design *IEEE Trans. Neural Syst. Rehab. Eng.* **11** 70–85.

Mason S G, Bohringer R, Borisoff J F and Birch G E 2004 Real-time control of a video game with a direct brain--computer interface *Clin. Neurophysiol.* **21** 404-8.

Mason S G, Moore M M and Birch G E 2003 Designing pointing devices using brain-computer interface technology *Proc. of the 1st Int. IEEE EMBS Conf. on Neural Engineering* (Capri, Italy) pp 610-13.

Millan J R and Mourino J 2003 Asynchronous BCI and local neural classifiers: An overview of the adaptive brain interface project *IEEE Trans. Neural Syst. Rehab. Eng.* **11** 159–61.

Nicolelis M A 2003 Brain-machine interfaces to restore motor function and probe neural circuits *Nat. Rev. Neurosci.* **4** 417– 22.

Scherer R, Muller G R, Neuper C, Graimann B and Pfurtscheller G 2004 An asynchronously controlled EEG-based virtual keyboard: improvement of the spelling rate *IEEE Trans. Biomed. Eng.* **51** 1979-84.

Townsend G, Graimann B and Pfurtscheller G 2004 Continuous EEG classification during motor imagery--simulation of an asynchronous BCI *IEEE Trans. Neural Syst. Rehab. Eng.* **12** 258-265.

Vaughan T M 2003 Guest editorial brain-computer interface technology: a review of the second international meeting *IEEE Trans. Neural Syst. Rehab. Eng.* **11** 94-109.

Wolpaw J R, Birbaumer N, McFarland D J, Pfurtscheller G and Vaughan T M 2002 Brain-computer interfaces for communication and control *Clin. Neurophysiol.* **113** 767-91.

Yom-Tov E and Inbar G F 2003 Detection of movement-related potentials from the electro-encephalogram for possible use in a brain-computer interface *Med. Biol. Eng. Comput.* **41** 85–93.

Chapter 7 Effects of Eye Blinks on a Self-paced Brain Interface Design[20]

7.1. Introduction

Many Brain Interface (BI) transducer designs have been presented in the literature (for a review of the field, see (Wolpaw et al., 2002; Vaughan, 2003; Mason et al., 2006; Nicolelis, 2003)). Few of them, however, have been designed specifically for self-paced control. The concept of self-paced control of brain interface systems was introduced in (Mason and Birch, 2000) as "asynchronous control". In a self-paced brain interface, the users affect the BI transducer output whenever they want by intentionally changing their brain state. Between periods of intentional control (IC), users are said to be in a no-control (NC) state - they may be idle, daydreaming, thinking about a problem or lunch, or performing any other action, but not trying to control the BI transducer. BI transducers are thus designed to respond only when there is intentional user control and to remain inactive when the user is in a no-control state.

In contrast, most BIs operate only during specific periods determined by the system (not the user). This operating paradigm is referred to as synchronous or synchronized control (Mason and Birch, 2000). Although self-paced control is the most natural mode of interaction, it has received less attention. Only a few BI transducers (Mason and Birch, 2000; Levine et al., 2000; Yom-Tov and Inbar, 2003; Birch et al., 1993; Millan and Mourino, 2003; Scherer et al., 2004; Graimann et al., 2004; Townsend et al., 2004; Borisoff et al., 2004) have been specifically designed and tested for self-paced control. As recognized by Wolpaw et al (2002), self-paced systems address a problem important for practical applications, i.e. detection of user commands without the timing cues provided by structured trials.

In developing a non-invasive brain interface system, the Low Frequency-Asynchronous Switch Design (LF-ASD) was first introduced as a brain interface for self-paced control applications (Mason and Birch, 2000). The LF-ASD seeks to recognize the movement related potentials (MRPs) in the EEG signal. Recent studies with the latest design of the LF-ASD

[20] A version of this chapter has been published. With kind permission of Springer Science and Business Media. Bashashati A., Noureddin B., Ward R., Lawrence P., and Birch G. (2007) Effects of Eye Blinks on the Performance of a Self-paced Brain Interface, *Clinical Neurophysiology* **118** 1639-47.

have demonstrated an average true positive (TP) rate of 66.5% for false positive (FP) rates of 2% (Bashashati et al., 2006 b). To aid the presentation, the latest two designs of the LF-ASD (Bashashati et al., 2006 a; Bashashati et al., 2006 b) will be referred to as LF-ASD-V4 and LF-ASD-V5, respectively, in this paper. Among the proposed asynchronous BI transducers whose offline performances have been reported in terms of true positives and false positives (Levine et al., 2000; Yom-Tov and Inbar, 2003; Graimann et al., 2004; Townsend et al., 2004), the LF-ASD generates less false positives. All these offline studies have reported average false positive rates in the range of 6% to 28% while the average true positive rates were between 73% and 94% (Levine et al 2000, Yom-Tov and Inbar 2003, Graimann et al 2004, Townsend et al 2004). It is difficult however to directly compare the results of the different studies, as the recording equipment, recording and classification protocols, decision rate and interval of time during which false positives could occur, and mental tasks considered are different. In addition, the amount of data involved and the degree of training the subjects received before participating in the BI experiments also vary between studies.

In the LF-ASD-V4 version, which is similar to the original design of the LF-ASD (Mason and Birch 2000), the output state of the system at time t_l, is only determined by the values of the feature vectors at that time. In contrast, the later design of the LF-ASD (LF-ASD-V5) was introduced to include the past information of the feature vectors in deciding whether or not there is a movement attempt at time t_l. Using this information has been shown to improve the BI's error rate (Bashashati et al 2006b). (Bashashati et al 2006a) showed that in order to detect the desired MRP pattern, some design parameters of the feature generator should be adjusted for each subject These parameter adjustments were not done for the LF-ASD-V5 version.

Previously, the testing system employed was the same as that used by (Mason and Birch 2000, Borisoff et al 2004). This system automatically detected eye-blinks and did not evaluate the system during these times. In the original version of the LF-ASD it was believed that eye-blinks generate excessive false activations of the system, and hence EEG data contaminated with eye-blinks were not evaluated. As the LF-ASD looks for a specific waveform (template) in the EEG signal to detect the presence of movements, eye movements can also easily generate such a template in the EEG signal and cause false activation of the output

Table 7.1 shows the details of eye-blink artifacts in our pre-recorded data that were used in this and previous studies (Bashashati et al., 2006 a; Bashashati et al., 2006 b). As this table shows, 15-34% of the NC state EEG data were contaminated with eye-blinks and 1-21.4% of the trials were rejected due to the presence of eye-blinks (Borisoff et al., 2004; Bashashati et al., 2006 a; Bashashati et al., 2006 b). As shown in the third row of Table 7.1, a significant amount of data (15-34%) was not evaluated due to the presence of eye-blinks. This reduced the available time that a user could control the BI system. Ideally, a BI system should be operational at any time. This is not the case for this brain interface system, thus reducing its usability. At the same time, according to the testing system employed, further devices are needed to record the electro-oculogram (EOG), which is used to detect eye-blinks. From the above, it is clear that a strategy that can handle eye-blink artifacts without the need for rejecting them or the need for EOG recording is desired.

TABLE 7.1 DETAILS OF THE EEG DATA OF THE EVALUATION SET THAT WERE BLOCKED BY THE TEST SYSTEM DUE TO EYE-BLINKS.

Subject	ID	CB	CS	KT	AJ	LB	BK	RT
Total duration of recorded EEG (minutes)	66	77	61	87	63	81	64	79
Percentage of data contaminated with eye-blinks (%)	17	19	15	28	34	22	19	23
Total number of movement attempts	320	411	294	397	324	415	356	322
Number of movement attempts blocked by the test system due to eye-blinks	21	16	12	4	43	25	76	10
Percentage of movement attempts blocked by the test system due to eye-blinks (%)	6.6	3.9	4.1	1.0	13.3	6.0	21.4	3.1

Since the LF-ASD-V5 design considers the history of features in decision making and improves the performance of the system, we thought it might handle the EEG data contaminated with eye-blink artifacts better than the previous versions. In such a case, we no longer need to block the decision of the system during eye-blink artifacts. This paper evaluates the performance of the LF-ASD-V4 (Bashashati et al., 2006 a) and the latest self-paced brain interface design, the LF-ASD-V5, (Bashashati et al., 2006 b) when eye-blinks are not excluded from data. In the meantime, the design parameters of the feature generator in (Bashashati et al., 2006 b) are customized according to (Bashashati et al., 2006 a) for each subject.

This study measures the performance of LF-ASD-V5 when eye-blinks are not excluded from the analysis and compares the performance of this design with LF-ASD-V4. The performance of the system is evaluated using EEG recordings of attempted finger movements of subjects with spinal cord injuries (SCI) as well as able-bodied subjects who were recorded previously in BI experiments.

In Section 7.2 of this paper, a brief description of the self-paced brain interface designs (LF-ASD-V4 and LF-ASD-V5), the description of the experiments, and the evaluation procedure are presented. The results and discussions are followed in Sections 7.3 and 7.4, respectively.

7.2. Methods

7.2.1. Brain Interface Designs

7.2.1.1. LF-ASD-V4

Fig. 7.1 shows the block diagram of the LF-ASD-V4 design, which is similar to the original design of the self-paced brain interface (Mason and Birch, 2000). This design uses features extracted from six bipolar EEG channels (defined with reference to the International 10-20 System at F1-FC1, Fz-FCz, F2-FC2, FC1-C1, FCz-Cz, and FC2-C2). After amplification, all six EEG channels are normalized with an Energy Normalization Transform (ENT) (Borisoff et al., 2004). A wavelet-like function is applied as the feature generator. The important design parameters of the feature generator are parameters that determine the shape of the subject-specific movement-related potential pattern that needs to be detected and are referred to as "delay parameters", as shown in Fig. 7.2 as αi, αj. The Karhunen-Loève Transform maps the six-dimensional feature space produced by the Feature Generator to a two-dimensional space. A one-nearest neighbour (1-NN) classifier is used as the feature classifier. The system's classification accuracy is further improved by using a moving average and a debounce block to reduce the number of false switch activations (for details, see (Mason and Birch, 2000; Borisoff et al., 2004)). Overall, every 1/16th of a second, the system classifies input patterns as either no-control (NC) or intentional control (IC).

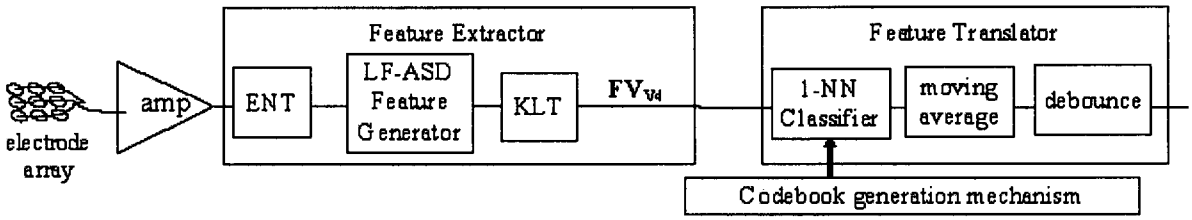

Figure 7.1 Components of the LF-ASD-V4 transducer (Borisoff et al., 2004), where ENT = Energy Normalization Transform, KLT = Karhunen-Loève Transform, 1-NN = 1-Nearest Neighbour, amp = amplifier, and FV_{V4} = extracted feature vector.

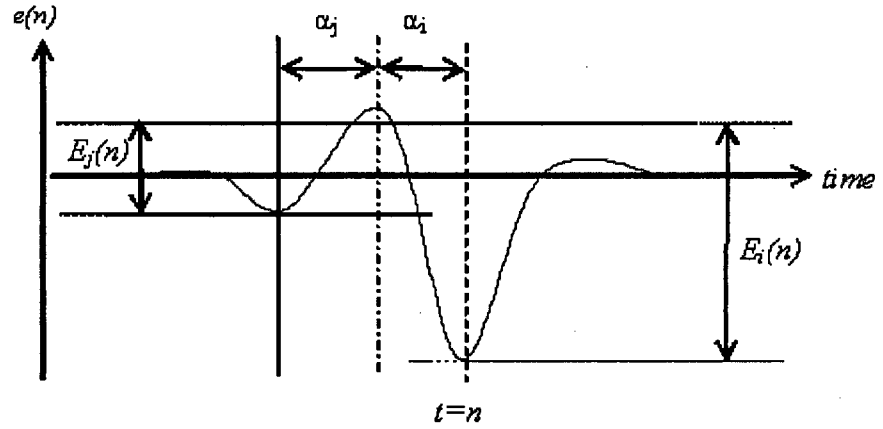

Figure 7.2 Desired pattern of the bipolar EEG during movement, where $e(n)$ = amplitude of the signal, $E_i(n)$ = amplitude difference between local maximum before the movement and local minimum after the movement, $E_j(n)$ = amplitude difference between local maximum before the movement and local minimum before the movement, $t=n$ is the time of the expected movement attempt, and α_i and α_j are the delay parameters.

The delay parameters of the feature generator in (Mason and Birch, 2000) were set to be the same for all subjects. In the LF_ASD-V4 design, these parameters were customized separately for each subject to increase the confidence that the system is triggered by the desired MRP pattern and not any other unwanted brain activity.

7.2.1.2. LF-ASD-V5

LF-ASD-V5 aimed at including the past values of the features in decision making at any specific time.

Fig. 7.3 shows the design of the LF-ASD-V5 (Bashashati et al., 2006 b). $FV_{V4}(t_1)$ is the value of the original features of the LF-ASD-V4, L is the length of the buffer, and

$FV_{V5}(t_1)$ represents the path that the original feature vectors traverse during time. This path represents the history of the original LF-ASD features in the multidimensional. As shown in Fig. 7.3, the LF-ASD-V5 has the same overall structure of the LF-ASD-V4 design (see Section 7.2.1.1) except for the feature extraction block which contains an additional buffer that captures the trajectory of the feature vector in the multi-dimensional space. As the movement-related potential pattern of each subject may vary in duration, the buffer length (L) is defined separately for each subject. Overall, every 1/16th of a second, the system classifies input patterns as either no- control or intentional control. For more details refer to (Bashashati et al., 2006 b).

In (Bashashati et al., 2006 b) the original parameters of the feature extraction block were used for all subjects. However, according to the findings of (Bashashati et al., 2006 a), these parameters should be adjusted for each subject. As such, in this paper, the parameters of the feature extraction block are customized according to (Bashashati et al., 2006 a).

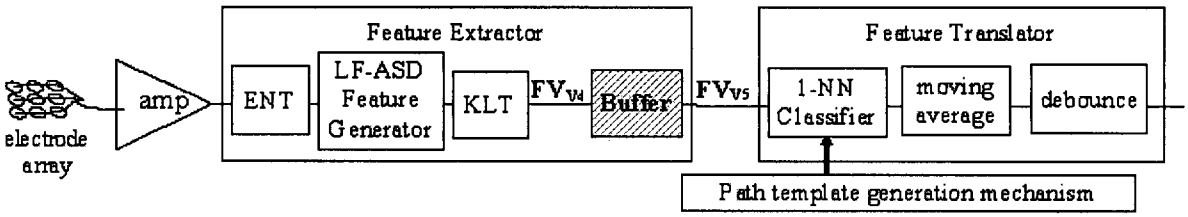

Figure 7.3 Components of the LF-ASD-V5 transducer (Bashashati et al., 2006 a), where ENT = Energy Normalization Transform, KLT = Karhunen-Loève Transform, 1-NN = 1-Nearest Neighbour, amp = amplifier, FV_{V4} = extracted feature vector of LF-ASD-V4, and FV_{V5} = extracted feature vector of LF-ASD-V4.

7.2.2. Experiments

The data used in this study were collected from subjects seated 150 cm in front of a computer monitor. The EEG signal was recorded from six bipolar electrode pairs positioned over the supplementary motor area and the primary motor cortex (defined with reference to the International 10-20 System at F1-FC1, Fz-FCz, F2-FC2, FC1-C1, FCz-Cz, and FC2-C2). Electro-oculographic (EOG) activity was measured as the potential difference between two electrodes, placed at the corner and below the right eye. Eye-blink artifacts were considered present when the difference between the EOG electrodes exceeded ±25 μV. All signals were amplified by an EEG amplifier, filtered to a pass-band between 0.1 to 30Hz and sampled at

128Hz by a PC equipped with a 12-bit analog to digital converter embedded on a data acquisition board.

The subjects participated in this study consisted of four subjects with a high-level spinal cord injury and four able-bodied subjects. All subjects were male (except subject KT), right handed between 31 and 57 years old. All SCI subjects had no residual sensation or motor function in the hands. All the subjects provided written consent according to the Behavioral Research Ethics Board (BREB) of the University of British Columbia.

The data were collected from the subjects while performing a guided task in 2-minute sessions. These sessions contained both the no-control and intentional control state periods as shown in Fig. 7.4. At random intervals of 5.6 to 7.0 seconds (mean of 6.7 seconds), a 2cm white circle was displayed on the subject's monitor for ¼ second, prompting them to attempt a movement. In response to this cue, the subject tried to activate the brain switch by attempting to move his right index finger one second after the cue appeared. The one-second delay was used to avoid visual evoked potential effects from the activity. The time, one second after the cue, is called "time of *expected* (attempted) movement (TEM)". As the time to perform the movement attempt depends on the user's response, the movement attempt is not necessarily performed at TEM and may change from subject to subject and attempt to attempt. Both subject groups used the same neurological mechanism to drive the brain switch: an attempted right index finger flexion. This resulted in no movement in subjects with high level spinal cord injury, and an actual finger flexion in able-bodied subjects. For each subject, an average of 80 trials was collected every day for 6 days.

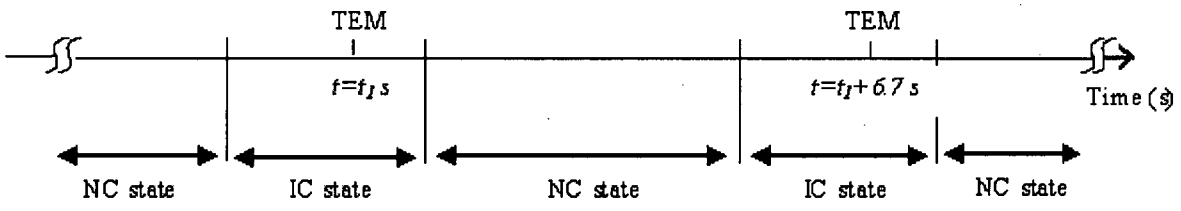

Figure 7.4 Structure of each 2-minute sub-session of EEG recording, where TEM = time of the expected (attempted) movement, NC = no-control, and IC = intentional control.

Besides recording the EEG data during movement attempts, the EEG data were also recorded for several 2-minute periods while the person was in a specific no-control state. These

sessions contained only no-control state EEG data and were gathered for different no-control states such as attentive eyes opened while looking at a picture on the monitor or doing a search task, and attentive eyes closed. The reason for recording this type of data was to evaluate the performance of the brain interface system for different no-control state periods.

7.2.3. Evaluation

The designs are evaluated on all the recorded data, i.e., the 2 minute sessions that contain mixed no-control (NC) and intentional control (IC) state data and the 2 minute sessions that include only NC state periods. The EEG data of the mixed NC and IC states contain movement attempts approximately every 6.7 seconds separated by periods of no-control state. The reasons behind the addition of the periods of pure no-control state data were: 1) to more thoroughly evaluate the performance of the system on different types of no-control state data, and 2) to approach the real-world paradigm where intentional control states are separated by longer periods of no-control state.

The ability of a subject to control the brain interface system was evaluated by 1) the percentage of correct activations during IC states (true positives, TPs) and 2) the percentage of false switch activations during NC states (false positives, FPs). A state was identified as true positive if the brain interface system was activated at least once in a TEM window starting at 0.5 seconds before the time of the expected movement (TEM) and ending at 1 second after it, a method similar to that employed in other studies (Yom-Tov and Inbar, 2003; Birch et al., 1993; Graimann et al., 2004; Townsend et al., 2004). Any activations before the appearance of a white circle and 1 second after the TEM were considered as false positives.

Artifact-free EEG data of the first day's recordings were used for training the 1-NN classifier. The EEG data of the subsequent 5 days recordings were used for evaluating the performance of the brain interface system in each of the following cases (refer to Fig. 7.5):

Case 1: Data during ocular artifact presence (OA_1, OA_2 and OA_3 periods) are not included at all in the analysis. The total length of data (**T**) is effectively reduced.

Case 2: Data during OA_1, OA_2 and OA_3 are included in the analysis, but the output is always set to inactive, even if the LF-ASD is activated (e.g., t_2 and t_3). All the data (**T**) is considered, but valid LF-ASD activations may be incorrectly suppressed (e.g. t_3). In this

case, in fact, the output is frozen and neither a hit nor a miss is registered during artifact presence.

Case 3: Data during OA_1, OA_2 and OA_3 are included in the analysis, and the output is never artificially set to inactive, even during artifacts. All the data (**T**) is considered, and no valid LF-ASD activations are suppressed.

To assess the effect of eye-blinks, the LF-ASD-V4 and LF-ASD-V5 were each evaluated by data from each of the above three cases resulting in six configurations: (1) LF-ASD-V4-Case1, (2) LF-ASD-V4-Case2, (3) LF-ASD-V4-Case3, (4) LF-ASD-V5-Case1, (5) LF-ASD-V5-Case2, (6) LF-ASD-V5-Case3.

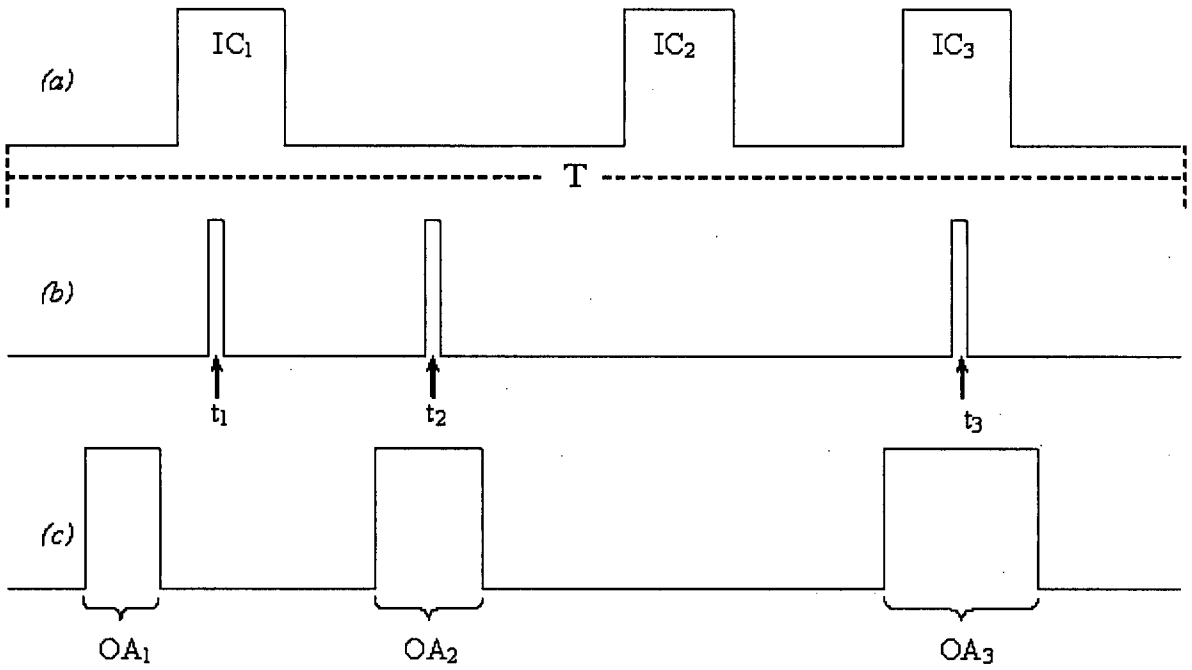

Figure 7.5 (a) Periods of intended control. Total length of experiment, in seconds, is **T**. (b) Timing of LF-ASD activations. (c) Timing of ocular artifacts detected using EOG electrodes, where IC = intentional control, $OA_{1,2,3}$ = ocular artifact periods.

7.3. Results

The performances of all six configurations are summarized via the receiver operating characteristic (ROC) curves (Egan, 1975).

For the LF-ASD-V5 design, different buffer lengths (refer to Section 7.2.1.2) were used to build the classifier. The buffer length that resulted in the best performance for each subject is reported here. Specifically, the buffer lengths tried were 3, 5, 7, 9 and 11.

In Table 7.2, we show the TP rates at fixed FP rates of 1% and 2% for able-bodied and SCI subjects using Case 1 and Case 3 evaluation methods and data (refer to Section 7.2.2). As shown in the last column of this table, the performance of the LF-ASD-V5-Case3 (67.9%) was better than the LF-ASD-V4-Case1 (63.0%) on average for a false positive rate of 2%. However, it should be noted that direct comparison of both the LF-ASD-V4 and LF-ASD-V5 systems with eye-blinks and without eye-blinks using the Case 1 and Case 3 evaluation methods can be misleading. Case 1 only evaluates the system on a portion of the available data and discards the eye-blink contaminated EEG data, whereas Case 3 evaluates the systems on all the available EEG data.

Direct comparison of both designs with eye-blinks and without eye-blinks is only possible if Case 2 and Case 3 evaluation methods are used since both evaluation schemes use all the EEG data (including EEG data containing eye-blinks). As such, Table 7.3 shows the TP rates at fixed FP rates of 1% and 2% for able-bodied and SCI subjects for Case 2 and Case 3. Table 7.3, thus, provides a more rigorous comparison between Case 2 and Case 3.

Table 7.4 shows the true positive (TP) rate change of the LF-ASD-V4 for Case 3 compared to Case 2. As shown in the last column of this table, the TP rate of the LF-ASD-V4 decreases by an average of 8.8% and 9.4% (for FP rates of 1% and 2%, respectively). Table 7.5 shows similar TP rate change in the LF-ASD-V5. In this case, the TP rate of the system decreases by an average of 6.7% and 5.5% (for FP rates of 1% and 2%, respectively), which suggests that the LF-ASD-V5 design performs better than the LF-ASD-V4 design when the EEG data containing eye-blinks are also included in evaluation.

Table 7.6 compares the LF-ASD-V5-Case3 with the LF-ASD-V4-Case2. In two spinal cord injured subjects (LB and BK), the performance of LF-ASD-V5 even with the presence of

eye-blinks are better than LF-ASD-V4 when the output is inactivated during eye-blinks. Overall, as shown in the last column of Table 7.6, the average true positive rate of LF-ASD-V5-Case3 was less than LF-ASD-V4-Case2 by 1.9% and 1.5% for false positive values of 1% and 2%, respectively. Fig. 7.6 summarizes the findings of Tables 7.4 and 7.5 and shows that the performance of the LF-ASD-V5 degrades less than the performance of the LF-ASD-V4 when the data containing eye-blinks are included in the evaluation.

TABLE 7.2 TRUE POSITIVE (TP) RATES AT FIXED FALSE POSITIVE (FP) RATES OF 1% AND 2% FOR BOTH ABLE-BODIED AND SPINAL CORD INJURED SUBJECTS FOR LF-ASD-V4 AND LF-ASD-V5 DESIGNS USING CASE 1 AND CASE 3 EVALUATION METHODS.

Subject		Spinal cord injured					Able-bodied					Overall average
		AJ	LB	BK	RT	Average	ID	CB	CS	KT	Average	
LF-ASD-V4-CASE1	TP (%) at FP=1 %	*42.1*	*35.6*	*27.3*	*36.5*	***35.4***	*45.2*	*40.4*	*46.9*	*23.4*	***39.0***	***37.2***
	TP (%) at FP=2%	64.3	61.1	52.6	65.4	**60.8**	69.9	68.4	73.3	49.1	**65.2**	**63.0**
LF-ASD-V4-CASE3	TP (%) at FP=1 %	*33.6*	*36.2*	*26.7*	*32.3*	***32.2***	*42.7*	*34.3*	*46.7*	*16.6*	***35.1***	***33.6***
	TP (%) at FP=2%	60.7	61.9	52.3	61.2	**59.1**	68.1	62.6	73.3	40.5	**61.1**	**60.1**
LF-ASD-V5-CASE1	TP (%) at FP=1 %	*46.9*	*40.1*	*40.9*	*40.2*	***42.0***	*45.3*	*46.5*	*49.1*	*31.2*	***43.0***	***42.5***
	TP (%) at FP=2%	72.1	68.7	67.4	76.3	**71.1**	67.2	72.0	74.3	53.0	**66.6**	**68.9**
LF-ASD-V5 - CASE3	TP (%) at FP=1 %	*40.0*	*45.7*	*40.3*	*33.5*	***39.9***	*43.5*	*40.8*	*48.5*	*32.1*	***41.2***	***40.5***
	TP (%) at FP=2%	66.9	71.7	66.5	72.4	**69.4**	67.3	68.2	74.2	56.4	**66.5**	**67.9**

The truncated ROC curves for all subjects for LF-ASD-V4 and LF-ASD-V5 and for Case 2 and Case 3 are provided in Figures 7.7-14. As we are interested in lower FP rate levels, only those values of FPs below 3% are shown in the ROC curves. For most of the FP rate levels, the LF-ASD-V5 generated a better TP rate than the LF-ASD-V4. For each figure, corresponding points for LF-ASD-V5-Case 2 and LF-ASD-V5-Case 3 using one set of identical classification parameters are indicated. This is included to highlight in each case whether the difference is due to an increase in true positives, false positives, or both.

TABLE 7.3 TRUE POSITIVE (TP) RATES AT FIXED FALSE POSITIVE (FP) RATES OF 1% AND 2% FOR BOTH ABLE-BODIED AND SPINAL CORD INJURED SUBJECTS FOR LF-ASD-V4 AND LF-ASD-V5 DESIGNS USING CASE 2 AND CASE 3 EVALUATION METHODS.

Subject		Spinal cord injured					Able-bodied					Overall average
		AJ	LB	BK	RT	Average	ID	CB	CS	KT	Average	
LF-ASD-V4-CASE2	TP (%) at FP=1 %	*47.5*	*42.2*	*26.2*	*42.9*	*39.7*	*50.3*	*46.3*	*51.2*	*32.8*	*45.2*	*42.4*
	TP (%) at FP=2%	70.8	68.1	49.9	77.9	**66.7**	70.8	75.2	77.5	65.3	**72.2**	**69.4**
LF-ASD-V4-CASE3	TP (%) at FP=1 %	*33.6*	*36.2*	*26.7*	*32.3*	*32.2*	*42.7*	*34.3*	*46.7*	*16.6*	*35.1*	*33.6*
	TP (%) at FP=2%	60.7	61.9	52.3	61.2	**59.1**	68.1	62.6	73.3	40.5	**61.1**	**60.1**
LF-ASD-V5-CASE2	TP (%) at FP=1 %	*51.8*	*48.1*	*38.8*	*48.6*	*46.8*	*45.8*	*50.4*	*54.7*	*40.0*	*47.7*	*47.3*
	TP (%) at FP=2%	77.1	73.2	59.5	84.0	**73.5**	70.2	76.9	77.8	68.8	**73.4**	**73.4**
LF-ASD-V5-CASE3	TP (%) at FP=1 %	*40.0*	*45.7*	*40.3*	*33.5*	*39.9*	*43.5*	*40.8*	*48.5*	*32.1*	*41.2*	*40.5*
	TP (%) at FP=2%	66.9	71.7	66.5	72.4	**69.4**	67.3	68.2	74.2	56.4	**66.5**	**67.9**

TABLE 7.4 TRUE POSITIVE (TP) RATE (%) CHANGE OF THE LF-ASD-V4 WHEN EYE-BLINKS ARE PRESENT (LF-ASD-V4-CASE3) VERSUS THE ORIGINAL LF-ASD-V4 WHEN THE OUTPUT IS BLOCKED DUE TO EYE-BLINKS (LF-ASD-V4-CASE2)

Subject		Spinal cord injured					Able-bodied					Overall average
		AJ	LB	BK	RT	Average	ID	CB	CS	KT	Average	
TP decrease	FP=1%	-13.9	-6.0	+0.5	-10.6	-7.5	-7.7	-12.0	-4.5	-16.2	-10.1	-8.8
	FP=2%	-10.1	-6.2	+2.4	-16.7	-7.6	-2.7	-12.6	-4.2	-24.8	-11.1	-9.4

TABLE 7.5 TRUE POSITIVE (TP) RATE (%) CHANGE OF THE LF-ASD-V5 WHEN EYE-BLINKS ARE PRESENT (LF-ASD-V5-CASE3) VERSUS THE ORIGINAL LF-ASD-V5 WHEN THE OUTPUT IS BLOCKED DUE TO EYE-BLINKS (LF-ASD-V5-CASE2)

Subject		Spinal cord injured					Able-bodied					Overall average
		AJ	LB	BK	RT	Average	ID	CB	CS	KT	Average	
TP decrease	FP=1%	-11.8	-2.4	+1.5	-15.1	-6.9	-2.3	-9.6	-6.2	-7.9	-6.5	-6.7
	FP=2%	-10.2	-1.5	+7.0	-11.6	-4.1	-2.9	-8.7	-3.6	-12.4	-6.9	-5.5

TABLE 7.6 TRUE POSITIVE RATE (%) CHANGE OF THE LF-ASD-V5 WHEN EYE-BLINKS ARE PRESENT (LF-ASD-V5-CASE3) VERSUS THE ORIGINAL LF-ASD WHEN THE OUTPUT IS BLOCKED DUE TO EYE-BLINKS (LF-ASD-V4-CASE2)

Subject		Spinal cord injured					Able-bodied					Overall average
		AJ	LB	BK	RT	Average	ID	CB	CS	KT	Average	
TP decrease	FP=1%	-7.5	+3.5	+14.1	-9.4	+0.2	-6.8	-5.5	-2.7	-0.7	-3.9	-1.9
	FP=2%	-3.9	+3.6	+16.6	-5.5	+2.7	-3.5	-7.0	-3.3	-8.9	-5.7	-1.5

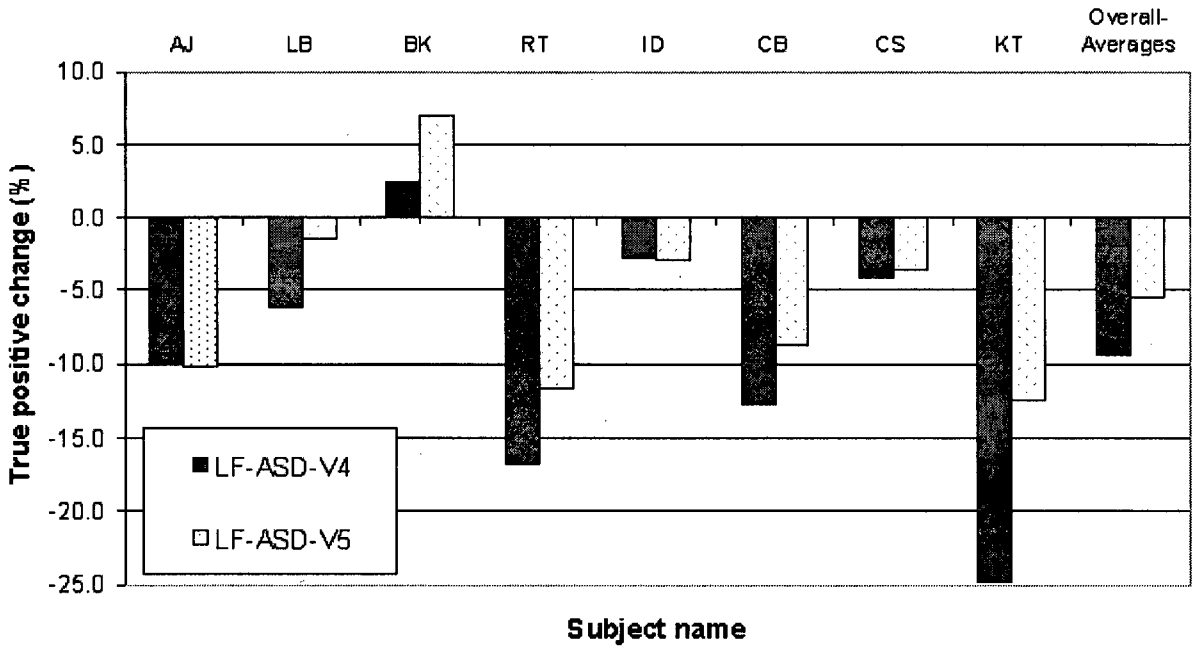

Figure 7.6 True positive rate change (at false positive rate of 2%) of the LF-ASD-V4 and LF-ASD-V5 designs between Case 2 and Case 3 evaluation methods.

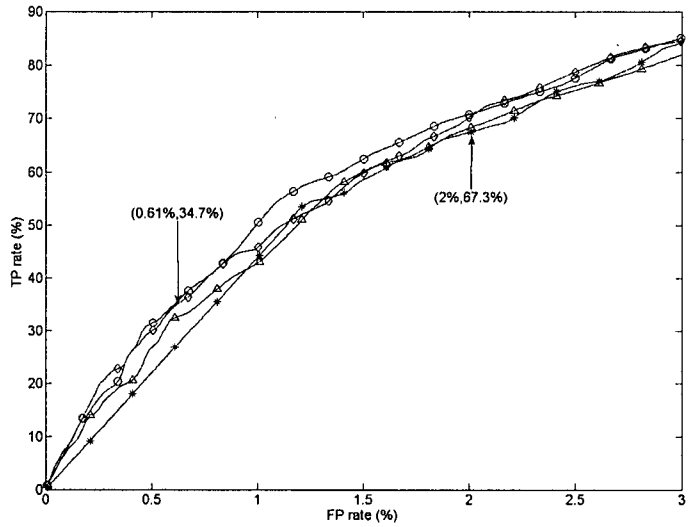

Figure 7.7 Truncated receiver operation characteristic (ROC) curves for subject ID (line with lozenges: LF-ASD-V5-Case2, line with circles: LF-ASD-V4-Case2, line with stars: LF-ASD-V5-Case3, line with triangles: LF-ASD-V4-Case3). As we are interested in lower FP rate levels, only those values of FPs below 3% are shown in the ROC curves. The numbers in the parentheses show the false positive and true positive percentages, respectively, for identical classification parameters for LF-ASD-V5-Case2 and LF-ASD-V5-Case3.

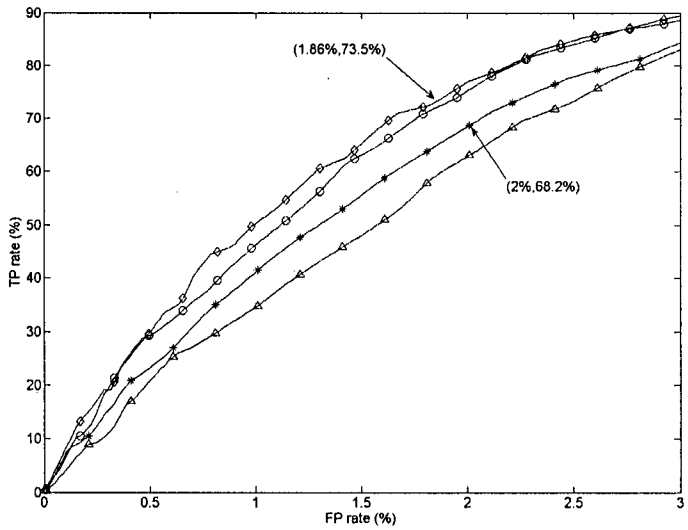

Figure 7.8 Truncated receiver operation characteristic (ROC) curves for subject CB (line with lozenges: LF-ASD-V5-Case2, line with circles: LF-ASD-V4-Case2, line with stars: LF-ASD-V5-Case3, line with triangles: LF-ASD-V4-Case3). As we are interested in lower FP rate levels, only those values of FPs below 3% are shown in the ROC curves. The numbers in the parentheses show the false positive and true positive percentages, respectively, for identical classification parameters for LF-ASD-V5-Case2 and LF-ASD-V5-Case3.

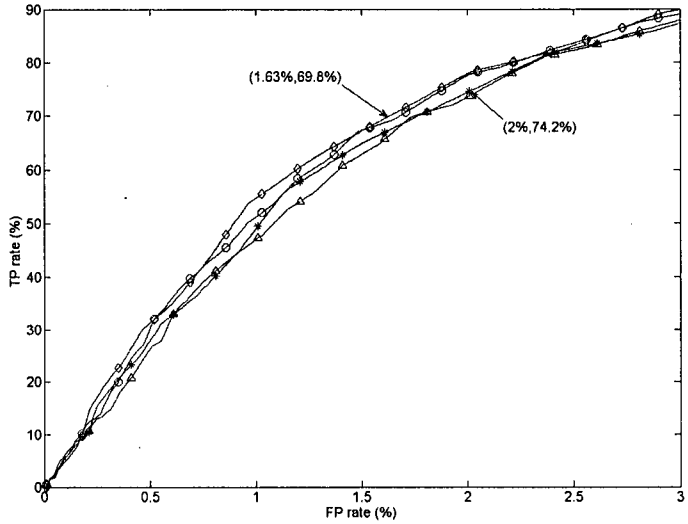

Figure 7.9 Truncated receiver operation characteristic (ROC) curves for subject CS (line with lozenges: LF-ASD-V5-Case2, line with circles: LF-ASD-V4-Case2, line with stars: LF-ASD-V5-Case3, line with triangles: LF-ASD-V4-Case3). As we are interested in lower FP rate levels, only those values of FPs below 3% are shown in the ROC curves. The numbers in the parentheses show the false positive and true positive percentages, respectively, for identical classification parameters for LF-ASD-V5-Case2 and LF-ASD-V5-Case3.

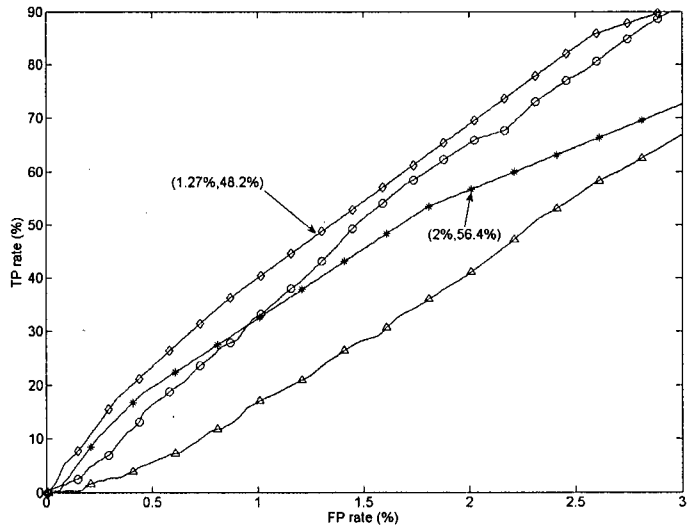

Figure 7.10 Truncated receiver operation characteristic (ROC) curves for subject KT (line with lozenges: LF-ASD-V5-Case2, line with circles: LF-ASD-V4-Case2, line with stars: LF-ASD-V5-Case3, line with triangles: LF-ASD-V4-Case3). As we are interested in lower FP rate levels, only those values of FPs below 3% are shown in the ROC curves. The numbers in the parentheses show the false positive and true positive percentages, respectively, for identical classification parameters for LF-ASD-V5-Case2 and LF-ASD-V5-Case3.

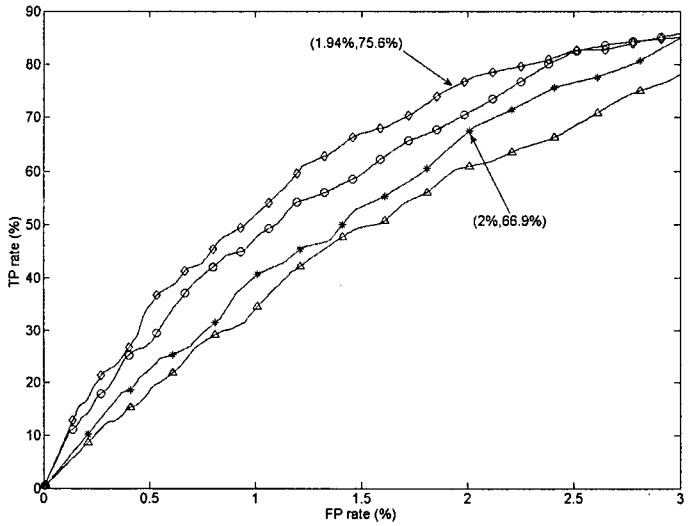

Figure 7.11 Truncated receiver operation characteristic (ROC) curves for subject AJ (line with lozenges: LF-ASD-V5-Case2, line with circles: LF-ASD-V4-Case2, line with stars: LF-ASD-V5-Case3, line with triangles: LF-ASD-V4-Case3). As we are interested in lower FP rate levels, only those values of FPs below 3% are shown in the ROC curves. The numbers in the parentheses show the false positive and true positive percentages, respectively, for identical classification parameters for LF-ASD-V5-Case2 and LF-ASD-V5-Case3.

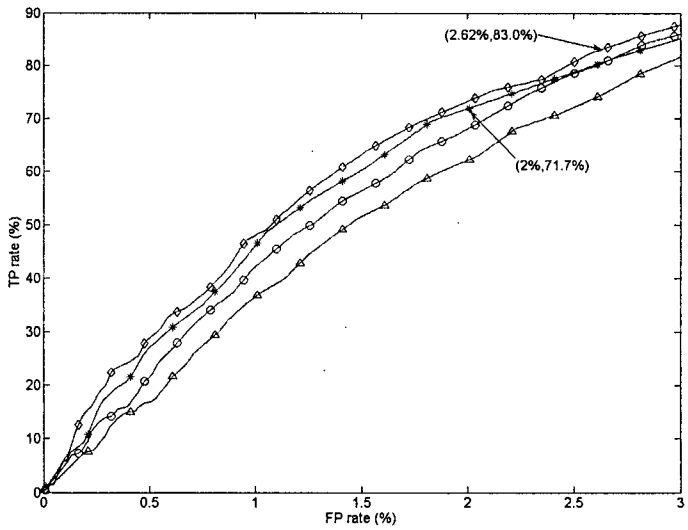

Figure 7.12 Truncated receiver operation characteristic (ROC) curves for subject LB (line with lozenges: LF-ASD-V5-Case2, line with circles: LF-ASD-V4-Case2, line with stars: LF-ASD-V5-Case3, line with triangles: LF-ASD-V4-Case3). As we are interested in lower FP rate levels, only those values of FPs below 3% are shown in the ROC curves. The numbers in the parentheses show the false positive and true positive percentages, respectively, for identical classification parameters for LF-ASD-V5-Case2 and LF-ASD-V5-Case3.

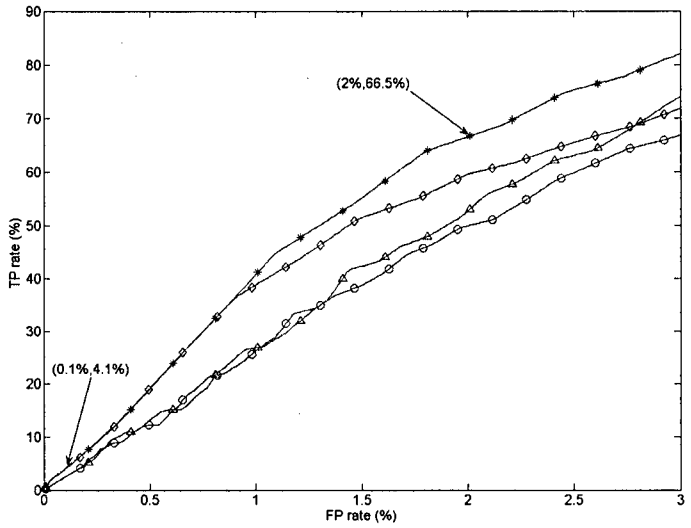

Figure 7.13 Truncated receiver operation characteristic (ROC) curves for subject BK (line with lozenges: LF-ASD-V5-Case2, line with circles: LF-ASD-V4-Case2, line with stars: LF-ASD-V5-Case3, line with triangles: LF-ASD-V4-Case3). As we are interested in lower FP rate levels, only those values of FPs below 3% are shown in the ROC curves. The numbers in the parentheses show the false positive and true positive percentages, respectively, for identical classification parameters for LF-ASD-V5-Case2 and LF-ASD-V5-Case3.

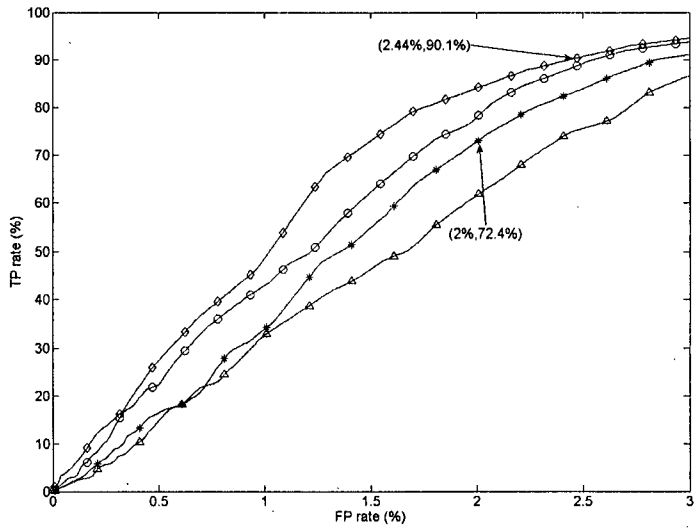

Figure 7.14 Truncated receiver operation characteristic (ROC) curves for subject RT ((line with lozenges: LF-ASD-V5-Case2, line with circles: LF-ASD-V4-Case2, line with stars: LF-ASD-V5-Case3, line with triangles: LF-ASD-V4-Case3). As we are interested in lower FP rate levels, only those values of FPs below 3% are shown in the ROC curves. The numbers in the parentheses show the false positive and true positive percentages, respectively, for identical classification parameters for LF-ASD-V5-Case2 and LF-ASD-V5-Case3.

7.4. Discussion

We have studied the performance of two self-paced brain interface designs when data containing eye-blinks are not excluded from analysis. The performance of the system for the case when data contaminated with eye-blinks are totally excluded from analysis were already known. Furthermore, we have evaluated the system's performance in a pseudo-online testing paradigms (Case 2 and Case 3 testing paradigms, refer to Section 7.2.3). The average true positive rate of LF-ASD-V5 when eye-blinks are included in the analysis degrades slightly (1.9% and 1.5% at false positive rate of 1% and 2%, respectively) compared to when the output was inactivated due to the presence of eye-blink artifacts in LF-ASD-V4.

As shown in Tables 7.2 and 7.3, the systems that inactivate the output during eye-blinks (Case 2) seem to perform better than the systems that exclude eye-blink contaminated data from analysis (Case 1). However, direct comparison of the systems using Case 1 and Case 2 evaluation methods is misleading, as the amount of data that are evaluated is different between them. Specifically, Case 1 evaluation method excludes eye-blink contaminated data from analysis and thus evaluates the system using only a portion of the data. In fact, excluding data (as in Case 1) is not even possible for on-line systems, and thus Case 1 cannot be used to analyze them. Such comparison between Case 1 and Case 3 is also misleading for the same reason mentioned above. However, inactivating the system's output during artifacts (as in Case 2) is possible, and thus it is best to compare Case 2 and Case 3, and not Case 1 and Case 3.

The results in Tables 7.4 and 7.5 show that although we have not inactivated the output due to eye-blinks, the system (the LF-ASD-V5-Case3) is performing worse than the case in which we inactivated the output due to eye-blinks (the LF-ASD-V5-Case2). This decrease in performance was much higher for LF-ASD-V4. This suggests that LF-ASD-V5 performs better than LF-ASD-V4 on the data that contain eye-blinks. As shown in Table 7.6, comparing LF-ASD-V5-Case3 with LF-ASD-V4-Case2 shows that the true positive rate decreases slightly with the addition of eye-blink contaminated data. As shown in the second row of Table 7.1, during 15-34% of the total available time, the subject was 'not allowed' to control the output of the system due to the presence of eye-blinks. Using the LF-ASD-V5-Case3 not only provides full control of the system at all times but also does not have any

significant impact on the performance of the subjects (only about 1.5%-1.9% average decrease in true positive rate) compared to the LF-ASD-V4-Case2.

A close examination of the ROC curves revealed an interesting point. When evaluating the performance of both the LF-ASD-V4 and LF-ASD-V5 systems, we expected to see a performance decrease or no change when EEG data containing eye-blinks were present (Case 3) compared to Case 2 when the output is inactivated (blocked) due to the presence of eye-blinks. In one subject, (BK), we noticed that the system performed even better when EEG data containing eye-blinks were present (Case 3). There are two possible causes for such a phenomenon:

(1) In Case 2, activations during some of the trials are blocked due to the presence of eye-blinks. Since in Case 3 no activations are blocked, the system may detect the previously blocked trials successfully even though they are contaminated with eye-blinks;

(2) In some cases, eye-blinks may actually trigger the system in the TEM window and be considered a true positive, even though the output is not activated by a real movement related potential (MRP) pattern.

For this subject, we specifically analyzed and investigated the system's output on a single trial basis for Case 2 and Case 3. As reported in Table 7.1, the output associated with 19% of the no-control (NC) data of this subject were inactivated (blocked) due to the presence of eye-blinks in Case 2. Note, however, that when these data were included in the analysis (Case 3), only a very small number of false positives appeared and this in fact caused a better overall performance of LF-ASD-V5-Case3 compared to LF-ASD-V5-Case2 for subject BK. In addition, we noted that 12 of the 76 previously rejected artifact-contaminated trials (intended control; IC) were correctly detected when data containing eye-blinks were included in the analysis. However, we are not sure whether these trials were detected due to eye-blink activity or the real intended movements. This is an issue that needs to be investigated in future studies.

In summary, this study evaluates two self-paced BIs in a pseudo-online testing paradigm, which was not the case before. Results show a slight decrease in the true positive rate of the LF-ASD-V5 design when the output during eye-blink artifacts is not inactivated compared to the LF-ASD-V4 design when the output is inactivated during eye-blinks. More importantly,

the system is available all the time, while in the previous design, it is unavailable for 15-34% of the time. Future studies will investigate the performance of such a system in an online testing paradigm.

LF-ASD was chosen for this study because so far it has the ability to generate less false positive rates than other BI designs. Our paper evaluates two different designs of the LF-ASD. The LF-ASD-V5 design utilizes all knowledge about the past values of feature vectors, thus it is more immune to eye-blink artifacts than the LF-ASD-V4 design. The implication of our findings is that in designing brain interfaces in general, incorporating the path of feature vectors is an effective way to increase the availability of the overall system without greatly reducing its performance in the presence of eye blink artifacts. In fact, this has implications for other BI designs and pattern recognition problems.

7.5. References

Bashashati A, Fatourechi M, Ward R and Birch G 2006a User Customization of the Feature Generator of an asynchronous Brain Interface *Annals of Biomedical Engineering* **34** 1051-60.

Bashashati A, Mason S G, Ward R K and Birch G E 2006b An Improved Asynchronous Brain Interface: Making Use of the Temporal History of the LF-ASD Feature Vectors *Journal of Neural Engineering* **3** 87-94.

Birch G E, Lawrence P D and Hare R D 1993 Single trial processing of event related potentials using outlier information. *IEEE Trans. Biomed. Eng.* **40** 59–73.

Borisoff J F, Mason S G, Bashashati A and Birch G E 2004 Brain Computer Interface (BCI) Design for Asynchronous Control Applications: Improvements to the LF-ASD Asynchronous Brain Switch. *IEEE Trans. Biomed. Eng.* **51** 985-92.

Egan J P 1975 Signal Detection Theory and ROC Analysis (New York: Academic Press).

Graimann B, Huggins J E, Levine S P and Pfurtscheller G 2004 Toward a direct brain interface based on human subdural recordings and wavelet-packet analysis *IEEE Trans. Biomed. Eng.* **51** 954-62.

Levine S P, Huggins J E, Bement S L, Kushwaha R, Schuh L A, Rohde M M, Passaro E A, Ross D A, Elisevich K V and Smith R J 2000 A direct brain interface based on event-related potentials *IEEE Trans. Rehab. Eng.* **8** 180–5.

Mason S G and Birch G E 2000 A Brain-Controlled Switch for Asynchronous Control Applications *IEEE Trans. Biomed. Eng.* **47** 1297-307.

Mason S G, Bohringer R, Borisoff J F and Birch G E 2004 Real-time control of a video game with a direct brain--computer interface *Clin. Neurophysiol.* **21** 404-8.

Mason S G, Bashashati A, Fatourechi M, Navarro K F and Birch G E 2007 A Comprehensive Survey of Brain Interface Technology Designs *Annals of Biomedical Engineering* **35** 137-69.

Millan J R and Mourino J 2003 Asynchronous BCI and local neural classifiers: An overview of the adaptive brain interface project *IEEE Trans. Neural Syst. Rehab. Eng.* **11** 159–61.

Nicolelis M A 2003 Brain-machine interfaces to restore motor function and probe neural circuits *Nat. Rev. Neurosci.* **4** 417– 22.

Scherer R, Muller G R, Neuper C, Graimann B and Pfurtscheller G 2004 An asynchronously controlled EEG-based virtual keyboard: improvement of the spelling rate *IEEE Trans. Biomed. Eng.* **51** 1979-84.

Townsend G, Graimann B and Pfurtscheller G 2004 Continuous EEG classification during motor imagery--simulation of an asynchronous BCI *IEEE Trans. Neural Syst. Rehab. Eng.* **12** 258-65.

Vaughan T M 2003 Guest editorial brain-computer interface technology: a review of the second international meeting *IEEE Trans. Neural Syst. Rehab. Eng.* **11** 94-109.

Wolpaw J R, Birbaumer N, McFarland D J, Pfurtscheller G and Vaughan T M 2002 Brain-computer interfaces for communication and control *Clin. Neurophysiol.* **113** 767-91.

Yom-Tov E and Inbar G F 2003 Detection of movement-related potentials from the electro-encephalogram for possible use in a brain-computer interface *Med. Biol. Eng. Comput.* **41** 85–93.

Chapter 8 Towards Development of a 3-State Self-Paced Brain Interface Based on Hand Extension Movements [21]

8.1. Introduction

Brain computer interface (BCI) systems form a possible alternative communication and control solution for individuals with severe disabilities. For a review of the field, see (Mason et al 2007, Wolpaw 2004). In BCI systems, the user's cortical activity associated with an intentional control of a device (such as attempted finger movements) is directly mapped to an application-specific control signal. This allows the user to control various devices such as a neural prosthetic by cognitive processes only, i.e., by bypassing traditional interface pathways (which cannot be used by individuals with severe disabilities).

In developing non-invasive BCI systems, the majority of research has concentrated on developing synchronous systems. These systems are only operational at specific periods. Asynchronous (self-paced) systems on the other hand have the advantage of being operational at all times. The 2-state Low Frequency-Asynchronous Switch Design (LF-ASD) was the first BCI introduced for self-paced or asynchronous control applications (Mason and Birch 2000). LF-ASD seeks to recognize the movement related potentials (MRPs) of a *finger flexion movement* in the EEG signal. As a self-paced BCI, it is activated only when a user intends control. In such instances, the user is said to be in an intentional control (IC) state. The system maintains an inactive state output when a user is not intending to control the device (i.e., the user may be idle, relaxed, thinking about a problem, or performing some other action). This state is called the No Control (NC) state. In fact, the NC state includes all mental states except for the IC state.

Like LF-ASD, the 2-state BCI systems tested in (Levine et al 2000, Townsend et al 2004, Yom-Tov and Inbar 2003) attempt to detect an intentional control state from the ongoing brain signal in a self-paced manner. The 3-state self-paced BCI implemented in (Scherer et al 2004) attempts to differentiate between right hand, left hand and foot movements to operate a virtual keyboard. However, this BCI requires the subject to constantly engage in control

[21] A version of this chapter has accepted for publication. Bashashati A., Ward R., and Birch G. (2007) Towards Development of a 3-State Self-Paced Brain Interface Based on Hand Extension Movements *J Computational Intelligence & Neuroscience,* In press.

without the option of going to the no control (NC) state. In a recent work, Scherer et al (Scherer et al 2007) has proposed a 4-state self-paced BCI that has mean true positive and false positive rates of 28.4% and 16.9%, respectively. In the study of (Millan et al 2004) the subjects were asked to perform one of the following three actions: (1) imagine right hand movement, (2) imagine left hand movement, and (3) relax. A 3-state self-paced BCI was designed to navigate a mobile robot in an 80cm*60cm house-like environment by differentiating amongst these three states. The system generates 'unknown state output' when there is not enough confidence in choosing one of the three above mentioned mental tasks. The classifier of this system was *not explicitly* trained to recognize idle (NC) state (Millan et al 2004). According to the authors, it could process them adequately by responding 'unknown'. It was also reported that the task of steering the robot between rooms was so engaging that the two tested subjects preferred to emit continuously mental commands *rather than to go through idle state*. Therefore, the response of this system on NC (idle) state was evaluated on a dataset with limited amount of idle-state. Moreover, having the choice of 'unknown state output' may represent some neutral output but it is not clear whether the unknown state output was caused by the actual idle (NC) state or by lack of confidence in detecting one of the three commands. Additionally, there is no evidence that the NC state will fall into the unknown state in these designs.

In this paper, a non-invasive 3-state self-paced BCI system is proposed. This system is the first multi-class BCI that is (a) designed specifically to support the NC state EEG signal (refer to Chapter 1 for definition of NC support), and (b) has a higher true positive rate at a considerably lower false positive rate (FP=1%) compared to existing 3-state and 4-state self-paced BCIs (Scherer et al 2007) that support the NC state. Unlike the 2-state self-paced system which detects the presence of a single movement from the ongoing EEG signal, the 3-state self-paced BCI design aims at detecting two different movements. Fig. 8.1 shows examples of outputs of the 2-state and 3-state self-paced BCIs. Overall, a 2-state self-paced BCI is in an inactive state (NC state) for most of the time and is in an IC state when a specific brain state (e.g. finger flexion movement) is detected in the brain signal. Unlike a 2-state self-paced BCI which has only one active (IC) state, a 3-state BCI has two active state outputs, IC1 and IC2, which are activated by two different brain states (e.g. right and left hand extensions). While a 2-state self-paced BCI can provide the user with the option of executing

only one command (e.g. turn right), a 3-state system gives the user two command options (e.g. turn right or turn left). This has the advantage of giving the user more control options.

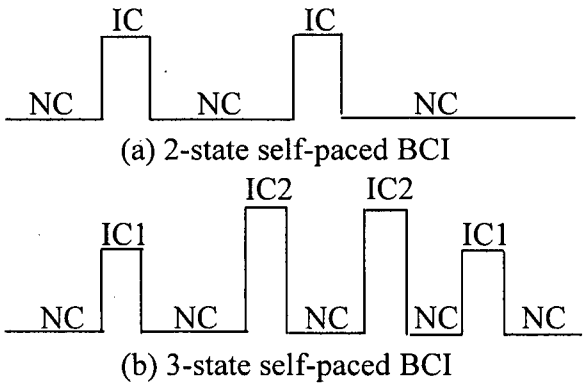

Figure 8.1 Samples of outputs of 2-state and 3-state self-paced BCIs, where NC = No Control state, IC = Intended Control state

The 2-state self-paced BCI (LF-ASD) in (Mason and Birch 2000) aimed at detecting attempted right finger flexions. Recent studies with the 2-state LF-ASD have demonstrated that this system correctly detects the presence of a movement (true positive (TP) rate) in 41% and 42% of the cases for able-bodied and spinal cord injured subjects, respectively (Bashashati et al 2006b). This is when the parameters were set so that the false positive rate is fixed at 1%. The TP rate of the system improves at higher FP rates, e.g. at an FP rate of 5%, the TP rate is almost 100%. Despite these encouraging results, our experience indicates that even a 1% false positive rate is too high for most practical self-paced control applications.

In the process of designing a three-state self-paced brain computer interface, it is prudent to investigate different movements (as neurophysiologic sources of activating a BCI) so as to find the movements that generate more differentiable patterns in the EEG. More differentiable patterns would make it easier for a BCI system to detect IC states and may yield improvements in the performance of the system. Many studies by the neurophysiologic research community have explored the effects of different movements on the EEG signal. These studies show that movements which involve more parts of the body (e.g. hand movement) or movements that need more effort (e.g. finger extension) generate more

differentiable patterns in the ongoing EEG signal than for example natural finger flexions (Stancak and Pfurtscheller 1996, Slobounov et al 2002, Yue et al 2000). It has also been reported that right and left movements (regardless of the type of movement) generate movement-specific patterns in different locations of the brain (Pfurtscheller and Lopez da Silva 1999). As our aim is to use movements that generate more differentiable patterns, based on the evidence in (Stancak and Pfurtscheller 1996, Slobounov et al 2002, Yue et al 2000, Pfurtscheller and Lopez da Silva 1999) we choose, the right hand and the left hand *extensions* in this study since a) hand movements involve more parts of the body than for example finger movements, b) extensions movements need more effort to execute compared to flexion movements and c) right and left movements generate movement-specific patterns in different locations of the brain. We speculate that these two movements generate more discriminative patterns than a finger flexion does. If that is the case, then using these movements would improve our BCI's performance in detecting the presence of a movement. To our best knowledge, the right and the left hand extension movements have not yet been studied in the context of BCI systems.

This paper reports on the preliminary results of a pilot study that investigates the feasibility of a 3-state 'self-paced' brain computer interface system whose aim is the detection of right and left hand extension movements in a self-paced manner. To our best knowledge, this system the first 3-state self-paced BCI that is specifically designed to support the no control (NC) state as well as two additional control options for the user.

Two consecutive detectors were designed to detect the presence of the left or the right hand extensions from the ongoing EEG. The first detector, DET1, determines whether or not a movement is present. If such a movement is detected then the second detector, DET2, classifies the movement as a right or a left hand extension.

Two designs of a 3-state self-paced BCI are proposed and implemented. Power spectral density and a specific template matching method (Mason and Birch 2000) are used in the feature extraction stages, and the k-nearest neighbour and linear discriminant analysis (LDA) classifiers are used in the classification stages.

The performances of the designs are evaluated using EEG recordings of right and left hand extension movements of four able-bodied individuals. The goals of this paper are two fold:

(1) to perform an initial investigation of the performance of the system as a 2-state self-paced BCI, i.e., detecting whether a left or a right hand movement (regardless of the type of movement) has occurred. If the performance of the system in detecting any such movement is better than detecting the previously used movement (i.e., the right finger flexion), then such these movements can be used in other 2-state self-paced brain computer interface designs.

(2) to introduce and carry out an initial evaluation of two possible designs of a 3-state self-paced BCI and to investigate whether a 3-state self-paced brain computer interface that handles the general no control (NC) state has promise.

In Sections 2 and 3 of this paper, the experimental paradigm, the structure of the proposed designs and the evaluation method are presented. The results and conclusions are discussed in Sections 4 and 5, respectively.

8.2. Experimental paradigm

The EEG data used in this study were recorded from 15 mono-polar electrodes positioned over the supplementary motor area and the primary motor cortex (defined with reference to the International 10-20 System at F1, F2, F3, F4, Fz, FC1, FC2, FC3, FC4, FCz, C1, C2, C3, C4, and Cz). Electro-oculographic (EOG) activity was measured as the potential difference between two electrodes, placed at the corner and below the right eye. The ocular artifact was considered present when the difference between the EOG electrodes exceeded +/-25μv, a threshold level similar to the one used in previous studies (Borisoff et al 2004, Mason and Birch 2000). All signals were sampled at 128 Hz. This study has been approved by the Behavioral Research Ethics Board (BREB) of the University of British Columbia.

Four able-bodied subjects participated in this study. All subjects were male (except subject 4), right handed (except subject 4) and 25-30 years old. Subjects were seated 150 cm in front of a computer monitor. The data were collected while the subjects were performing a guided task. At random intervals of 5.6-7s (mean of 6.7 s), a target window was displayed on the subject's monitor. As shown in Fig. 8.2, a box moved from the right side to the left side of the screen. When the box reached the target window, the subject attempted to activate the custom-made switch by extending his/her right or left hand. The length of the target window was more than the length of the moving box and the subjects were free to activate the switch any time they want while the box is inside the target window. An arrow in the moving box,

pointing to the left or the right showed the subject whether to move the right or the left hand. *In the NC period, i.e. the time between the subject activates the switch and the next opportunity to activate the switch, the subject were free to perform any mental task except the two predefined movements.* For each subject, an average of 150 trials for each movement was collected in two sessions carried in the same day.

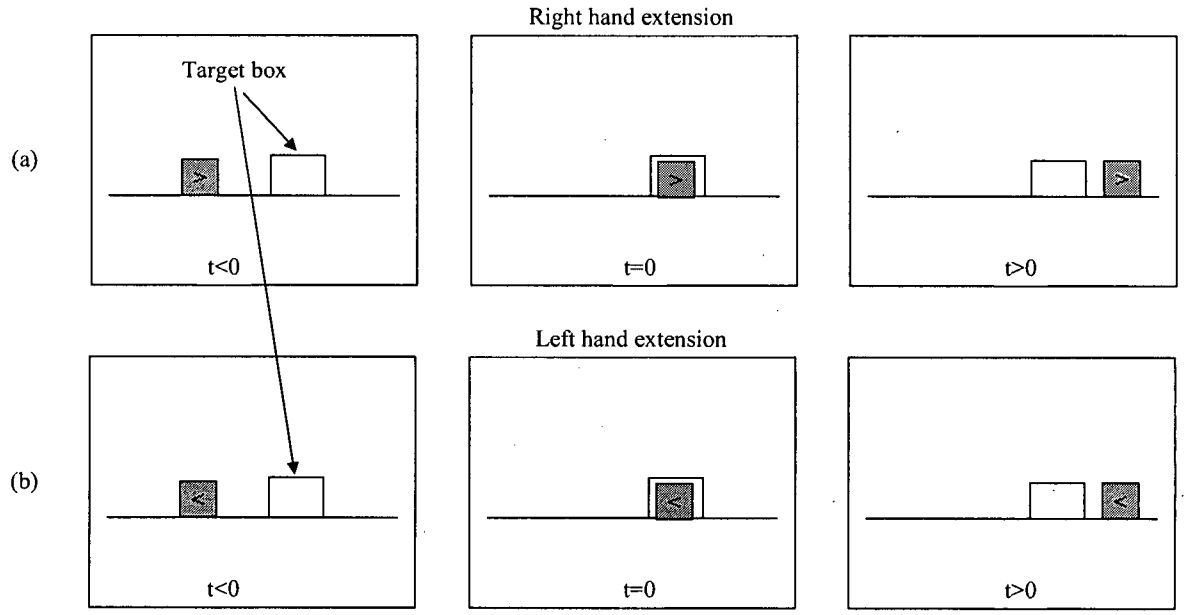

Figure 8.2 Screen contents for each of the right hand (a) and left hand (b) extension movement trials, t=0 is the time of movement execution.

8.3. Proposed 3-state self-paced Brain computer interface

Fig. 8.3 shows the overall structure of the proposed designs. These designs include two major blocks:

a) "*Detector 1*" which determines whether or not a movement is performed, and

b) "*Detector 2*" which determines whether the detected movement is a right hand or a left hand extension. In this study, two different designs for Detector 1 and one design for Detector 2 have been proposed and evaluated. The details of both detectors are explained below. Detectors 1 and 2 are referred to as DET1 and DET2.

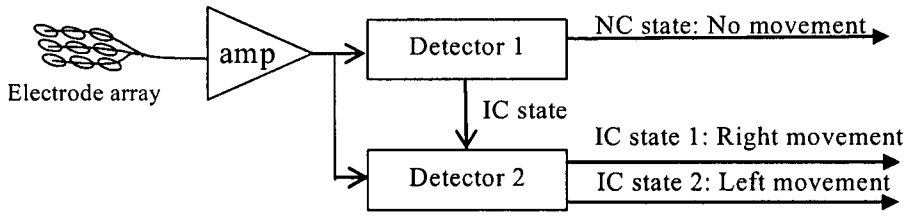

Figure 8.3 Structure of the 3-state self-paced brain computer interface design

8.3.1. Detector 1

Two different designs for DET1 are proposed and compared. These are referred to as DET1-LF-1NN and DET1-PSD-LDA.

DET1-LF-NN uses one of the latest designs of the LF-ASD (Bashashati et al 2006a) as shown in Fig. 8.4.a. It employs features extracted from the 0-4Hz band in six bipolar EEG channels (defined with reference to the International 10-20 System at F1-FC1, Fz-FCz, F2-FC2, FC1-C1, FCz-Cz, and FC2-C2). After amplification, a low-pass FIR filter (0-4Hz) is used to decrease the interference with the features in the high-frequency band.

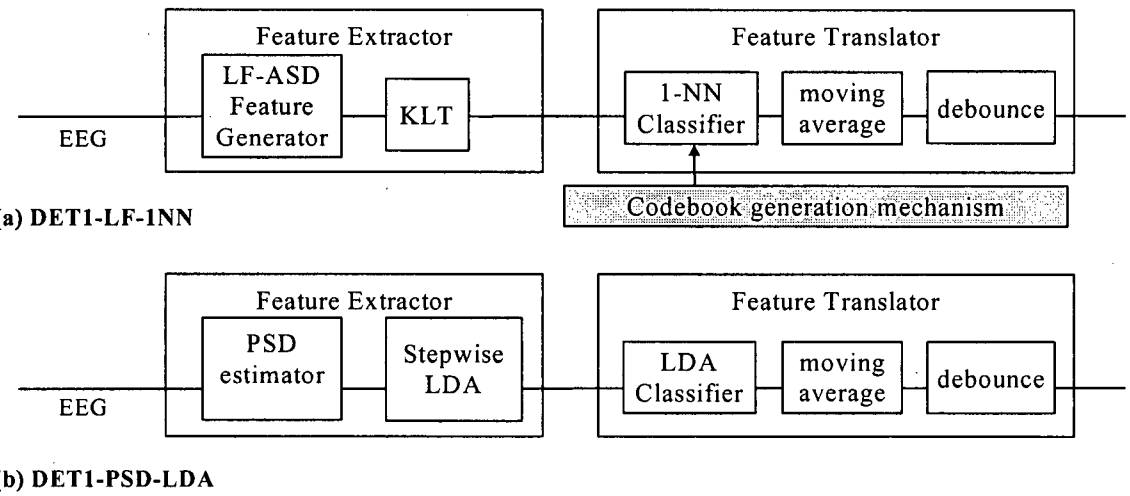

Figure 8.4 Structure of the two designs of DET1, where KLT = Karhunen-Loève Transform, and 1-NN = 1-Nearest Neighbour, PSD = power spectral density, and LDA: linear discriminant analysis.

Previous studies show that when a movement is performed, a bipolar pattern similar to the one shown in Fig. 8.5 is generated in the ongoing EEG (Mason and Birch 2000). A specific template matching algorithm based on the one employed in (Mason and Birch 2000) is implemented. This algorithm generates large feature values when there is such a pattern in the spontaneous EEG. The delay parameters α_i and α_j, shown in Fig. 8.5, determine the locations of the peaks of the pattern that need to be detected. Thus, these delay parameters need to be properly determined in order to detect the presence of a specific movement. For each subject, the ensemble averages of the EEG around the movements of the training data are generated and then used to determine the values of α_i and α_j according to the method presented in (Bashashati et al 2006a). Table 8.1 shows the estimated values of α_i and α_j for each subject. This feature extraction procedure is repeated for each of the six bipolar channels. The resulting feature vector is a six-dimensional vector, with each dimension reflecting the value of the feature in each channel.

TABLE 8.1 ESTIMATED α_i AND α_j PARAMETERS FOR EACH SUBJECT. NOTE ALL VALUES ARE IN MILLISECONDS.

	Subject1	Subject2	Subject3	Subject4
α_i	125	195	398	195
α_j	578	141	297	313

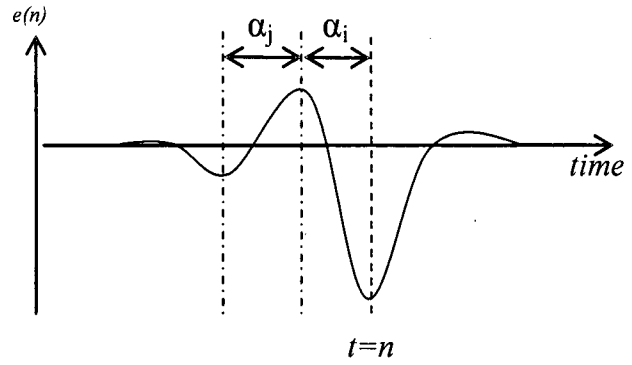

Figure 8.5 Description of delay terms (α_i, α_j), where e(n) is the amplitude of the bipolar signal

The Karhunen-Loève Transform (KLT) component is used to reduce the 6-dimensional feature vector to a 2-dimensional feature vector. A 1-NN (1-nearest neighbour) classifier is used as the feature classifier. Finally, a moving average (with length of 39ms) and a debounce block (with length of 125ms) are employed to further improve the classification accuracy of DET1 by reducing the number of false activations (for details, see (Borisoff et al 2004, Mason and Birch 2000]). DET1 classifies the input patterns, at every 1/16th of a second, to one of the two classes, No Control (NC) or Intentional Control (IC) states.

The second design of DET1 (referred to as DET1-PSD-LDA) is shown in Fig. 8.4.b. It extracts the power spectral density features of the EEG from a group of bipolar EEG channels and then selects the most informative channels for classification. Specifically, thirty bipolar combinations of EEG channels that may contribute to the detection of movements were generated. These bipolar EEG channels were Cz-C1, Cz-C2, Cz-C3, Cz-C4, C1-C2, C1-C4, C1-C3, C2-C3, C2-C4, C3-C4, FCz-Cz, FC1-C1, FC2-C2, FC3-C3, FC4-C4, Fz-FCz, F1-FC1, F2-FC2, F3-FC3, F4-FC4, FCz-FC1, FCz-FC2, FCz-FC3, FCz-FC4, FC1-FC2, FC1-FC4, FC1-FC3, FC2-FC3, FC2-FC4, FC3-FC4. These bipolar channels were chosen to capture possible discriminatory information between left and right and also between frontal and central areas of the head. In the feature extraction block, the power spectral density (PSD) components of each of the 30 bipolar EEG channels are calculated in each frequency bin from 1Hz to 25Hz using Welch's Periodogram method (Welch 1967) with window length of one second (equivalent to 128 samples). This results in 25 frequency components for each of the 30 bipolar channels and a total of 25*30 features at each time instant. We then use stepwise linear discriminant analysis (stepwise LDA) (Lachenbruch 1975) to find the most informative features that better discriminate between IC and NC classes. Stepwise LDA is a method that results in a linear combination of selected features that contribute to the classification and omits the features that have redundant information for discrimination. Once the features are extracted and selected, a linear discriminant classifier (LDA) (Lachenbruch 1975) is used for classification. Other details about the other components of the feature translator (moving average and debounce blocks) are the same as in DET1-LF-1NN above.

8.3.2. Detector 2

Existing studies show that the cortical activation related to movement preparation and execution desynchronizes the Mu (8-12Hz) rhythm and increases the Beta (13-25Hz) rhythm of the EEG. These phenomena are known as event related desynchronization (ERD) and event related synchronization (ERS), respectively (Pfurtscheller and Aranibar 1979, Pfurtscheller and Lopez da Silva 1999). The ERD of a hand movement is more prominent over contralateral sensorimotor areas during motor preparation and extends bilaterally after movement initiation (Pfurtscheller et al 1997, Pfurtscheller and Lopez da Silva 1999). Some studies however show that the frequency bands of the ERD and ERS patterns are variable from subject to subject (Pregenzer and pfurtscheller 1999).

As shown in Fig. 8.6, DET2 which aims at differentiating between right and left hand movements is similar to the second design of DET1 (DET1-PSD-LDA), except that it does not have the averaging and debounce blocks of DET1. This design intends to extract subject specific ERD/ERS frequency bands that lead to more discrimination between the two classes, i.e., the left and right hand movements. As in DET1, the stepwise linear discriminant analysis (LDA) method is employed to select the subject specific ERD/ERS frequency bands and bipolar EEG channels. We have evaluated a similar design of DET2 when the inputs were mono-polar EEG channels. Preliminary analysis of the data shows that using bipolar electrodes yield better performances. As such, we used bipolar electrodes as input to the system and did not further evaluate the overall performance of the 3-state brain computer interface using mono-polar electrodes.

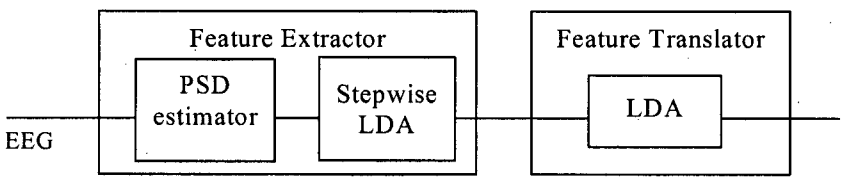

Figure 8.6 Structure of DET2-PSD-LDA, where PSD = power spectral density, and LDA = linear discriminant analysis.

Two designs of a 3-state self-paced BCI system are evaluated. The first design uses combination DET1-LF-1NN and DET2-PSD-LDA and the second one uses the combination DET1-PSD-LDA followed by DET2-PSD-LDA.

8.4. Evaluation

The designed 3-state self-paced BCI first detects whether or not a movement is performed. If a movement is detected, then the system classifies it as one of two classes, the right hand (IC1) or the left hand (IC2) extension classes. If the system does not detect a movement, the output reports an inactive state.

We use a 5-fold stratified cross-validation method to evaluate the performance of the proposed 3-state self-paced BCI. The ability of the subjects to control the 3-state BCI system is evaluated using three performance measures. At a fixed false positive rate, these measures report the correct detection rates of the right and the left hand extensions (from the ongoing EEG), respectively. These three measures are:

(1) the percentage of correct right hand movement detection during IC states (i.e., the true positive rate for right hand movement, TP_R) calculated using equation (1) below:

TP_R = (number of correctly detected right movements)/(total number of right movements) (1)

(2) the percentage of correct left movement detection during IC states (true positives of left hand movements, TP_L) calculated using equation (2) below:

TP_L = (number of correctly detected left movements)/(total number of left movements) (2)

(3) the percentage of false switch activations during NC states (false positives, FPs) calculated using equation (3) below:

FP = (number of false activations)/(total number of the systems' decisions during NC state) (3)

Note that the system makes a decision every $1/16^{th}$ of a second.

A TP is identified if the BCI system is activated at least once in a response window, i.e., a time window spanning 0.25 seconds before the time of movement till 0.5 seconds after it, a method similar to that employed in (Birch et al 1993, Graimann et al 2004, Mason and Birch

2000, Townsend et al 2004, Yom-Tov and Inbar 2003). FPs are assessed in the periods outside the response window as explained above. Periods during which ocular artifacts occurred are blocked from analysis.

We also report the overall true positive and false positive rates of DET1 (regardless of the type of movement). We refer to these measures as TP_{IC} and FP_{IC}. The TP_{IC} is the percentage of correct detection of a movement whether it is a right hand or a left hand one. Thus it reflects the performance of the system if used as a 2-state self-paced BCI. We report this measure to compare the findings of this study with our latest 2-state self-paced BCI as stated in goal (1) of this study.

5. Results

The performance of DET1 (TP_{IC}) in detecting the presence of hand movements, regardless of the type of movement, from the background EEG is shown in Table 8.2. This table shows the TP rates at a fixed FP rate of 1% for the two designs of DET1. As we are interested in low false positive rates, we do not report the performance of the system for higher false positive rates. For higher false positive rates (e.g. FP>3%) the true positive rate is almost 100%. As shown in the last column of Table 8.2, the average performance of DET1-LF-1NN is slightly better than DET1-PSD-LDA. Except for subject 2 for which DET1-PSD-LDA significantly outperforms DET1-LF-1NN, for the rest of the subjects DET1-LF-1NN yields higher true positives rates.

Table 8.3 shows the performance of the whole 3-state self-paced BCI for the two proposed designs (i.e., <DET1-LF-1NN + DET2-PSD-LDA> and <DET1-LF-1NN + DET2-PSD-LDA>) at a fixed false positive rate of 1%.

TABLE 8.2 PERCENTAGE OF TRUE POSITIVES (TP_{IC}) AT FIXED FALSE POSITIVE RATE OF 1% FOR THE TWO DESIGNS OF DET1

DET1 Design	Subject1	Subject2	Subject3	Subject4	Average
DET1-LF-1NN	50.1	38.4	56.5	71.0	54.0
DET1-PSD-LDA	38.2	54.7	60.2	60.3	53.4

On average, 36% of the right and left hand extensions of the 4 subjects are correctly identified by the 3-state <DET1-PSD-1NN + DET2-PSD-LDA> design (for a false positive rate of 1%). As shown in Table 8.3, <DET1-LF-1NN + DET2-PSD-LDA> outperforms <DET1-PSD-LDA + DET2-PSD-LDA> in three of the tested subjects. A close analysis of the results shows that for subject2, <DET1-PSD-LDA + DET2-PSD-LDA> performs significantly better than the other design. For this subject, 35.6% and 47% of the right and left hand extensions are correctly differentiated from the no control (NC) state.

TABLE 8.3 PERCENTAGE OF RIGHT AND LEFT TRUE POSITIVES (TP_R AND TP_L) OF THE TWO PROPOSED 3-STATE BRAIN COMPUTER INTERFACES (WHEN FALSE POSITIVE RATE IS SET AT 1%) . THE TP_R AND TP_L VALUES OF THE BEST DESIGN COMBINATION FOR EACH SUBJECT IS HIGHLIGHTED.

3-state BCI Design structure	Subject1		Subject2		Subject3		Subject4		Average
	TPR	TPL	TPR	TPL	TPR	TPL	TPR	TPL	
<DET1-LF-1NN + DET2-PSD-LDA>[22]	**30.6**	**32.6**	16.1	33.4	**30.5**	**36.7**	**53.3**	**54.7**	36.0
<DET1-PSD-LDA + DET2-PSD-LDA>	19.5	22.2	**35.6**	**47.0**	30.1	34.3	37.4	45.2	33.9

TABLE 8.4 BEST DESIGN COMBINATION FOR EACH SUBJECT TOGETHER WITH THE PERFORMANCES OF THE 2-STATE AND 3-STATE SYSTEMS (AT FALSE POSITIVE OF 1%), WHERE A = <DET1-LF-1NN + DET2-PSD-LDA> AND B = <DET1-PSD-LDA + DET2-PSD-LDA>.

Subject	**Best design**	**2-state BCI**	**3-state BCI**		
		TP_{IC}	**TP_R**	**TP_L**	**Average TP ($TP_{3\text{-State}}$)**
Subject 1	A	50.1	30.6	32.6	31.6
Subject 2	B	54.7	35.6	47	41.3
Subject 3	A	60.2	30.5	36.7	33.6
Subject 4	A	71.0	53.3	54.7	54
Average	-	58.1	37.5	42.8	40.1

[22] Note that <DET1-LF-1NN + DET2-PSD-LDA> indicates a design of a 3-state BCI that uses DET1-LF-1NN design for DET1 and DET2-PSD-LDA design for DET2. A similar description applies to <DET1-LF-1NN + DET2-PSD-LDA> design as well.

Table 8.4 shows the best performing 3-state self-paced BCI design for each individual subject. As the last column of Table 8.4 shows, the average performance of the 3-state system achieves an overall true positive rate of 40.1% (at false positive rate of 1%). If used as a 2-state BCI its average true positive is 58.1%.

8.5. Discussion

This study introduced and evaluated two designs of a 3-state self-paced brain computer interface based on movement related potentials. This 3-state self-paced brain computer interface is the first of its kind in its capability of handling the no control (NC) state. In fact, this BCI intends to differentiate the right and the left hand extensions from the NC state. Ideally, in this system, the user can perform any brain activity (other than the predefined IC states of right and left hand extensions) when he/she does not intend to control the BCI. While the true positive rate of the latest 2-state self-paced BCI is 41% (at FP=1%) (Bashashati et al 2006b), the best average true positive rate of the proposed 3-state system is 40.1% (at FP=1%). These results show that the 3-state system performs almost the same as the latest 2-state self-paced BCI (Bashashati et al 2006b) with the advantage of providing more control options than a 2-state system.

The proposed 3-state self-paced BCI was specifically designed to support NC state. This system was tested in a specific experimental paradigm and on NC state data that were supposed to be the most difficult one as they were surrounded by IC state data. However, a more thorough study is needed to investigate the performance of the system under *different experimental paradigms and on different sets of NC state data*, e.g. when the person perform different mental tasks except for the IC task. This study would provide a better estimate of the performance of a self-paced BCI system in a real-world application.

There have been numerous BCIs, e.g. (Blankertz et al 2006, Brunner et al 2006, Millan et al 2004, Scherer et al 2004, Scherer et al 2007, Wang et al 2004, Wolpaw and Mcfarland 2004), that differentiate between two or more classes of movements, e.g. right and left hand (imagined) movements, or operate based on subject modulating the Mu and Beta brain rhythms. It should, however, be mentioned that it is difficult to directly compare the results of our study with these studies because: (a) the system implemented in this study performs in a self-paced manner, i.e., it is different from most other studies, (b) the recording equipment,

recording and classification protocols, and mental tasks considered are different, and (c) the amount of data involved and the degree of training the subjects received before and during participation in the BCI experiments varies for different studies, (d) there is not a unified framework of reporting performance of BCI systems, i.e. the performance metrics are different across different studies.

The performance of DET1-LF-1NN and DET1-PSD-LDA in detecting the presence of a movement (regardless of its type) yielded average true positive rates of 54% and 53.4% at false positive (FP) rate of 1%, respectively. In the meantime, as shown in the third column of Table 8.4, the average TP_{IC} rate for the best performing design across the subjects was 58.1% at false positive rate of 1%. In other words, if the current system was used as a 2-state self-paced BCI, the true positive rate would be 58.1% at false positive of 1%. In comparison, the results of the latest 2-state self-paced BCI (Bashashati et al 2006b) for four able-bodied subjects yielded an average true positive rate of 41% at the same false positive rate of 1%. Thus, when used as a 2-state system the proposed BCI performs significantly better than the 2-state self-paced BCI system in (Bashashati et al 2006b). It should be noted that while this 2-state self-paced brain computer interface detects finger flexions, DET1 of the 3-state self-paced BCI detects the presence of a left or a right hand extension movement. This improvement should be the result of using hand extension movements instead of a finger flexion one. It should be noted however that direct comparison of the current system with (Bashashati et al 2006b) is not completely accurate as the data and experimental paradigms used in testing the two systems were different; a more thorough study is needed to verify these findings. Verifying these results on a very large subject pool would eventually provide a better neurophysiological source for controlling current 2-state self-paced BCIs.

As shown in Table 8.2, for three of the four tested subjects, DET1-LF-1NN performs better than DET1-PSD-LDA. However, for subject 2, DET1-PSD-LDA outperforms DET1-LF-1NN, specifically, the true positive rate increases significantly from 38.4% to 54.7%. The overall performance of the 3-state BCI varies across the subjects and depends on the type of the design used. Such performance variability across different designs and subjects has also been observed in other BCI systems (e.g. (Graimann et al 2004, Muller-Putz et al 2005)). Given the variable performance of subjects across the two designs, an approach that can select a suitable design and adapt to each subject is expected to achieve better detection rates.

Significant gains may also be achieved from the combination of several single designs if these designs provide complementary information for the classification task. Several studies have demonstrated some evidence of existing independent features related to movement tasks that could be used to achieve better classification accuracies (Babiloni et al 1999, Dornhege et al 2003, Dornhege et al 2004).

Subject 4 yielded the best right and left true positive rates (TP_R and TP_L) overall performance of 53.3% and 54.7% at false positive rate of 1%, respectively. Although DET1's true positive rate in detecting the presence of a movement (TP_{IC}) for subject 3 was the second best, overall the system has poor performance in differentiation between right and left movements. The following reasons might have caused the poor performance related to this subject:

(a) this subject did not generate significantly differentiable ERD/ERS patterns for the left and right hand movements. Many factors such as task complexity, effort and attention during the task can also contribute to the quality of the ERD/ERS patterns (Pfurtscheller and Lopes da Silva 1999). Other studies such as (Blankertz et al 2006) have reported some subjects who poorly performed (classification rates of close to chance) compared to the rest of the subjects.

(b) in the experimental paradigm used in this study, no feedback during the performed tasks was provided to the subjects. While we adopted this paradigm to simulate a more natural mode of control, this may have caused a lower performance in some subjects. As shown by some researchers (e.g. Millan et al 2002), providing feedback during experiments may increase the performance of subjects over time.

(c) no subject pre-screening and prior training was performed before the sessions,

This preliminary study was performed to examine the feasibility of a 3-state 'self-paced' brain computer interface design. Although the results are promising, more improvements are needed in both of its components, that for detecting a movement and that for differentiating between two movements. The true positive rate of the system is reported at a false positive rate of 1%. Even a false positive rate of 1% is still not suitable for real-world applications as it corresponds to one false activation every six seconds and may cause excessive user frustration. Use of more efficient feature extraction and classification methods, subject training, providing online feedback during the performed task and verifying the results on a large number of subjects are in the scope of our future directions to improve these results.

8.6. References

Babiloni C, Carducci F, Cincotti F, Rossini P M, Neuper C, Pfurtscheller G and Babiloni F 1999 Human movement-related potentials vs desynchronization of EEG alpha rhythm: A high-resolution EEG study *NeuroImage* **10** 658–65.

Bashashati A, Fatourechi M, Ward R K and Birch G E 2006a User customization of the feature generator of an asynchronous brain interface *Ann. Biomed. Eng.* **34** 1051-60.

Bashashati A, Mason S, Ward R K and Birch G E 2006b An improved asynchronous brain interface: making use of the temporal history of the LF-ASD feature vectors *J. Neural Eng.* **3** 87-94.

Birch G E, Lawrence P D and Hare R D 1993 Single Trial Processing of Event Related Potentials Using Outlier Information *IEEE Trans. Biomed. Eng.* **40** 59-73.

Blankertz B, Dornhege G, Krauledat M, Muller K R, Kunzmann V, Losch F and Curio G 2006 The Berlin Brain-Computer Interface: EEG-based communication without subject training *IEEE Trans. Neural Syst. Rehabil. Eng.* **11** 147-52.

Borisoff J F, Mason S G, Bashashati A and Birch G E 2004 Brain-computer interface design for asynchronous control applications: improvements to the LF-ASD asynchronous brain switch *IEEE Trans. Biomed. Eng.* **51** 985-92.

Brunner C, Scherer R, Graimann B, Supp G and Pfurtscheller G 2006 Online Control of a Brain-Computer Interface Using Phase Synchronization *IEEE. Trans. Biomed. Eng.* **53** 2501-6.

Dornhege G, Blankertz B, Curio G and Müller K R 2003 Combining features for BCI *Advances in Neural Inf. Proc. Systems (NIPS 02)*, eds Becker S, Thrun S and Obermayer K **15** 1115-22.

Dornhege G, Blankertz B, Curio G and Müller K R 2004 Boosting bit rates in non-invasive EEG single-trial classifications by feature combination and multi-class paradigms *IEEE Trans. Biomed. Eng.* **51** 993–1002.

Graimann B, Huggins J E, Levine S P and Pfurtscheller G 2004 Toward a direct brain interface based on human subdural recordings and wavelet-packet analysis *IEEE Trans. Biomed. Eng.* **51** 954-62.

Lachenbruch P A 1975 *Discriminant Analysis* (NY: Hafner Press)

Levine S P, Huggins J E, Bement S L, Kushwaha R K, Schuh L A, Rohde M M, Passaro E A, Ross D A, Elisevich K V and Smith B J 2000 A Direct Brain Interface Based on Event-Related Potentials *IEEE Trans. Rehabil. Eng.* **8** 180-5.

Mason S G and Birch G E 2000 A brain-controlled switch for asynchronous control applications *IEEE Trans. Biomed. Eng.* **47** 1297-307.

Mason S G, Bashashati A, Fatourechi M, Navarro K F and Birch G E 2007 A Comprehensive Survey of Brain Interface Technology Designs *Ann. Biomed. Eng.* **35** 137-69

Muller-Putz G R, Scherer R, Brauneis C and Pfurtscheller G 2005 Steady-state visual evoked potential (SSVEP)-based communication: impact of harmonic frequency components *Journal of Neural Engineering* **2** 123-30.

Millan J R, Mourino J, Franze M, Cincotti F, Varsta M, Heikkonen J, Babiloni F 2002 A local neural classifier for the recognition of EEG patterns associated to mental tasks *IEEE Trans. Neural Networks* **13** 678-86.

Millan J R, Renkens F, Mourino J and Gerstner W 2004 Noninvasive brain-actuated control of a mobile robot by human EEG *IEEE Trans. Biomed. Eng.* **51** 1026-33.

Pfurtscheller G and Lopes da Silva F H 1999 Event-related EEG/MEG synchronization and desynchronization: basic principles *Clin. Neurophysiol.* **110** 1842-57.

Pfurtscheller G and Aranibar A 1979 Evaluation of event-related desynchronization (ERD) preceding and following voluntary self-paced movement *Electroencephalogr. Clin. Neurophysiol.* **46** 138-46.

Pfurtscheller G, Neuper C, Andrew C and Edlinger G 1997 Foot and hand area mu rhythms *Int. J. Psychophysiol.* **26** 121-35.

Pregenzer M and Pfurtscheller G 1999 Frequency Component Selection for an EEG-Based Brain to Computer Interface *IEEE Trans Reh Eng* **7** 413-9.

Scherer R, Muller G R, Neuper C, Graimann B and Pfurtscheller G 2004 An asynchronously controlled EEG-based virtual keyboard: improvement of the spelling rate *IEEE Trans. Biomed. Eng.* **51** 979-84.

Scherer R, Lee F, Schlogl A, Leeb R, Bischot H and Pfurtscheller G 2007 Towards Self-Paced Brain-Computer Communication: Navigation through Virtual Worlds *IEEE Transactions on Biomedical Engineering*, In press.

Stancak A and Pfurtscheller G 1996 Event-related desynchronisation of central beta-rhythms during brisk and slow self-paced finger movements of dominant and nondominant hand *Brain Res. Cogn. Brain Res.* **4** 171-83.

Slobounov S, Johnston J, Chiang H and Ray W 2002 Movement-related EEG potentials are force or end-effector dependent: evidence from a multi-finger experiment *Clin. Neurophysiol.* **113** 1125-35.

Townsend G, Graimann B and Pfurtscheller G 2004 Continuous EEG classification during motor imagery--simulation of an asynchronous BCI *IEEE Trans. Neural Syst. Rehabil. Eng.* **12** 258-65.

Wang Y, Zhang Z, Li Y, Gao X, Gao S and Yang F 2004 BCI Competition 2003--Data set IV: an algorithm based on CSSD and FDA for classifying single-trial EEG *IEEE Trans Biomed. Eng.* **51** 1081-6.

Welch P 1967 The use of fast Fourier transform for the estimation of power spectra: A method based on time averaging over short, modified periodograms *IEEE Trans. Audio and Electroacoustics* **15** 70-3.

Wolpaw J R and McFarland D J 2004 Control of a two-dimensional movement signal by a noninvasive brain-computer interface in humans *Proc. Natl. Acad. Sci. U. S. A.* **101** 17849-54.

Wolpaw J R 2004 Brain-computer interfaces (BCIs) for communication and control: a mini-review *Suppl. Clin. Neurophysiol.* **57** 607-13.

Yom-Tov E and Inbar G F 2003 Detection of Movement-Related Potentials from the Electro-Encephalogram for possible use in a Brain-Computer Interface *Med. Bio. Eng. Comp.* **41** 85-93.

Yue G H, Liu J Z, Siemionow V, Ranganathan V K, Ng T C and Sahgal V 2000 Brain activation during human finger extension and flexion movements *Brain Res.* **856** 291-300.

Chapter 9 Improving the Performance of a 3-State Self-Paced Brain Computer Interface [23]

9.1. Introduction

Over the past decade, several research groups have developed direct brain computer interface (BCI) systems as a possible alternative communication and control solution for individuals with severe disabilities. By using a BCI, control of various devices such as a neural prosthetic is made possible by cognitive processes only, in other words a BCI system bypasses the traditional interface pathways which cannot be used by individuals with severe disabilities.

Many BCI designs have been presented in the literature (for a review of the field see (Bashashati et al 2007a, Mason et al 2007, Wolpaw 2004)). Few of these, however, have been designed specifically for self-paced (asynchronous) control as defined in (Mason and Birch 2000). For a self-paced BCI system, the users can affect the BCI system output whenever they want by intentionally changing their brain state. In such instances, the user is said to be in an intentional control (IC) state. In between periods of intentional control (IC), the user is in a no control (NC) state, i.e., he/she may be idle, daydreaming, thinking about a problem or lunch, or performing some other action, but they are not trying to control the BCI system. In fact, the NC state includes all mental states except for the IC state. Self-paced BCI systems should respond only when the user intends to affect control and should maintain an inactive state output during times when the user is in a NC state. In contrast, for a synchronous BCI system, the allowable times for intentional user control are restricted to periods defined by the system. Thus, these systems are tested and evaluated only during intentional user control and the response during NC states is not tested.

Only a few BCI designs have been specifically designed for self-paced control (Bashashati et al 2007b, Levine et al 2000, Mason and Birch 2000, Millan et al 2004, Scherer et al 2004, Townsend et al 2004, Yom-Tov and Inbar 2003). The low frequency asynchronous switch design (LF-ASD) was the first BCI system implemented for asynchronous (self-paced) applications (Mason and Birch 2000). Like LF-ASD, the BCI systems introduced in (Levine et al 2000, Townsend et al 2004, Yom-Tov and Inbar 2003) attempt to detect a specific

[23] A version of this chapter will be submitted for publication.

intentional control state, e.g. imagined right hand movement, from the ongoing brain signal. The BCI implemented in (Scherer et al 2004) attempts to differentiate between imagined right hand, imagined left hand and imagined foot movements. However, this BCI requires the subject to constantly engage in control without the option of staying in a no control state. Therefore, the response of this BCI to NC state is not studied. In a recent work, Scherer et al (Scherer et al 2007) has proposed a 4-state self-paced BCI that has mean true positive and false positive rates of 28.4% and 16.9%, respectively. In the study of (Millan et al 2004) the subjects were asked to perform one of the following three actions: (1) imagine right hand movement, (2) imagine left hand movement, and (3) relax. A 3-state self-paced BCI was designed to navigate a mobile robot in an 80cm*60cm house-like environment by differentiating amongst these three states. The system generates 'unknown state output' when there is not enough confidence in choosing one of the three above mentioned mental tasks. The classifier of this system was not explicitly trained to recognize idle (NC) state (Millan et al 2004). According to the authors, it could process them adequately by responding 'unknown'. It was also reported that the task of steering the robot between rooms was so engaging that the two tested subjects preferred to emit continuously mental commands *rather than to go through idle state*. Therefore, the response of this system on NC (idle) state was evaluated on a dataset with limited amount of idle-state. Moreover, having the choice of 'unknown state output' may represent some neutral output but it is not clear whether the unknown state output was caused by the actual idle (NC) state or by lack of confidence in detecting one of the three commands. Additionally, there is no evidence that the NC state will fall into the unknown state in these designs.

A 3-state self-paced BCI system that extends the 2-state self-paced systems has been introduced in (Bashashati et al 2007b). This system is designed to have the ability to support the no-control (NC) state as well as detecting right and left hand extension movements.

Fig. 9.1 shows an output sample of a self-paced 3-state BCI. A 3-state self-paced BCI remains in an inactive state (NC state) for most of the time and is activated (IC state) when specific brain states associated with IC1 and IC2 outputs are detected in the brain signal. A 2-state self-paced BCI has only one active state output (IC1), and thus provides the user with the option of executing only one command (e.g. turn right). A 3-state system, on the other

hand, gives the user two command options (e.g. turn right or turn left) which has the advantage of providing more control options.

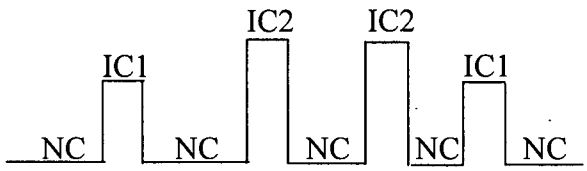

Figure 9.1 Sample of output of a 3-state self-paced BCIs, where NC = No Control state, IC = Intended Control state

The 2-state self-paced BCI (LF-ASD) in (Mason and Birch 2000) aimed at detecting attempted right finger flexions. Recent studies with the 2-state self-paced BCI have demonstrated that this system correctly detects the presence of a movement (true positive (TP) rate) in 41% of the cases for able-bodied (Bashashati et al 2006b). This is when the parameters were set so that the false positive rate is fixed at 1%. The TP rate of the system improves at higher FP rates, e.g. at an FP rate of 5%, the TP rate is almost 100%. Results of the evaluation of the 3-state self-paced BCI system introduced in (Bashashati et al 2007b) show an average true positive rate of 58.1% when it is used as a 2-state BCI and an average of 40.1% true positive rate in correct detection of right and left hand extension movements (Bashashati et al 2007b). These results show a higher mean true positive rate at a lower false positive rate compared to the only multi-state self-paced BCI that supports NC state (Scherer et al 2007). Despite these encouraging results, however, more improvements are still needed.

The original design of the 3-state self-paced BCI system is comprised of two major decision blocks. The first block (DET1) determines whether or not a movement (regardless of the type of the movement) is executed. If a movement is detected, the second block (DET2) determines the type of the movement, i.e., whether it is a right or a left hand extension movement.

The aims of this paper are: (a) to improve the performance of the original 3-state self-paced BCI system, and (b) to improve the performance of the 2-state self-paced BCI that detects hand extensions (Bashashati et al 2007b).

Several design variations for both DET1 and DET2 are implemented. One of the new designs of DET1 uses the past history of features to detect movements. In other words, instead of using the features values at $t=t_1$ to detect the presence of a movement at $t=t_1$, the past history of the features values are also used. In the previous design, the output class at $t=t_1$ was determined based on the values of features at $t=t_1$, only. Using the past trajectory of features has proven to increase the performance of a 2-state self-paced BCI system in (Bashashati et al 2006b) and we expect that using the same idea should also improve the results of a 3-state self-paced BCI. Another improved design of DET1 uses a nonlinear classifier, i.e. 1-nearest neighbor classifier, instead of a linear classifier, i.e. linear discriminant analysis, to detect movements. This design uses features related to power spectrum of the EEG. A new design of DET2 is also evaluated. This design uses the logarithm of the extracted power spectral features to differentiate between right and left hand extensions.

The performance of the proposed design is evaluated using EEG recordings of right and left hand extension movements of four able-bodied individuals. Results show improvements for both the 2-state and the 3-state self-paced BCI systems.

In Sections 2 and 3, the design of the 3-state self-paced BCI system and the experimental paradigm are presented. The results and conclusions are in Sections 4 and 5, respectively.

9.2. 3-State Self-Paced BCI

Fig. 9.2 shows the overall block diagram of the 3-state self-paced BCI design (Bashashati et al 2007b). This system aims at detecting the right and the left hand extensions from the ongoing EEG in a self-paced manner. This design includes two detectors: a) Detector 1 (DET1) which determines whether or not a movement is performed, and b) Detector 2 (DET2) which determines whether the detected movement is a right hand or a left hand extension. The details of both detectors are explained below.

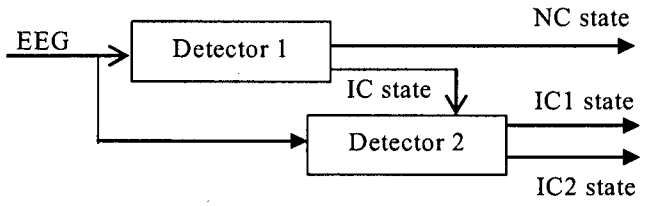

Figure 9.2 Overall structure of the 3-state self-paced BCI design

9.2.1. Detector 1 (DET1)

Two new designs of DET1, as explained below, are implemented and compared to the designs that were evaluated in (Bashashati et al 2007b).

9.2.1.1. DET1-LF$_{V5}$-1NN

The latest 2-state self-paced BCI design, LF-ASD-V5, that models the trajectories the features move on during movements is used to detect movements (Bashashati et al 2006b).

One of the original designs of DET1, DET1-LF$_{V4}$-1NN, was based on LF-ASD-V4 design (Borisoff et al 2004) in which the output class at $t=t_1$ was determined based on only the values of features at t_1. In the proposed design (DET1-LF$_{V5}$-1NN), we use all the past values of the features and not only those at t_1, i.e., the paths the features traverse in the multidimensional space during both the IC states and the NC states. As in (Bashashati et al 2006b), the relation between the output class of the system and its input can be expressed by equations (1) and (2):

$$O(t_1) = g(FV_{V5}(t_1)) \qquad (1)$$

$$FV_{V5}(t_1) = [FV_{V4}(t_1 - L) \quad \ldots \quad FV_{V4}(t_1 - 1) \quad FV_{V4}(t_1)] \qquad (2)$$

where $O(t_1)$ is the output class at $t=t_1$, $FV_{V5}(t_1)$ is the feature matrix of DET1-LF$_{V5}$-1NN at $t=t_1$, $[FV_{V4}(t_1 - L) \quad \ldots \quad FV_{V4}(t_1 - 1) \quad FV_{V4}(t_1)]$ are the values of the DET1-LF$_{V4}$-1NN design in the time window $t=t_1$-L to $t=t_1$ and L is the length of the window. $g(.)$ is the function that maps the feature values to the output of the system. In DET1-LF$_{V5}$-1NN, the feature matrix $FV_{V5}(t_1)$ represents the path that the original feature vectors ($FV_{V4}(t_1)$) traverse during time. Basically, the new feature space captures the paths of the feature vectors.

Our goal is to find the representative feature vectors (codebooks) that correspond to the IC and to the NC states. Conceptually these representative feature vectors show the paths the features move on during NC and IC states and are used as the codebooks the classifier uses to detect IC and NC states. To find the classifier codebooks, we use the k-Means and learning vector quantization (LVQ) methods (Kohonen 1990).

Figs. 9.3.a & 9.3.b show the block diagram of DET1-LF_{V4}-1NN and DET1-LF_{V5}-1NN. Both designs use features extracted from the 0-4Hz band in six bipolar EEG channels (defined with reference to the International 10-20 System at F1-FC1, Fz-FCz, F2-FC2, FC1-C1, FCz-Cz, and FC2-C2). After filtering the input EEG, all six bipolar EEG channels are normalized with an energy normalization transform (ENT). The LF-ASD feature generator extracts features related to movement related potentials using a template matching algorithm. The parameters values of this block are customized for each subject according to the procedure explained in (Bashashati et al 2006a). The Karhunen-Loève Transform (KLT) component (Jayant 1984) is used to reduce the 6-dimensional feature vector to a 2-dimensional feature vector. The resulting 2-dimensional feature vector corresponds to the feature vectors of the DET1-LF_{V4}-1NN design, i.e. FV_{V4}. A buffer (with length L) is used to capture the trajectory of features over time and the output of this block represents the feature vectors of the DET1-LF_{V5}-1NN design, i.e. FV_{V5}. A 1-NN (1-nearest neighbor) classifier is used as the feature classifier to detect movements. Finally, a moving average (length of 5 samples) and a debounce block (length of 16 samples) are used to further improve the classification accuracy of DET1 by reducing the number of false switch activations (for details, see (Borisoff et al 2004, Mason and Birch 2000)). DET1 classifies the input patterns, every 1/16th of a second, to one of two classes, no control (NC) or intentional control (IC) states.

9.2.1.2. DET1-PSD-1NN

Figs. 9.3.c & 9.3.d shows another design of DET1, DET1-PSD-LDA, implemented in (Bashashati et al 2007b) and the modified design of this detector, DET1-PSD-1NN implemented in this study. Both designs extract the power spectral density features of the EEG from a group of bipolar EEG channels and then select the most informative channels for classification. Specifically, thirty bipolar combinations of EEG channels that may contribute to the detection of movements were generated. These bipolar EEG channels were Cz-C1, Cz-

C2, Cz-C3, Cz-C4, C1-C2, C1-C4, C1-C3, C2-C3, C2-C4, C3-C4, FCz-Cz, FC1-C1, FC2-C2, FC3-C3, FC4-C4, Fz-FCz, F1-FC1, F2-FC2, F3-FC3, F4-FC4, FCz-FC1, FCz-FC2, FCz-FC3, FCz-FC4, FC1-FC2, FC1-FC4, FC1-FC3, FC2-FC3, FC2-FC4, FC3-FC4. These bipolar channels were chosen to capture possible discriminatory information between left and right and also between frontal and central areas of the head. In the feature extraction block, the power spectral density (PSD) components of each of the 30 bipolar EEG channels are calculated in each frequency bin from 1Hz to 25Hz using Welch's Periodogram method (Welch 1967) with window length of one second (equivalent to 128 samples). This results in 25 frequency components for each of the 30 bipolar channels and a total of 25*30 features at each time instant. We then use stepwise linear discriminant analysis (stepwise LDA) (Lachenbruch 1975) to find the most informative features that better discriminate between IC and NC classes. Stepwise LDA is a method that results in a linear combination of selected features that contribute to the classification and omits the features that have redundant information for discrimination. Once the features are extracted and selected, DET1-PSD-LDA uses a linear discriminant classifier (LDA) (Lachenbruch 1975), and DET1-PSD-1NN uses a 1-NN classifier for classification. The codebooks for the 1-NN classifier are generated using the same approach explained for DET1-LF_{V5}-1NN. For more details about the other components of the feature translator (moving average and debounce blocks) refer to the previous description of DET1-LF_{V5}-1NN.

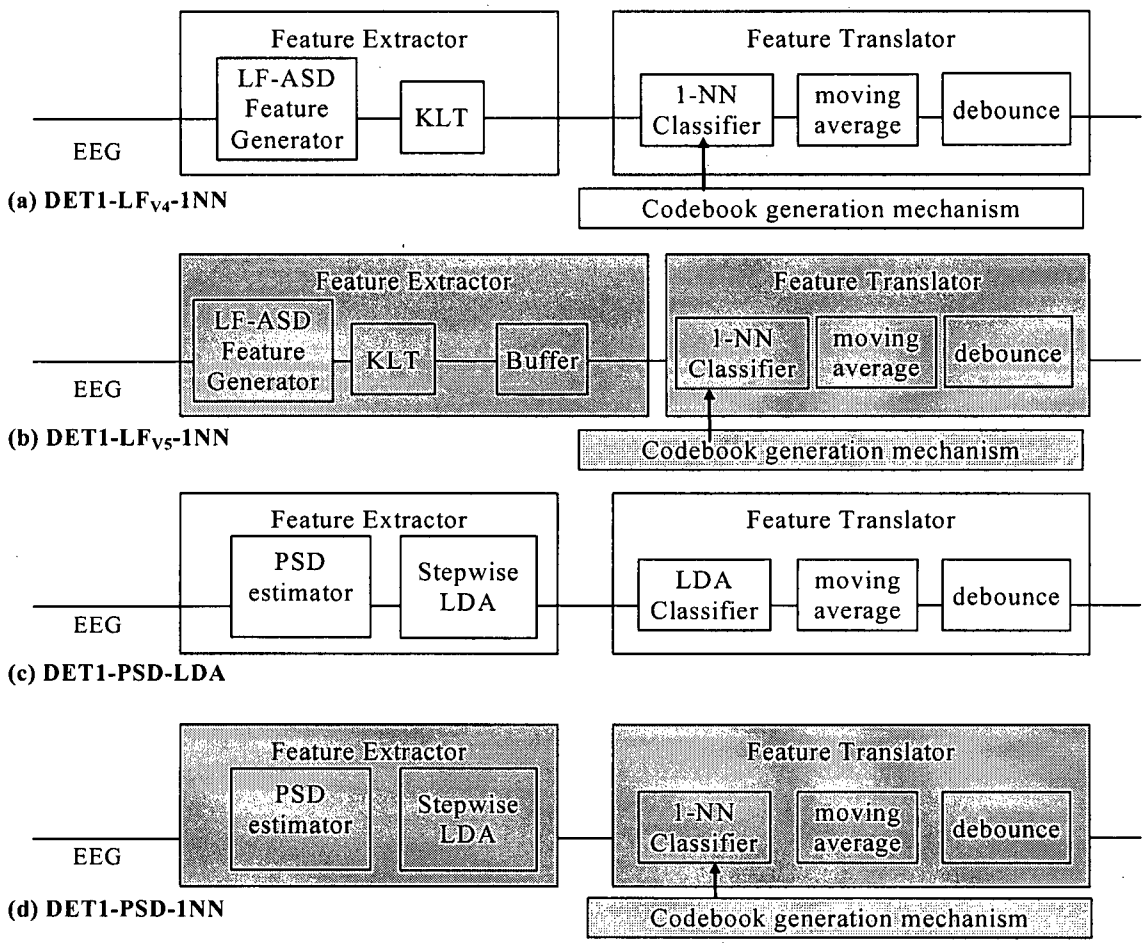

Figure 9.3 Structure of the two designs of DET1, where KLT = Karhunen-Loève Transform, and 1-NN = 1-Nearest Neighbour, PSD = power spectral density, and LDA: linear discriminant analysis. Note, shaded designs are new designs of DET1 implemented in this study.

9.2.2. Detector 2 (DET2)

The same design of DET2 as implemented in (Bashashati et al 2007b) and a modified version of this design that applies a logarithm function on the extracted features are used. DET2 uses the power spectral density (PSD) features of the input signal to capture the 8-12Hz Mu rhythm event related desynchronization (ERD) and the 14-25Hz Beta rhythm event related synchronization (ERS) which are generated during movement preparation and execution.

Fig. 9.4 shows the block diagram of DET2. The input for DET2 is comprised of several bi-polar combinations of EEG electrodes: Cz-C1, Cz-C2, Cz-C3, Cz-C4, C1-C2, C1-C4, C1-C3, C2-C3, C2-C4, C3-C4, FCz-Cz, FC1-C1, FC2-C2, FC3-C3, FC4-C4, Fz-FCz, F1-FC1, F2-FC2, F3-FC3, F4-FC4, FCz-FC1, FCz-FC2, FCz-FC3, FCz-FC4, FC1-FC2, FC1-FC4, FC1-FC3, FC2-FC3, FC2-FC4, FC3-FC4. A feature selection algorithm (stepwise linear

discriminant analysis (LDA)) (Lachenbruch 1975) is used to select the most informative electrode combinations for further processing. DET2 contains a feature extraction block which calculates the power spectral density features of the EEG. Specifically, the Welch's Periodogram method (Welch 1967) with a window length of 128 samples and a 90% overlap is used to extract the PSD features. Some studies show that the frequency band of ERD patterns varies from subject to subject (Pregenzer and Pfurtschller 1999); thus we employ the stepwise LDA method to select the subject's specific ERD frequency bands that yield better differentiation between right and left hand movements. In the modified version of DET2, instead of classifying the PSD feature values, the logarithm of PSD features are classified. This design is referred to as DET2-logPSD-LDA. The reason behind applying logarithm function on PSD features is to generate features with normal distribution.

We implemented another design of DET2 that used a nonlinear classifier, i.e., a 1-NN classifier trained with LVQ. However, the results were lower than the linear classifier used and thus are not reported in this paper.

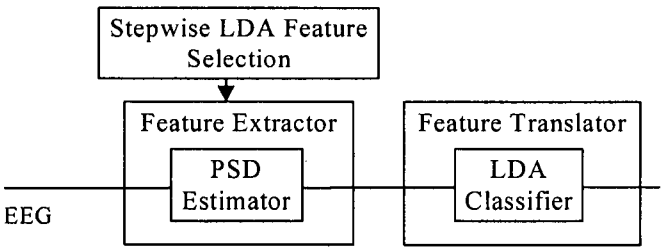

Figure 9.4 Structure of DET2, where LDA = Linear Discriminant Analysis, PSD = Power Spectral Density

Finally, when DET1 detects a movement in the ongoing EEG, then DET2 determines whether the input pattern belong to one of the two right hand movement (IC1) or left hand movement (IC2) classes. If DET1 does not detect any movement, the output will be in inactive (NC) state.

9.3. Experimental Paradigm

The EEG data used in this study were recorded from 15 mono-polar electrodes positioned over the supplementary motor area and the primary motor cortex (defined with reference to

the International 10-20 System at F1, F2, F3, F4, Fz, FC1, FC2, FC3, FC4, FCz, C1, C2, C3, C4, and Cz referenced to linked ear lobes). Electro-oculographic (EOG) activity was measured as the potential difference between two electrodes, placed at the corner and below the right eye. The ocular artifact was considered present when the difference between the EOG electrodes exceeded ±25μv, a threshold level similar to the one used in previous studies (Bashashati et al 2006b, Borisoff et al 2004, Mason and Birch 2000). All signals were sampled at 128 Hz. This study has been approved by the Behavioral Research Ethics Board (BREB) of the University of British Columbia.

Four able-bodied subjects participated in this study. All subjects were male (except subject 4), right handed (except subject 4) and 25-30 years old. Subjects were seated 150 cm in front of a computer monitor. The data were collected while the subjects were performing a guided task. At random intervals of 5.6-7s (mean of 6.7 s), a target window was displayed on the subject's monitor. A box moved from the left side to the right side of the screen. When the box reached the target window, the subject attempted to activate the custom-made switch by extending his/her right or left hand. The length of the target window was more than the length of the moving box and the subjects were free to activate the switch any time they want while the box is inside the target window. An arrow in the moving box, pointing to the left or the right showed the subject whether to move the right or the left hand. *In the NC period, i.e. the time between the subject activates the switch and the next opportunity to activate the switch, the subject was free to perform any mental task except the two predefined movements.* For each subject, an average of 150 trials for each movement was collected in two sessions carried out in the same day.

9.4. Evaluation

The designed 3-state self-paced BCI detects whether or not a movement is performed and then classifies the input to one of two classes, the right hand (IC1) or the left hand (IC2) extension classes. If the system does not detect a movement, the output will report an inactive NC state.

We use a 5-fold stratified cross-validation method (Witten and Frank 2000) to evaluate the performance of the proposed 3-state self-paced BCI designs. In a 5-fold *stratified* cross-validation, the data files are randomly divided into *five* groups of equal trial numbers, with

approximately the same frequency of classes. As in conventional cross-validation schemes, the classifier is trained based on the data of four of the five groups and the system's performance is evaluated based on the unseen data of the remaining group. This process is repeated for each group. The average of these five performance measures gives the overall performance of the system.

For each specific design, the ability of the subjects to control the 3-state BCI system is evaluated using three performance measures. At a fixed false positive rate, these measures report the correct detection rates of the right and the left hand extensions (from the ongoing EEG), respectively:

(1) the percentage of correct right hand movement detection during IC states (true positives for right hand movement, TP_R) as in equation (1) below:

TP_R = (number of correctly detected right movements)/(total number of right movements) (1)

(2) the percentage of correct left movement detection during IC states (true positives of left hand movements, TP_L) as in equation (2) below:

TP_L = (number of correctly detected left movements)/(total number of left movements) (2)

(3) the percentage of false switch activations during NC states (false positives, FPs) as in equation (3) below:

FP = (number of false activations)/(total number of the systems' decisions during NC state) (3)

Note that the decision rate of the system is $1/16^{th}$ of a second.

A TP is identified if the BCI system is activated at least once in a time window (response window) spanning 0.25 seconds before the time of movement till 0.5 seconds after it, a method similar to that employed in [4-6,11,12]. FPs are assessed in the periods outside the 'response window' as explained above. Periods during which ocular artifacts occurred are blocked from analysis.

We also report on the overall true positive and false positive rates of DET1 regardless of the type of movement. We refer to these measures as TP_{IC} and FP_{IC}. These measures reflect the

performance of the system as if it was used as a 2-state self-paced BCI. These measures are used to compare the performance of the proposed designs with our latest 2-state self-paced BCI.

9.5. Results

Four new designs of a 3-state self-paced BCI system are evaluated:

1) DET1-LF_{V5}-1NN followed by DET2-PSD-LDA (<DET1-LF_{V5}-1NN + DET2-PSD-LDA>),

2) DET1-PSD-1NN followed by DET2-PSD-LDA (<DET1-PSD-1NN + DET2-PSD-LDA>),

3) DET1-LF_{V4}-1NN followed by DET2-logPSD-LDA (<DET1-LF_{V4}-1NN + DET2-logPSD-LDA>), and

4) DET1-LF_{V5}-1NN followed by DET2-logPSD-LDA (<DET1-LF_{V5}-1NN + DET2-logPSD-LDA>).

These designs are compared to the previously implemented designs, i.e., DET1-LF_{V4}-1NN followed by DET2-PSD-LDA (<DET1-LF_{V4}-1NN + DET2-PSD-LDA>) and DET1-PSD-LDA followed by DET2-PSD-LDA (<DET1-PSD-LDA + DET2-PSD-LDA>) as in (Bashashati et al 2007b).

Table 9.1 shows the true positive (TP_{IC}) rate of DET1 when the false positive (FP_{IC}) rate is set at 1%. The results are shown for the designs of DET1 implemented in (Bashashati et al 2007b), i.e., DET1-LF_{V4}-1NN and DET1-PSD-LDA, and the present designs of DET1, DET1-LF_{V5}-1NN and DET1-PSD-1NN. As we are only interested in low FP rates, we do not report the TP rates at higher FPs. However, it is worth mentioning that the TP rate of the system, in the cases when FPs>3%, is about 100%. As Table 9.1 shows, for all the four tested subjects, the new designs of DET1 outperform the previous designs. As shown in the last column of Table 9.1, DET1-PSD-1NN design yields the largest average TP_{IC} rate of 73.4%. This is 19.4% higher than the TP_{IC} rate of 54% achieved in the previous study (Bashashati et al 2007b). The TP_{IC} rate of DET1-LF_{V5}-1NN is significantly higher than the ones for DET1-PSD-LDA and DET1-LF_{V4}-1NN designs by more than 11%. By using a paired t-test, both new designs of the DET1-LFV5-1NN and DET1-PSD-1NN outperform DET1-LF_{V4}-1NN and DET1-PSD-LDA designs by a significance level greater than 95%.

TABLE 9.1 PERCENTAGE OF TRUE POSITIVES (TP_{IC}) AT FIXED FALSE POSITIVE RATE OF 1% FOR THE TWO DESIGNS OF DET1

DET1 Design	Subject1	Subject2	Subject3	Subject4	Average
DET1-LF$_{V4}$-1NN	*50.1*	*38.4*	*56.5*	*71*	*54.0*
DET1-PSD-LDA	*38.2*	*54.7*	*60.2*	*60.3*	*53.4*
DET1-LF$_{V5}$-1NN	57.7	54	76.4	72.2	65.1
DET1-PSD-1NN	80.8	71.8	68	73	73.4
Best Design	80.8	71.8	76.4	73	75.5

Table 9.2 shows the performance of the whole 3-state self-paced BCI, at a fixed false positive rate of 1%, for the six design versions: 1) <DET1-LF$_{V4}$-1NN + DET2-PSD-LDA>, 2) <DET1-LF$_{V5}$-1NN + DET2-PSD-LDA>, 3) <DET1-LF$_{V5}$-1NN + DET2-PSD-LDA>, 4) <DET1-LF$_{V5}$-1NN + DET2-PSD-LDA>, 5) <DET1-LF$_{V5}$-1NN + DET2-logPSD-LDA>, 6) <DET1-LF$_{V5}$-1NN + DET2-logPSD-LDA>. On average, 47.0% of the right and the left hand extensions of the four subjects are correctly identified by the 3-state <DET1-PSD-1NN + DET2-PSD-LDA> design (for a false positive rate of 1%). Results of a paired t-test shows that <DET1-LF$_{V5}$-1NN + DET2-PSD-LDA> outperforms <DET1-LF$_{V4}$-1NN + DET2-PSD-LDA> by significance level greater than 93% and <DET1-PSD-1NN + DET2-PSD-LDA> outperforms <DET1-PSD-LDA + DET2-PSD-LDA> by a significance level greater than 99%. As shown in the last two columns of Table 9.2, DET2-logPSD-LDA performs slightly better than DET2-PSD-LDA when used as DET2 in a 3-state self-paced BCI.

TABLE 9.2 PERCENTAGE OF RIGHT AND LEFT TRUE POSITIVES (TP_R AND TP_L) OF THE TWO PROPOSED 3-STATE BRAIN COMPUTER INTERFACES (WHEN FALSE POSITIVE RATE IS SET AT 1%) . THE TP_R AND TP_L VALUES OF THE BEST DESIGN COMBINATION FOR EACH SUBJECT IS HIGHLIGHTED.

3-state BCI Design structure	Subject1		Subject2		Subject3		Subject4		Average
	TPR	TPL	TPR	TPL	TPR	TPL	TPR	TPL	
<DET1-LF$_{V4}$-1NN + DET2-PSD-LDA>[24]	*30.6*	*32.6*	*16.1*	*33.4*	*30.5*	*36.7*	*53.3*	*54.7*	*36.0*
<DET1-PSD-LDA + DET2-PSD-LDA>	*19.5*	*22.2*	*35.6*	*47.0*	*30.1*	*34.3*	*37.4*	*45.2*	*33.9*
<DET1-PSD-1NN + DET2-PSD-LDA>	**33.6**	**46**	**41.5**	**59**	39.8	45.5	53.7	57	47.0
<DET1-LF$_{V5}$-1NN + DET2-PSD-LDA>	36.8	39.2	29.8	46.4	**39.0**	**51.0**	53.1	55.6	43.9
<DET1-LF$_{V4}$-1NN+DET2-logPSD-LDA>	30.6	40.5	18.1	31.2	31.5	36.0	49.3	59.4	37.1
<DET1-LF$_{V5}$-1NN+DET2-logPSD-LDA>	**35.0**	**44.3**	28.5	47.5	41.4	48	**50.0**	**62.2**	44.6

[24] Note that <DET1-LF-1NN + DET2-PSD-LDA> indicates a design of a 3-state BCI that uses DET1-LF-1NN design for DET1 and DET2-PSD-LDA design for DET2. A similar description applies to other designs of 3-state self-paced BCI as well.

9.6. Conclusions

This study introduced and evaluated four new designs of a 3-state self-paced brain computer interface based on movement related potentials. Similar to the 3-state self-paced BCI in (Bashashati et al 2007b), the proposed systems intend to continuously differentiate the right and the left hand extensions from the NC state. While the true positive rate of the latest 2-state self-paced BCI based on finger flexion movements is 41% (at FP=1%) (Bashashati et al 2006b), the average true positive rate of the improved designs of the 3-state system reach have reached 47.0% (at FP=1%). These results show that the 3-state self-paced BCI system that detects hand extensions movements performs better than the latest 2-state self-paced BCI (Bashashati et al 2006b) that detects finger flexion movements with the added advantage of providing more control flexibility than a 2-state system. It should be noted, however, that the 3-state system implemented in this study aims at detecting hand extension movements while the 2-state self-paced BCI (Bashashati et al 2006b) detects finger flexion movements. The performance superiority of the 3-state self-paced BCI of the present study over the 2-state self-paced BCI in (Bashashati et al 2006b) is primarily due to the use of the new set of movements.

There have been numerous BCIs, e.g. (Blankertz et al 2006, Brunner et al 2006, Millan et al 2004, Scherer et al 2004, Scherer et al 2007, Wang et al 2004, Wolpaw and Mcfarland 2004), that differentiate between two or more classes of movements, e.g. right and left hand (imagined) movements, or operate based on subject modulating the Mu and Beta brain rhythms. It should, however, be mentioned that it is difficult to directly compare the results of our study with these studies because: (a) the system implemented in this study performs in a self-paced manner, i.e., it is different from most other studies, (b) the recording equipment, recording and classification protocols, and mental tasks considered are different, and (c) the amount of data involved and the degree of training the subjects received before and during participation in the BCI experiments varies for different studies, (d) there is not a unified framework of reporting performance of BCI systems, i.e. the performance metrics are different across different studies.

The performance of DET1-LF_{V5}-1NN and of DET1-PSD-1NN in detecting the presence of a movement (regardless of its type) yielded average true positive rates of 65.1% and 73.4%

with the false positive (FP) rate of 1%, respectively. The latest results of the 2-state self-paced brain computer interface shows an average true positive rate of 41% at the same false positive rate of 1% across four tested able-bodied subjects (Bashashati et al 2006b). Comparing the true positive (TP_{IC}) results of DET1 with the performance of able-bodied subjects of the latest 2-state self-paced BCI (Bashashati et al 2006b) shows a significant true positive rate increase of 32.4% at false positive rate of 1%. In other words, if the current system was used as a 2-state self-paced BCI, the true positive rate would be 73.4% at the false positive rate of 1%. It should be noted that while the latest 2-state self-paced brain computer interface detects finger flexions, DET1 of the 3-state self-paced BCI detects the presence of left or right hand extension movements. Such an improvement should be the result of the use of hand extension movements instead of finger flexion movements. However, it should be noted that direct comparison of the current system with (Bashashati et al 2006b) is not completely accurate as the data and experimental paradigms used in testing the two systems were different; a more thorough study is needed to verify these findings. Verifying these results on a very large subject pool would potentially provide a neurophysiological source that results in significantly better performances in controlling current 2-state self-paced brain computer interfaces without the need to change the design components of the systems.

As shown in Table 9.1, DET1-LF_{V5}-1NN outperforms DET1-LF_{V4}-1NN in movement detection by an average of 11.1% across the four subjects. This finding suggests that the past history of features provide better information for movement detection. In this study, this approach is performed on the original 2-state self-paced BCI features (Mason and Birch 2000); it may also yield improvements in other design variations. The results also show that DET1-PSD-1NN performed 20% better than DET1-PSD-LDA. Since these two designs differ in the classification stage, it is concluded that the 1-NN nonlinear classifier performs better than the linear discriminant analysis (LDA) classifier on power spectral density features, in detecting the presence of movements.

As shown in Table 9.2, the <DET1-PSD-1NN+DET2-PSD-LDA> design yields the best average true positive rate ((TP_R+TP_L)/2) of 47.0% in detecting the right and the left hand movements in the context of a 3-state self-paced BCI. This is higher than the 40.1% best average true positive rate achieved in the previous study ((Bashashati et al 2007b)).

The design of DET2 that uses the logarithm of PSD features yield better performance than the design that uses the PSD features, since <DET1-LF_{V5}-1NN+DET2-logPSD-LDA> performs better than <DET1-LF_{V5}-1NN+DET2-PSD-LDA>. The results also show that the use of DET1-LF_{V5}-1NN and DET1-PSD-1NN in a 3-state self-paced BCI yield 7.9% and 13.1% better average true positive rates $((TP_R+TP_L)/2)$ than the use of DET1-LF_{V4}-1NN and DET1-PSD-LDA, respectively. This is when all these designs are followed by the same design of DET2, i.e., DET2-PSD-LDA.

The overall performance of both the 2-state and the 3-state BCI systems vary across the subjects depending on the type of the design used. Given the variable performance of subjects across the two designs, an approach that can select a suitable design and adapt to each subject might achieve better detection rates. Significant gains may also be achieved from the combination of several single designs if these designs provide complementary information for the classification task. Several studies have demonstrated some evidence that existing independent features related to movement tasks could be used to achieve better classification accuracies (Babiloni et al 1999, Dornhege et al 2003, Dornhege et al 2004).

In this study, we evaluated several design combinations of DET1 and DET2, however, there are still other possible combinations (e.g. <DET1-PSD-1NN + DET2-logPSD-LDA>) that need to be evaluated in the future and may improve the performance of the system. We have shown that logarithm of PSD features yield superior results than PSD features when used in DET2 design. Applying this function to the PSD features of DET1 may also improve the performance of this detector and overall performance of the system.

Both the 2-state and the 3-state self-paced BCIs in this study and in the previous studies (Bashashati et al 2006b, Bashashati et al 2007b) were specifically designed to support NC state (refer to Chapter 1 for definition of NC support). In our studies, both BCIs were tested on a NC state data that would be expected to be the most difficult one as it is surrounded by the IC state data. *However, a more thorough study is needed to evaluate the performance of such systems on different and a larger variety of NC state data. Ideally, the NC state data include all the brain states except for the intentional control state and the system should not be activated during NC state periods.*

In the experimental paradigm used in this study, no feedback during the performed tasks was provided to the subjects. While we adopted this paradigm to simulate a more natural mode of control, this may have caused a lower performance in some subjects. Moreover, no subject pre-screening and no prior training were performed before the sessions. Thus, providing feedback during sessions and also training subjects like shown by other researchers (e.g. Millan et al 2002) may also improve the results of this study. Use of more efficient feature extraction and classification methods, subject training, providing online feedback during the performed task and verifying the results on more subjects are in the scope of our future directions to improve these results.

9.7. References

Babiloni C, Carducci F, Cincotti F, Rossini P M, Neuper C, Pfurtscheller G and Babiloni F 1999 Human movement-related potentials vs desynchronization of EEG alpha rhythm: A high-resolution EEG study *NeuroImage* **10** 658–65.

Bashashati A, Fatourechi M, Ward R K and Birch G E 2006a User customization of the feature generator of an asynchronous brain interface *Annals of Biomedical Engineering* **34** 1051-60

Bashashati A, Mason S, Ward R K and Birch G E 2006b An improved asynchronous brain interface: making use of the temporal history of the LF-ASD feature vectors *J. Neural Eng.* **3** 87-94.

Bashashati A, Fatourechi M, Ward R K and Birch G E 2007a A survey of signal processing algorithms in brain-computer interfaces based on electrical brain signals *J Neural Eng* **4** R35-57.

Bashashati A, Ward R and Birch G 2007b Towards Development of a 3-State Self-Paced Brain Interface Based on Hand Extension Movements *J Computational Intelligence & Neuroscience* In press.

Blankertz B, Dornhege G, Krauledat M, Muller K R, Kunzmann V, Losch F and Curio G 2006 The Berlin Brain-Computer Interface: EEG-based communication without subject training *IEEE Trans. Neural Syst. Rehabil. Eng.* **11** 147-52.

Borisoff J F, Mason S G, Bashashati A and Birch G E 2004 Brain-computer interface design for asynchronous control applications: improvements to the LF-ASD asynchronous brain switch *IEEE Trans. Biomed. Eng.* **51** 985-92.

Brunner C, Scherer R, Graimann B, Supp G and Pfurtscheller G 2006 Online Control of a Brain-Computer Interface Using Phase Synchronization *IEEE. Trans. Biomed. Eng.* **53** 2501-6.

Dornhege G, Blankertz B, Curio G and Müller K R 2004 Boosting bit rates in non-invasive EEG single-trial classifications by feature combination and multi-class paradigms *IEEE Trans. Biomed. Eng.* **51** 993–1002.

Dornhege G, Blankertz B, Curio G and Müller K R 2003 Combining features for BCI *Advances in Neural Inf. Proc. Systems (NIPS 02)*, eds Becker S, Thrun S and Obermayer K **15** 1115-22.

Jayant N S and Noll P 1984 Digital Coding of Waveforms (NJ: Prentice Hall).

Kohonen T 1990 Self-organizing map *Proceedings of IEEE* **78** 1464-80

Lachenbruch P A 1975 *Discriminant Analysis* (NY: Hafner Press)

Levine S P, Huggins J E, Bement S L, Kushwaha R K, Schuh L A, Rohde M M, Passaro E A, Ross D A, Elisevich K V and

Mason S G, Bashashati A, Fatourechi M, Navarro K F and Birch G E 2007 A Comprehensive Survey of Brain Interface Technology Designs *Ann. Biomed. Eng.* **35** 137-69

Mason S G and Birch G E 2000 A brain-controlled switch for asynchronous control applications *IEEE Trans. Biomed. Eng.* **47** 1297-307.

Millan J R, Mourino J, Franze M, Cincotti F, Varsta M, Heikkonen J, Babiloni F 2002 A local neural classifier for the recognition of EEG patterns associated to mental tasks *IEEE Trans. Neural Networks* **13** 678-86.

Millan J R, Renkens F, Mourino J and Gerstner W 2004 Noninvasive brain-actuated control of a mobile robot by human EEG *IEEE Trans. Biomed. Eng.* **51** 1026-33.

Pregenzer M and Pfurtscheller G 1999 Frequency Component Selection for an EEG-Based Brain to Computer Interface *IEEE Trans Reh Eng* **7** 413-9.

Scherer R, Muller G R, Neuper C, Graimann B and Pfurtscheller G 2004 An asynchronously controlled EEG-based virtual keyboard: improvement of the spelling rate *IEEE Trans. Biomed. Eng.* **51** 979-84.

Scherer R, Lee F, Schlogl A, Leeb R, Bischot H and Pfurtscheller G 2007 Towards Self-Paced Brain-Computer Communication: Navigation through Virtual Worlds *IEEE Transactions on Biomedical Engineering*, In press.

Smith B J 2000 A Direct Brain Interface Based on Event-Related Potentials *IEEE Trans. Rehabil. Eng.* **8** 180-5.

Townsend G, Graimann B and Pfurtscheller G 2004 Continuous EEG classification during motor imagery--simulation of an asynchronous BCI *IEEE Trans. Neural Syst. Rehabil. Eng.* **12** 258-65.

Wang Y, Zhang Z, Li Y, Gao X, Gao S and Yang F 2004 BCI Competition 2003--Data set IV: an algorithm based on CSSD and FDA for classifying single-trial EEG *IEEE Trans Biomed. Eng.* **51** 1081-6.

Welch P 1967 The use of fast Fourier transform for the estimation of power spectra: A method based on time averaging over short, modified periodograms *IEEE Trans. Audio and Electroacoustics* **15** 70-3.

Witten I H and Frank E 2000 Data Mining (San Diego, CA: Academic Press).Wolpaw J R 2004 Brain-computer interfaces (BCIs) for communication and control: a mini-review *Suppl. Clin. Neurophysiol.* **57** 607-13.

Wolpaw J R and McFarland D J 2004 Control of a two-dimensional movement signal by a noninvasive brain-computer interface in humans *Proc. Natl. Acad. Sci. U. S. A.* **101** 17849-54.

Yom-Tov E and Inbar G F 2003 Detection of Movement-Related Potentials from the Electro-Encephalogram for possible use in a Brain-Computer Interface *Med. Bio. Eng. Comp.* **41** 85-93.

Chapter 10 Summary and Conclusions

10.1. Summary and Concluding Remarks

This research was motivated by the need for an assistive device for individuals with severe disabilities such as spinal cord injury (SCI) and amyotrophic lateral sclerosis (ALS). These individuals need a device that can directly translate brain signals to commands. BCIs can replace the neural pathways that are impaired by such disabilities.

This project had two goals:

(1) Improving a 2-state self-paced BCI that is capable of generating lower false positive rates. Initial evaluations of this system showed an average true positive rate of 51.3% with false positive rate of 2% (Borisoff *et al* 2004). The high false positive rate of the system made it unsuitable for practical applications. For example, a false positive rate of 2%, in this system, corresponds to an average of two false activations every six seconds.

(2) Performing a preliminary study to design and test the feasibility of the first 3-state self-paced BCI[25] that continuously monitors the intent of the user and is specifically designed to support the NC state.

To improve the 2-state self-paced BCI, three studies concerning the different building blocks (refer to Chapter 1) of the system were conducted. Through our different studies, the feature extraction and feature classification blocks of the 2-state system were improved. In these studies (Bashashati *et al* 2006a, 2006b) the response of the system during periods contaminated with EOG artifacts was not evaluated as these artifacts were believed to cause high false positive rates in the system. Since the improved self-paced BCI was customized for each user (Bashashati *et al* 2006a) and incorporated the past history of feature values in detecting user intents (Bashashati *et al* 2006b), it was thought to be more immune to electroculogram (EOG) artifacts. Therefore, another study was conducted to evaluate the 2-state self-paced BCI when the data contaminated with electroculogram (EOG) artifacts were not excluded from analysis. As a result, the self-paced BCI system is available to control all

[25] A 4-state self-paced BCI has been introduced very recently after we introduced the 3-state self-paced BCI (Scherer et al Aug 2007). Performance of the system introduced in this dissertation is compared to other BCI systems later in this section.

the time including the 15-34% of the time that the system was unavailable due to the presence of EOG artifacts (Bashashati *et al* 2006b).

Evaluation of the latest 2-state self-paced BCI, improved during this dissertation, on both able-bodied and disabled subjects show true positive (TP) rates of 73.5% and 47.3% at the fixed false positive rates of 2% and 1%, respectively (Bashashati *et al* 2007c). These are when the output of the system was blocked during EOG artifacts. Evaluation of the same system, when data including periods contaminated with EOG artifacts are included, show true positive rates of 68.0% and 40.6% at the fixed false positive rates of 2% and 1%, respectively. Based on these results, for example at a false positive rate of 2%, the user can activate the output by performing one to two attempts on average.

To achieve the second goal of this dissertation, several designs of a 3-state self-paced BCI were proposed and evaluated on four able-bodied subjects. Ideally, these systems can distinguish the intended control (IC) states from the no control (NC) state. The aim of this initial investigation was to examine the feasibility of a 3-state self-paced BCI and determine whether such a system has promise. While a 2-state self-paced BCI allows the user to execute only one command type, a 3-state one provides the user two types of command options, i.e. more control options. To our best knowledge, no 3-state BCI that is both continuously available for control, and is designed to support the NC state (as defined in Section 1.2.1) has been proposed before. The implemented 3-state self-paced BCI expands the latest design of the 2-state self-paced system discussed earlier in this thesis.

The proposed design of the 3-state self-paced BCI is comprised of two detectors: DET1 and DET2. DET1 determines whether a movement is present or not, and DET2 differentiates between the two movements. Since DET1 determines whether or not a movement is performed, it can be considered and independently used as a 2-state self-paced BCI. Thus, in the initial design of the 3-state self-paced BCI, the latest designs of the 2-state self-paced BCI developed in Chapters 5 and 6 are used in the design of DET1. Several design versions of the 3-state self-paced system were proposed and evaluated by data from able-bodied subjects. If used as a 2-state self-paced BCI, i.e. to determine whether or not a movement has occurred, the latest results show that the percentage of the true positive rate increases from 41.1% to 73.4% at a fixed rate of 1%. This is when hand extension movements are used instead of a

finger flexion. When the system is used as a 3-state self-paced BCI, the latest results show average right and left true positive rates of 42.2% and 51.9%, respectively.

Tables 10.1 and 10.2 compare the latest results of the 2-state and 3-state self-paced BCI systems developed during this dissertation with other BCI system in the literature. As shown in these two tables, the 2-state and 3-state self-paced BCI systems proposed in this thesis generate higher true positive rates at considerably lower false positive rates compared to other self-paced BCI systems. Note that the self-paced BCI system introduced in (Scherer et al 2007) has an additional output state; i.e. it is a 4-state self-paced BCI, however, the false positive rate of this system is too high compared to the false positive rate of the 3-state self-paced BCI introduced in this thesis. It should be, however, mentioned that it is difficult to directly compare the results of our study and other studies, as the recording equipment, recording and classification protocols, and mental task considered are different. In addition, the amount of data involved, the degree of training the subjects received before participating in the BCI experiments and the decision rate of the systems vary for different studies.

The techniques and ideas introduced in different parts of this dissertation not only have value for the 2-state and 3-state self-paced BCI systems introduced in this thesis but also can be applied to other self-paced and system-paced BCI systems .

TABLE 10.1 COMPARISON BETWEEN 2-STATE SELF-PACED BCI SYSTEMS

Reference	Self-paced	Supporting NC	True positive rate	False positive rate
(Graimann et al 2004, Levine et al 2000, Townsend et al 2004, Yom-Tov and Inbar 2003)	Yes	Yes	73%-94%	6%-28%
(Bashashati et al 2007c)[26]	Yes	Yes	47.3%	1%
(Bashashati et al 2007d&e)	Yes	Yes	73.4%	1%

[26] Note that the mean true positive rates of the 2-state self-paced BCI systems introduced in (Bashashati et al 2007c & 2007d & 2007e) are 100% at false positive rates of more than 6%.

TABLE 10.2 COMPARISON BETWEEN MULTI-STATE BCI SYSTEMS

Reference	Number of output states	Self-paced	Supporting NC	True positive rate	False positive rate
(Millan et al)	3	Yes	No	Not reported	Not reported
(Scherer et al 2007)	4	Yes	Yes	28.4%	16.9%
(Bashashati et al 2007d&e)[27]	3	Yes	Yes	47.0%	1%

10.2. Summary of Contributions

1- An important contribution of this dissertation relates to the comprehensive survey we carried out on the signal processing algorithms used in BCI systems (Bashashati et al 2007a). This survey is the first survey that covers more than 300 papers in the field of brain computer interfaces. It addresses the following key research questions: 1) what are the key signal processing components of a BCI, 2) what signal processing algorithms have been used in BCIs, and 3) which signal processing techniques have received more attention. This information is valuable for present researchers as well as newcomers to the field, as it allows them to find out which signal-processing methods have been used for a certain type of a BCI system.

Most of the contributions listed below are not only useful for the self-paced BCI system being developed during this dissertation but also have value for other BCI systems.

2- Like any control system that depends on pattern recognition or machine learning, any BCI system needs to be trained before a user can operate it. System training typically refers to training the classifier component of the system and requires well-defined training-data that include representative samples of each class of data. The proposed methods for generating training-data introduced in Chapter 4 (Bashashati *et al* 2007b) generate higher quality training-data from a population comprised of fuzzy training-data. In other words, these methods select a subset of the training-data that has a higher probability of being real events. As such, the proposed methods are directly applicable to other BCI designs, including

[27] Note that the mean true positive rates of the 3-state self-paced BCI system introduced in (Bashashati et al 2007d & 2007e) is close to 75% at false positive rates of more than 4%.

synchronized BCIs and other neuroscience applications where mental tasks such as imagined movements are involved.

3- In Chapter 5, the feature extraction parameters of the 2-state self-paced BCI were customized for each subject. The customization showed improvements in the system performance (Bashashati *et al* 2006a). This study emphasizes the variability of brain signals across subjects and the need for such personalization in any BCI design. More importantly, in our current 2-state self-paced system, such customization is crucial to ensure that the system is triggered only by movement-related potential patterns associated with the attempted finger flexion task.

4- In Chapter 6, a study that proposed the use of the past values of the features to detect the presence of an intentional control state at a certain instance showed improvements in the performance of the 2-state self-paced BCI (Bashashati *et al* 2006b). We expect that the idea of using past feature values might also be useful for other BCI systems and pattern recognition problems.

5- The last study related to the 2-state self-paced BCI system evaluated the BCI's performance when the output during eye-blink artifacts was not inactivated (Bashashati *et al* 2007c). In previous evaluation schemes, the data containing eye-blinks were *excluded* from further analysis. This study emphasized that comparing the results of the two types of BCI systems (those which include and those which block the data contaminated with artifacts from the analysis) is only possible in a pseudo-online testing paradigm, i.e. when the system continuously classifies the input signals as when used in a real application. This testing paradigm, for the case when the artifact contaminated data is blocked from the analysis, forces the output to remain in the NC state during artifact presence. Such a testing paradigm is crucial in the sense that it provides a better estimate of the performance of the system for real online applications. Another contribution of this study relates to the fact that the performance of the system does not significantly degrade when the data containing eye-blink artifacts are included in the analysis. In addition, the system provides the user full control of the BCI which was not the case before. When the output was blocked during periods of artifacts, the system was found to be not usable for 15-34% of the time.

6- The 3-state self-paced BCI proposed in this study is the first 3-state BCI system that is available for control at all times and supports the no control (NC) state. In other words, the currently developed system continuously differentiates the predefined intended control states (i.e. right and the left hand extensions) from the NC state. Ideally, the NC state should include any brain state other than the predefined IC states.

7- The study for designing a 3-state self-paced BCI system also led us to a new set of movements, i.e. right and left hand extension movements that has more promise in controlling a 2-state BCI system. Using a right or a left hand extension movement instead of a finger flexion significantly improved the performance in detecting the presence of a movement (Bashashati *et al* 2007d). This finding is important since it is shown that improvements were significant when hand extension movements were used instead of a finger flexion as the neurophysiological control source.

8- The designs of DET1, which detects the presence of a movement in the 3-state self-paced BCI, are directly usable in the design of a 2-state self-paced system. For example, the design of DET1 that is based on the power spectral density features and a 1-nearest neighbor classifier outperformed the design of the latest 2-state self-paced BCI. As such, it can be used in the context of a 2-state self-paced BCI.

10.3. Discussions and Future Directions

Non-muscular communication and control are no longer a merely speculation. The results presented in this dissertation along with many studies in the field of BCI show that direct communication from the brain to the external world is possible and can serve useful purposes. At the same time, the reality does not yet match the fantasy: BCIs are not yet able to fly airplanes and are not likely to be doing so anytime soon. However, for people with no voluntary muscle control or in whom the remaining control (e.g. eye movement) is weak, easily fatigued, or unreliable, the current modest capacity of BCI systems may be valuable. For people who are totally paralyzed (e.g. by ALS, brainstem stroke, or severe polyneuropathy) or lack any useful muscle control (e.g. due to severe cerebral palsy), a BCI might give them the ability to answer simple questions, control the environment (e.g. lights, temperature, television, etc.), perform slow word processing, or even operate a neuroprosthesis.

There are a number of related issues that can be investigated as an extension to the research presented in this thesis. Some of these topics are presented in this section.

The algorithms developed in this dissertation were all tested in an offline setting, i.e. the data to test the different designs for a BCI system were first recorded and then analyzed. Offline analysis of the data is necessary to evaluate the different designs before performing an online test of the final design. A study that confirms the findings of this research in an online setting is needed in the future.

The study in (Bashashati et al 2006a) showed that user customization of a BCI is useful. In this study, the parameter values of the BCI system were customized based on the training data. Since the performance of the subjects over time is an issue that needs to be extensively studied, and since the brain signals are variable over time, developing a customization scheme that continuously tunes the parameters of the BCI system over time is useful for real-world applications.

In this research, we showed that the 2-state self-paced BCI system is better at detecting a right or a left hand extension movement than a finger flexion movement (Bashashati et al 2007d). However, since the data for hand extension movements and finger flexion movements were gathered in separate studies, this comparison is not totally accurate. A study that records the data related to these movements in the same experimental setting and on a large number of subjects is necessary to confirm these findings.

Although the performance of the BCI system in detecting the presence of any of a right or a left hand movement was better than the finger flexion, these movements may not be optimal when used in the context of a 3-state self-paced BCI. In other words, there might be alternative movements that are more differentiable from each other and also from the NC state. Therefore, a study that investigates other movements, such as right and left hand flexions, right and left finger flexion and right and left foot movements, is useful in finding the optimal movements. If such movements exist, they can potentially yield more improvements in the performance of the 3-state self-paced system.

The aim of the study on the 3-state self-paced BCI was to examine whether or not such a self-paced BCI has promise. Results of the evaluation of the system on four able-bodied subjects show promising results. However, more studies are needed to improve this system.

The use of nonlinear classifiers and exploring other approaches that combine the different feature extraction and feature classification methods should also be in the scope of future studies.

Although both the 2-state and 3-state self-paced BCI system in this thesis were tested in a specific experimental paradigm and on NC state data that were supposed to be the most difficult one as they were surrounded by IC state data, a more thorough study is needed to investigate the performance of the systems under *different experimental paradigms and on different sets of NC state data*, e.g. when the person perform different mental tasks except for the IC task. This study would provide a better estimate of the performance of a self-paced BCI system in a real-world application.

We implemented a specific design of a 3-state self-paced BCI. This system detects a right or a left hand extension via a sequential decision making paradigm. The system, at first, detects whether or not a movement is present. If a movement is detected, the system classifies it as a right or a left hand one. Another possible design of a 3-state BCI would be a system that consists of three decision modules in parallel. Each module differentiates between one of IC1 and IC2 classes from the NC class. Finally, by using a voting system, the output can be classified to any of the three states, i.e. NC, IC1 and IC2. Since this system uses three decision modules and majority voting (instead of the two modules used for the current design (Bashashati et al 2007d)), it may result in a better performance of the 3-state self-paced BCI.

The false positive rate of 1% for both the 2-state and the 3-state self-paced BCIs is still high for most practical applications. A false positive rate of 1% corresponds to a false activation of the system, on average, every six seconds. Therefore, future studies are still needed to decrease the false positive rate.

The overall performance of both the 2-state and the 3-state BCI systems vary across the subjects depending on the type of the design used. Given the variable performance of subjects across the two designs, an approach that can select a suitable design and adapt to each subject might overcome the subject performance variability across different designs and achieve better detection rates. Significant gains may also be achieved when combining several single designs if these designs provide complementary information for the classification task. Several studies have demonstrated some evidence that existing

independent features related to movement tasks could be used to achieve better classification accuracies (Babiloni et al 1999, Dornhege et al 2003, Dornhege et al 2004).

The study on the 3-state self-paced BCI did not focus on training subjects and did not provide any online feedback during the data recording. A future study that investigates the effect of subject training and provides biofeedback might be useful in achieving better performances. Specifically, this might be useful for subjects that do not perform well in the first few sessions. There have been some studies that showed that BCI performance increase after a few training sessions (e.g. Millan and Mourino 2002).

While synchronized control requires a cuing mechanism in its design, the presence of a cuing mechanism in an experimental protocol does not imply that the system operates in a synchronized control paradigm. Cues are an essential part of the synchronized system design. They let the user know when the system is about to start interpreting their data as control. For synchronized BCI systems, the cues are generally used to tell the user 'get ready to start controlling'. In BCI systems that support the NC state and that evaluate the system in a specific time, the cues indicate that a control period will be starting soon if they want to control the system at that time but the user has the option of not controlling the device. Cues are also used as experimental constraints (i.e., not part of the BCI system design). As experimental constraints, cues are used to guide the user into some state, such as IC or NC. In this way, one could set up an experimental system with a user operating a self-paced BCI system (design) and using a separate cuing mechanism to force the user to control the self-paced system when desired by the experimenters. Such a setup does not imply a synchronized transducer, but instead indicate a tightly constrained experimental setup. However, true testing of BCI technology for individuals with severe motor disabilities will require self-paced actions and timing. Ideally, a self-paced testing protocol is desired to test the developed system in this thesis although this type of protocol involves many issues related to how to generate the estimated intended output and must rely on user self-report of true positives and false negatives.

10.4. Applications of 2-State and 3-State Self-Paced BCIs

Assistive Technology (AT) is a generic term that includes assistive, adaptive, and rehabilitative devices and the process used in selecting, locating, and using them. AT

promotes greater independence for people with disabilities by enabling them to perform tasks they were formerly unable to accomplish, or had great difficulty accomplishing, by providing enhancements or changed methods for interaction with the technology needed to accomplish such tasks. Brain computer interfaces can be used in many assistive devices to help individuals with severe disabilities to interact with different devices. In this section, we provide a simple example application of 2-state and 3-state self-paced BCI systems that can be used to assist individuals with disabilities.

In this example application, the user interface can display a menu system (for an example see Fig.10.1(a)) with several action items such as 'Turn TV on', 'Turn lights on', etc. A 2-state self-paced BCI can be used to help the user select the desired item. In such a case, each menu item is sequentially highlighted for a specific period (e.g. 1s). If the user decides to activate an item in the menu, e.g. turn the TV on, he/she should wait until the desired button is highlighted (Fig.10.1(b)). Then the user can click the item by activating the 2-state self-paced BCI. The same user interface can be controlled more conveniently by a 3-state self-paced BCI. In such a case, the user does not need to wait until the desired menu item is highlighted by the system. Instead, he/she can use the first intentional control state (IC1), e.g. right hand extension, to navigate through different menu items and highlight the desired item. Then, the desired item can be activated by performing the second intentional control state (IC2), e.g. left hand extension.

If the system goes to a standby mode after clicking the 'stand by' item in the menu, a 3-state system (compared to a 2-state one) may also provide an easier way of resuming the function of the system. This task can be achieved by, for example, executing a specific sequence of IC1 and IC2 tasks. However, by using a 2-state self-paced BCI, a more complicated strategy may be needed to resume the function of the system.

The above example showed a possible application of 2-state and 3-state self-paced BCIs. This idea can be simply implmented for other applications like wheelchair control or word procesors. For a wheelchair control application, the same menu system with desired control options can be implemented in a palm pilot mounted on the wheelchair. A word processing application could be implemneted using a scanning keyborad and either a 2-state or a 3-state self-paced BCI.

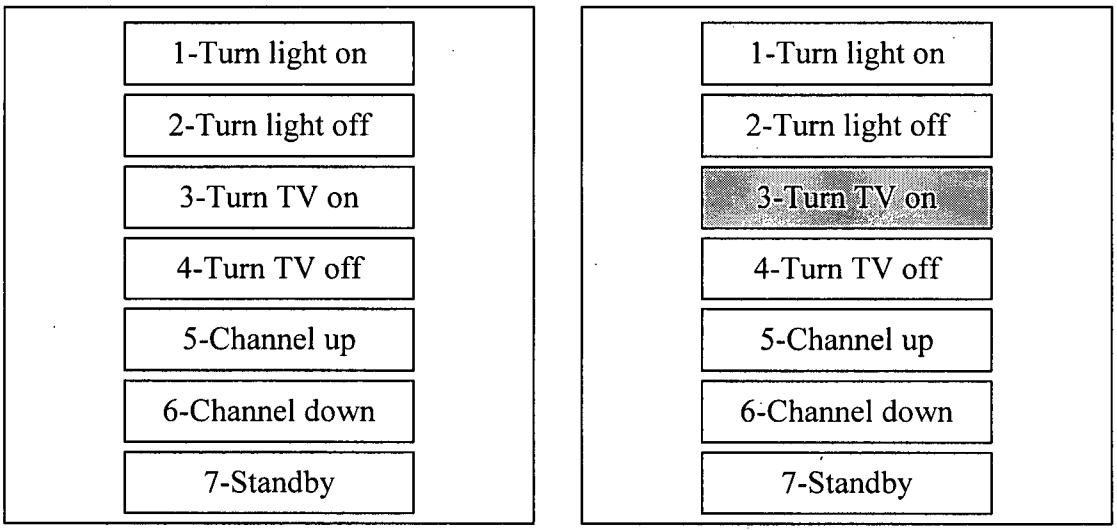

(a) (b)

Figure 10.1 Example of a BCI user interface

10.5. References

Bashashati A, Fatourechi M, Ward R K and Birch G E 2006a User customization of the feature generator of an asynchronous brain interface *Annals of Biomedical Engineering* **34** 1051-60

Bashashati A, Fatourechi M, Ward R K and Birch G E 2007a - A Survey of signal processing algorithms in brain-computer interfaces based brain electrical signals *J of Neural Engineering* **4** R35-57

Bashashati A, Mason S, Ward R K and Birch G E 2006b An improved asynchronous brain interface: Making use of the temporal history of the LF-ASD feature vectors **3**(2) 87-94

Bashashati A, Mason S G, Borisoff J F, Ward R K and Birch G E 2007b A comparative study on generating training-data for self-paced brain interfaces *IEEE transactions on neural systems and rehabilitation engineering* **15** 59-66

Bashashati A, Noureddin B, Ward R, Lawrence P and Birch G 2007c Effects of eye blinks on the performance of a self-paced brain interface *Clinical Neurophysiology* **118** 1639-47.

Bashashati A, Ward R and Birch G 2007d Towards development of a 3-state self-paced brain interface based on hand extension movements *J Computational Intelligence & Neuroscience* In press.

Bashashati A, Ward R and Birch G 2007e Improving the performance of a 3-state self-paced brain computer interface *To be submitted.*

Birch G E, Bozorgzadeh Z and Mason S G 2002 Initial on-line evaluations of the LF-ASD brain-computer interface with able-bodied and spinal-cord subjects using imagined voluntary motor potentials *IEEE Transactions on Neural Systems and Rehabilitation Engineering* **10** 219-24

Levine S P, Huggins J E, Bement S L, Kushwaha R K, Schuh L A, Rohde M M, Passaro E A, Ross D A, Elisevich K V and

Millan J R, Mourino J, Franze M, Cincotti F, Varsta M, Heikkonen J, Babiloni F 2002 A local neural classifier for the recognition of EEG patterns associated to mental tasks *IEEE Trans. Neural Networks* **13** 678-86.

Scherer R, Muller G R, Neuper C, Graimann B and Pfurtscheller G 2004 An asynchronously controlled EEG-based virtual keyboard: improvement of the spelling rate *IEEE Trans. Biomed. Eng.* **51** 979-84.

Scherer R, Lee F, Schlogl A, Leeb R, Bischot H and Pfurtscheller G 2007 Towards Self-Paced Brain-Computer Communication: Navigation through Virtual Worlds *IEEE Transactions on Biomedical Engineering*, In press.

Townsend G, Graimann B and Pfurtscheller G 2004 Continuous EEG classification during motor imagery--simulation of an asynchronous BCI *IEEE Trans. Neural Syst. Rehabil. Eng.* **12** 258-65.

Yom-Tov E and Inbar G F 2003 Detection of Movement-Related Potentials from the Electro-Encephalogram for possible use in a Brain-Computer Interface *Med. Bio. Eng. Comp.* **41** 85-93.

Appendix B. Expanded Tables of Chapter 2[28]

TABLE B.0.1 FEATURE EXTRACTION METHODS IN BCI DESIGNS

Neurological phenomenon		Feature Extraction method			Reference ID
Sensorimotor Activity	***Changes in brain rhythms (Mu, Beta, and Gamma)***	**Spectral parameters**	***Using AR parameters***		(Fabiani *et al* 2004, Kubler *et al* 2005, McFarland and Wolpaw 1998, McFarland *et al* 1997, McFarland *et al* 2003, McFarland *et al* 2005, Schalk *et al* 2000, Sheikh *et al* 2003, Wolpaw *et al* 1997, Wolpaw *et al* 2000, Wolpaw and McFarland 2004)
			Using BPF - squaring		(Guger *et al* 2003a, Ivanova *et al* 1995, Kalcher *et al* 1992, Krausz *et al* 2003, Neuper *et al* 2003, Neuper *et al* 2005, Pfurtscheller *et al* 2005, Pfurtscheller *et al* 1994, Pfurtscheller *et al* 1996, Pfurtscheller and Neuper 2001, Pfurtscheller *et al* 2003a, Pregenzer and Pfurtscheller 1995, Jia *et al* 2004)
			Using BPF		(Trejo *et al* 2003)
			Using FFT-based methods	***FFT***	(Coyle *et al* 2005, Pfurtscheller *et al* 2000, Pregenzer and Pfurtscheller 1999, Wolpaw and McFarland 1994, Wolpaw *et al* 2000)
				Periodograms such as Welch algorithm	(Babiloni *et al* 2000, Babiloni *et al* 2001a, Babiloni *et al* 2001b, Cincotti *et al* 2001, Cincotti *et al* 2003a, Cincotti *et al* 2003b, Kelly *et al* 2002b, Lal *et al* 2004, Millan *et al* 2002a, Millan *et al* 2002b)
				FFT - VEFD	(Pineda *et al* 2003)
				CSP - FFT	(Blanchard and Blankertz 2004)
			CSP - log-transformation of the variance of the resulting time series (captures ERD/ERS)		(Guger *et al* 2000b, Krauledat *et al* 2004, Pfurtscheller *et al* 2000, Pfurtscheller and Neuper 2001, Ramoser *et al* 2000, Townsend *et al* 2004)
			CSSP - log-transformation of the variance of the resulting time series		(Lemm *et al* 2005)
			Details not mentioned		(Boostani and Moradi 2004, Flotzinger *et al* 1994, Kalcher *et al* 1993, Leeb and Pfurtscheller 2004, Mahmoudi and Erfanian 2002, Mason and Birch 2000, Muller *et al* 2003c, Muller-Putz *et al* 2005b, Pfurtscheller *et al* 1993, Pfurtscheller *et al* 1997, Pfurtscheller *et al* 1998, Pfurtscheller and Neuper 2001, Pfurtscheller *et al* 2003b, Wolpaw *et al* 1991, Wolpaw *et al* 2003, Li *et al* 2004a)
		Parametric modeling	***BPF in the Mu band - AR parameters***		(Peters *et al* 2001)

[28] The extended tables of Chapter 2 are published online by the Journal of Neural Engineering.

TABLE B.0.1 FEATURE EXTRACTION METHODS IN BCI DESIGNS (CONTINUED)

	BPF-ICA-dipole analysis		(Qin *et al* 2004a, Qin *et al* 2005)
	BPF-ICA-dipole analysis-cortical current density		(Qin *et al* 2004a)
	TFR method	***Wavelet transform***	(Lemm *et al* 2004, Qin *et al* 2005)
		Wavelet transform - difference between Left/Right hemisphere features	(Qin and He 2005)
		{Wavelet- BPF} - ICA - dipole analysis	(Qin *et al* 2004b)
		{Wavelet- BPF} - ICA - dipole analysis - cortical current density	(Qin *et al* 2004b)
	Signal envelope (calculated by Hilbert transform) – Cross- correlation		(Wang *et al* 2004b, Wang *et al* 2004a)
	Analog circuit to extract Mu-band (8-12Hz) power		(LaCourse and Wilson 2003)
	Contralateral and ipsilateral rebound maps		(Hung *et al* 2005)
MRP	**Parametric modeling**	***AR parameters***	(Burke *et al* 2005)
		ARX parameters	(Burke *et al* 2005)
	TFR method	***A custom made TFR method***	(Birch *et al* 2002, Birch *et al* 2003, Borisoff *et al* 2004, Bozorgzadeh *et al* 2000, Fatourechi *et al* 2004, Fatourechi *et al* 2005, Lisogurski and Birch 1998, Mason and Birch 2000, Mason *et al* 2004, Yom-Tov and Inbar 2003)
		Wavelet transform	(Glassman 2005)
		A custom made TFR method - construction of the trajectory of features	(Bashashati *et al* 2005)
	LRP features (sub-sampling the data - FFT and taking the bins in the interested pass band - IFFT)		(Blankertz *et al* 2002a, Blankertz *et al* 2003, Krauledat *et al* 2004)
	Combination of different feature extraction methods	***LRP + {CSP - log-transformation of the variance of the resulting time series }***	(Dornhege *et al* 2003)
	Matched filter		(Yom-Tov and Inbar 2003)
	None		(Barreto *et al* 1996a, Barreto *et al* 1996b, Blankertz *et al* 2002a)
Other Sensorimotor activity	**Spectral parameters**	***Using AR parameters***	(Cho *et al* 2004)
		Using FFT	(Garcia *et al* 2003b)
		Details not mentioned	(Mahmoudi and Erfanian 2002, Scherer *et al* 2004)
	Parametric modeling	***AAR parameters using Kalman filtering method***	(Graimann *et al* 2003b, Schlogl *et al* 2003)

TABLE B.0.1 FEATURE EXTRACTION METHODS IN BCI DESIGNS (CONTINUED)

	AAR parameters using LMS method	(Huggins *et al* 2003, Neuper *et al* 1999, Obermaier *et al* 2001b, Pfurtscheller *et al* 1998, Pfurtscheller *et al* 2000, Pfurtscheller and Neuper 2001, Schloegl *et al* 1997a, Schloegl *et al* 1997b)
	AAR parameters (details not mentioned)	(Guger *et al* 1999, Guger *et al* 2000a, Guger *et al* 2003a, Guger *et al* 2003b, Haselsteiner and Pfurtscheller 2000, Obermaier *et al* 2001a, Pfurtscheller and Guger 1999)
	AR parameters	(Burke *et al* 2002, Kelly *et al* 2002b, Kelly *et al* 2002a, Lal *et al* 2004, Peters *et al* 2001, Schröder *et al* 2005, Sykacek *et al* 2003, Yoon *et al* 2005)
	ARX parameters	(Burke *et al* 2002, Kelly *et al* 2002b, Kelly *et al* 2002a)
TFR methods	***Wavelet transform***	(Huggins *et al* 2003)
	AGR	(Costa and Cabral 2000)
	CTFR	(Garcia *et al* 2003a, Garcia *et al* 2003b)
	Time-frequency expansion (part of a commercial software: Thoughtform Interpretation Studio TIS 2.0)	(Pineda *et al* 2000)
CCTM		(Balbale *et al* 1999, Graimann *et al* 2003b, Huggins *et al* 1999, Huggins *et al* 2003, Levine *et al* 1999, Levine *et al* 2000)
Quadratic modeling		(Huggins *et al* 2003)
Hjorth parameters		(Boostani and Moradi 2004, Lee and Choi 2002, Obermaier *et al* 2001a, Obermaier *et al* 2001c, Pfurtscheller and Neuper 2001)
SOFNN one step ahead prediction - mean square error (MSE) or mean squared of the predicted signal		(Coyle *et al* 2004)
OPM		(Mason and Birch 2000)
Signal complexity	***Fractal dimension***	(Boostani and Moradi 2004)
	Coarse-grained entropy rate (CER)	(Trejo *et al* 2003)
	Gaussian process entropy rates (GPER)	(Trejo *et al* 2003)
	spectral entropy (SE)	(Trejo *et al* 2003)
	wavelet entropy (WE)	(Trejo *et al* 2003)
	Embedding space decomposition	(Roberts *et al* 1999)
Combination of different feature extraction methods	***AR + PSD + Barlow + mean + STD***	(Yom-Tov and Inbar 2001, Yom-Tov and Inbar 2002)
	Relative power of specific frequency band + mean absolute value + variance	(Mahmoudi and Erfanian 2002)
	Mean absolute value + variance	(Mahmoudi and Erfanian 2002)

TABLE B.0.1 FEATURE EXTRACTION METHODS IN BCI DESIGNS (CONTINUED)

	CSP - log-transformation of the variance of the resulting time series		(Xu *et al* 2004b)
	{ Combined PCA + CSP} - log-transformation of the variance of the resulting time series		(Xu *et al* 2004b)
	Feature coherence (part of a commercial software: Thoughtform Interpretation Studio TIS 2.0)		(Pineda *et al* 2000)
	None		(Lee and Choi 2002, Lee and Choi 2003, Mahmoudi and Erfanian 2002, Parra *et al* 2002, Parra *et al* 2003a, Schroder *et al* 2003, Trejo *et al* 2003)
MN: Changes in brain rhythms (Mu, Beta, and Gamma) + Other sensorimotor activity	**Spectral parameters**	***Details not mentioned***	(Garrett *et al* 2003)
	CCTM		(Graimann *et al* 2004)
	TFR method	***Wavelet transform***	(Graimann *et al* 2003a, Graimann *et al* 2004)
	Shrinking LORETA-FOCUSS - 3-D micro-state analysis		(Liu *et al* 2003)
	Combination of different feature extraction methods	***Power spectra in Mu band + time features (ratio of two areas under the energy accumulation curve)***	(Cheng *et al* 2004)
MN: Changes in brain rhythms (Mu, Beta, and Gamma) + MRP + Other sensorimotor activity	**Combination of different feature extraction methods**	***LRP features + AR + {CSP - log-transformation of the variance of the resulting time series } + variance***	(Muller *et al* 2003b)
MN: Changes in brain rhythms (Mu, Beta, and Gamma) + MRP	**BPF in 0-4Hz and Mu bands - CSSD**		(Li *et al* 2004b, Wang *et al* 2004d)
	Combination of different feature extraction methods	***{CSP - log-transformation of the variance of the resulting time series } + LRP features***	(Krauledat *et al* 2004)
		LRP features + AR + {CSP - log-transformation of the variance of the resulting time series } + variance	(Dornhege *et al* 2004)

TABLE B.0.1 FEATURE EXTRACTION METHODS IN BCI DESIGNS (CONTINUED)

	Amplitude between N2 and P2 peaks			(Lee *et al* 2005)
	None			(Guan *et al* 2005, Vidal 1977)
Response to Mental Tasks[29]	**Spectral parameters**	***Using FFT-based methods***	***FFT***	(Bashashati *et al* 2003, Kostov and Polak 1997, Liu *et al* 2005, Polak and Kostov 1997, Polak and Kostov 1998, Wang *et al* 2005a)
			Periodograms such as Welch's method	(Peterson *et al* 2005)
		Using WK method		(Keirn and Aunon 1990, Palaniappan *et al* 2002)
		Using AR parameters		(Keirn and Aunon 1990, Palaniappan *et al* 2002)
		Method not mentioned		(Millan *et al* 1998, Palaniappan 2005)
	Parametric modeling	***AR parameters***		(Anderson *et al* 1995b, Anderson *et al* 1998, Garrett *et al* 2003, Huan and Palaniappan 2004, Keirn and Aunon 1990, Kostov and Polak 2000, Huan and Palaniappan 2005, Polak and Kostov 1998, Polak and Kostov 1999, Sykacek *et al* 2003)
		AAR using LMS method		(Huan and Palaniappan 2004, Huan and Palaniappan 2005)
		Multivariate AR coefficients		(Anderson *et al* 1995b, Anderson *et al* 1998)
	Signal Complexity	***Fractal dimension***		(Bashashati *et al* 2003, Tavakolian *et al* 2004)
	Eigen values of correlation matrix			(Anderson *et al* 1998)
	LPC using Burg's method			(Kostov and Polak 1997)
	None			(Anderson *et al* 1995a, Panuccio *et al* 2002)
ANC	**Cross-covariance of each neuron's activity with one another - Principal Component Analysis (PCA)**			(Isaacs *et al* 2000)
	LBG vector quantization (VQ)			(Darmanjian *et al* 2003)
	Filtering - rectification - thresholding			(Karniel *et al* 2002, Kositsky *et al* 2003, Reger *et al* 2000a, Reger *et al* 2000b)
	Averaging			(Laubach *et al* 2000, Otto *et al* 2003, Vetter *et al* 2003)
	TFR methods	***Wavelet transform***		(Laubach *et al* 2000, Musallam *et al* 2004)
	None - Most of these designs model the relationship between neural firing rates and 'position and/or velocity and/or acceleration' of hand			(Black *et al* 2003, Byron *et al* 2005, Carmena *et al* 2003, Carmena *et al* 2005, Chapin *et al* 1999, Gao *et al* 2002, Gao *et al* 2003a, Hatsopoulos *et al* 2004, Hu *et al* 2004, Karniel *et al* 2002, Kemere *et al* 2004, Kennedy *et al* 2000, Kim *et al* 2005a, Kim *et al* 2005b, Lebedev *et al* 2005, Olson *et al* 2005, Patil *et al* 2004, Rao *et al* 2005, Roushe *et al* 2003, Sanchez *et al* 2002a, Sanchez *et al* 2002b, Sanchez *et al* 2003, Serruya *et al* 2003, Serruya *et al* 2002, Taylor *et al* 2002, Taylor *et al* 2003, Wessberg *et al* 2000, Wu *et al* 2002a, Wu *et al* 2002b)

[29] Designs that differentiate between relaxed state and movement tasks are considered in "Sensorimotor activity + Response to Mental Tasks" category.

TABLE B.0.1 FEATURE EXTRACTION METHODS IN BCI DESIGNS (CONTINUED)

MN: Sensorimotor activity + Response to Mental Tasks	**Spectral parameters**	***Using FFT-based methods*** ***Periodograms such as Welch's method***	(Gysels and Celka 2004, Gysels *et al* 2005, Millan *et al* 2004a, Millan *et al* 2002b, Millan *et al* 2000a, Millan *et al* 2000b, Millan and Mourino 2003b, Millan *et al* 2004b, Varsta *et al* 2000, Millan *et al* 2003a)
		Using BPF	(Obermaier *et al* 2001d)
		Method not mentioned	(Millan *et al* 2002b, Millan 2004)
	Parametric modeling	***AR parameters***	(Curran *et al* 2004, Penny *et al* 2000, Roberts and Penny 2003, Sykacek *et al* 2004, Varsta *et al* 2000)
	TFR method	***Wavelet transform***	(Varsta *et al* 2000)
		CTFR	(Garcia and Ebrahimi 2002, Garcia *et al* 2002, Garcia *et al* 2003c, Molina *et al* 2003)
	Combination of different features	***PSD components + mean absolute value + variance + AR parameters etc.***	(Erfanian and Erfani 2004)
	PLV		(Gysels and Celka 2004, Gysels *et al* 2005)
	Mean spectral coherence		(Gysels and Celka 2004)
	None		(Mourino *et al* 2002, Rezek *et al* 2003)
MN: SCP + other brain rhythms	**SCP calculation + Power spectral parameters**		(Hinterberger and Baier 2005)
	Combination of SCP features (averaging technique) + Gamma band features (using Welch Periodogram method)		(Mensh *et al* 2004)

TABLE B.0.2 FEATURE CLASSIFICATION METHODS IN BCI DESIGNS THAT USE EEG AND ECOG RECORDING TECHNOLOGY

Feature Extraction method	Feature translation method		Reference ID
Spectral parameter	**Neural networks**	***MLP***	(Anderson *et al* 1995a, Ivanova *et al* 1995, Mahmoudi and Erfanian 2002, Palaniappan 2005, Su Ryu *et al* 1999)
		Committee of MLP neural network	(Millan *et al* 2002b, Millan *et al* 2000b, Varsta *et al* 2000)
		Committee of Plat's RAN algorithm (Platt 1991)	(Millan *et al* 1998)
		Committee of neural networks trained with Adaboost	(Boostani and Moradi 2004)
		TBNN	(Ivanova *et al* 1995)
		LVQ	(Flotzinger *et al* 1994, Ivanova *et al* 1995, Kalcher *et al* 1992, Kalcher *et al* 1993, Pfurtscheller *et al* 1993, Pfurtscheller *et al* 1994, Pfurtscheller *et al* 1996, Pfurtscheller *et al* 1997, Pfurtscheller *et al* 1998, Pfurtscheller *et al* 2000, Pfurtscheller and Neuper 2001, Pregenzer and Pfurtscheller 1999)
		kMeans - LVQ	(Mason and Birch 2000)
		DSLVQ	(Muller-Putz *et al* 2005a, Neuper *et al* 2005, Pregenzer and Pfurtscheller 1995, Pregenzer and Pfurtscheller 1999)
		Growing Hierachical SOM	(Liu *et al* 2005)
		ALN	(Kostov and Polak 1997, Polak and Kostov 1998)
		ANN	(Cincotti *et al* 2003b)
		Custom designed local neural network	(Millan *et al* 2002b, Millan *et al* 2000a, Millan and Mourino 2003b)
		Fuzzy ARTMAP	(Palaniappan *et al* 2002)
	(R)LDA[30]		(Boostani and Moradi 2004, Coyle *et al* 2005, Fabiani *et al* 2004, Garcia *et al* 2003b, Guger *et al* 2003a, Kelly *et al* 2002b, Kelly *et al* 2004, Kelly *et al* 2005c, Kelly *et al* 2005a, Krausz *et al* 2003, Lalor *et al* 2005, Leeb and Pfurtscheller 2004, Muller *et al* 2003c, Muller-Putz *et al* 2005a, Muller-Putz *et al* 2005b, Neuper *et al* 2003, Pfurtscheller *et al* 2003b, Jia *et al* 2004)
	(R)FLD		(Babiloni *et al* 2001b, Cincotti *et al* 2001, Cincotti *et al* 2003a, Pfurtscheller *et al* 2003a, Scherer *et al* 2004, Li *et al* 2004a)
	MD-based classifier		(Babiloni *et al* 2001a, Cincotti *et al* 2003a, Cincotti *et al* 2003b)

[30] Regularization may be applied before LDA classification scheme.

TABLE B.0.2 FEATURE CLASSIFICATION METHODS IN BCI DESIGNS THAT USE EEG AND ECOG RECORDING TECHNOLOGY (CONTINUED)

		Nonlinear discriminant function	(Fabiani *et al* 2004)
		Bayes quadratic classifier	(Keirn and Aunon 1990)
		Gaussian classifier	(Millan *et al* 2004a, Millan 2004, Millan *et al* 2004b, Milln *et al* 2003a)
		SSP	(Babiloni *et al* 2000, Babiloni *et al* 2001a, Babiloni *et al* 2001b, Cincotti *et al* 2001, Cincotti *et al* 2003a, Millan *et al* 2002b, Millan *et al* 2000b)
		SOM-based SSP	(Millan *et al* 2002b, Millan *et al* 2000b)
		HMM	(Cincotti *et al* 2003b, Obermaier *et al* 2001d)
		SVM	(Garrett *et al* 2003, Gysels and Celka 2004, Gysels *et al* 2005, Lal *et al* 2004, Peterson *et al* 2005)
		NID3	(Ivanova *et al* 1995)
		CN2	(Ivanova *et al* 1995)
		C4.5	(Ivanova *et al* 1995, Millan *et al* 2002a)
		k-NN	(Pregenzer and Pfurtscheller 1999)
		Threshold detector	(Calhoun and McMillan 1996, Cheng Ming *et al* 2005, Cheng and Gao 1999, Cheng *et al* 2001, Cheng *et al* 2002, Gao *et al* 2003b, Kelly *et al* 2005b, Kostov and Polak 1997, McMillan and Calhoun 1995, Middendorf *et al* 2000, Pfurtscheller *et al* 2005, Pineda *et al* 2003, Polak and Kostov 1997)
		Linear combination - Continuous feedback	(Fabiani *et al* 2004, Krausz *et al* 2003, Kubler *et al* 2005, McFarland and Wolpaw 1998, McFarland *et al* 1997, McFarland *et al* 2003, McFarland *et al* 2005, Schalk *et al* 2000, Sheikh *et al* 2003, Wolpaw and McFarland 1994, Wolpaw *et al* 1997, Wolpaw *et al* 2000, Wolpaw *et al* 2003, Wolpaw and McFarland 2004)
		Continuous feedback	(Bashashati *et al* 2003, Cho *et al* 2004, LaCourse and Wilson 2003, Middendorf *et al* 2000, Trejo *et al* 2003, Wolpaw *et al* 1991)
Parametric modeling	**AAR parameters**	**LDA**	(Guger *et al* 2003a, Guger *et al* 2003b, Huggins *et al* 2003, Neuper *et al* 1999, Obermaier *et al* 2001b, Pfurtscheller *et al* 1998, Pfurtscheller and Guger 1999, Pfurtscheller *et al* 2000, Pfurtscheller and Neuper 2001, Schloegl *et al* 1997a, Schloegl *et al* 1997b)
		FLD	(Guger *et al* 1999, Guger *et al* 2000a, Obermaier *et al* 2001a)

TABLE B.0.2 FEATURE CLASSIFICATION METHODS IN BCI DESIGNS THAT USE EEG AND ECOG RECORDING TECHNOLOGY (CONTINUED)

		Neural networks	***MLP neural network***	(Haselsteiner and Pfurtscheller 2000, Huan and Palaniappan 2005)
			FIR- MLP neural network	(Haselsteiner and Pfurtscheller 2000)
		Threshold detector		(Graimann *et al* 2003b)
		Continuous feedback using MD		(Schlogl *et al* 2003)
	(multivariate) AR parameters	**LDA**		(Burke *et al* 2002, Burke *et al* 2005, Garrett *et al* 2003, Huan and Palaniappan 2004, Kelly *et al* 2002b, Kelly *et al* 2002a)
		Bayesian logistic classifier (linear classifier)		(Curran *et al* 2004, Penny *et al* 2000, Roberts and Penny 2003)
		Bayes quadratic classifier		(Keirn and Aunon 1990)
		Neural networks	***MLP neural network***	(Anderson *et al* 1998, Garrett *et al* 2003, Huan and Palaniappan 2004, Huan and Palaniappan 2005, Schalk *et al* 2004)
			Committee of MLP neural network	(Varsta *et al* 2000)
			Committee of single Perceptrons with no hidden layers	(Peters *et al* 2001)
			ALN	(Kostov and Polak 2000, Polak and Kostov 1998, Polak and Kostov 1999)
		HMM		(Sykacek *et al* 2003)
		SVM		(Garrett *et al* 2003, Lal *et al* 2004, Schröder *et al* 2005, Yoon *et al* 2005)
		Variatioanal Kalman filter		(Sykacek *et al* 2004)
		Static classifier that is inferred with sequential variational inference (nonlinear generative classifier)		(Curran *et al* 2004, Sykacek *et al* 2004)
	ARX	**LDA**		(Burke *et al* 2002, Burke *et al* 2005, Kelly *et al* 2002b, Kelly *et al* 2002a)
X-Correlation		**Threshold detector**		(Balbale *et al* 1999, Bayliss and Ballard 1999, Bayliss and Ballard 2000a, Bayliss and Ballard 2000b, Farwell and Donchin 1988, Graimann *et al* 2003b, Graimann *et al* 2004, Huggins *et al* 1999, Huggins *et al* 2003, Levine *et al* 1999, Levine *et al* 2000, Sutter 1992, Wang *et al* 2004b, Wang *et al* 2004a)
TFR methods	***CTFR***	**LDA**		(Garcia *et al* 2003b)
		MD-based classifier		(Garcia and Ebrahimi 2002, Molina *et al* 2003)

TABLE B.0.2 FEATURE CLASSIFICATION METHODS IN BCI DESIGNS THAT USE EEG AND ECOG RECORDING TECHNOLOGY (CONTINUED)

	Neural networks	***Single layer neural network***	(Garcia *et al* 2002)
	SVM		(Garcia *et al* 2003a, Garcia *et al* 2003b, Garcia *et al* 2003c)
AGR	**Neural networks**	***MLP neural network***	(Costa and Cabral 2000)
A custom made TFR method	**Neural networks**	***kMeans - LVQ***	(Bashashati *et al* 2005, Birch *et al* 2002, Birch *et al* 2003, Borisoff *et al* 2004, Bozorgzadeh *et al* 2000, Fatourechi *et al* 2004, Fatourechi *et al* 2005, Lisogurski and Birch 1998, Mason and Birch 2000, Mason *et al* 2004, Yom-Tov and Inbar 2003)
		fART - LVQ	(Borisoff *et al* 2004)
	Threshold detector		(Yom-Tov and Inbar 2003)
	SVM		(Yom-Tov and Inbar 2003)
Wavelet transform	**LDA**		(Bostanov 2004, Fukada S *et al* 1998, Hinterberger *et al* 2003)
	ZDA		(Hinterberger *et al* 2003)
	Baysian classifier		(Lemm *et al* 2004)
	Neural networks	***MLP neural network***	(Fukada S *et al* 1998)
		Committee of MLP neural network	(Varsta *et al* 2000)
	SVM		(Glassman 2005)
	Threshold detector		(Donchin *et al* 2000, Graimann *et al* 2003a, Graimann *et al* 2004, Huggins *et al* 2003, Jansen *et al* 2004, Kawakami *et al* 1996, Qin and He 2005)
Matched filtering	**Threshold detector**		(Serby *et al* 2005)
Hjorth parameters	**LDA**		(Boostani and Moradi 2004)
	LDS		(Lee and Choi 2002)
	HMM		(Obermaier *et al* 2001a, Obermaier *et al* 2001c, Pfurtscheller and Neuper 2001)
	Neural networks	***Committee of neural networks trained with Adaboost***	(Boostani and Moradi 2004)
LRP features: (sub-sampling the data - FFT - taking the bins in the pass-band - IFFT)	**(R)LDA**		(Krauledat *et al* 2004)
	(R)FLD		(Blankertz *et al* 2002a, Blankertz *et al* 2003)
	Sparse FLD		(Blankertz *et al* 2002a)
	SVM		(Blankertz *et al* 2002a)
	k-NN		(Blankertz *et al* 2002a)

TABLE B.0.2 FEATURE CLASSIFICATION METHODS IN BCI DESIGNS THAT USE EEG AND ECOG RECORDING TECHNOLOGY (CONTINUED)

Calculation of SCP amplitude		**Continuous feedback followed by threshold detector**		(Birbaumer *et al* 1999, Birbaumer *et al* 2000, Hinterberger *et al* 2003, Hinterberger *et al* 2004a, Hinterberger *et al* 2004b, Hinterberger *et al* 2005b, Hinterberger *et al* 2005a, Kaiser *et al* 2001, Kaiser *et al* 2002, Kubler *et al* 1999, Kubler *et al* 2001b, Kubler *et al* 1998, Neumann *et al* 2003, Neumann *et al* 2004)
None		**LDA**		(Hinterberger *et al* 2003)
		Logistic regression		(Parra *et al* 2002, Parra *et al* 2003a)
		(R)FLD		(Blankertz *et al* 2002a)
		Sparse FLD		(Blankertz *et al* 2002a)
		ZDA		(Hinterberger *et al* 2003)
		Linear Bayian decision rule		(Vidal 1977)
		Neural networks	***MLP neural network***	(Anderson *et al* 1995a, Mahmoudi and Erfanian 2002, Yan Wang *et al* 2004)
			A custom designed local neural network	(Mourino *et al* 2002)
			Static neural classifier (Adaline)	(Barreto *et al* 1996a, Barreto *et al* 1996b)
			TDNN	(Barreto *et al* 1996a, Barreto *et al* 1996b)
			Gamma neural network	(Barreto *et al* 1996a, Barreto *et al* 1996b)
		HMM Based techniques	***CHMM***	(Rezek *et al* 2003)
			AR HMM	(Panuccio *et al* 2002)
			HMM + SVM	(Lee and Choi 2002, Lee and Choi 2003)
			HMM	(Lee and Choi 2003)
		SVM		(Blankertz *et al* 2002a, Guan *et al* 2004, Hill *et al* 2004, Guan *et al* 2005, Kaper and Ritter 2004a, Kaper and Ritter 2004b, Kaper *et al* 2004, Schroder *et al* 2003, Thulasidas *et al* 2004, Trejo *et al* 2003)
		k-NN		(Blankertz *et al* 2002a)
		LDS		(Lee and Choi 2002)
		Threshold detector		(Jansen *et al* 2004)
CSP	***CSP - log-transformation of the variance of the resulting time series***	**LDA**		(Guger *et al* 2000b, Krauledat *et al* 2004, Pfurtscheller *et al* 2000, Pfurtscheller and Neuper 2001, Townsend *et al* 2004)
		Linear combination – Threshold detector		(Townsend *et al* 2004)
		Linear classifier (no details)		(Ramoser *et al* 2000)

TABLE B.0.2 FEATURE CLASSIFICATION METHODS IN BCI DESIGNS THAT USE EEG AND ECOG RECORDING TECHNOLOGY (CONTINUED)

		SVM		(Xu *et al* 2004b)
	{Combined PCA-CSP} - log-transformation of the variance of the resulting time series	**SVM**		(Xu *et al* 2004b)
	CSP - FFT in Mu and Beta frequency bands	**(R)FLD**		(Blanchard and Blankertz 2004)
CSSP - log-transformation of the variance of the resulting time series		**LDA**		(Lemm *et al* 2005)
BPF in 0-4Hz and Mu bands - CSSD		**Single layer Perceptron model (a linear classifier)**		(Li *et al* 2004b, Wang *et al* 2004d)
Combination of different features	***LRP features + AR + CSP-based features + variance***	**(R)LDA**		(Dornhege *et al* 2004, Muller *et al* 2003b)
	LRP + CSP-based features	**(R)LDA**		(Dornhege *et al* 2003, Krauledat *et al* 2004)
	Relative power of specific frequency band + mean absolute value + variance	**Neural networks**	***MLP***	(Mahmoudi and Erfanian 2002)
	PSD components + mean absolute value + variance + AR parameters etc.	**Neural networks**	***MLP***	(Erfanian and Erfani 2004)
	Power in Mu+ time features (ratio of two areas under the energy accumulation curve)	**2-dimensional linear classifier trained by a non-enumerative search procedure**		(Cheng *et al* 2004)
	AR + PSD + Barlow + mean + STD	**SVM (using SVM-light software)**		(Yom-Tov and Inbar 2001, Yom-Tov and Inbar 2002)
	Combination of SCP features (averaging technique) and Gamma band features	**LDA**		(Mensh *et al* 2004)

TABLE B.0.2 FEATURE CLASSIFICATION METHODS IN BCI DESIGNS THAT USE EEG AND ECOG RECORDING TECHNOLOGY (CONTINUED)

Other methods		**Threshold detector**		(Allison and Pineda 2003, Bayliss 2003, Bayliss *et al* 2004, Donchin *et al* 2000, Farwell and Donchin 1988, Hinterberger *et al* 2003, Huggins *et al* 2003, Jansen *et al* 2004, Lee *et al* 2005, Polikoff *et al* 1995, Xu *et al* 2004a)
		HMM		(Liu *et al* 2003)
		FLD		(Hung *et al* 2005)
		LDA		(Coyle *et al* 2004)
		Linear classifier based on time-warping		(Mason and Birch 2000)
		Neural networks	***MLP neural network***	(Anderson *et al* 1998, Hung *et al* 2005, Mahmoudi and Erfanian 2002)
			ALN	(Kostov and Polak 1997)
			RBF-NN	(Hung *et al* 2005)
		SVM		(Gysels and Celka 2004, Gysels and Celka 2004, Gysels *et al* 2005, Hung *et al* 2005)
		Random forest algorithm		(Neuper *et al* 1999)
		k-NN		(Pineda *et al* 2000)
		Continuous audio feedback		(Hinterberger and Baier 2005)
Signal complexity	***Fractal dimension***	**LDA**		(Boostani and Moradi 2004)
		Neural networks	***Committee of neural networks trained with Adaboost***	(Boostani and Moradi 2004)
			MLP neural network	(Tavakolian *et al* 2004)
		Continuous feedback		(Bashashati *et al* 2003)
	Embedding space decomposition	**Threshold detector**		(Roberts *et al* 1999)
	Coarse-grained entropy rate (CER)	**Continuous feedback**		(Trejo *et al* 2003)
	Gaussian process entropy rates (GPER)	**Continuous feedback**		(Trejo *et al* 2003)
	spectral entropy (SE)	**Continuous feedback**		(Trejo *et al* 2003)
	wavelet entropy (WE)	**Continuous feedback**		(Trejo *et al* 2003)
Dipole analysis (wavelet transform may be applied before BPF)	***BPF-ICA-dipole analysis***	**Threshold detector**		(Qin *et al* 2004b, Qin *et al* 2004a)
	BPF-ICA-dipole analysis-cortical current density	**Threshold detector**		(Qin *et al* 2004b, Qin *et al* 2004a)

TABLE B.0.3 FEATURE CLASSIFICATION METHODS IN BCI DESIGNS THAT ARE BASED ON NEURAL CORTICAL RECORDINGS

Feature Extraction		Feature Classification		Reference ID
None - Most of these designs model the relationship between neural firing rates and 'position and/or velocity and /or acceleration of hand		**Neural Networks**	***Recurrent multi layer Perceptron Neural network (RNN)***	(Sanchez *et al* 2002a, Sanchez *et al* 2002b, Sanchez *et al* 2003)
			MLP	(Kim *et al* 2005b)
			Feed-forward ANN	(Patil *et al* 2004)
			ANN recurrent dynamic back-propagation	(Chapin *et al* 1999)
			ANN model	(Hatsopoulos *et al* 2004, Wessberg *et al* 2000)
			Other	(Karniel *et al* 2002)
		Support vector machine regression (SVR) model		(Kim *et al* 2005b)
		Cosine tuning model (a linear model)		(Black *et al* 2003, Kemere *et al* 2004, Taylor *et al* 2002, Taylor *et al* 2003)
		Linear Gaussian models (LGM) implemented by Kalman filter		(Black *et al* 2003, Gao *et al* 2003a, Patil *et al* 2004, Sanchez *et al* 2002a, Wu *et al* 2002a, Wu *et al* 2002b)
		Generalized linear models (GLA)		(Black *et al* 2003, Gao *et al* 2003a)
		Generalized additive models (GAM)		(Black *et al* 2003, Gao *et al* 2003a)
		Weighted linear combination of neuronal activity (Wiener filter: a linear model)		(Carmena *et al* 2005, Hatsopoulos *et al* 2004, Kim *et al* 2005a, Kim *et al* 2005b, Lebedev *et al* 2005, Patil *et al* 2004, Sanchez *et al* 2002b, Serruya *et al* 2003, Serruya *et al* 2002)
		Gamma filter (a linear model)		(Sanchez *et al* 2002b)
		Mixture of multiple models based on NMF (non-negative matrix factorization)		(Kim *et al* 2005a)
		Echo State Networks (ESN) - Optimal sparse linear mapping		(Rao *et al* 2005)
		Linear model (no details mentioned)		(Carmena *et al* 2003, Wessberg *et al* 2000)
		Threshold detector		(Roushe *et al* 2003)
		SVM		(Byron *et al* 2005, Hu *et al* 2004, Olson *et al* 2005)
		Direct translation of firing rate to cursor movement		(Kennedy *et al* 2000)
		Bayesian classifier		(Gao *et al* 2002, Hu *et al* 2004)
		Maximum likelihood-based model		(Hatsopoulos *et al* 2004, Kemere *et al* 2004, Serruya *et al* 2003)
TFR methods	**Wavelet transform**	**Neural Networks**	***LVQ***	(Laubach *et al* 2000)
		Bayesian classifier		(Musallam *et al* 2004)
Averaging		**Neural Networks**	***LVQ***	(Laubach *et al* 2000)
		Threshold detector		(Otto *et al* 2003, Vetter *et al* 2003)

TABLE B.0.3 FEATURE CLASSIFICATION METHODS IN BCI DESIGNS THAT ARE BASED ON NEURAL CORTICAL RECORDINGS (CONTINUED)

Filtering - rectification - thresholding	**LPF (continuous signal)**	(Karniel *et al* 2002, Kositsky *et al* 2003, Reger *et al* 2000a, Reger *et al* 2000b)
Cross-covariance of each neuron's activity with one another - Principal Component Analysis (PCA)	**k-NN**	(Isaacs *et al* 2000)
LBG vector quantization	**HMM**	(Darmanjian *et al* 2003)

Appendix C. Details of Methods

In this chapter details of the methods that have been used in this thesis are presented.

C.1. Linear Discriminnat Analysis (Lachenbruch 1975)

Linear discriminant analysis (LDA) is used in classification problems to find the linear projection of features which best separate two or more classes of object or event. The resulting combinations may be used as a linear classifier, or in dimensionality reduction before later classification.

LDA is also closely related to principal component analysis (PCA) in that both look for linear combinations of variables which best explain the data. LDA explicitly attempts to model the difference between the classes of data. PCA on the other hand does not take into account any difference in class.

More formally, given a number of independent features relative to which the data is described, LDA creates a linear combination of these (by applying a projection matrix W) which yields the largest mean differences between the desired classes. Mathematically speaking, for all the samples of all classes, two measures are defined: 1) one is called within-class scatter matrix, as given by:

$$S_w = \sum_{j=1}^{c} \sum_{i=1}^{N_j} (x_i^j - \mu_j)(x_i^j - \mu_j)^T$$

where x_i^j is the *i*th sample of class j, μ_j is the mean of class j, c is the number of classes, and N_j the number of samples in class j; and 2) the other is called between-class scatter matrix, given by:

$$S_b = \sum_{j=1}^{c} (\mu_j - \mu)(\mu_j - \mu)^T$$

where μ represents the mean of all classes.

The goal is to maximize the between-class measure while minimizing the within-class measure. One way to do this is to maximize the ratio $\frac{\det(S_b)}{\det(S_w)}$. It can be proven that this ratio is maximized when the column vectors of the projection matrix, W, are the eigenvectors of $S_w^{-1}S_b$.

C.2. Principal Components Analysis (Jolliffe 2002)

Principal components analysis (PCA; also known as Karhounen-Loeve transform) is a technique for simplifying a dataset, by reducing multidimensional datasets to lower dimensions for analysis.

PCA is an orthogonal linear transformation that transforms the data to a new coordinate system such that the greatest variance by any projection of the data comes to lie on the first coordinate (called the first principal component), the second greatest variance on the second coordinate, and so on. PCA can be used for dimensionality reduction in a dataset while retaining those characteristics of the dataset that contribute most to its variance, by keeping lower-order principal components and ignoring higher-order ones.

Assuming zero empirical mean (the empirical mean of the distribution has been subtracted from the data set), the principal component W_1 of a dataset X can be defined as:

$$W_1 = \arg \max_{\|W\|=1} \operatorname{var}\{W^T X\} = \arg \max_{\|W\|=1} E\{(W^T X)^2\}$$

With the first k -1 components, the k^{th} component can be found by subtracting the first k-1 principal components from X:

$$\hat{X}_{k-1} = X - \sum_{i=1}^{k-1} W_i W_i^T X$$

and by substituting this as the new dataset to find a principal component in

$$W_k = \arg \max_{\|W=1\|} E\left\{\left(W^T \hat{X}_{k-1}\right)^2\right\}$$

The Karhunen-Loève transform is therefore equivalent to finding the singular value decomposition of the data matrix X, $X = W \Sigma V^T$ and then obtaining the reduced-space data

matrix Y by projecting X down into the reduced space defined by only the first L singular vectors, W_L:

$$Y = W_L^T X = \sum_L V_L^T$$

The matrix W of singular vectors of X is equivalently the matrix W of eigenvectors of the matrix of observed covariances $C = XX^T$,

$$XX^T = W \sum^2 W^T$$

The eigenvectors with the largest eigen values correspond to the dimensions that have the strongest correlation in the dataset.

C.3. K-Means Clustering (Hartigan 1979)

K-means is one of the simplest unsupervised learning algorithms that solve the well known clustering problem. The procedure follows a simple and easy way to classify a given data set through a certain number of clusters (assume k clusters) fixed a priori. The algorithm is composed of the following steps:

Step 1: Place K points into the space represented by the objects that are being clustered. These points represent initial group centroids.

Step 2: Assign each object to the group that has the closest centroid.

Step 3: When all objects have been assigned, recalculate the positions of the K centroids.

Repeat Steps 2 and 3 until the centroids no longer move. Basically, this algorithm aims at minimizing an *objective function*, in this case a squared error function. The objective function is:

$$J = \sum_{j=1}^{k} \sum_{i=1}^{n} \left\| x_i^{(j)} - c_j \right\|^2$$

where $\left\| x_i^{(j)} - c_j \right\|^2$ is a chosen distance measure between a data point $x_i^{(j)}$ and the cluster centre c_j, is an indicator of the distance of the n data points from their respective cluster centers.

Although it can be proved that the procedure will always terminate, the k-means algorithm does not necessarily find the most optimal configuration, corresponding to the global objective

function minimum. The algorithm is also significantly sensitive to the initial randomly selected cluster centers. The k-means algorithm can be run multiple times to reduce this effect.

There is no general theoretical solution to find the optimal number of clusters (k) for any given data set. A simple approach is to compare the results of multiple runs with different k classes and choose the best one according to a given criterion, but we need to be careful because increasing k results in smaller error function values by definition, but also an increasing risk of over-fitting.

The way to initialize the means (initial group centroids) is not specified in the algorithm. One popular way to start is to randomly choose k of the samples. Moreover, the results produced depend on the initial values for the means, and it frequently happens that suboptimal partitions are found. The standard solution is to try a number of different starting points.

C.4. Parzen Probability Density Estimation Method (Parzen 1962)

Given N samples $X_1,...,X_N$ drawn from a population with density function *f(x)*. The Parzen density estimate at x is given as

$$\hat{f}_h(x) = \frac{1}{N}\sum_{i=1}^{N}\frac{1}{h}k(\frac{x-X_i}{h})$$

where $k(.)$ is a window or kernel function and h is the window width, smoothing parameter, or simply the kernel size. $\hat{f}_h(x)$ is the maximum likelihood estimate of *f(x)*.

Traditionally, it is assumed that $\int k(u)d(u) = 1$ and $k(.)$ is symmetric, that is, $k(u) = k(-u)$.

The kernel function and kernel size are the most important characteristics of the Parzen density estimate. There are several types of kernel functions such as rectangular, triangular and Gaussian. Gaussian kernel is the popular choice for the kernel function.

The ideal or optimal value of *h* can be computed as

$$h_{0,sym}(x) = (\frac{f(x)\int k^2(u)du}{N\left[f''(x)\int u^2 k(u)du\right]^2})^{1/5}$$

provided that $h \longrightarrow 0, N \longrightarrow \infty, and \quad Nh \longrightarrow \infty$.

C.5. Description of the LF-ASD Feature Generator (Mason and Birch 2000)

The desired bipolar EEG pattern associated with the MRPs is similar to that shown in Fig. C.1. The time of the executed movement is around $t=n$. The output of the LF-ASD is activated when it detects the pattern shown in Fig. C.1.

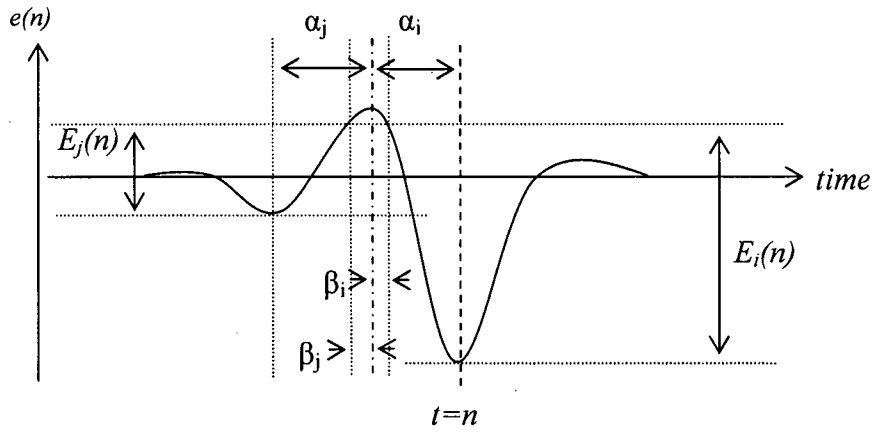

Fig. C.1. Desired pattern of the bipolar EEG during movement

As Fig. C.1 shows, each of the elemental features $E_i(n)$ and $E_j(n)$ are defined as the difference of a filtered signal (e(n)) at two points in time as calculated in equations (1) and (2). e(n) is the filtered signal measured from a pair of bipolar electrodes (filtered to 1-4 Hz using a 121-point, zero-phase FIR filter based on a Hamming window). There are six such pairs and six such signals.

$$E_i(n) = e(n - \alpha_i + \beta_i) - e(n) \quad (1)$$

$$E_j(n) = e(n - \alpha_i - \beta_j) - e(n - \alpha_i - \alpha_j) \quad (2)$$

In this thesis we used the general term "delay parameters" of the feature generator when referring to the above parameters ($\alpha_i, \alpha_j, \beta_i, \beta_j$).

The delay terms are initially estimated from the ensemble averages based on the minimum peak near the trigger (at time $t=n$ in Fig. C.1), the first local maximum, and the local minimum before

the trigger as shown in Fig. C.1. The trigger point is defined as the point around which the movement is performed.

Compound features are defined in equation (3) by pairing elemental features (E_i, E_j) to emphasize the samples in which two large elemental features appear concurrently.

$$\begin{aligned} g_{ij}(n) &= E_i(n).E_j(n) \qquad if \quad E_i(n) \times E_j(n) \geq 0 \\ &= 0 \qquad\qquad\qquad otherwise \end{aligned} \tag{3}$$

For robustness, the compound features are maximized over a window as follows.

$$G_{ij}(n) = \max\{g_{ij}(n-8), g_{ij}(n-7), \ldots, g_{ij}(n-1), g_{ij}(n)\} \tag{4}$$

This procedure is repeated for each channel. The resulting feature vector is an equally weighted six-dimensional vector, with each dimension reflecting the value of the feature ($G_{ij}(n)$) in each channel.

C.6. Fuzzy Adaptive Resonance Theory (Carpenter et al 1991)

Adaptive resonance theory (ART) describes a family of self-organizing neural networks, capable of clustering arbitrary sequences of input patterns into stable recognition codes. Many different types of ART-networks have been developed to improve clustering capabilities.

The common algorithm used for clustering in any kind of ART network is closely related to the well-known k-means algorithm. Both use single prototypes to internally represent and dynamically adapt clusters. The k-means algorithm clusters a given set of input patterns into groups. The parameter thus specifies the coarseness of the partition. In contrast, ART uses a minimum required similarity between patterns that are grouped within one cluster. The resulting number of clusters then depends on the distances (in terms of the applied metric) between all input patterns, presented to the network during training cycles. This similarity parameter is called *vigilance* [3]. Specifically, fuzzy ART like many other iterative clustering algorithms is based on (a) 'finding the nearest' cluster seed (also known as prototype, template, or codebook) to the input x, and (b) updating that cluster seed to be 'closer' to the input where "nearest" and "closer" can be defined in hundreds of different ways. In fuzzy ART, the framework is modified slightly by introducing the concept of "resonance" so that each case is processed by:

(1) Finding the "nearest" cluster seed that "resonates" with the input

(2) Updating that cluster seed to be "closer" to the input

Given input X as an M-dimensional vector $(X_1,...,X_M)$ and a cluster seed W as $(W_1,...,W_M)$, nearness is assessed by a similarity measure called the "choice function":

$$\left(\sum_{i=1}^{M}\min(X_i,W_i)\right)/\left(\alpha+\sum_{i=1}^{M}W_i\right)$$

where α is a user-specified parameter usually equal to a very small positive number such as 1e-6.

Resonance is based on a slightly different similarity measure called the "match function". A seed resonates with the case if:

$$\left(\sum_{i=1}^{M}\min(X_i,W_i)\right)/\left(\sum_{i=1}^{M}X_i\right)\geq\rho$$

where ρ is a user-specified "vigilance" parameter between 0 and 1.

If no seed resonates with an input sample, a new cluster is created, usually with a seed equal to the input sample. If a resonant seed is found, the seed is updated according to the formula:

$$W_{new}=\beta*(\min(X,W_{old})+(1-\beta)*W_{old})$$

where β is a user-specified learning rate, usually 1 for "fast learning."

C.7. Learning Vector Quantization (Kohonen 1990)

The Learning Vector Quantization (LVQ) is an algorithm for learning class labels from labeled data samples. Instead of modeling the class densities, LVQ models the discrimination function defined by the set of labeled codebook vectors (m_i) and the nearest neighborhood search between the codebook and data. In classification, a data point x_i is assigned to a class according to the class label of the closest codebook vector (m_i).

To define the optimal placement of m_i in an iterative learning process, initial values for them must first be set using any classical vector quantization approach, e.g. k-means. In the learning process, the codebooks are pulled away from the decision surfaces to demarcate the class borders more

accurately. If m_c is the closest codebook (winner codebook) to input x in the Euclidean metric, m_c is updated according to the following equation:

$m_c(t+1)= m_c(t)+\alpha(t)[x(t)-m_c(t)]$ if x is classified correctly,

$m_c(t+1)= m_c(t)-\alpha(t)[x(t)-m_c(t)]$ if x is classified incorrectly,

$m_i(t+1)= m_i(t)$ for $i \neq c$

where $\alpha(t)$ is a scalar gain ($0<\alpha(t)<1$), which should decrease monotonically in time.

In fact, the direction of the gradient update depends on the correctness of the classification using a nearest neighborhood rule in Euclidean space. If a data sample is correctly classified (the labels of the winner unit and the data sample are the same), the model vector closest to the data sample is attracted towards the sample; if incorrectly classified, the data sample has a repulsive effect on the model vector.

For different picks of data samples from the training set, the procedure explained above is repeated iteratively until convergence. Finally, the set of m_i form the final codebook for classification. Several variations of LVQ such as LVQ2 and LVQ3 have also been proposed. While in LVQ (also known as LVQ1) only one m_i is updated, in LVQ2 and LVQ3 the two closest codebook vectors are changed simultaneously (Kohonen 1990).

C.8. k-Nearest Neighbor Classification:

k-nearest neighbor alngorithm (k-NN) is a methos of classifying objects based on closest training samples in the feature space. In k-NN algorithm, the k closest codebooks to the input sample X_{new} are found based on some distance measure like Euclidean distance. X_{new} is assigned to the class c if it is the most frequent class label among the k closest codebooks.

The codebooks which are representative of the features of each class can be determined by different algorithms like learning vector quantization.

C.9. References

Cacoullos T 1966 Estimation of a multivariate density *Annals of the Institute of Statistical Math.* **18** 179-89

Carpenter G, Grossberg S and Rosen D B 1991 Fuzzy ART: Fast stable learning and categorization of analog patterns by an adaptive resonance system *Neural Networks* **4** 759-71

Hartigan JA and Wong MA 1979 A K-means clustering algorithm JR Stat. Soc. **28** 100-8

Jolliffe IT 2002 *Principal Component Analysis* (Springer)

Kohonen T 1990 The Self-Organizing Map *Proc IEEE* **78** 1464-80

Lachenbruch P A 1975 *Discriminant Analysis* (NY: Hafner Press)

Mason SG and Birch GE 2000 A brain-controlled switch for asynchronous control applications *IEEE Trans. Biomed. Eng.* **47** 1297-307

Parzen E 1962 On estimation of a probability density function and mode *Annals Math. Statistics* **33** 1065-76